Durability of concrete in saline environment

Sandberg, Paul

1996

Durability of Concrete in Saline Environment

Contents

Foreword

In the last 10-15 years durability issues have been increasingly important for the concrete industry. Especially so for large infrastructure projects such as the Great Belt Link and the Öresund Link. Previously durability of concrete was assessed by experience from old-fashion structures, or by simple extrapolations of test results from simplified accelerated durability tests. Recent research has shown that accelerated laboratory tests cannot be used to assess the durability of concrete, unless long term field exposure tests are performed simultaneously for the calibration of test data.

Extensive field- and laboratory exposure tests of modern bridge concrete have been carried out in the Nordic countries in the last five years. Several of the projects have been lead or sponsored by Cementa AB. The results regarding freezing and thawing, chloride and moisture transport, and reinforcement corrosion, all indicate that the field performance of modern high quality concrete in a marine environment is far better than the performance indicated by accelerated laboratory tests.

In this publication some of the most important results are presented and evaluated by some of the leading experts in the field of concrete durability. Some of the information presented is based on a previous publication in the same field - "Marina betongkonstruktioners livslängd" (Service life of marine concrete structures, in Swedish/Danish), Edited by K. Tuutti, Cementa, Danderyd 1993.

Lund, Maj 1996

Paul Sandberg, Cementa AB

Systematic Collection of Field Data for Service Life Prediction of Concrete Structures

P. Sandberg
Cementa AB / Lund Inst. of Tech., Building Materials
Ideon, S-223 70 Lund, Sweden

Abstract

Results from laboratory testing of the potential durability of reinforced concrete cannot be used for service life prediction, unless the results are carefully calibrated against the long term field performance under relevant exposure conditions. The marine field station at Träslövsläge on the Swedish west coast was established in 1991 for the purpose of collecting relevant field data for the planning of the Öresund Link between Copenhagen and Malmö. The field station is briefly described and a procedure for systematic collection of relevant durability-related data from field exposed concrete is outlined.

Introduction

Several long-term field studies of concrete have revealed the need for a systematic approach for collecting field data for service life prediction of concrete structures /1-5/. These field studies among others indicated that field testing of concrete will generate a wide spread of data for a given concrete mix, depending mainly on the exposure conditions on the micro level, and on the exposure length.

Most laboratory testing of the potential durability of concrete involves accelerated and simplified exposure conditions. Tests for the evaluation of chloride permeability, for instance, are usually accelerated by the use of an electrical field or immersion in very strong chloride solutions. Such laboratory testing produces some permeability-related results, which are only valid for that specimen at the testing age and the specific exposure conditions used. Today it is obvious that laboratory tests cannot be used for service life prediction unless they are carefully calibrated against long term experience from field exposure tests.

General procedures for the development of testing methods for service life prediction, by simultaneous field and laboratory testing, has been presented by CIB/RILEM and ASTM /6-7/, as illustrated in Figure 1. The key to the

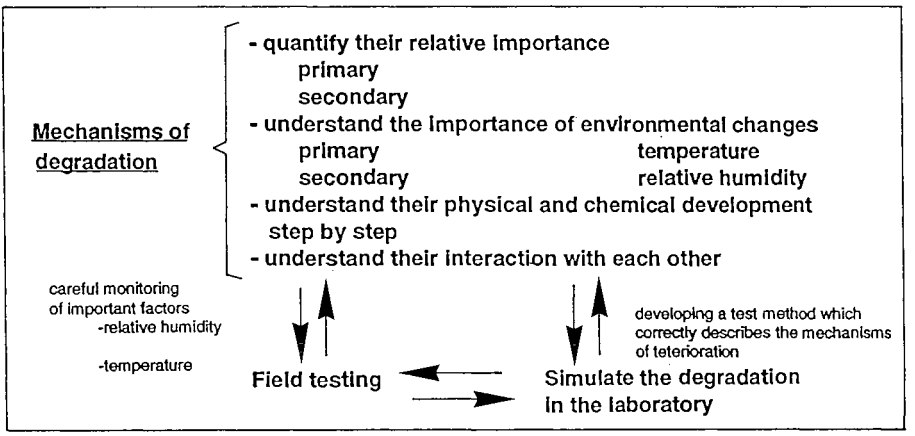

Fig. 1. General procedure for the development of testing methods for service life prediction, derived from recommendations by CIB/RILEM and ASTM/6-7/.

development of better test methods and prediction models is to identify and understand the various degradation mechanisms at work in the field.

It has become evident from the field testing that concrete in most cases perform much better in the field as compared to the expected performance based on results from laboratory testing. This is true f.i. when considering chloride transport rates and frost attack on marine exposed concrete. Thus it is important to identify the mechanism(s) behind this improvement, and to quantify its (their) relative importance. As illustrated in Figure 2, one important mechanism

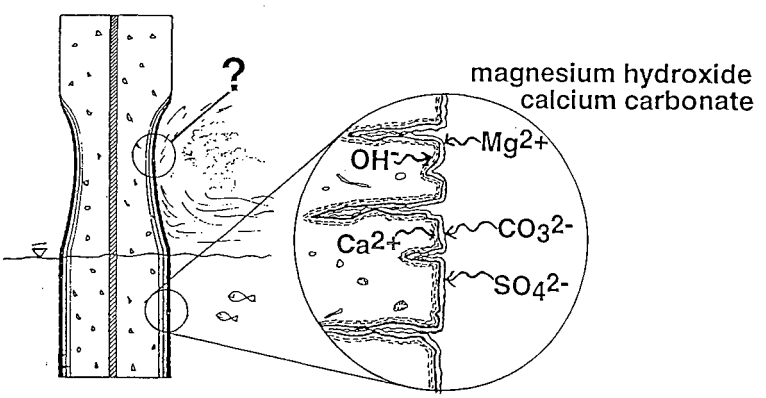

Fig. 2. Magnesium and carbonates from sea water combine with calcium and hydroxides from concrete to form a dense precipitate on the concrete surface and in cracks. This self sealing effect is very pronounced for marine concrete /8/, but remains to be studied more in detail for concrete exposed to deicing salts.

appears to be the surface densification of concrete, a phenomenon which is much stronger in the marine exposure as compared to the simplified laboratory exposure conditions.

Field exposure tests are naturally very time consuming and can also be very costly, if the aim is to follow the time dependent changes in the concrete microstructure with respect to all relevant properties. Therefore it is important to establish a common approach for field monitoring of concrete, to make it possible to compare and evaluate experiences from different exposure sites. However, such a program should not limit the freedom of research to certain methods.

A common approach to field studies would make it possible to correlate the performance of concrete in certain laboratory testing to the actual field behaviour, for a given type of structure in a given environment. A common approach for field monitoring of concrete would also help to create a database of experience for future planning and design of concrete structures.

The Träslövsläge Field Station

The need for reliable field data for service life prediction lead to the establishment of a marine field station at Träslövsläge on the Swedish west coast in the end of 1991, Figure 3. Today 3 pontoons are carrying more than 50 different concrete qualities, with water to binder ratios ranging from 0.25 to 0.75. Most of the mix designs are shown in Appendix 1.

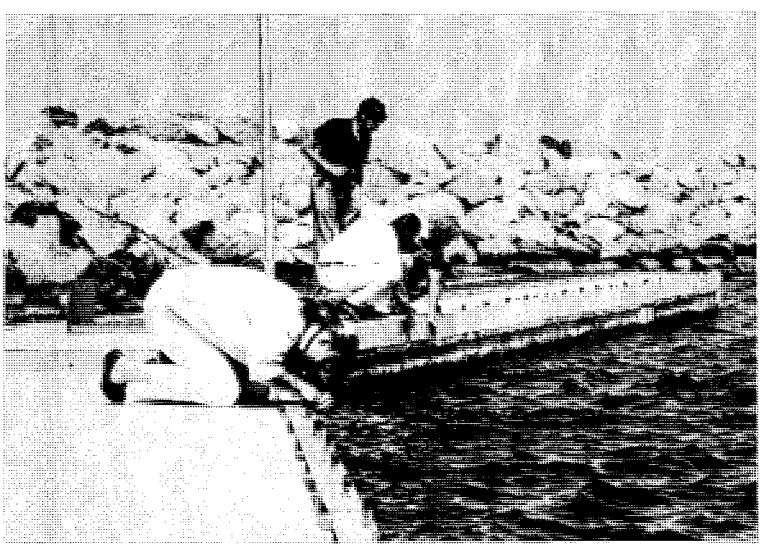

Fig. 3. *The Träslövsläge Marine Field Station.*

In general, two designs of concrete specimens are field exposed at Träslövsläge:

- 15 cm cubes for field studies of the frost attack on concrete in the salt spray zone. The cubes are mounted on top of the pontoons. Besides studies of the surface scaling at field exposure, field exposed concrete is also tested for resistance to salt scaling in a standard laboratory test (the Borås Method, SS 13 72 44) /9,10/.
- Reinforced concrete slabs, height 100 cm, width 70 cm, thickness 10-20 cm, are mounted on the sides of the pontoons. A submerged- a splash- and an atmospheric / upper splash zone are thus obtained for each slab as illustrated in Figure 4. The concrete slabs are used for the following studies:

- chloride threshold levels /11,12/
- corrosion rates /11,12/
- steel potentials /11,12/
- chloride profiles /13/
- chloride transport coefficients* /14/
- moisture profiles /15/
- moisture transport coefficients* /16/
- changes in the concrete microstructure /17/
- surface scaling /9/
- resistance to salt scaling* /10/

* indicates standard laboratory exposure test on field exposed concrete.

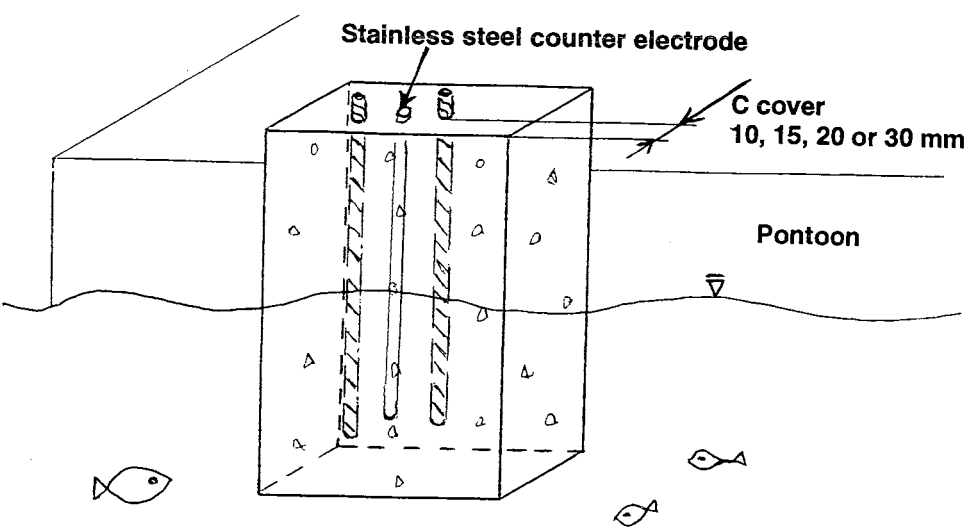

Fig. 4. Exposure conditions at the Träslövsläge Field Station.

In some cases special set-ups have been used:

- A test method for laboratory or field testing of the chloride threshold level for initiation of active reinforcement corrosion, APM 303 /18/, has been developed within the BMB-project. In this test the reinforcement is kept under potentiostatic control, which allows for the chloride threshold level to be obtained as a function of the steel potential. In a given structure, the reinforcement potential is controlled by the moisture state and other exposure conditions.
- Concrete "dummies" (same dimensions as for reinforced concrete specimens) are exposed parallel to the main samples, for the continuos logging of moisture- /15/ and temperature /19/ data inside the concrete using cast-in probes.

Recently a data logger system has been designed and implemented for continuously logging of reinforcement potentials, and occasionally for logging of corrosion currents (if the reinforcement is kept under potentiostatic control).

Suggested procedure for investigations on existing structures

Several durability-related concrete parameters changes with time, such as the moisture state and the coefficient of chloride transport in concrete. The breakdown of concrete in the field gradually continues from the beginning of field exposure to the end of the service life, as illustrated in Figure 5 /20/.

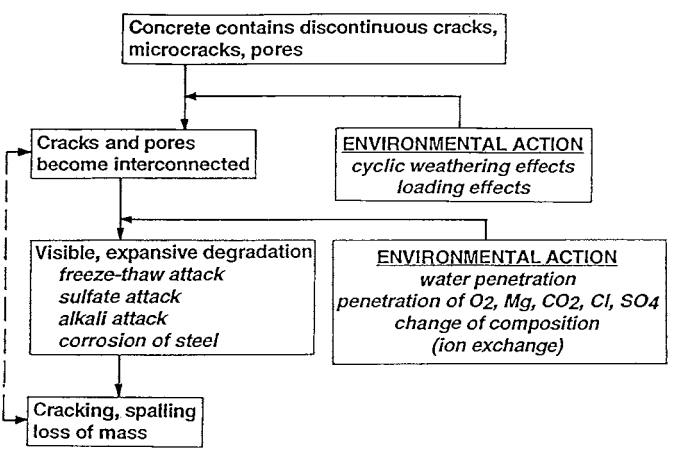

Fig. 5. *A schematic sketch of the gradual degradation of concrete /20/.*

The net rate of concrete breakdown is non-linear over time. During the first years of exposure, the permeability of a good quality marine concrete cover decreases over time, due to continued hydration, densification of the concrete surface, etc. The net effect on the chloride transport coefficient, evaluated as a diffusion coefficient by fitting an obtained chloride distribution to a solution to Fick's second law of diffusion, is illustrated in Figure 6 /21/, for exposure in the tidal zone.

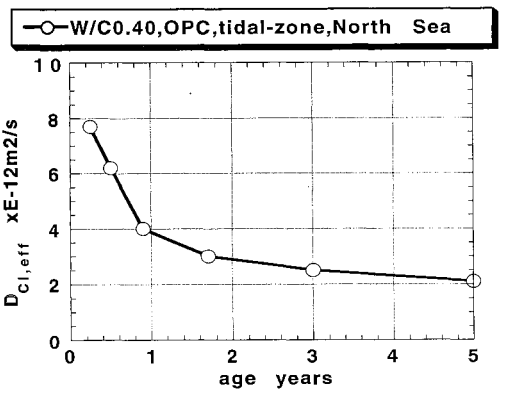

Fig. 6. The relation between the "effective diffusion coefficient" and time for a field exposed concrete in the tidal zone /21/.

Various degradation mechanisms initiate and proceed at various rates. After some 10-20 years of service, freeze-thaw attack etc. may become a dominant degradation mechanisms. At this stage the chloride permeability may increase rapidly over time, as illustrated schematically in Figure 7 /22/.

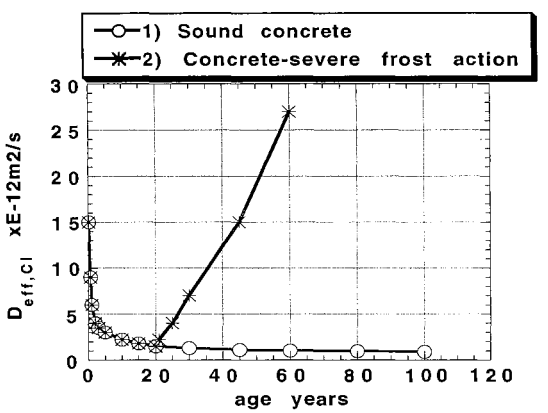

Fig. 7. Scenarios for the chloride transport coefficient "effective diffusivity" over time in field exposed concrete. Scenario 1) No frost attack on the concrete cover. 2) Servere freeze-thaw attack initiated after 20 years of field exposure /22/.

Planning for recurrent inspection

Due to changes in concrete properties over time, recurrent inspection should be planned at various ages. Since most properties are believed to roughly follow a square root dependency, the inspection frequency may be higher at early ages.

Results from recurrent inspections of concrete field exposed for 0-9 years, indicate that the following scheme could be useful for planning. The field data obtained from 0-5 years of exposure is intended for planning of future inspections and service life prediction. Present models for service life prediction may of course later on become adjusted for the knowledge achieved from future inspections.

Inspection number	time of exposure (years)	
1	0	(inspection at the day of field exposure)
2	1	
3	2	
4	5	
5	10	
6	20	
7	35	
8	50	
9	70	
10	100	

Classification into exposure zones

The main factors affecting the degradation rate of a given reinforced concrete structure are the moisture state, the oxygen availability and the temperature /23/.

The moisture state controls the transport of moisture and aggressive ions through a given concrete, thereby affecting chemical and physical degradation of concrete. Once ions aggressive to the steel reinforcement, such as chlorides and carbonates, have penetrated the concrete cover, reinforcement corrosion may be initiated.

The rate of initiation and propagation of the corrosion process is strongly affected by the moisture state, the oxygen availability and the temperature.

As a consequence, it is practical to subdivide a given reinforced concrete structure into different exposure zones, reflecting mainly the variations in the concrete moisture state in different exposure zones.

The effect of varying exposure conditions

The chloride penetration profiles, measured in a marine concrete bridge column, as a function of the distance from the water level are illustrated in Figure 8. As indicated the chloride penetration rate at a given exposure time may vary extensively with the local exposure conditions.

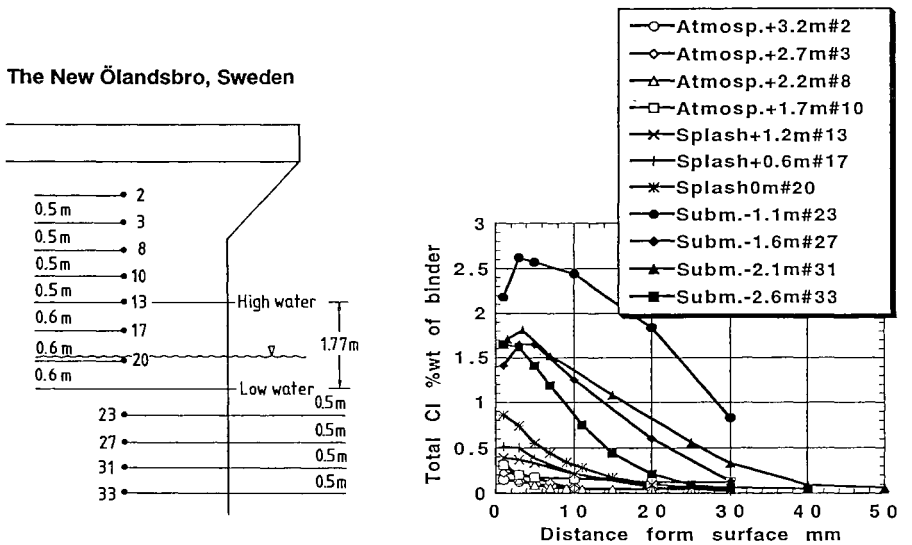

Fig. 8. The effect of micro environment on the chloride penetration in the New Ölandsbro at various heights from the mean water level, after 4 years of exposure /24/.

Recent research /23,24/ has indicated that the reinforcement corrosion threshold level and the active corrosion rate may vary with orders of magnitudes as controlled by the exposure conditions. In submerged concrete, where chloride penetration rates are relatively high, the chloride threshold level is normally very high, and the active corrosion rate is depressed to often insignificant levels - due to a lack of oxygen at the depth of the reinforcement /23,24/. On the other hand, in splash zone concrete subjected to wetting and drying, chloride penetration rates can be slower, but the potential corrosion damage can be high due to the abundance of oxygen at the depth of the reinforcement.

As a consequence, various criteria must be established regarding the accepted performance range in various exposure zones.

Exposure zones in a marine environment

The following exposure zones are suggested when applicable:

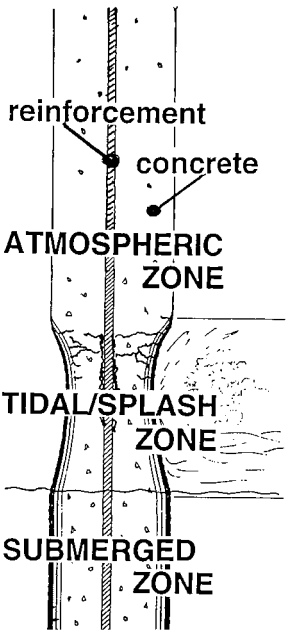

Fig. 9. Exposure zones in a marine environment.

Atmospheric zone not sheltered from rain

No regular splashing from waves. However, the salt spraying by wind may be significant. Significant temperature cycles, wetting and drying, freezing and thawing may occur.

Atmospheric zone sheltered from rain

As above, but the effect of stronger drying may cause significant capillary chloride transport. Carbonation may be important.

Splash zone not sheltered from rain

Regular splashing from waves. Significant temperature cycles, wetting and drying, freezing and thawing, erosion may occur.

Splash zone sheltered from rain

As above, but the effect of stronger drying may cause significant capillary chloride transport. Carbonation may be important. Occasionally very high salt levels and scaling has been observed in this climate, due to continuous capillary suction and evaporation of water at the concrete surface.

Tidal zone

Tidal cycles cause temperature cycles, wetting and drying, freezing and thawing. Long term field studies indicated the tidal zone as the most servere zone, since tidal water causes 2 cycles of freezing and thawing each day /25/.

Submerged zone

The environmental load is relatively constant. This zone is an important reference zone when evaluating chloride ingress etc. in zones above the water table. Swedish field studies indicated that for good quality concrete with no or little damage, the chloride penetration is most rapid in the submerged zone (due

to continuous chloride exposure). However, the reverse appears to be true once significant deterioration take place in the splash zone /24/.

Zones of primary interest

The splash and tidal zones are by far the most servere exposure zones in a marine environment. However, it is strongly recommended also to monitor the submerged and atmospheric zones, since these less servere zones will submit reference data of importance when evaluating the degradation path in more damaged concrete.

Parameters of primary interest

Measurements of ***corrosion potentials and -rates*** are useful for evaluating if the reinforcement is actively corroding or not. It is often difficult to establish if the reinforcement is actively corroding or not by measuring potentials only, since potential gradients may be the result of both active corrosion and of variations in the concrete moisture state. However, a simple potential mapping is often useful as the first step for the identification of the local parts of the structure which are most likely to have a corrosion problem.

Thus the results from the potential mapping may serve as a guide for where to measure field chloride profiles.

Field chloride profiles are of primary concern when evaluating resistance to chloride penetration. A large number of rapid chloride profiles can be obtained in a short time by simply drilling powder samples at various depths using a hammer drill. The ***rapid chloride profiles*** are not always accurate, but they provide a guide for where to measure more accurate chloride profiles by means of the more time consuming ***profile grinding*** technique.

A field chloride profile reflects the net result of all kinds of environmental action and the materials properties from the beginning of exposure to the time of measurement. However, field chloride profiles alone may not be sufficient for prediction of the future chloride ingress. A laboratory measurement of the ***bulk diffusivity in unexposed bulk concrete*** will give useful indications on the "intrisinic" permeability of the concrete itself.

Since most degradation mechanisms are governed by moisture transport, registration of ***moisture state and moisture transport data*** is also of primary concern for improving service life prediction.

Studies of the ***steel potential and the moisture state*** is important also when evaluating the hazard of future active corrosion in a reinforcement which is passive at present. Measurements of the ***pore solution chemistry*** may also give important information on the hazard for active corrosion, although no inexpensive and accurate method exists for such measurements in high quality concrete of low water/binder ratios.

Optical microscopy will supply very useful general information about micro structural degradation such as cracking, leaching, densification, carbonation, expansive reactions etc. Furthermore, the microstructure at the steel-concrete interface appears to be most important for the chloride threshold level.

References

1. *Tuutti, K.* "Reinforcement corrosion" (in Swedish), Marina betongkonstruktioners livslängd - Seminars in Sweden and Denmark, Dansk Betoninstitut/Aalborg Portland /Cementa 1993.
2. *Concrete in the Oceans* technical report No. 24 "Effectiveness of concrete to protect steel reinforcement from corrosion in marine structures", OTH 87 247, London 1988.
3. *Maage, M., Helland, S., Carlsen, J. E.* "Chloride penetration in high performance concrete exposed to marine environment", 3rd int. symp. on Utilization of High Strength Concrete, Lillehammer, Norway 1993.
4. *Vejdirektoratet Broområdet* "Chloride induced corrosion - a study of chloride load and reinforcement corrosion in bridge columns" (in Danish), Köpenhamn 1991.
5. *Vegdirektoratet Bruavdelning/Norges Byggforskningsinstitutt (NBI)* "Chloride durability of marine concrete bridges" (in Norwegian), Oslo 1993.
6. *Masters, L., W., Brandt, E.* "Prediction of service life of building materials and components", CIB W80/RILEM 71-PSL Final Report, 1987.
7. *ASTM E632*, "Standard practise for developing accelerated tests to aid prediction of the service life of building components and materials, 1988.
8. *Buenfeld, N.R., Newman, J.B.* "The Permeability of concrete in a marine environment", Magazine of Concrete Research, 1984, 36, No. 127, pp. 67-80.
9. *Pettersson, P.-E.* "The resistance of concrete to salt scaling - Field studies" (in Swedish), SP Report 1995:73, the Swedish National Testing and Research Institute (SP), Borås 1995.
10. *SS 13 72 44*, "Betongprovning - Hårdnad betong - Frostresistens" (Swedish standard for testing of freeze-thaw resistance of concrete in saline environment.), Byggstandardiseringen, Stockholm 1988.

11. *Schiessl, P.* "Corrosion of Steel in Concrete", London/New York: Chapman and Hall, Nov 1988, RILEM-report TC 60-CSC.
12. *Pettersson, K.* "Corrosion threshold value and corrosion rate in reinforced concrete", Swedish Cement and Concrete Research Institute, CBI report 2:92, Stockholm 1992.
13. *Sörensen, H., Frederiksen, J.M.* "Testing and modelling of chloride penetration into concrete", Nordic Concrete Research, Seminar Trondheim 1990, pp. 354-356.
14. *Tang, L., Nilsson. L.-O.* "Transport of ions", Chapter 9.6 and 9.8 in "Performance Criteria for Concrete Durability", State-of-the-art Report by RILEM TC 116-PCD, RILEM Report 12, ed. J. Kropp and H.K. Hilsdorf, Chapman & Hall, 1995.
15. *Nilsson, L.-O.* "Methods of measuring moisture penetration into concrete submerged in sea water", Proc. Nordic Seminar on Corrosion of Reinforcement - Field & Laboratory Studies for Modelling & Service Life, Lund, Sweden, February 2-3, pp. 199-208, 1995.
16. *Hedenblad, G.* "Moisture permeability of mature concrete, cement mortar and cement paste", Report TVBM-1014, Lund Inst. of Tech., Building Materials, Lund 1993.
17. *Hansen, T. S.* "Micro- and Macrostructural Analysis of Concrete" using Thin Section and Polished Section Microscopy, APM 201-202, AEC, Vedbaek, 1993.
18. *Arup, H., Sørensen, H.* "A proposed technique for determining chloride thresholds", Proc. Int. RILEM Workshop on Chloride Penetration into Concrete, Saint-Rémy-Les-Chevreuse, October 15-18, 1995.
19. *Ewertson, C.* "Consecutive climate data from Träslövsläge", Internal report BMB, SP Borås, available since 1992.
20. *Mehta, P.K.* "Concrete Technology at the Crossroads - Problems and Opportunities", Concrete Technology: Past, Present and Future, San Francisco, March 1994.
21. *Mangat, P.S., Molloy, B.T.* "Prediction of long term chloride concentration in concrete", Materials and Structures, 27, pp. 338-346, 1994.
22. *Sandberg, P.* "A proposed methodology for recurrent collection of fieldperformance data from bridges" (in Swedish), Internal report BMB, Cementa AB, Lund 1993.
23. *Pettersson, K., Sandberg, P.* "Chloride threshold levels and corrosion rates in cracked high performance concrete exposed in a marine environment - Considerations for a definition of service life time for high performance concrete", to be presented at the 4th CANMET/ACI Int. Conf. Durability of Concrete, Sydney, August 17- 22, 1997.
24. *Sandberg, P.* "Critical evaluation of factors affecting chloride initiated reinforcement corrosion in concrete", Report TVBM-3068, 1995, Lund Inst. of Tech., Building Materials, p. 43, 62.

25. *Moskvin, V., Ivanov, F., Alekseyev, S., Guzeyev, E.* "Concrete and Reinforced Concrete Deterioration and Protection", Mir Publishers, Moscow 1983.

Data for concrete exposed at the Träslövsläge Marine Field Station

W/(C+SF+0.3FA) Mix design	0.35	0.40	0.50	0.60	0.75
SRPC kg/m3 / air cast. date slump/remould f´c 28d cube/slab	450 / 6.0% cast 920122 10cm/10rev 70/62 MPa	420 / 6.2% cast 920122 12cm/9 rev 58/50 MPa	370 / 6.4% cast 920122 10cm/10rev 41/31 MPa		240 / 6.1% cast 920122 11 cm/8 rev 21/16 MPa
OPC kg/m3 / air cast. date slump/remould f´c 28d cube/slab	450 / 5.7% cast 911210 13cm/14rev 60/57 MPa	420 / 6.25 % cast 911209 12cm/10rev 54/49 MPa	390 / 5.8% cast 911205 9cm / 9 rev 42/36 MPa	310 / 6.3 % cast 911205 10cm/11rev 35/29 MPa	250 / 5.8 % cast 911204 10cm / 8rev 26/23 MPa
SRPC kg/m3 / air **5% SF** cast. date slump/remould f´c 28d cube/slab	427.5 / 5.8% cast 920127 6cm / 18rev 72/62 MPa	399 / 6.1 % cast 920123 8 cm/14rev 61/52 MPa	351.5 / 6.0% cast 920123 8 cm/11rev 45/37 MPa		233 / 5.9% cast 920122 14 cm/8 rev 21/19 MPa
SRPC kg/m3 / air **10% SF** cast. date slump/remould f´c 28d cube/slab		378 /6.6% cast 920224 6 cm/16 rev 65/49 MPa			
SRPC kg/m3 / air **5% SF** cast. date slump/remould f´c 28d cube/slab		399 / 2.9% cast 920225 9 cm/ 14 rev 81/64 MPa			
SRPC kg/m3 / air **5% SF** cast. date slump/remould f´c 28d cube/slab	427.5 / 2.1% cast 920225 4 cm / 27 rev 93/72 MPa	399 / 1.7% cast 920225 7 cm / 18 rev 87/69 MPa			
SRPC kg/m3 / air cast. date slump/remould f´c 28d cube/slab	450 / 2.4% cast 920225 6 cm / 17 rev 91/81 MPa	420 / 2.1% cast 929225 5 cm / 23 rev 79/68 MPa			265 / 1.1% cast 920126 5 cm/16 rev 32/24 MPa
OPC kg/m3 / air cast. date slump/remould f´c 28d cube/slab	470 / 2.1% cast 911203 8 cm / 16rev 73/71 MPa	440 / 2.1% cast 911203 8 cm / 15 rev 67/56 MPa	410 / 1.4% cast 911203 9 cm / 10rev 56/47 MPa	330 / 1.6% cast 911204 7 cm / 13rev 45/39 MPa	330 / 1.6% cast 911204 7 cm / 12rev 37/30 MPa
SRPC kg/m3 / air **4.5%SF** cast. date **17%FA** slump/rem f´c 28d cube/slab		345 / 6.1% cast 920303 10cm / 13rev 69/58 MPa			
SRPC kg/m3 / air **5% SF** cast. date **10%FA** slump/rem f´c 28d cube/slab	382.5 / 5.7% cast 920226 18cm / 11rev 84/68 MPa				

W/(C+SF+FA) mix design	0.25 Anl C	0.30 Anl C	0.30 Deg 400	0.40 Anl C
0 % Pozzolan		**H 3**	**H 9**	**Öland Bridge**
casting date		cast 920401	cast 920401 500	cast 920407
cement/super		492 kg /2.7 %	kg /2.3 %	420 kg / 0.8%
silica fume/fly ash		- / -	- / -	- / -
%air entr./%air		- / 3.6 %	- / 2.9 %	0.03%L14/6.2
slump/remould		>27cm/<5rev.	21cm/8 rev.	13cm / 9 rev.
aggregate 0-8/8-16		47 % / 53 %	47 % / 53 %	52% / 48%
f'c 28d cube/slab		96 / 91 MPa	102 / 98 MPa	58 / 53 MPa
5 % Silica fume	**H 5**	**H 1**	**H 7**	**H 4**
casting date	cast 920406 525	cast 920406 475	cast 920401 475	cast 920402 399
cement/super	kg /3.0 %	kg / 2.3 %	kg / 2.3 %	kg /0.8 %
silica fume/fly ash	26.2 kg / -	25 kg / -	25 kg / -	21 kg / -
%air entr./%air	- / 1.3 %	- / 0.8 %	- / 1.3 %	0.055L14/5.9
slump/remould	>27cm/<10rev.	>27cm/ <5rev.	>27cm/ <5rev.	18cm/10 rev.
aggregate 0-8/8-16	46 % / 54 %	47 % / 53 %	47 % / 53 %	50 % / 50 %
f'c 28d cube/slab	125 / 119MPa	112 / 105MPa	117 / 108MPa	63 / 59MPa
10 % Silica fume		**H 2**		
casting date		cast 920402 450		
cement/super		kg / 2.1 %		
silica fume/fly ash		50 kg / -		
%air entr./%air		- / 1.1 %		
slump/remould		14cm/ 16 rev.		
aggregate 0-8/8-16		46 % / 54 %		
f'c 28d cube/slab		117 /108MPa		
5 % Fly ash		**H 6**		
casting date		cast 920401 492		
cement/super		kg / 2.5 %		
silica fume/fly ash		- / 25.9 kg		
%air entr./%air		- / 2.8 %		
slump/remould		>27cm/ <5 rev.		
aggregate 0-8/8-16		47 % / 53 %		
f'c 28d cube/slab		95 / 90MPa		
20 % Fly ash		**H 8**		
casting date		cast 920401 493		
cement/super		kg / 2.8 %		
silica fume/fly ash		- / 123.3 kg		
%air entr./%air		- / 3.0 %		
slump/remould		27cm/ <5 rev.		
aggregate 0-8/8-16		44 % / 56 %		
f'c 28d cube/slab		98 / 90MPa		

w/(C+SF) mix design	0.25	0.30	0.35	0.40	0.50
0% silica fume casting date cement/super air entr./%air slump/remould aggregate0-8/8-16 f´c28d cube		**H3 air** cast 930518 500kg/2.3% 0.60%L14/3.4 >25cm/7rev. 47% / 53% 82 MPa			
5% silica fume casting date cement/super air entr./%air slump/remould aggregate0-8/8-16 f´c28d cube	**H5 air** cast 930518 522.5kg/2.6% 0.50%L14/5.5 20cm/15rev. 45% / 55% 101 MPa	**H1 air/30-5** cast 930510 475kg/2.0% 0.10%L14/6.2 26cm/<5rev. 46% / 54% 91 MPa	**35-5** cast 930510 427.5kg/1.2% 0.09%L14/5.6 13cm/14rev. 48% / 52% 79 MPa	**40-5** cast 930512 399kg/0.8% 0.08%L14/6.1 13cm/11rev. 50% / 50% 62 MPa	**50-5** cast 930513 351.5kg/-- 0.07%L14/5.8 8.0cm/15rev. 50% / 50% 48 MPa
8% silica fume casting date cement/super air entr./%air slump/remould aggregate0-8/8-16 f´c28d cube		**30-8** cast 930510 460kg/2.1% 0.11%L14/5.5 >26cm/5rev. 46% / 54% 95 MPa	**35-8** cast 930512 414kg/1.4% 0.10%L14/5.3 15cm/14rev. 47% / 53% 82 MPa	**40-8** cast 930512 386.4kg/0.9% 0.10%L14/5.6 9.5cm/15rev. 49% / 51% 66 MPa	**50-8** cast 930513 340.4kg/-- 0.09%L14/5.4 6.0cm/21rev. 50% / 50% 51 MPa
10% silica fume casting date cement/super air entr./%air slump/remould aggregate0-8/8-16 f´c28d cube		**H2 Air** cast 930518 450kg/2.2% 0.55%L14/6.4 >25cm/5rev. 45% / 55% 97 MPa			

Moisture in Marine Concrete Structures
- studies in the BMB-project 1992-1996

Lars-Olof Nilsson, Department of Building Materials
Chalmers University of Technology, S-412 96 Göteborg

Abstract

The moisture distribution in a concrete structure is determined by the concrete composition and curing and the micro-climate in the different parts of the structure. A prediction requires access to data on the time-dependency of the binder reactions, moisture fixation and moisture flow, ambient temperature and humidity and a computer software for more complicated cases. A summary of the present knowledge and examples of relevant material properties are given in the paper.

In a four-year project on durability of marine concrete structures, special attention was put to the moisture properties and moisture conditions of relevant concretes submerged in sea water and exposed to splash from sea water. Measured moisture properties and moisture distribution for a number of concretes in a field exposure site and in a number of structures are given in the paper. One surprising discovery was the low RH and degree of saturation in structures submerged in sea water for decades.

Introduction

A project on durability of marine concrete structures (BTB in short in Swedish) was run 1992-1996 in Sweden. A number of Swedish and Danish researchers worked together on various topics. The moisture conditions of marine concrete structures were especially studied by the Department of Building Materials at Chalmers University of Technology in Göteborg.

The moisture conditions of a concrete structure have a decisive effect on many parts of deterioration processes and consequently have a significant effect on the service-life of a structure. In this respect it is important to consider both material parameters and climatic parameters.

The moisture conditions of indoor, normal concrete are fairly well known and possible to predict. The conditions of outdoor concrete structures and properties

and conditions of high performance concrete are less known and studied to a very small extent.

Significance of moisture

The moisture condition is one of the parameters that governs the hardening of concrete, especially close to the surface, and consequently governs the impermeability to gases, water and ions. Moisture variations causes shrinkage and shrinkage cracking.

Moisture plays a significant role in chemical reactions in concrete and in parts of physical and chemical processes in various deterioration phenomena. The effect of moisture in frost damage is obvious. In alkali-aggregate reactions moisture is required for the alkalis to reach the aggregate and the reaction product imbibe moisture resulting in large expansive forces.

The initiation time for reinforcement corrosion is highly influenced by the moisture content since moisture delays the intrusion of carbon dioxide but is a pre-requisite for the penetration of chlorides. In the splash zone of a marine structure moisture plays a more active role when salts are penetrating by convection when moving with the water and deposit where and when the moisture evaporates.

When the corrosion starts the rate of corrosion is influenced by moisture to a great extent. In dry conditions or very wet conditions the rate is slow but intermediate moisture conditions give an electrolyte and permits the intrusion of oxygen to the corrosion process.

What is most important to consider?

To be able to predict the moisture conditions of a specific case knowledge is required on both a number of material properties and the micro-climate of the different parts of the structure. An example of what this means is given in Figure 1 for a concrete bridge deck with a membrane as a top cover.

In the upper part of the bridge deck it is decisive to predict the self-desiccation correctly by predicting the concrete binder reactions. The moisture conditions in the concrete cover for the reinforcement at the bottom of the bridge deck, however, depends to a great extent on the temperature of the structure and its micro-climate.

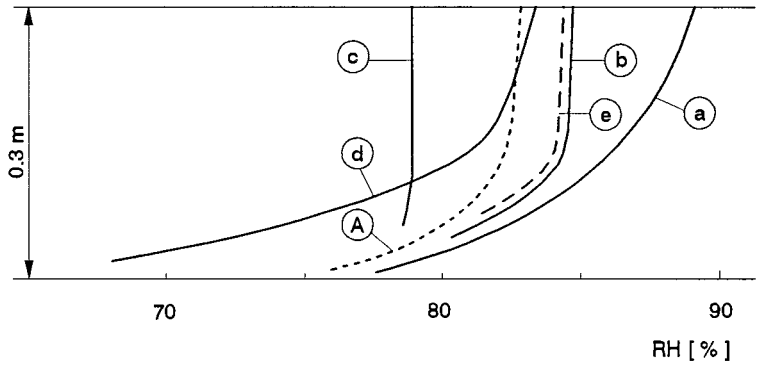

Fig. 1. *Predicted moisture distribution in a 5 year old concrete bridge deck with a tight top cover(A). The effect of lack of knowledge on material properties [a) without, b) slow hydration, c) larger moisture flow ability, e) very early form stripping and start of drying] and boundary conditions [d) dry micro climate due to sun radiation].*

PART A: THEORY

Definitions and basic laws

The moisture condition of air is defined by the water vapour content c [kg/m^3], the water vapour content at saturation c_s and the relative humidity

$$RH = \frac{c}{c_s} \tag{1}$$

The moisture content of concrete may be described in several ways:

w	moisture content per volume [kg/m^3]
u	moisture content in per cent by weight of dry material [%]
S_{cap}	degree of capillary saturation [-]

The water chemically fixed to the binder is described as the non-evaporable water content w_n.

The relationship between the RH and the water content is shown in the section on physical fixation of moisture.

The moisture distribution of the different parts of a concrete structure can be predicted by solving the "law of mass conservation". In one dimension it is

$$\frac{\partial w_e}{\partial t} = -\frac{\partial q_m}{\partial t} - \frac{\partial w_n}{\partial t} \qquad [2]$$

For the temperature calculation a similar equation for energy conservation is used.

The solution of Eq. [2] requires initial conditions. Usually the calculation starts at a time t_0 when the moisture distribution is known or may be estimated in a simple way. Required initial conditions in a one-dimensional description are

$$\begin{aligned} w_e(x, t = t_0) &= w_{e0}(x) \\ w_n(x, t = t_0) &= w_{n0}(x) \end{aligned} \qquad [3]$$

The boundary conditions must be known. The surface temperature T(x=0, t) and the surface humidity RH(x=0, t) are calculated from the micro-climatic data.

For solving Eq. [2] computer software is usually required, at least in more complicated cases and for accurate predictions. A number of PC-programs are available, also for two-dimensional predictions.

The solutions will not, however, be more accurate than the accuracy of the input data. The data is to a large extent available today, even though it may require some effort to collect it.

Chemical fixation of water

A large part of the mixing water in concrete is chemically bound to the binder. Data is required on the development of hydration of the cement in question and the effect of additives and admixtures. Temperature (T) and moisture conditions (ϕ) will influence the time-dependency. The rate of the chemical binding of water is described by

$$\frac{\partial w_n}{\partial t} = \beta_T \cdot \beta_\phi \cdot \left(\frac{\partial w_n}{\partial t}\right)_0 \qquad [1]$$

where index 0 refer to the hydration in a reference climate, usually curing in water at +20 °C.

The effect of moisture on the rate of hydration, described by the factor β_ϕ, is shown in Figure 2 where RH is the relative humidity in the concrete pores.

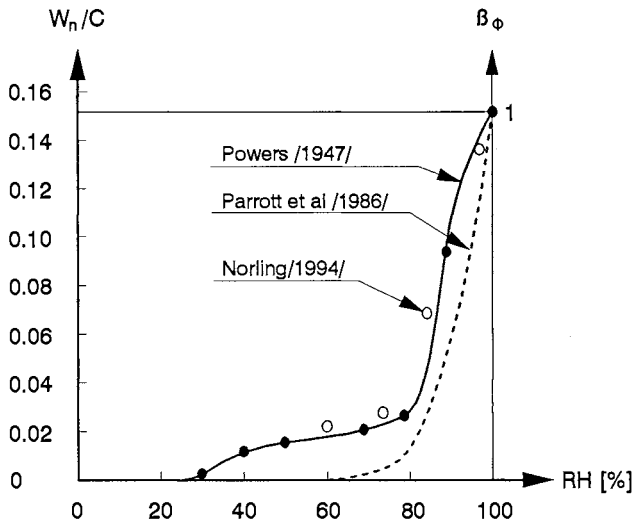

Fig. 2. The effect of the state of moisture on the cement hydration (o shows recent measurements by Norling (1994))

Also below 80 % RH the hydration continues. This is clearly shown in self-desiccation of concretes with a low water-binder ratio where the self-desiccation can reach as low RH:s as 70 %.

Physical fixation of water

The water that is not chemically fixed to the binder is physically fixed in the pores of the concrete. In the smallest pores the water is most firmly bound and this water can dry out only in a very low RH. The relationship between the amount of physically bound water w_e [kg/m^3] and the state of moisture RH can be calculated from available sorption curves, see the example in Figure 3.

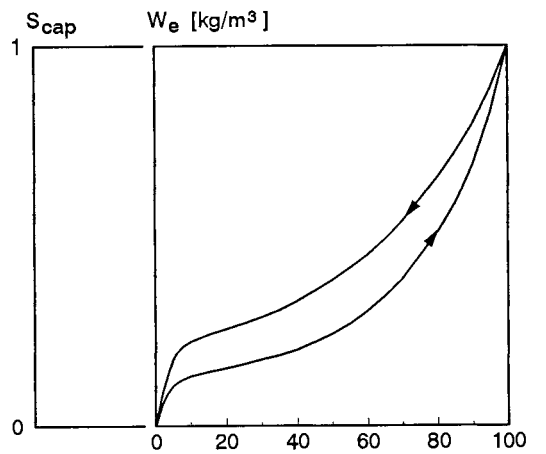

Fig. 3. The sorption isotherm in principle.

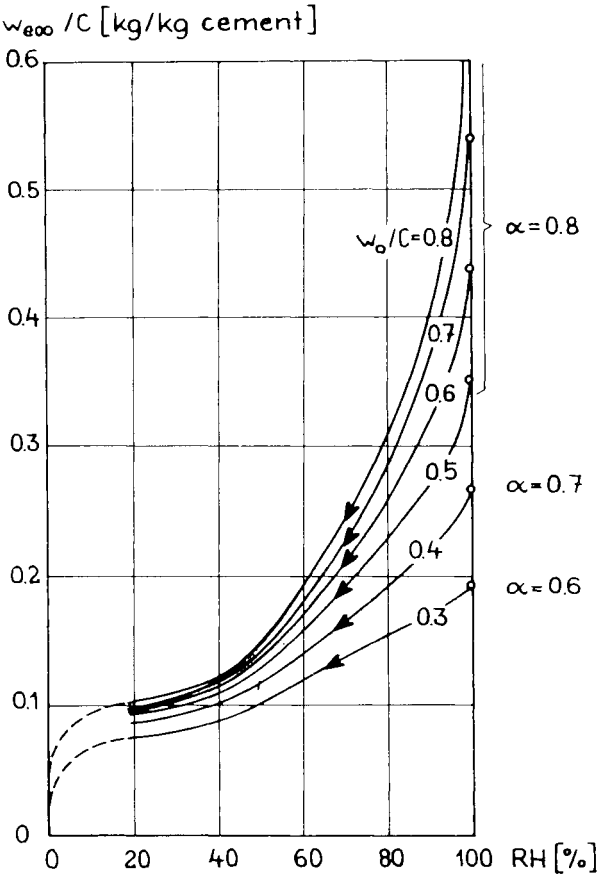

Fig. 4. Desorption curves for OPC concrete of various compositions, Nilsson (1980).

The sorption curves depend mainly on the cement content C, the water-cement ratio w_0/C, the age or degree of hydration α and the amount of microsilica. They also vary to some extent with type of cement, temperature and amount of additives, Atlassi et al (1989).

For accurate predictions of moisture conditions the salt content in the pore water should be considered since the sorption curves should depend on the salt content and type of salt. For instance the alkali content is considered by Hedenblad (1993).

Moisture transport

The moisture flow in the concrete pores takes place as vapour diffusion, with the vapour content as driving potential, and liquid flow with the pore water pressure

as potential. All sorts of complicated descriptions of the moisture flow have been used. Since measured data is lacking for the most complicated ones and the vapour flow and liquid flow usually occur in the same direction a simple description of the total moisture flow q_m [kg/(m^2·s)] can be used as a reasonable assumption.

A description with the vapour content v [kg/m^3] as a potential for the total flow and the moisture flow coefficient δ is

$$q_m = -\delta \cdot \frac{\partial v}{\partial x} \qquad [2]$$

The moisture flow coefficient δ increases very much above 90 % RH, see Figure 5, since more and more of the flow is liquid flow.

The moisture flow must be described in a more accurate way to consider the effect of temperature variations and the effect of salts on the moisture flow. In those cases separate terms for the vapour flow and the liquid flow must be utilised.

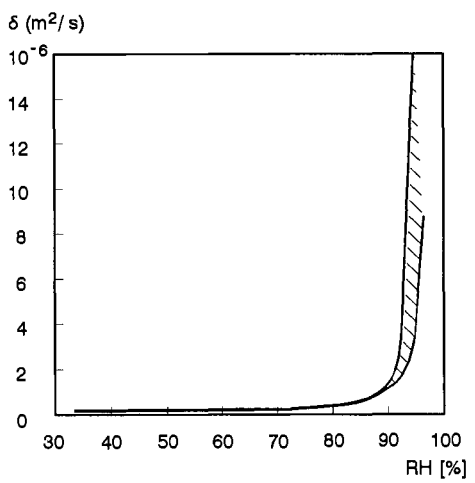

***Fig 5**. The moisture flow coefficient δ for well cured concrete of different water-cement ratios 0.4-0.8, Hedenblad (1993).*

Water absorption

At present the flow equations above can not describe the process of water absorption from a free water surface, for i e a concrete surface exposed to rain, sea water or splashing. An estimation of the depth of penetration z [m] and the

amount of water absorbed Q_m [kg/m^2], after a certain exposure time t [s], can be done with the "resistance number" m and the capillary absorption coefficient k

$$t = m \cdot z^2 \qquad z = \frac{1}{\sqrt{m}} \cdot \sqrt{t}$$

$$Q_m = \int_0^t q_m \cdot dt = k\sqrt{t} \qquad [4]$$

An example of how the resistance number m depends on the capillary porosity of the concrete is shown in Figure 6.

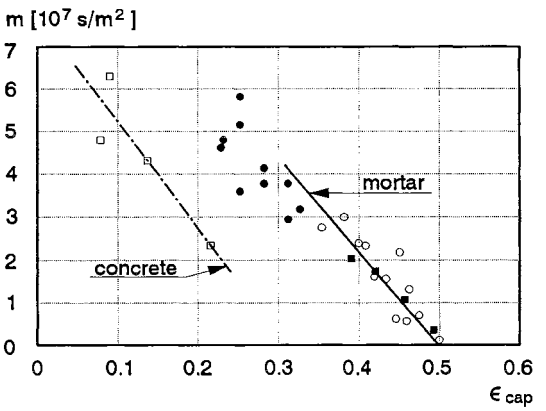

Fig. 6. Resistance number m for cement mortar as a function of the capillary porosity, Fagerlund (1982) (mortar) & Persson (1992) (concrete).

Low water-cement ratios give a very high resistance number and consequently a very slow absorption of water.

Water absorption in air pores

Air pores in concrete will contain entrapped air when water is absorbed into an exposed surface. Eventually those pores will be water filled after the air has been dissolved and diffused to larger air pores or the concrete surface. This process of extremely slow water absorption is of decisive importance for predicting the moisture distributions as a basis for estimating the service-life due to frost damage of air-entrained concretes. The water absorption process is described by Fagerlund (1993).

Micro climate

Relevant parameters in the description of the micro-climate of a concrete surface of a structure is

- Equivalent air temperature (with long wave and short wave radiation taken into account)
- RH of the concrete surface (with the temperature difference between the air and the surface taken into account)
- Time of wetness of the surface, which is the duration and time of occurrence of those periods when the surface is wet from rain, sea water, condensation, splashing water etc.

These parameters requires access to meteorological data and data on the geometry and the exact location of the structural part.

Self-desiccation

Even when no moisture transport occurs, as in structures with tight surface coverings or in dense concretes with low water-binder ratios, the concrete may undergo internal drying due to the chemical fixation of water to the binder since the reaction products have a lower volume than the reactants. The explanation is shown in Figure 7.

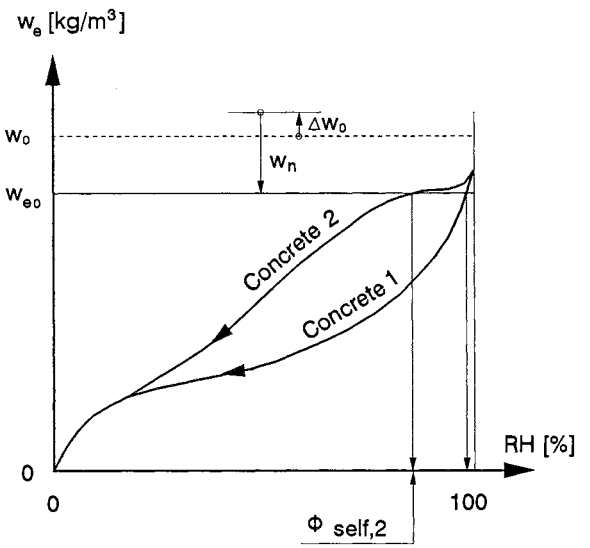

Fig. 7. *Self-desiccation for two concretes. Δw_0 is additional water during curing. w_{e0} is the remaining moisture and Φ_{self} is the RH after self-desiccation.*

Self-desiccation will increase with lower water-cement ratios and water-binder ratios, addition of silica fume and with some types of cement. RH can reach 70% in some cases only because of self-desiccation!

The time dependency of self-desiccation may be predicted from Eq [2], the rate of hydration and the age dependent desorption isotherms.

PART B: EXPERIMENTAL

Materials

Concrete specimens were cast in the Building Technology laboratories of the Swedish Testing and Research Institute (SP) in Borås. Specimen slabs 1.0x0.6x0.1m were cast lying down. The concrete compositions are shown in Table 1.

Material properties

In the project a number of material properties were determined: sorption isotherms, moisture flow coefficients and water absorption properties.

Sorption isotherms

Thin slices sawed from cores taken from the slabs were saturated in water and stored in several climate boxes with a series of RH:s. After reaching equilibrium, the moisture contents were determined before and after saturated in water once again. From the weights, the degree of saturation was calculated.

All measured desorption isotherms are shown in Figure 8 as degree of capillary saturation as a function of RH. The water-binder ratio varies from 0.25 to 0.50, cf. Table 1. Samples from the concrete in Esbjerg harbour are also included, see below.

The variation between the concretes is surprisingly small when the desorption isotherms are expressed in terms of degree of capillary saturation. The differences coincide rather well with what would be expected from Figure 4. OPC concretes with a high w/C have somewhat lower S_{cap} than HPC.

Moisture flow coefficients

The steady-state moisture flow coefficients were determined in experiments using an "upside-down cup". 18 mm thick specimens were placed as lids on a glass cup containing water. The cups were stored upside-down in a climate room at 85 % RH. Consequently, the top surface was exposed to 100 % RH (water) and the bottom surface to 85 % RH. After reaching steady-state conditions, the moisture flow was measured by determining the weight loss as a function of time. From the flow and the boundary conditions, the average moisture flow coefficient was calculated. The results are shown in Table 1 and 2.

For High Performance Concrete (HPC), with very low water-binder ratios and additions of silica fume or fly ash, the moisture transport coefficient may be very much lower, see Figure 9. In that figure the moisture transport coefficient is the average in an interval between 85% RH and complete saturation, i. e. the

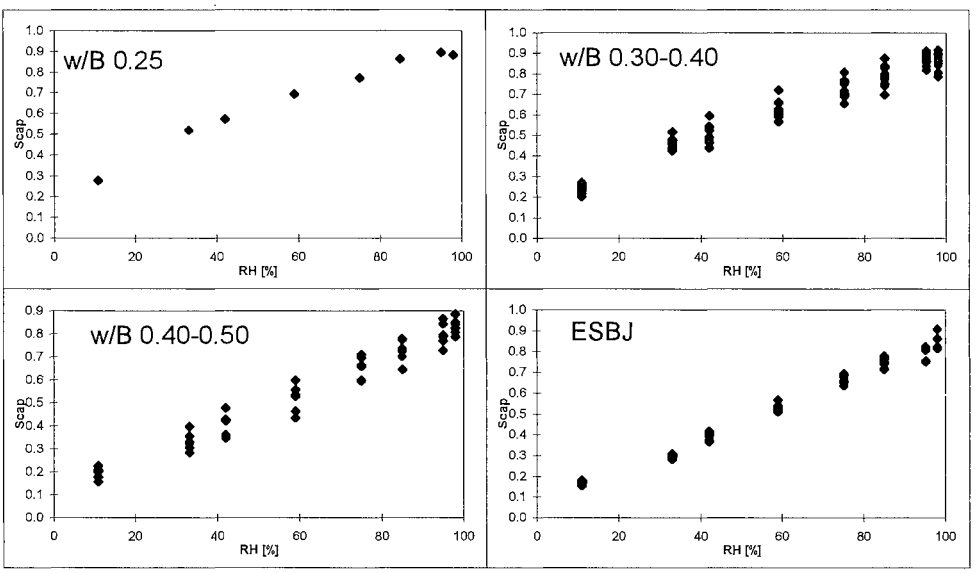

Fig. 8. Measured desorption isotherms for the concretes in Table 1.

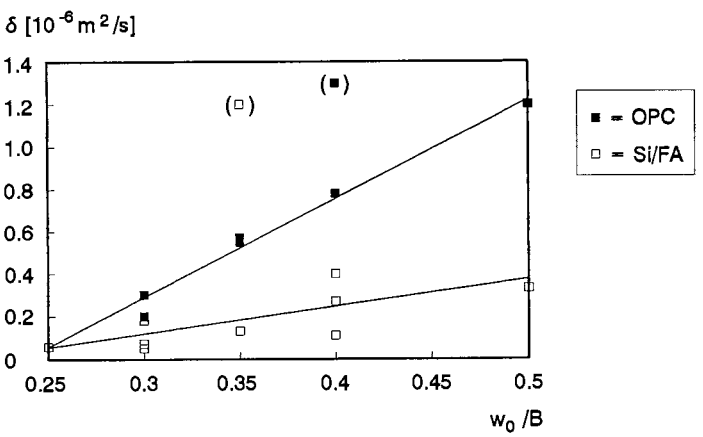

Fig. 9. The average moisture flow coefficients δ in the interval 85-100% RH for some HPCs with addition of silica fume and fly ash.

flow involves a large proportion of liquid flow. Additives seem to change the average moisture transport coefficient δ by a factor of 1/3. Decreasing the water-cement ratio has a significant effect. A factor of 1/10 to 1/20 is found when going from w_0/C=0.5 to 0.25.

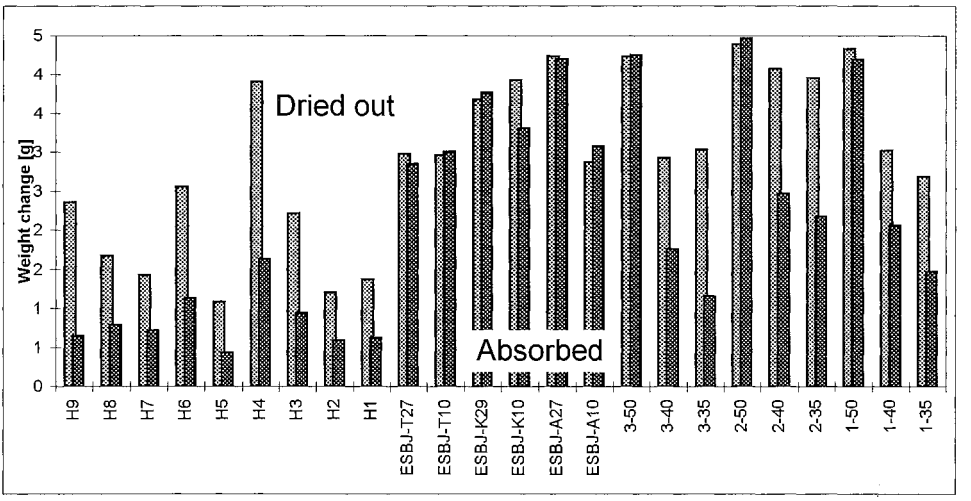

Fig 10. The amount of moisture absorbed during 12 days of capillary suction into 18 mm thick specimens of various concretes, cf. Table 1. The amount of moisture dried out of the saturated specimens before the test is shown for comparison.

Water absorption

A capillary suction test was done on all the concretes in Table 1. 18 mm slices were dried in 85 % RH until equilibrium. The circumference was sealed and the top surface was covered with a plastic bag. The specimens were then placed with the bottom surface in contact with water and the increase in weight was regularly determined.

The amount of moisture absorbed by the denser concretes was extremely small and consequently the suction test was very difficult to perform with a good accuracy. The amount of absorbed water after 12 days is compared to the water dried out before the test in Figure 10. Obviously, 12 days are far too short a time for capillary suction through 18 mm of high performance concrete. The concretes with a water-cement ratio of 0.5, however, have absorbed an equal amount of moisture as was dried out before the test.

Field exposure

Concrete specimens were cast in the Building Technology laboratories of the Swedish Testing and Research Institute (SP) in Borås. Specimens 1.0x0.6x0.1m were cast lying down. The penetration depth is referred to as the distance from the bottom surface in the mould. Some of the specimens were containing tubes or cast-in probes for in situ measurements.

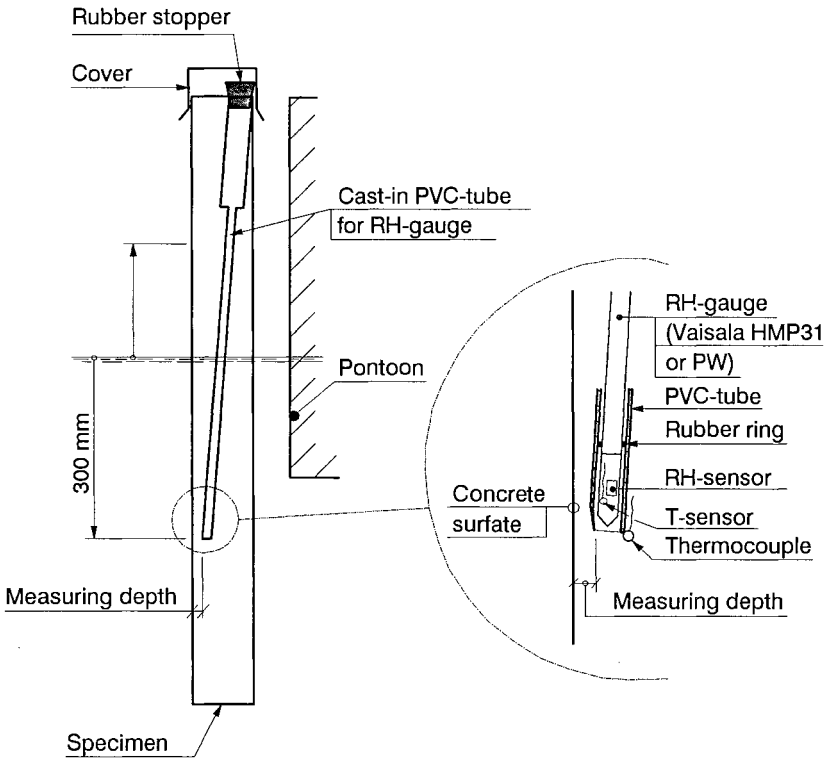

***Fig. 11**. A concrete slab attached vertically to the pontoon and submerged 0.6 m below the water table. Cast-in tubes for in situ measurement of RH.*

After a curing period the specimens were exposed to sea water at the SP field station in Träslövsläge some 100 km south of Göteborg at the west coast of Sweden. The specimens were exposed in such a way that 0.6 m of them was submerged into the sea water at a pontoon floating in the harbour of Träslövsläge. The 0.4 m above sea level are simulating a kind of a splash zone. However, since the pontoon is floating and positioned inside the harbour, the upper part is not frequently wetted by sea water. Driving rain, however, may hit the surface now and then. The climate is continuously registered by SP. Today (1996) most of the specimens have been exposed for some three and a half year.

The concrete qualities in the specimens are several, from plain OPC concretes with water-cement ratios 0.4-0.7, with and without air entrainment, to high performance concretes with a sulphate resistant low alkali cement sometimes blended with silica fume and fly ash to water-binder ratios down to 0.25. The concrete compositions are shown in Table 1.

A specimen, with cast-in tubes for in situ measurement of RH, attached to the pontoon is shown in Figure 11.

Methods of measuring moisture profiles

Attempts to measure moisture profiles in situ have been done in three different ways. Tubes have been cast in the specimens for later insertion of two kinds of RH-probes; the Vaisala probe and the PW-probe.

At some occasions a vertical slice of the specimens has been cut off. From that slice cores through the 0.1 m thick slice have been drilled out at different levels. From the cores samples have been taken to measure RH and degree of capillary saturation (S_{cap}).

RH in situ by Vaisala-probes

Vaisala-probes contain a capacitive sensor with a polymeric material as the moisture sensitive element. The changes in RH in the air surrounding the sensor material changes the moisture content of the sensor material. These changes of the moisture content, changes the capacitance of the sensor material, which is measured.

The cast-in plastic tubes for the Vaisala-probe are shown in Fig. 11. The bottom of the tube was sealed against the fresh concrete with a surgical tape that permits moisture to penetrate. A thermocouple was cast in close to the end of the tube to measure the temperature of the concrete. The Vaisala probe includes a temperature sensor. From those two sensors a possible temperature difference between the concrete material and the RH-sensor can be detected.

The top of the plastic tube is sealed with a rubber stopper. The top of the specimen, and the rubber stopper, is covered with a steel plate to protect the tube from sea water and rain.

A measurement is done by removing the rubber stopper, insert a Vaisala RH-probe and wait for equilibrium to be obtained. In the measurements done here some 4-6 hours were used. The reading from the sensor is translated into RH by a calibration curve, individual for each probe.

The results obtained from the measurements by the Vaisala-probes were obviously not correct. The RH:s were very low and had a large, inconsistent variation with depth. The probable explanation is a too short a period to obtain equilibrium between the sensor and the concrete since the concrete surface in "vapour contact" with the sensor is extremely small and the concrete qualities used are very dense and evaporates moisture to the sensor very slowly.

The results from the Vaisala measurements is not further discussed. A much longer equilibration time is needed.

RH in situ by PW-probes

PW-probes have a sensor made of a woven synthetic tube containing two wires that act as electrodes. A particular salt solution is impregnated into the woven tube when the sensor is assembled at the start of the measurement. An assembled PW-sensor is only some 10x15 mm. It is placed in a plastic tube and connected to an instrument by two wires during measurements.

Some of the water in the salt solution in the sensor is evaporated and absorbed by the concrete surface at the bottom of the plastic tube. Eventually, usually after a few days, the water content of the sensor is in equilibrium with the RH of this small concrete surface at a defined depth.

The conductance between the two electrodes in the sensor is then measured. Since the probe is continuously present in the plastic tube, and close to the concrete surface at the end of the tube, continuous equilibrium between the sensor and the concrete is expected. Consequently the measurement is done within a few minutes.

A reference probe continuously placed above a small container with a saturated salt solution (KCl) giving 85 % RH is also placed in a similar plastic tube in each specimen. The reading from each sensor is divided by the reading from the reference sensor, which has a temperature very close to the other sensors. The quotient is translated into an RH-value by a calibration curve valid for all PW-sensors. In this way the temperature effects on conductance measurements are heavily reduced.

The cast-in plastic tubes for the PW-probe are similar to the tubes for the Vaisala-probes, see Figure 11. The bottom of the tubes ends at four depths from the exposed surface, 20, 30, 40 and 50 mm.

RH on samples

Cores taken from the specimen through the whole thickness were sealed and brought to the laboratory. The cores were split length-wise in four sections. Two of those sections were used for taking samples to measure RH. Samples were taken using hammer and chisel from the inner parts of the sections to avoid parts that could have absorbed drilling water. Each sample was put in a test tube that were sealed by a rubber stopper. Samples were taken from several depths from the exposed surfaces.

The RH of a sample was measured by inserting a Vaisala RH-probe into the test tube and seal the gap between the test tube and the probe with an expandable rubber ring, see Figure 12.

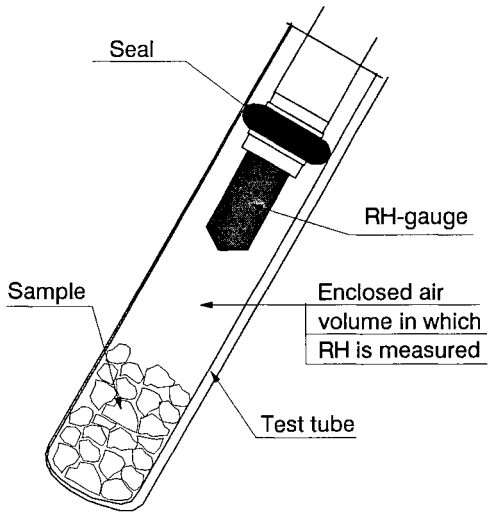

Fig. 12. *The method of measuring RH of a sample in a test tube using a Vaisala RH-probe with an expandable rubber ring, Nilsson (1980).*

The reading from the sensor is stable after some hours, depending on the concrete quality and a few other parameters. Usually the reading is taken after 8 hours. The reading is translated to RH by a calibration curve that is individual for each RH-probe and taken every other month or so.

S_{cap} on samples

The two remaining sections of the cores from the specimens were used to take samples for determining the degree of capillary saturation, S_{cap}. The samples were somewhat larger than the samples taken for the RH-measurements, but not too large too obtain a certain resolution with depth.

The original weight m_0 of each sample was carefully determined. One side of the sample were then put in contact with free water and evaporation from the other side was prevented. When the sample was saturated with water the wet weight m_{wet} was determined. The condition of saturation was usually obtained after some days and visible as a darkening of the upper side of the sample. For the samples of high performance concrete a very long time was needed to reach a "constant" weight gain. This procedure needs more investigation for high performance concrete to ensure a saturated condition.

Finally the samples were dried in an oven at +105 °C and the dry weight m_{dry} was determined. From those three weights the degree of capillary saturation is calculated as

$$S_{cap} = \frac{m_0 - m_{dry}}{m_{wet} - m_{dry}}$$

The advantage of the degree of capillary saturation is that the possible lack of representativity of a small sample from a concrete containing large aggregate is excluded.

Measured moisture profiles

A few examples of measured profiles are shown here. For complete information on all results are given in Nilsson et al (1994-95).

RH in situ

Only the in situ measurements with the PW-probes were successful. Measurements were done on three slabs. The variations were small between different depths and different exposure times (within a nine month period), only some + 2-3 % RH. Since the first measuring depth was 20 mm almost only self-desiccation was visible in the moisture profiles. In slab 3, however, an indication of a penetration depth of 20-25 mm is found, see Figure 13.

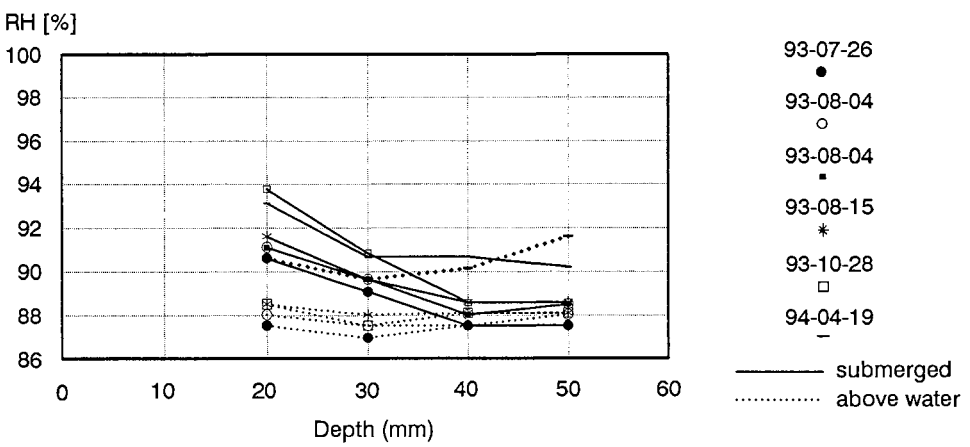

Fig. 13. RH measured in situ with PW-probes on slab 3 July/August 1993, October 1993 and April 1994.

RH on samples

The RH was measured on two core sections and throughout the whole thickness of the slabs. An example is shown in Figure 14. Since no significant difference was visible between the two core sections and the two opposite parts of the slab, all the results are shown as a function of the depth from one of the two exposed surfaces.

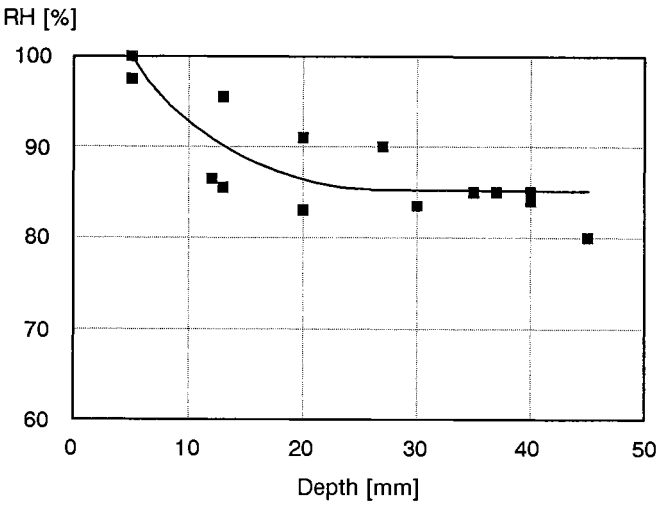

***Fig. 14**. Moisture profiles from samples as RH after two years of exposure in sea water. Slab H4, Degerhamn cement with 5 % silica fume, water-binder ratio 0.40.*

The results show a larger variation, + 5 % RH in the central part of the slab, than usually expected from measurements on samples. A variation larger than + 1 % RH is normally not satisfactory. Compared to the in situ measurements with the PW-probes, the variation when taking samples is much higher. The explanation for this has not yet been found, but it is obvious that improvement is essential.

In the example in Figure 14 a penetration depth of some 20-30 mm can be estimated.

S_{cap} on samples

The degree of capillary saturation, cf. Figure 15, has a somewhat smaller variation, some $\pm$ 2-3 %. In some cases the S_{cap} is far from 1.0 also very close to the surface. This is strange and should be further analysed. The method of removing "loose" water at the surfaces of the samples after saturation must be carefully performed, especially on small samples. This could be one explanation.

General observations

In spite of the somewhat large variations, a few general trends were obvious from the results:

- w/C = 0.75: more or less complete saturation after a year in the submerged zone; around 95 % RH and S_{cap}=0.8 some 0.3 m above sea level.

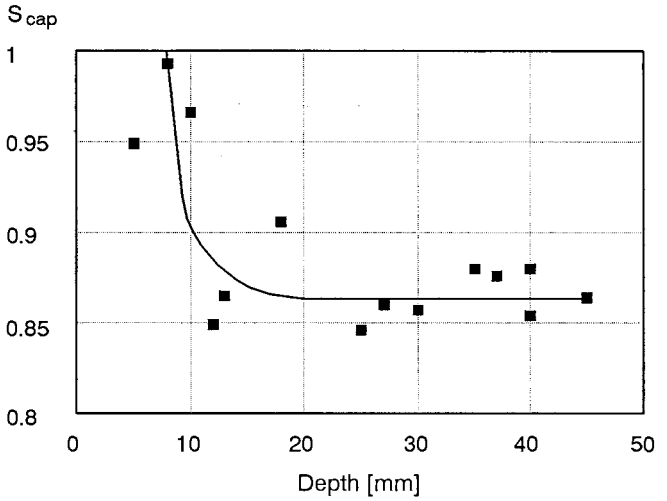

Fig. 15. Moisture profiles from samples as S_{cap} after two years of exposure in sea water. Slab H4, Degerhamn cement with 5 % silica fume, water-binder ratio 0.40.

- w/C = 0.75: more or less complete saturation after a year in the submerged zone; around 95 % RH and S_{cap}=0.8 some 0.3 m above sea level.
- w/C = 0.50: saturated surface, and close to complete saturation in the centre, after a year.
- w/C = 0.40 or lower: less than 20 mm depth of penetration in the submerged zone; beneath that only self-desiccation.
- In most cases the measured RH and S_{cap} in the exposed specimens do not fit the desorption isotherm measured on unexposed cores. The measured point lies clearly above the desorption isotherm. A possible explanation is the differences in age in the two cases, but this point needs further studies.

Marine structures

Moisture profiles have been measured in a few structures with different ages and different concretes. Cores were taken at different levels above and below sea level. The cores were split length-wise and samples taken from the central parts at different depths from the surface. Small samples were used for measuring RH and larger samples were used for determining S_{cap}.

Öland Bridge

The Öland Bridge in the Baltic Sea, at the east coast of Sweden, was recently repaired using an SRPC concrete with w/C = 0.40 as a thick shell around the old columns. After four years of exposure, cores were taken for moisture profile

measurements. The measured RH was 60-70 %, also below sea level, and S_{cap} was 0.85-0.90 in the submerged zone and 0.75-0.80 in the splash zone, with very little variations with depth. These values were surprisingly low and errors in the measurements were suspected.

Esbjerg Harbour

A 36 year old quay in Esbjerg harbour, at the west coast of Jutland in Denmark, was studied in the same way. Cores were taken below, at and above sea level from a 0.28 m thick, vertical slab of a concrete with w/C = 0.60, according to available information. The concrete, however, was very dense and had a strength of some 90 MPa!

The cores were stored in sealed bags for a couple of months before the measurements were done. RH and S_{cap} were measured in the same way as before. All the results are given in Nilsson et al (1994-95).

The 36 year old, continuously submerged concrete was saturated only to a depth smaller than 30 mm! Beneath that RH was around 80 % and S_{cap} was 0.75-0.80.

Once again the values were surprisingly low and the long storage before the measurements were done, was suspected as the cause of drying of the cores.

Vejlefjord Bridge

The 18 year old Vejlefjord Bridge, at the east coast of Jutland, was constructed with slag cement concrete in the submerged zone and up to 2 m above sea level and OPC concrete above that. Cores were taken and RH and S_{cap} were measured in the same way as before. This time, however, the samples for moisture measurements were taken from the cores on site and the weight was determined immediately before any drying could occur. The results are shown in Figure 16.

RH was close to 100 % at the surface in the submerged zone, but at depths larger than 20 mm the concrete was certainly not saturated. RH was around 85 % and S_{cap} was 0.85-0.90 at depths from 40 to 270 mm in the submerged zone.

In the splash zone, and 2 m above sea level, RH was below 80 % at all depths.

Discussion and conclusions

The moisture conditions in marine concrete structures are obviously not easy to predict. The sorption isotherms of exposed concrete seem to be different from unexposed ones. Knowledge on moisture flow properties is lacking to a large extent. Concrete submerged in sea water for 36 years is not saturated more than some 30 mm! The samples for measuring degree of capillary saturation, however, easily absorb tap water to reach capillary saturation in the laboratory.

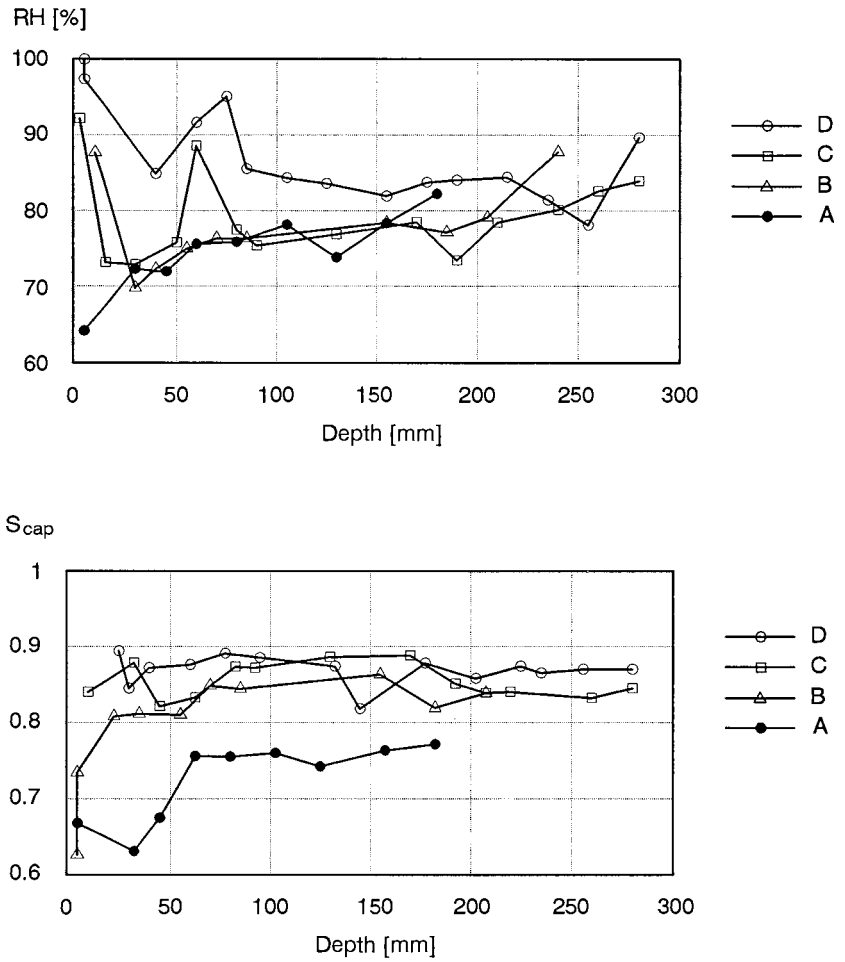

Fig. 16. *Measured moisture profiles in the 18 year old Vejlefjord Bridge. RH (top) and S_{cap} (bottom) in the submerged zone(D), the splash zone (C) and 2 m above sea level (B in slag concrete below a casting joint and A in OPC concrete above the joint), Andersen (1996).*

Whether the original concrete surface absorbs tap water or not has not yet been tested.

Well known moisture mechanics for indoor concrete does not seem to be applicable for structures exposed to sea water. It is obvious that further study is required.

References

Andersen, A. (1996) Moisture and chloride profiles in a column in the Vejlefjord Bridge after 18 years of exposure to marine environment. Work report May 1996, Department of Building Materials, Chalmers University of Technology, Göteborg.

Atlassi, E., Nilsson, L.-O. & Xu, A. (1989) Moisture sorption properties of concrete with admixtures and industrial by-products - implications for durability. BFR Document D9:1989, Svensk Byggtjänst, Stockholm.

Fagerlund, G. (1982) Fuktmekaniska egenskaper (Moisture properties). Chapter 8.6 in Betonghandboken. Material (Concrete Hand Book), 2nd edition, Svensk Byggtjänst, Stockholm.

Fagerlund, G. (1993) The long time water absorption in the air pore structure of concrete. Building Materials, Lund Institute of Technology. Report TVBM-3051, Lund.

Hedenblad, G. (1993) Moisture permeability of mature concrete, cement mortar and cement paste. Report TVBM-1014, Building Materials. Lund Institute of Technology, Lund.

Hedenblad, G. & Nilsson, L.-O. (198x) Degree of capillary saturation - A tool for accurate determination of the moisture content in concrete. TVBM-7005, Division of Building Materials, Lund Institute of Technology, Lund.

Nilsson, L.-O. (1980) Hygroscopic moisture in concrete - drying, measure-ments and related material properties. TVBM-1003, Division of Building Materials, Lund Institute of Technology, Lund.

Nilsson, L.-O. (1994) The relation between the composition, moisture transport and durability of conventional and new concretes - Concrete composition, moisture and durability. Contech '94, Int RILEM Workshop on Technology Transfer of the New Trends in Concrete, 7-9 November 1994, Barcelona, Spain.

Nilsson, L.-O. & Aavik, J. (1993) Moisture measurement in concrete slabs with PW-probes during construction - an evaluation of a new equipment and methodology (in Swedish). Publication P-93:5, Department of building materials, Chalmers University of Technology, Göteborg.

Nilsson, L.-O., Rodhe, M., Sahlén, S. & Roczak, W. (1994-95) Moisture distributions in marine concrete structures as a basis for service-life predictions. Parts 1-7. Working reports. Department of Building Materials, Chalmers University of Technology.

Norling-Mjörnell, K. (1994) Self-desiccation in Concrete. Licentiate thesis, Report P-94:2, Dept. of Building Materials, Chalmers University of Technology, Göteborg.

Powers, T. C. (1947) A discussion of cement hydration in relation to the curing of concrete, Highway Research Board.

Parrott, L. J., Killoh, D. C. & Patel, R. G. (1986) Cement hydration under partially saturated curing conditions, 8th Int Congr on Chem of cement, Rio de Janeiro.

Persson, B. (1992) Hydration, structure and strength of High Performance Concrete (in Swedish). Report TVBM-1009, Building Materials. Lund Institute of Technology, Lund.

TABLE 1. Materials

		Binder				Agg	Water	Air	Density		w/C	w/B	Moisture Flow	Properties
		Cement		Additives									δ	μ
Mix	Anl	Slite	Aalborg	Flyash	Silica			%	calc	meas			m^2/s	
H9	500.0					1831.9	150.0		2456.9		0.30	0.30	**2.0E-7**	**123**
H8	493.0			123.3		1628.6	184.9		2399.0		0.38	0.30	**7.1E-8**	**351**
H7	475.0				25.0	1822.8	150.0		2447.8		0.32	0.30	**7.2E-8**	**349**
H6	492.0			25.9		1799.9	155.4		2447.2		0.32	0.30	**1.8E-7**	**138**
H5	525.0				26.2	1811.6	137.8		2500.6		0.26	0.25	**5.6E-8**	**450**
H4	399.0				21.0	1684.8	168.0	6.0	2209.8	2202.0	0.42	0.40	**2.7E-7**	**92**
H3	492.0					1845.0	147.6		2460.0		0.30	0.30	**3.0E-7**	**82**
H2	450.0				50.0	1813.7	150.0		2438.7		0.33	0.30	**4.9E-8**	**511**
H1	475.0				25.0	1822.8	150.0		2447.8		0.32	0.30	**7.1E-8**	**352**
3-50	351.5				148.5	1353.9	250.0	6.0	1978.9		0.71	0.50	**3.3E-7**	**76**
3-40	399.0				94.0	1519.5	197.2	6.0	2135.8		0.49	0.40	**4.0E-7**	**62**
3-35	427.5				47.5	1633.6	166.3	6.0	2227.3	2263.0	0.39	0.35	**1.2E-6**	**21**
2-50		390.0				1646.2	195.0	6.0	2133.7		0.50	0.50	**1.2E-6**	**22**
2-40		420.0				1692.5	168.0	6.0	2217.5		0.40	0.40	**1.3E-6**	**19**
2-35		450.0				1695.1	157.5	6.0	2257.6		0.35	0.35	**5.7E-7**	**44**
12-35	382.5			45.0	22.5	1682.1	157.5	6.0	2244.6	2224.0	0.41	0.35	**1.3E-7**	**194**
10-40			345.0	59.0	16.0	1680.4	168.0	6.0	2205.4	2206.0	0.49	0.40	**1.1E-7**	**234**
1-50	370.0					1689.5	185.0	6.0	2152.0		0.50	0.50	**1.2E-6**	**21**
1-40	420.0					1692.5	168.0	6.0	2217.5		0.40	0.40	**7.8E-7**	**32**
1-35	450.0					1695.1	157.5	6.0	2257.6	2260.0	0.35	0.35	**5.5E-7**	**45**

TABLE 2. Measured moisture flow properties

Mix	Binder					Air	w/C	w/B		
	Cement			Additives					δ	μ
	Degerhamn	Slite	Aalborg	Fly ash	Silica	%			m^2/s	
w/C										
1-50	370					6.0	**0.50**	0.50	**1.2E-6**	**21**
1-40	420					6.0	**0.40**	0.40	**7.8E-7**	**32**
1-35	450					6.0	**0.35**	0.35	**5.5E-7**	**45**
2-50		390				6.0	**0.50**	0.50	**1.2E-6**	**22**
2-40		420				6.0	**0.40**	0.40	**1.3E-6**	**19**
2-35		450				6.0	**0.35**	0.35	**5.7E-7**	**44**
w/B										
H4	399				21.0	6.0	0.42	**0.40**	**2.7E-7**	**92**
H7	475				25.0		0.32	**0.30**	**7.2E-8**	**349**
H5	525				26.2		0.26	**0.25**	**5.6E-8**	**450**
Silica - w/B										
3-50	352				**148.5**	6.0	0.71	**0.50**	**3.3E-7**	**76**
3-40	399				**94.0**	6.0	0.49	**0.40**	**4.0E-7**	**62**
3-35	428				**47.5**	6.0	0.39	**0.35**	**1.2E-6**	**21**
Equal mix										
H1	475				25.0		0.32	0.30	**7.1E-8**	**352**
H7	475				25.0		0.32	0.30	**7.2E-8**	**349**
H3	492						0.30	0.30	**3.0E-7**	**82**
H9	500						0.30	0.30	**2.0E-7**	**123**
Fly ash										
H8	493			**123.3**			0.38	0.30	**7.1E-8**	**351**
H6	492			**25.9**			0.32	0.30	**1.8E-7**	**138**
H3	492			**0.0**			0.30	0.30	**3.0E-7**	**82**

Scaling Resistance of Concrete Field Exposure Tests

Per-Erik Petersson,
SP - Swedish National Testing and Research Institute
Box 857, S-501 15 BORÅS, Sweden

Summary

This paper presents results from field exposure tests to investigate scaling resistance. Concrete specimens were exposed to the marine environment in Träslövsläge on the Swedish west coast and to the environment close to the highway between Borås and Gothenburg. Large amounts of de-icing agents are used on this highway every winter.

Thirty-four different concrete qualities were used in the investigation, ranging from very poor (water/binder ratio=0.90, no entrained air) to very good scaling resistance (water/binder ratio=0.37, air content=6%). Three different Portland cement qualities were used and silica fume, or pulverised fly-ash, was added to some of the concrete mixes.

The scaling resistance at 28 days was determined using Swedish standard SS 13 72 44 for all the concrete qualities. After two to four years of field exposure the specimens were inspected visually and then tested again in the laboratory. The results for the aged specimens were compared with the results for the 28 days old specimens.

The following conclusions can be drawn from the test results:

- SS 13 72 44 is useful for classifying concrete intended for use in environments aggressive to concrete structures.
- The scaling resistance of concrete in a marine environment or in the environment close to a highway normally improves with age.
- The highway environment is much more aggressive than the marine environment, at least as far as scaling resistance is concerned.

Key words: *concrete, scaling resistance, field exposure testing*

Introduction

Knowledge about the scaling resistance of concrete is mainly based on experience. In Sweden, Portland cement has been used as binder in concrete for over a century, and we have had access to airentraining agents for more than 40 years. This has made it possible to gain experience on how "common" concrete functions under normal conditions in the Swedish climate. It is known that a sufficiently low water/binder ratio, a sufficiently high content of air and a good air pore structure normally produces concrete with good scaling resistance for the majority of areas of use. Testing methods have also been developed, e.g. SS 13 72 44 /2/, which make it possible to estimate the quality of concrete. However, it must be kept in mind that our knowledge is based on experience and not on basic knowledge of deterioration mechanisms. If we use other types of cement than Portland cement, other admixtures than pure air-entraining agents, very low water/binder ratios, etc., we often do not have sufficient experience and knowledge either of how a frostresistant concrete should be composed, or of how it should be tested. Better knowledge and more experience must be gained!

Rapid development takes place in the field of concrete technology. High performance concrete with low water/binder ratios and very high strengths are being produced. It is possible to produce concrete with extremely good casting characteristics. Surface treatment and impregnation affect the characteristics of the concrete. Fibres of steel, polymer and coal give tough concrete, etc. Full use of these products in real structures requires experience from exposure under actual conditions as a complement to the extensive laboratory experiments that have been carried out.

The Swedish tradition is to almost exclusively use Portland cement as the binder in concrete. In other countries, fly-ash, slag, silica fume and other additions are used to a great extent as a complement to Portland cement. Surface treatment products are also used in other countries to a much greater extent than in Sweden. These materials and applications, new to Sweden, can probably contribute to cheaper and perhaps also better constructions and possibly also to more environmentally friendly constructions. It is therefore of great importance that knowledge and experience be gained, for example in field exposure experiments, of how these products function under Swedish environmental conditions and with Swedish construction practices.

The aim of the work presented in this report was to gain experience of the scaling resistance of concrete from realistic exposure conditions and to calibrate results from field exposure tests with laboratory results obtained by the Swedish standardised freeze/thaw testing method SS 13 72 44. The paper gives the results of an extensive field exposure experiment in a marine environment that was car-

ried out in Träslövsläge, south of Varberg on the Swedish west coast, as well as the results of a smaller study performed in a road environment on national highway 40 between Borås and Gothenburg. More detailed information is presented in /1/.

Field exposure in a marine environment

Field exposure site in Träslövsläge

The field exposure stite consists of three approximately 20 meter long and three meter wide floating concrete pontoons. They are situated in Träslövsläge harbour about seven kilometres south of Varberg on the Swedish west coast. The pontoons are protected from direct wave forces by a pier, however, they are also exposed to salt spray when the waves hit the protective pier that separates the outer dock from the sea. The pier is located only a few meters beyond the pontoons.

Test panels of concrete, with the dimensions 100x800x1000 mm, were attached to the sides of the pontoons, so that half the height of the panels (500 mm) was over and half under the water line. The surface of the panel that was cast against the mould was turned outward and was usually used as the test surface. Because the pontoons float, the water line was always at half the panel height. The panels were mounted so that it was relatively simple to dismount them when they were to be tested after exposure.

Moreover, on the deck of the pontoons, specimens with the dimensions of 50x150x150 mm were placed with the sawn test surface (150x150 mm) turned upwards. After being aged for different times, the specimens were taken in for testing in the laboratory.

In many ways the climate on the Swedish west coast represents a very aggressive environment for concrete constructions, owing to salt and high humidity. As regards temperature, however, the climate is relatively mild, as the temperature seldom falls below -10° C. This is probably of great significance for the scaling resistance of concrete.

Concrete qualities

In the investigation, 34 concrete mixtures were tested, see Table 1. The mixtures ranged from concrete with an expected very poor scaling resistance (water/binder ratio=0.75, no air) to very good resistance (water/binder ratio=0.35, 6% air).

Three different types of Swedish Portland cement were used: Slite std, Degerhamn anl and Degerhamn 400. Compared with Slite std, Degerhamn anl is a low alkaline cement with an equivalent alkaline content of below 0.6%. The C_3A content is also low, and the cement can be considered sulphate-resistant. The Degerhamn cement also shows low heat development, making this type of cement generally suitable for use in large, compact constructions in environments aggressive towards concrete. This cement is, for example, used for all bridge constructions in Sweden. Degerhamn 400 is a finer-ground variant of the Degerhamn cement.

The fly-ash was added in the form of dry powder, together with the cement. The silica fume used was in the form of a slurry, which yields a good dispersion of the silica fume particles. The slurry was added with the first mixing water.

The aggregate used was a frost-resistant natural gravel, primarily gneiss, the largest particle size being 16 mm. The air-entraining agent was Cementa L14 (pine oil) except for the mixtures containing silica fume, in which Cementa 88L (Vinsol resin) was used. Cementa 92M (melamine) was used as plasticizer. The admixtures were added with the mixing water.

As can be seen in Table 1, the concrete qualities can be separated into two groups: "normal" concrete (1-35 to 8-75) and high performance concrete (H1 to H9). The normal concrete strengths are between 21 and 91 MPa, with slump values between 45 and 140 mm. The strength of the high performance concretes is higher (except for H4) and the consistency in all cases is fluid. Air-entrainment admixtures were used in only one of the nine high performance concrete qualities. In spite of this, the air content is often relatively high. One explanation may be that the plasticizer was used in high dosages for the high performance concrete qualities, which may have resulted in the high air content.

***Table 1**. Concrete qualities used for the field exposure tests in Träslövsläge on the Swedish west coast.*

Quality no.	Cement	Binder content	Silica fume	Fly ash	Water/ binder ratio	Admixtures[1)]	Air	Slump	Compr strength
		kg/m3	*%*	*%*			*%*	*mm*	*MPa*
1-35	Anl	450			0.35	AE+PL	6.0	105	68
1-40	Anl	420			0.40	AE+PL	6.2	125	57
1-50	Anl	370			0.50	AE	6.4	105	41
1-75	Anl	240			0.75	AE	6.1	100	21
2-35	Slite	450			0.35	AE+PL	5.7	135	60
2-40	Slite	420			0.40	AE+PL	6.2	125	55
2-50	Slite	390			0.50	AE	5.8	95	42
2-60	Slite	310			0.60	AE	6.3	100	35
2-75	Slite	250			0.75	AE	5.8	115	26
3-35	Anl	450	5[2)]		0.35	AE+PL	5.8	60	71
3-40	Anl	420	5		0.40	AE+PL	6.1	75	60
3-50	Anl	370	5		0.50	AE	6.0	80	45
3-75	Anl	245	5		0.75	AE	5.9	140	21
4-40	Anl	420	10		0.40	AE+PL	6.6	60	65
5-40	Anl	420	5		0.40	AE+PL	2.9	90	81
6-35	Anl	450	5		0.35	AE+PL	2.1	45	93
6-40	Anl	420	5		0.40	AE+PL	1.7	70	87
7-35	Anl	450			0.35	PL	2.4	55	91
7-40	Anl	420			0.40	PL	2.1	50	79
7-75	Anl	265			0.75	-	1.1	45	32
8-35	Slite	470			0.35	PL	2.1	85	73
8-40	Slite	440			0.40	PL	2.1	80	67
8-50	Slite	410			0.50	-	1.4	95	56
8-60	Slite	330			0.60	-	1.6	70	45
8-75	Slite	270			0.75	-	1.4	70	37
H1	Anl	500	5		0.30	PL	0.8	>265	112
H2	Anl	500	10		0.30	PL	1.1	145	117
H3	Anl	492			0.30	PL	3.6	>265	90
H4	Anl	420	5		0.40	AE+PL	5.9	180	56
H5	Anl	551	5		0.25	PL	1.3	>265	116
H6	Anl	518		5	0.30	PL	2.8	>265	90
H7	De400	500	5		0.30	PL	1.3	>265	114
H8	Anl	616		20	0.30	PL	3.0	>270	90
H9	De400	500			0.30	PL	2.9	210	99

1) AE=air entraining agent (Cementa 88L or Cementa L14), PL=plasticizer (Cementa 92M)
2) percent by weight of the total binder content

Manufacturing and curing of specimens

Concrete manufacturing

All mixtures were made in a 350-litre paddle mixer. The concrete was mixed for three minutes, after which tests were made of the consistency and air content.

Specimens for normal time testing

For testing the scaling resistance, 150-mm cubes were produced according to process IA in SS 13 72 44, second edition /2/. Directly after casting, the moulds were covered with plastic foil to prevent drying. The cubes were demoulded after 24 hours and then placed in water (20± 2° C), where they were stored for six days. They were then placed in a climate chamber with a temperature of 20± 2°C, a relative humidity of 50±5% and an air flow of <0.1 m/s.

After 21 days, 50-mm thick specimens were sawn from the cubes. The specimens were immediately placed in the climate chamber, where they were stored for another seven days.

When the specimens were 26 days old, a rubber sheet was glued to the specimens on all sides except the test surface. The rubber sheet reached 20±1 mm over the test surface, according to the test set-up shown in Figure 1.

When the concrete was 28 days old, water was poured on to the test surface. This resaturation continued for three days, after which the water was replaced with 3% NaCl solution, and the freeze/thaw testing began.

Specimens for field testing

Specimens with the dimensions 50x150x150 mm were manufactured and cured for 28 days in the exact same way as for the normal time specimens, with the exception of the fact that no rubber sheet was glued to the surfaces. They were then placed at the field exposure site on the decks of the pontoons with the sawn test surface turned upwards.

When the specimens were taken in to the laboratory for testing after certain periods of exposure, they were stored in a climate chamber (20°C, 50% RH) for one week. During this time, rubber sheets were glued onto the sides of the specimens. They were then resaturated for three days, after which the freeze/thaw tests started.

Panels with the dimensions of 100x1000x800 mm were also manufactured for exposure at the test site. Directly after being cast, the specimens were covered with plastic foil. After 24 hours, the panels were removed from the moulds and again covered with plastic foil for another six days. The panels were then stored

in the laboratory until they were placed at the field exposure site when they were 28 days old.

After exposure periods, the panels were taken back to the laboratory and specimens with the dimensions of 50x100x100 mm were sawn from the panels. The specimens were then treated in the same way as the specimens for normal time testing.

Freeze/thaw testing

The freeze/thaw tests were carried out according to SS 13 72 44, version 2, procedure IA.

Before the start of the freeze/thaw testing, all the surfaces of the specimens except for the test surface were insulated with a 20±1 mm thick layer of celluar polystyrene according to Figure 1. A 3 mm thick layer of 3% NaCl solution was poured onto the freeze surface. To prevent evaporation during testing, polyethylene foil was stretched over the salt solution.

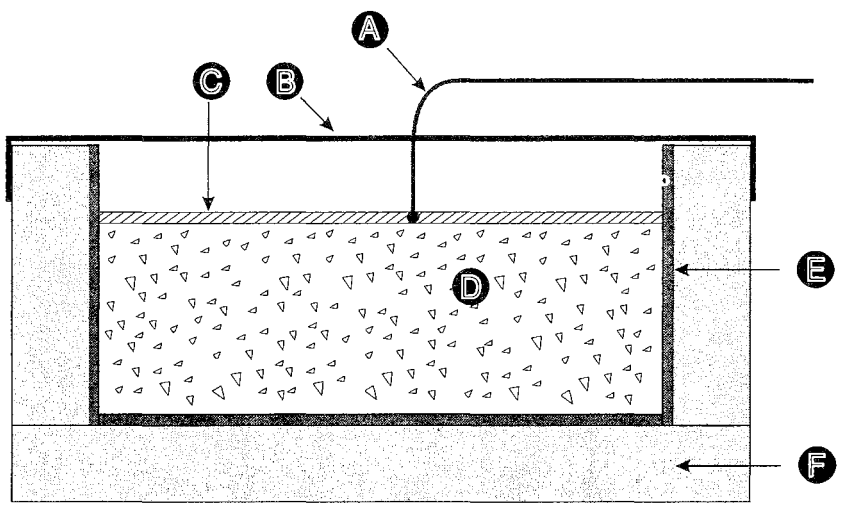

Fig. 1. Test set-up according to SS 13 72 44. A=temperature sensor, B=plastic sheet, C=salt solution, D=specimen, E=rubber sheet, F=heat insulation

The specimens were then exposed to repeated freezing and thawing between 18 and +20 °C. The time for each cycle was 24 hours. The temperature was continuously measured in the salt solution for one specimen in each freezer.

The material scaled from the test surface was collected after 7, 14, 28, 42 and 56 cycles and then dried at 105 °C and weighed. The results are given as the amount of scaled material per surface unit as a function of the number of freeze/thaw cycles.

Three or four specimens of each quality of concrete were tested.

Results of the normal time test

The results of the normal time tests are reported in Table 2.

In Table 2, the following observations can be made:

- The requirements for good or very good scaling resistance are fulfilled for all 12 concrete qualities having a water/binder ratio less than or equal to 0.5 and in which air-entraining agents have been used.

- Of the four air-entrained qualities having a water/binder ratio exceeding 0.5, none fulfill the requirement for acceptable scaling resistance.

- Of the 18 qualities in which no air entraining agent was used, 14 do not fulfill the requirement for acceptable scaling resistance. The four concretes without air and with acceptable scaling resistance, all have a water/binder ratio of 0.30 or lower. Moreover, three of these four qualities have a high natural content of air, about 3%.

- Only one quality with a low air content, 1.3%, fulfills the requirement for good scaling resistance. This quality, however, has a low water/binder ratio of 0.25.

The test method thus completely classified the qualities of concrete as could be expected. It can also be seen that the scaling resistance of the concretes were either judged to be very good/good or unacceptable, while no concrete was classified in the region of acceptable, between these levels. Consequently, a functioning test method must primarily differentiate between very good and very poor qualities, and these experiments show that the method used here does that. For the method to be useful, however, it is also necessary that the expected results agree with the results achieved in actual structures. Field experiments must be carried out to obtain answers.

Table 2. *Freeze/thaw test results (mean values) for normal time tests. Italicised figures are uncertain owing, for example, to leakage of salt solution during the test.*

Quality No.	Cement	Silica fume	Fly ash	Water/ binder	Air	Scaling (g/m²)					Rating[1]
		%	%		%	*7c*	*14c*	*28c*	*42c*	*56c*	
1-35	Anl			0.35	6.0	56	74	85	95	106	G
1-40	Anl			0.40	6.2	71	91	97	101	105	G
1-50	Anl			0.50	6.4	80	97	111	124	131	G
1-75	Anl			0.75	6.1	400	620	920	1080	1160	NA
2-35	Slite			0.35	5.7	20	27	40	50	56	VG
2-40	Slite			0.40	6.2	57	76	91	104	109	G
2-50	Slite			0.50	5.8	133	203	264	280	290	G
2-60	Slite			0.60	6.3	310	560	940	1160	1290	NA
2-75	Slite			0.75	5.8	700	1280	2090	2650	3090	NA
3-35	Anl	5		0.35	5.8	17	21	28	39	57	VG
3-40	Anl	5		0.40	6.1	9	14	16	19	21	VG
3-50	Anl	5		0.50	6.0	27	32	38	40	43	VG
3-75	Anl	5		0.75	5.9	420	603	880	995	1050	NA
4-40	Anl	10		0.40	6.6	18	22	27	31	38	VG
5-40	Anl	5		0.40	2.9	56	75	92	113	135	G
6-35	Anl	5		0.35	2.1	140	420	1240	2410	4520	NA
6-40	Anl	5		0.40	1.7	350	1020	2540	4510	7550	NA
7-35	Anl			0.35	2.4	210	600	1280	1870	2410	NA
7-40	Anl			0.40	2.1	850	2250	4710	6700	9450	NA
7-75	Anl			0.75	1.1	1910	4810	*12000*	SF[2]	SF	NA
8-35	Slite			0.35	2.1	320	880	1830	2660	3520	NA
8-40	Slite			0.40	2.1	1030	2360	4540	6840	9120	NA
8-50	Slite			0.50	1.4	2180	5070	*11000*	SF	SF	NA
8-60	Slite			0.60	1.6	2460	6790	16610	*33000*	SF	NA
8-75	Slite			0.75	1.4	2510	7130	*23000*	SF	SF	NA
H1	Anl	5		0.30	0.8	29	84	209	352	545	NA[3]
H2	Anl	10		0.30	1.1	43	83	405	923	1958	NA
H3	Anl			0.30	3.6	15	21	33	45	60	VG
H4	Anl	5		0.40	5.9	25	35	48	53	59	VG
H5	Anl	5		0.25	1.3	18	41	78	104	151	G
H6	Anl		5	0.30	2.8	18	29	41	60	77	VG
H7	De400	5		0.30	1.3	12	31	86	306	593	NA[3]
H8	Anl		20	0.30	3.0	25	38	55	88	152	NA[3]
H9	De400			0.30	2.9	14	20	28	42	69	VG

1) Rating of scaling resistance according to SS 13 72 44; VG=very good, G=good, A=acceptabel, NA= not acceptable 2) SF means that the specimen is totally disintegrated 3) Accelerated scaling (normally not acceptable according to SS 13 72 44

Results of the field tests

Specimens aged on the decks of the pontoons

For all qualities of concrete, specimens for freeze/thaw tests (50x150x150 mm) were manufactured according to the procedure described in SS 13 72 44. The specimens were treated as specimens for normal time testing until the 28th day after casting. Then, between December 1991 and February 1992, they were placed on the pontoons with the sawn test surface turned upwards.

After three years of exposure, the specimens were taken to the laboratory from December 1994 to March 1995 for freeze/thaw testing. The aim was to compare the results with the normal time tests in order to study effects of ageing. All "normal" concrete qualities, i.e. 1-35 to 8-75, were analysed in this way.

No visible freeze/thaw damage could be observed for any specimens on the exposure site, with the exception of those with a water/binder ratio of 0.75. The surfaces of these specimens were weakly etched and the edges showed damage. The specimens were weighed in air and in water, and the volume was determined and compared with corresponding values at an age of 28 days, i.e. before ageing. The reduction in volume did not exceed 1.5% for any specimen. Thus the damage was relatively limited, even in the case of high water/binder ratios.

The results of freeze/thaw testing of the aged specimens are shown in Table 3. It was found that the specimens made of concrete with water/binder ratios of 0.75 often leaked at relatively low scaling. This explains the gaps in the table. The values for the specimens that leaked are not representative and have not, of course, been considered in the analyses.

The results for the aged specimens show even more clearly than the normal time tests that there is a well-defined zone between good and poor qualities of concrete. All qualities but one were classified as having either very good or unacceptable scaling resistance. Only one concrete quality had good scaling resistance, while no quality was classified as having acceptable scaling resistance. It can again be pointed out that a good freeze/thaw test method must primarily be able to distinguish between very good and very poor concrete, as it seems to be rare that concrete qualities are classified in the zone between very good and poor scaling resistance.

In a comparison between the results of Tables 2 and 3, it is seen that aged specimens, almost without exception, showed better scaling resistance than those that were tested at 28 days! In this marine environment on the west cost of Sweden the concrete seems to have experienced positive ageing.

Table 3. *Freeze/thaw test results (mean values) for specimens aged on the decks of the pontoons for about four years at the field exposure site in Träslövsläge. Italicised figures are uncertain due, for example, to leakage of salt solution during the tests.*

Quality no.	Cement	Silica fume	Fly ash	Water/ binder	Air	Scaling (g/m^2)					Rating[1]
		%	%		%	7c	14c	28c	42c	56c	
1-35	Anl			0.35	6.0	6	10	12	14	18	VG
1-40	Anl			0.40	6.2	7	10	12	13	15	VG
1-50	Anl			0.50	6.4	10	14	18	20	23	VG
1-75	Anl			0.75	6.1	617	840	1052			NA
2-35	Slite			0.35	5.7	7	9	11	14	18	VG
2-40	Slite			0.40	6.2	7	10	13	15	17	VG
2-50	Slite			0.50	5.8	13	20	26	34	36	VG
2-60	Slite			0.60	6.3	37	63	140	183	214	G
2-75	Slite			0.75	5.8	268	*378*				?
3-35	Anl	5		0.35	5.8	4	8	12	14	16	VG
3-40	Anl	5		0.40	6.1	4	8	11	14	16	VG
3-50	Anl	5		0.50	6.0	7	12	16	19	23	VG
3-75	Anl	5		0.75	5.9	1030	1260	1580	1740	1880	NA
4-40	Anl	10		0.40	6.6	8	13	17	22	25	VG
5-40	Anl	5		0.40	2.9	6	10	14	18	27	VG
6-35	Anl	5		0.35	2.1	4	7	11	116	2050	NA
6-40	Anl	5		0.40	1.7	4	8	18	2730	SF[2]	NA
7-35	Anl			0.35	2.4	8	11	13	15	18	VG
7-40	Anl			0.40	2.1	8	12	15	18	23	VG
7-75	Anl			0.75	1.1	801	*1010*				NA
8-35	Slite			0.35	2.1	7	9	12	16	19	VG
8-40	Slite			0.40	2.1	6	9	14	17	20	VG
8-50	Slite			0.50	1.4	18	29	51	143	683	NA[3]
8-60	Slite			0.60	1.6	40	57	192	1944	8694	NA
8-75	Slite			0.75	1.4	418	*576*				?

1) Rating of scaling resistance according to SS 13 72 44;
VG=very good, G=good, A=acceptabel, NA= not acceptable
2) SF means that the specimen is totally disintegrated
3) Accelerated scaling (normally not acceptable according to SS 13 72 44

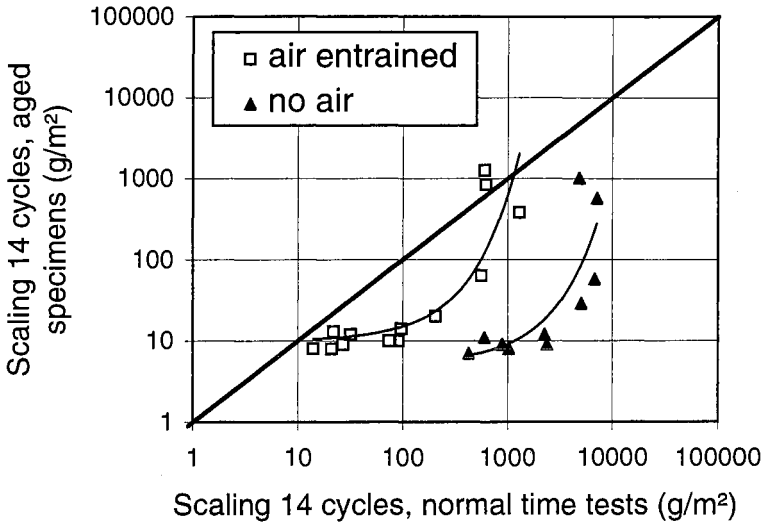

Fig. 2. Relation between test results for aged concrete and for concretetested at 28 days after 14 freeze/thaw cycles.

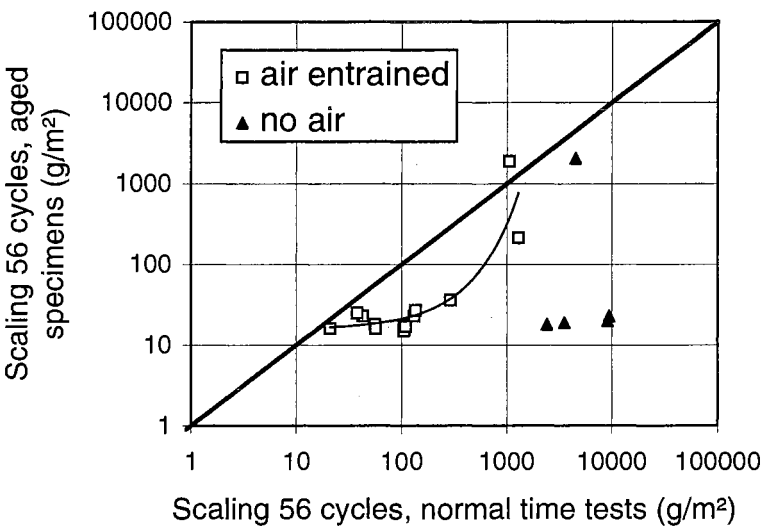

Fig. 3. Relation between test results for aged concrete and for concrete tested at 28 days after 56 freeze/thaw cycles.

Figures 2 and 3 compare scaling for aged specimens with results from the normal time tests. The two figures represent 14 and 56 freeze cycles, respectively. Almost all of the results lie to the right of the diagonal line, which means that scaling is lower for aged than for non-aged specimens.

As can be seen in the figures, it is possible to divide the qualities of concrete into two clearly identifiable groups: concrete with and without entrained air. The results show that the ageing effect is especially pronounced for the concretes in which no air entraining agent was used. It can also be seen that some of the aged concretes without entrained air showed low scaling even after 56 freeze cycles. This is discussed in greater detail below.

For the air-entrained concrete qualities, the scaling is often 10 times lower for aged than for non-aged specimens. The difference decreases with increasing scaling and, at a value of about 1 kg/m^2 after 56 cycles, there no longer seems to be any difference. This is important, as this value represents the limit between acceptable and unacceptable scaling resistance according to SS 13 72 44. For air-entrained concrete, the present acceptance limit for scaling-resistant concrete thus seems to be applicable to the marine environment of Sweden. For concrete with lower scaling, the method yields results on the safe side, i.e. the scaling in the case of normal time testing is higher than the corresponding results for aged specimens. For concrete without entrained air, scaling for aged concrete is often up to 100 times lower than the normal time values, and the difference does not seem to disappear until scaling after 56 freeze cycles exceeds about 10 kg/m^2. According to these results, SS 13 72 44 appears to underestimate the scaling resistance of concrete without entrained air, at least in the marine environment. There is, nevertheless, justification for having a high safety margin for concrete without entrained air until the degradation mechanisms and ageing effects of salt and frost have been completely clarified.

Figure 4 shows scaling as a function of water/binder ratio after different numbers of freeze cycles for the aged qualities of concrete 8-35 - 8-75, i.e. concrete without entrained air and with Slite std as binder. It is clear from the results that the concrete scales in freezing in an accelerated process when the water/binder ratio is 0.50 or higher. On the other hand, scaling is very small, even after 56 freeze/thaw cycles, when the water/binder ratio is equal to or less than 0.40. The low water/binder ratio together with the natural air (about 2%) seems to be sufficient to give good resistance. This indicates that it may be possible to produce concrete without entrained air that has good scaling resistance in the marine environment, providing that the water/binder ratio is sufficiently low.

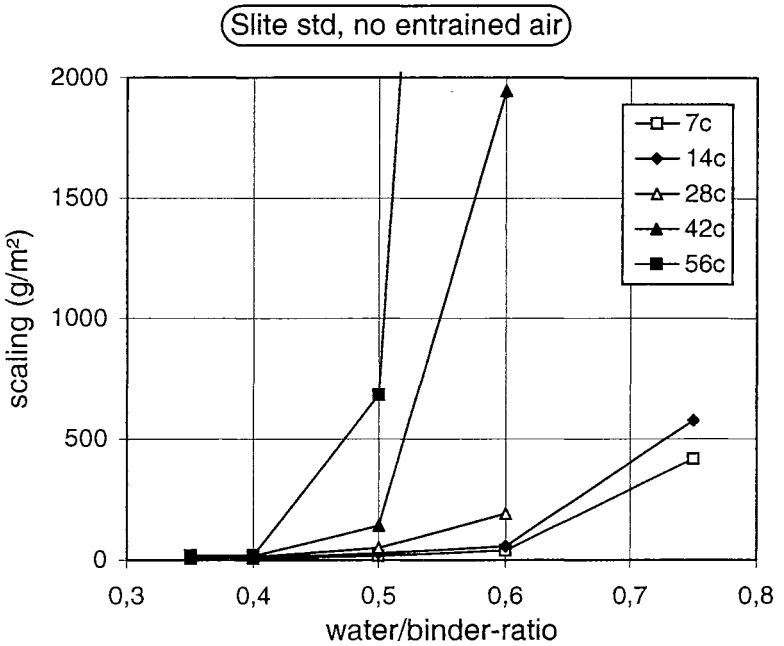

Fig. 4. *Scaling as function of the water/binder ratio and the number of freeze/thaw cycles for aged concrete without entrained air and Slite std as binder.*

Concrete with the cement Degerhamn anl without entrained air also has good scaling resistance when the water/binder ratio is 0.4 or lower, see Table 3. However, concrete with 5% silica fume addition (concret qualities 6-35 and 6-40) also seems to scale at low water/binder ratios. There is very little scaling for these concrete qualities until 28 or 42 cycles, after which it accelerates rapidly, and the concrete is completely disintegrated within only a few cycles. This is generally the same process as is reported in /3/ for concrete with silica fume. However, it is not possible to explain the reason why the concrete with silica fume disintegrates in freezing on the basis of the results of this investigation. It is indicated in /4/ that the reason might be alkali-silica reactions owing to the silica fume being insufficiently dispersed in the concrete. However, this cannot explain the course of events here, as the silica fume was added as a slurry and was therefore well dispersed in the concrete.

Scaling in concrete without entrained air or silica fume accelerates quickly for higher values of the water/binder ratio, as can be seen in the results for 8-50 and 8-60. To study how stable the scaling resistance is for lower values of water/binder ratio, the freezing experiments were continued for 112 cycles for two of the concrete qualities without entrained air, 7-35 (Degerhamn anl 0.35) and 8-

40 (Slite std 0.40). The results are given in Figure 5, together with the results for concrete with silica fume with low water/binder ratios.

It can be seen in Figure 5 that scaling also remains relatively small after 112 freeze/thaw cycles for concrete with Degerhamn anl or Slite std concrete as the binder. There is no rapid acceleration, as for concrete with silica fume, and, to judge by these results, the scaling resistance of concrete with OPC as the only binder seems to be stable.

Some experiments were performed with aged specimens to study the influence of the surface layer on ageing effects. For this purpose, a 5 mm

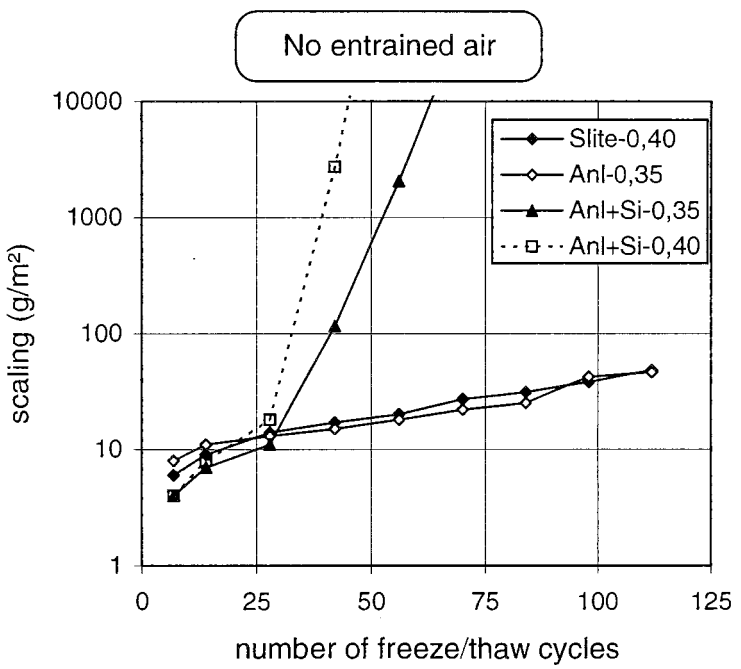

Fig. 5. *Scaling for concrete qualities with and without addition of silica fume as function of the number (up to 112) of freeze/thaw cycles.*

thick layer was sawn from the exposed surface. The specimens were then treated in a normal way, i.e. they were conditioned at +20¡C and RH=65% for seven days and then re-saturated for three days before the start of the freeze/thaw testing. The results are given in Table 4. Two specimens were included in each test series. The results for the specimens whose outer layer had been sawn away (Table 4) are compared with the results for the normally aged specimens (Table 3) in Figures 6 and 7.

It can be seen in Figure 6 that there is good agreement between the results for concrete with entrained air, at least in the case of low scaling. In the case of scaling of about 1 kg/m2, there is a tendency for the exposed outer layers to have somewhat poorer scaling resistance than the newly-sawn freeze surfaces.

However, Figure 7 shows that the scaling resistance for concrete without entrained air is poorer for the newly-sawn surfaces, at least in the case of low scaling. This implies that after ageing concrete without entrained air is protected by a thin layer that gives significantly improved scaling resistance in the marine environment in question in many cases.

Table 4. *Freeze/thaw test results (mean values) for specimens aged for four years on the decks of the pontoons after which a five mm thick layer was sawn from the exposed surfaces of the specimens before the start of the test. Italicised figures are uncertain owing, for example, to leakage of salt solution during the test.*

Quality no.	**Cement**	**Silica fume**	**Fly ash**	**Water/ binder**	**Air**	**Scaling (g/m²)**					**Rating[1)]**
		%	%		%	*7c*	*14c*	*28c*	*42c*	*56c*	
1-40	Anl			0.40	6.2	11	14	20	23	26	VG
1-75	Anl			0.75	6.1	100	261				?
2-40	Slite			0.40	6.2	11	13	19	26	31	VG
2-75	Slite			0.75	5.8	203	600				?
3-40	Anl	5		0.40	6.1	11	15	23	27	28	VG
3-75	Anl	5		0.75	5.9	121	225	435	670	1040	NA
4-40	Anl	10		0.40	6.6	15	21	28	36	40	VG
6-40	Anl	5		0.40	1.7	58	460	2255	6260	SF[2]	NA
7-40	Anl			0.40	2.1	37	525	2595	4660	8090	NA
7-75	Anl			0.75	1.1	705	3860	SF			NA
8-40	Slite			0.40	2.1	29	60	217	520	990	NA[3]
8-75	Slite			0.75	1.4	2125	4880				NA

1) Rating of scaling resistance according to SS 13 72 44; VG=very good, G=good, A=acceptabel, NA= not acceptable 2) SF means that the specimen is totally disintegrated 3) Accelerated scaling (normally not acceptable according to SS 13 72 44)

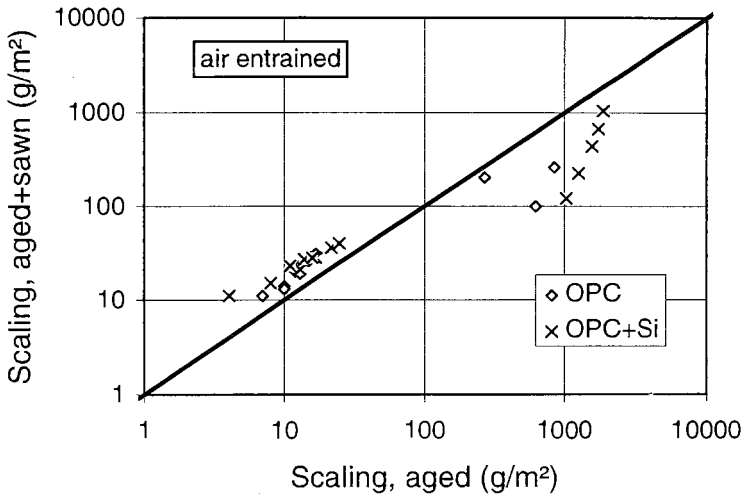

Fig. 6. The relation between the scaling resistance for aged specimens and aged specimens where a 5 mm thick layer is sawn from the test surface before testing. Air-entrained concrete.

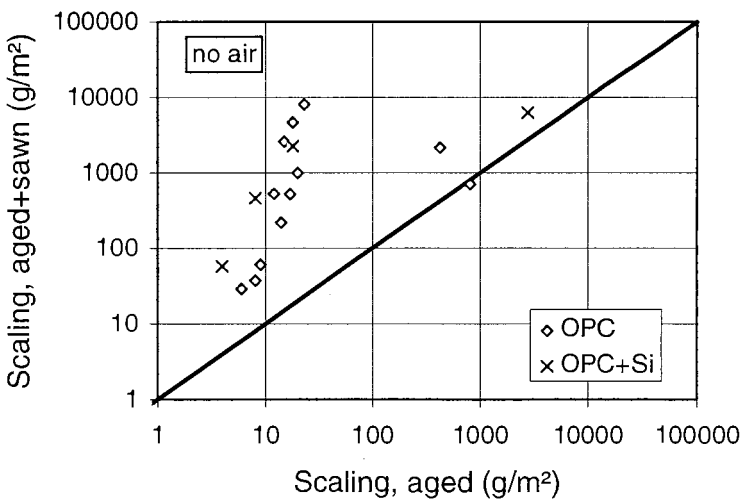

Fig. 7. The relation between the scaling resistance for aged specimens and aged specimens where a 5 mm thick layer is sawn from the test surface before testing. No air entraining agent was used.

Table 5 shows the water absorption during three days of re-saturating directly prior to the freeze/thaw testing for aged specimens and for aged specimens whose surfaces were sawn off. According to the test results, the water absorption is 2 - 3 times lower for the aged surfaces than for the corresponding surfaces whose outer layer were sawn off. Concrete with entrained air seems to tolerate an increased absorption, while concrete without entrained air does not. This explains why the scaling resistance is normally poorer for concrete without entrained air when the outer surface layer has been sawn off. It is not possible, however, on the basis of the results of this investigation, to explain why the surface is so much less water-permeable after ageing.

Table 5. *Water suction during the resaturation period directly before the freeze/thaw test. The results are relevant for aged specimens and also for aged specimens where a 5 mm thick layer is sawn off the test surface before the test.*

Quality No.	Cement	Silica fume	Fly ash	Water/ binder	Air	Water suction (g/m²)	
		%	%			*aged*	*aged+sawn*
1-40	Anl			0.40	6.2	132	327
1-75	Anl			0.75	6.1	633	1978
2-40	Slite			0.40	6.2	104	227
2-75	Slite			0.75	5.8	831	1635
3-40	Anl	5		0.40	6.1	97	260
3-75	Anl	5		0.75	5.9	711	1404
4-40	Anl	10		0.40	6.6	127	292
6-40	Anl	5		0.40	1.7	64	140
7-40	Anl			0.40	2.1	142	248
7-75	Anl			0.75	1.1	591	2044
8-40	Slite			0.40	2.1	92	135
8-75	Slite			0.75	1.4	585	1400

Concrete panels aged on the sides of the pontoons

Between December 1991 and March 1992, concrete panels with dimensions of 100x800x1000 mm were placed on the sides of the pontoons so that half the panel was under and half the panel over the water line.

After about two years of exposure, the panels were brought to the laboratory of the Swedish National Testing and Research Institute in Borås for analysis. It should be noted that no frost damage had been observed up to this point in time on the panels in the field, except for concrete with a water/binder ratio of 0.75. On these, a small amount of damage was observed on the horizontal upper surfaces.

A 5 cm wide strip was sawn from one of the sides of the panels to eliminate any possible edge effects. A 100-mm wide strip was then sawn to be used for the tests. The strip was split so that 100-mm cubes were obtained. Some of these cubes were used for freeze/thaw testing.

The cubes used for freeze/thaw testing were divided in the middle, using a diamond saw, so that two specimens with the approximate dimensions of 50x100x100 mm were obtained. For one of the specimens, the cast surface was used as the test surface. This was the surface that was cast against the mould and which had been directly exposed to the sea water. For the other specimen, the sawn surface was used for testing. This was thus concrete from the inner portion of the panel, about 50 mm from the surface that had been exposed to sea water.

Specimens for freeze/thaw testing were taken either from the upper part of the panel, least 150 mm over the water line, or from the part of the panel that had been in the splash zone, i.e. $\pm$150 mm from the water line. Table 6 shows the designations of the specimens with respect to the part of the panel from which they had been taken.

Table 6. *Designation of specimens according to their location on the panel.*

	Over the waterline	In the **Sp**lash zone
Cast surface	Ov/Ca	Sp/Ca
Sawn surface	Ov/Sa	Sp/Sa

After sawing, the specimens were treated in the same way as specimens for normal time testing. This means that the specimens were dried for seven days and then resaturated for three days before the start of freeze/thaw testing.

The results are shown in Table 7. Two specimens were normally tested for each combination of concrete quality and location of the specimen, although in some cases only one specimen was tested.

The results for the sawn specimens can not, of course, be expected to be directly comparable with the results for the normal time tests on cast cubes. Production and storage until the 28th day were different. Moreover, sawnsurfaces were tested in some cases and cast surfaces in others, etc. It is, however, of interest to examine how well the predictions according to the normal time tests can be used for classifying the aged concrete in the panels.

Table 7. *Test results after 56 freeze/thaw cycles for specimens sawn from panels aged on the sides of the pontoons. Thedesignations of the specimens are given in Table 6.*

Quality No.	Cement	Silica fume	Fly ash	Water/ binder	Air	Scaling, 56 cycles (g/m²)				Normal time results[1]
		%	%		%	Ov/Ca	Ov/Sa	Sp/Ca	Sp/Sa	(g/m²)
1-50	Anl			0.50	6.4	80	60	540	55	131
2-40	Slite			0.40	6.2	65	45	110	50	109
3-40	Anl	5		0.40	6.1	55	60	860	60	21
3-50	Anl	5		0.50	6.0	80	60	1420	75	43
H1	Anl	5		0.30	0.8	9260	19360	170	14650	545
H2	Anl	10		0.30	1.1	12300	5250	210	15900	1958
H3	Anl			0.30	3.6	265	75	130	60	60
H4	Anl	5		0.40	5.9	95	65	155	55	59
H5	Anl	5		0.25	1.3	1660	5500	210	790	151
H8	Anl		20	0.30	3.0	285	220	940	240	152

1) Normal time results, 56 cycles, according to Table 2.

Scaling for the aged specimens was, without exception, low for the four "normal" qualities of concrete (1-50, 2-40, 3-40, 3-50), which agrees well with the normal time tests. Scaling is higher, however, for the wettest specimen surfaces, i.e. cast surfaces that were exposed to the splash zone (Sp/Ca). The effect is especially pronounced for mixtures with additions of silica fume, and for one of these, 3-50, scaling in the splash zone exceeds the limit for acceptable scaling resistance. The reason for the higher scaling in the splash zone is probably a higher moisture content owing to long-term capillary suction without the possibility of intermediate drying periods.

For the high performance qualities of concrete, scaling for cast surfaces in the splash zone is low or moderate. However, scaling for sawn surfaces and cast surfaces above the splash zone is high or even very high for some of the concrete qualities. This applies to H1, H2 and H5, all without entrained air and with silica fume. These surfaces seems to have suffered some form of negative ageing. This may have to do with the fact that all surfaces except for the cast surfaces in the splash zone were continuously or periodically exposed to drying, either as exposure to the air or as internal self-drying.

Scaling is low for H3, a concrete without silica fume addition and H4, a concrete with entrained air and silica fume addition. It should be noted, however, that the

concrete without silica fume has a high natural air content, 3.6%, which must certainly contribute to the low scaling. H8, which contains fly-ash, also shows relatively low scaling.

The normal time test according to SS 13 72 44 seems to classify the four "normal" concrete qualities satisfactorily, with some doubt in the case where silica fume was added. Moreover, the first four high performance concrete qualities in Table 7 were classified correctly, while the scaling resistance was overestimated for the fifth quality, H5. This is an extreme quality of concrete with a very low water/binder ratio of 0.25. The scaling resistance of H8, containing fly-ash, was somewhat underestimated, although the field specimens from the splash zone are very close to the limit for unacceptable scaling resistance, when tested on the cast surface.

Figure 8 plots all the freeze/thaw results for the high performance qualities of concrete against the air content. As can be seen in the figure, there is a clear correlation between air content and scaling resistance. The results indicate that a relatively low natural content of air of about 2% can yield scaling resistance for low values of the water/binder ratio.

Field exposure tests in an environment with de-icing salts

Field exposure site at Swedish national highway 40 (R40)

In a limited investigation, some qualities of concrete were exposed to an environment along a highway. The goal was primarily to calibrate the freeze/thaw test method SS 13 72 44 against results obtained under realistic exposure conditions.

The exposure site is located immediately outside the road area along national highway 40 (R40), west of Borås. Specimens with the dimensions of 50x150x150 mm were placed in rows in special rigs with ten specimens in each rig. The rigs were oriented in a direction alongside the road and were set into the roadbank so that the test surface was on a level with the surface of the road. As the entire width of the road is used for traffic along the test area, vehicles passed very close to the specimens, sometimes at a distance of only a few decimetres. The traffic intensity is high and there is intensive use in winter of de-icing agents. This environment can be therefore be considered to be very aggressive for concrete.

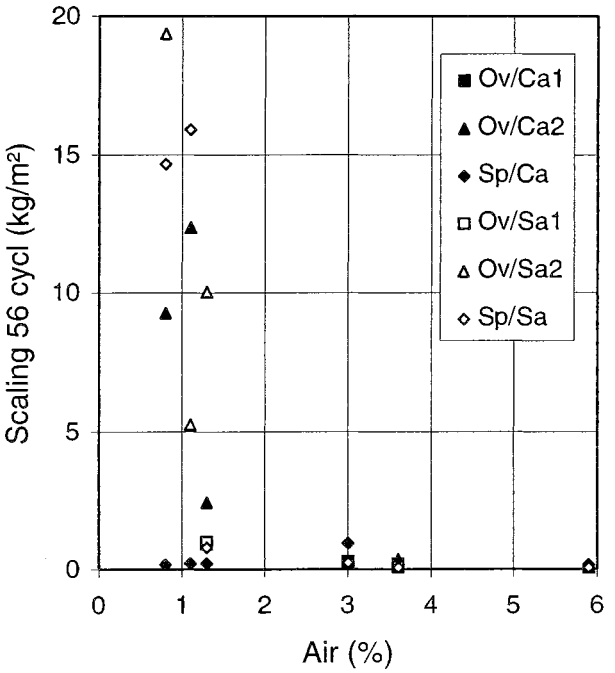

Fig. 8. *Scaling resistance after 56 cycles as function of air content for the high performance concrete qualities studied. The designations are given in Table 6.*

The Swedish Road Administration has a weather station located about 300 meters from the test area, which can be reached by telephone. Information is updated every 30 minutes. It was not possible to make continuous registrations, but the weather station was called three or four times each day and their observations were registered.

For the test period, autumn 1990 to spring 1993, observations were made according to Table 8. No temperature registrations were made during the 1993-1994 winter season. As the observations are relatively few, it is likely that the values in the table are somewhat underestimated. The number of "zero point passages" is relevant for the ground close to the road surface, and the lowest air temperatures were probably somewhat lower. The winters in question are considered relatively mild.

Table 8. *Climate observations at the exposure site close to R40 during the period from autumn -90 to spring -91.*

Period	Number of passages through 0°C	Lowest temperature (°C)
Nov 90-March 91	46	-10.1
Nov 91-March 92	68	-11.8
Nov 92-March 93	58	-13.3

Concrete qualities

A total of 15 concrete qualities were included in the investigation, as described in Table 9. The mixtures range from concrete with expected very poor scaling resistance (water/binder ratio=0.90, no entrained air) to very good scaling resistance (water/binder ratio=0.37, 6% entrained air).

Swedish ordinary Portland cement Degerhamn anl was used for all mixtures. As mentioned in section 2.2, this is a low alkaline, sulphate-resistant concrete with low heat development.

The air-entraining agent used is a neutralised Vinsol resin (C88L). In addition to the air-entraining agent, a water-reducing agent, a melamine (V33), was also used for mixtures with the water/binder ratio 0.37. The aggregate used was a natural material, primarily gneiss. The largest particle size was 16 mm.

Manufacturing and curing of specimens

All mixtures were made in a 350-litre paddle mixer. When an air-entraining agent was used, it was added with the mixing water. When a water reducing agent was used, it was added after the air-entraining agent, with the last mixing water. All batches were mixed for 180 seconds.

Specimens with the dimensions of 50x150x150 mm were manufactured according to the procedure described in section 2.3.2, specimens for normal time tests. Four specimens per concrete quality were used for the normal time test, while two specimens per quality were placed in the test area for field exposure about 28 days after casting.

Freeze/thaw testing

Normal time testing was carried out according to the methodology described in SS 13 72 44, procedure IA.

Results of normal time testing

The results of the normal time tests are reported in Table 10. The results generally agree with expected values and with the results presented in Table 2

Table 9. Concrete qualities used for the field exposure tests a the R40.

Quality No.	Cement content	W/C	Admix-tures	Air	Slump	Compr. strength
	kg/m³			*%*	*mm*	*MPa*
A-37	464	0.37	PL	2.1	80	77.2
A-45	426	0.45	-	1.9	80	65.2
A-60	302	0.63	-	1.7	80	39.8
A-75	278	0.74	-	1.2	85	29.3
A-90	219	0.93	-	1.1	80	16.2
B-37	458	0.37	PL+AE	3.8	80	74.9
B-45	398	0.45	AE	4.2	80	56.4
B-60	310	0.59	AE	4.0	80	36.0
B-75	255	0.72	AE	4.0	85	24.5
B-90	209	0.87	AE	4.0	80	16.4
C-37	449	0.37	PL+AE	5.9	80	70.7
C-45	404	0.44	AE	6.3	80	46.2
C-60	300	0.59	AE	6.3	80	32.3
C-75	240	0.74	AE	6.0	80	20.8
C-90	198	0.90	AE	6.1	80	13.0

1) AE=air entraining agent (C88L), PL=plasticizer (V33)

for normal time testing of concrete for Träslövsläge. The results for C-75 may be uncertain, owing to leakage during testing. This quality of concrete was, therefore, not considered in the continued analysis.

It is remarkable that scaling is so high for concrete with a water/binder ratio of 0.37 and 4% added air. Its scaling resistance is judged as even worse than that of concrete with the same air content and with a water/binder ratio of 0.45. One probable explanation is that the combination of air-entrainment agent and water-reducing agent, used only for the water/binder ratio 0.37, is unsuitable and gives an unsatisfactory air pore structure. A corresponding effect was reported in /5/.

Field exposure results

Two specimens of each quality were placed at the field exposure site in October 1990. The aim was to study the development of damage visually. The specimens were taken to the laboratory for examination after one year. A measurement was then made of the volume of each specimen by weighing it in air and in water. The specimens were then again placed at the test area. The same procedure was repeated after two and three years of exposure. Unfortunately, the experiment then had to be stopped, as the road was to be re-built and it was impossible to continue our work.

Table 10. *Scaling resistance results (mean values) for normal time tests of concrete used at the field exposure site at R40.*

Quality No.	W/C	Air	Scaling (g/m^2)					Ra-ting[1]
		%	7c	14c	28c	42c	56c	
A-37	0.37	2.1	1020	2450	5520	9310	11880	NA
A-45	0.45	1.9	1190	3320	7630	10630	12280	NA
A-60	0.63	1.7	1300	4050	10870	16740	19760	NA
A-75	0.74	1.2	2060	6490	15580	20160	SF[2]	NA
A-90	0.93	1.1	1610	4300	6890	10130	SF	NA
B-37	0.37	3.8	190	430	790	1080	1270	NA
B-45	0.45	4.2	50	70	90	100	110	G
B-60	0.59	4.0	200	440	790	1040	1130	NA
B-75	0.72	4.0	360	700	1210	1460	1600	NA
B-90	0.87	4.0	540	870	1200	1470	1580	NA
C-37	0.36	5.9	30	50	60	70	80	VG
C-45	0.44	6.3	20	30	40	50	60	VG
C-60	0.59	6.3	40	60	70	80	80	VG
C-75	0.74	6.0	250	360	*420*	*440*	*450*	(G)
C-90	0.90	6.1	470	720	940	1040	1130	NA

1) Rating of scaling resistance according to SS 13 72 44;
VG=very good, G=good, A=acceptabel, NA= not acceptable
2) SF means that the specimen is totally disintegrated
3) Accelerated scaling (normally not acceptable according to SS 13 72 44

The volume change after different exposure times proved to be an excellent measure of concrete scaling. Unfortunately, no determination of volume was made before the specimens were first placed at the test site and thus there are no values for the first winter's exposure. The results are shown in Table 11.

It can be seen in the table that the reductions in volume vary from very small, 0.1% after three years of exposure, to total disintegration of the specimens of the poorest qualities. As expected, frost damage was most severe for concrete without entrained air. When air was entrained, 4% and 6% air appears to give the same results.

In Träslövsläge on the Swedish west coast, no damage at all was observed after three years of exposure, with the exception of the poorest qualities. This shows that the road environment is much more aggressive than the marine environment on the Swedish west coast, at least with respect to freeze/thaw and scaling.

Table 11. *Volume change of the specimens after exposure during three winters at R40. Each value is the mean result from two specimens.*

Quality No.	W/C	Air	Volume change (%)			
		%	9110-9209	9209-9311	9311-9407	**1991-1994**
A-37	0.37	2.1	0	0	0.1	**0.1**
A-45	00.45	1.9	0.1	0.9	0.4	**1.4**
A-60	0.63	1.7	0.1	7.8	33.5	**41.4**
A-75	0.74	1.2	0.4.1	95.9	-	**100**
A-90	0.93	1.1	14.2	85.8	-	**100**
B-37	0.37	3.8	0	0	0.1	**0.1**
B-45	0.45	4.2	0	0	0.1	**0.1**
B-60	0.59	4.0	0.1	0.1	0.2	**0.4**
B-75	0.72	4.0	0.2	2.0	0.6	**2.8**
B-90	0.87	4.0	0.4	4.4	1.5	**6.3**
C-37	0.36	5.9	0	0	0.1	**0**
C-45	0.44	6.3	0.1	0	0.1	**0.2**
C-60	0.59	6.3	0	0.3	0.2	**0.5**
C-75	0.74	6.0	0.2	1.6	0.6	**2.4**
C-90	0.90	6.1	0.5	6.1	1.9	**8.5**

Figure 9 shows the volume reduction after exposure over three winters as a function of water/binder ratio and air content. The darker the colour, the stronger the scaling. Concrete with the water/binder ratio over 0.6 and without entrained air was completely disintegrated. Concrete with entrained air with a water/binder ratio of 0.9 also showed severe damage. Very good scaling resistance was achieved for concrete with entrained air when the watwr/binder was 0.45 or lower, which is in good agreement with present norms. It is also possible to achieve scaling-resistant concrete without air, according to the results in Figure 9, provided there is a low water/binder ratio, in this case 0.37. This is in good agreement with the results from the field tests in Träslövsläge.

Figure 10 shows the relationship between the results from the field exposure tests at R40 and the normal time tests according to SS 13 72 44. Two lines are marked in the figure. The vertical line at 1 kg/m^2 after 56 cycles corresponds to the limit for acceptable scaling resistance according to SS 13 72 44. The vertical line at a volume reduction of 1% corresponds to an example of a possible acceptance limit after three years of field exposure.

The figure shows that the four concrete qualities that fulfilled the requirement of 1 kg/m^2 in the normal time test also all fulfilled the requirement of 1% volume

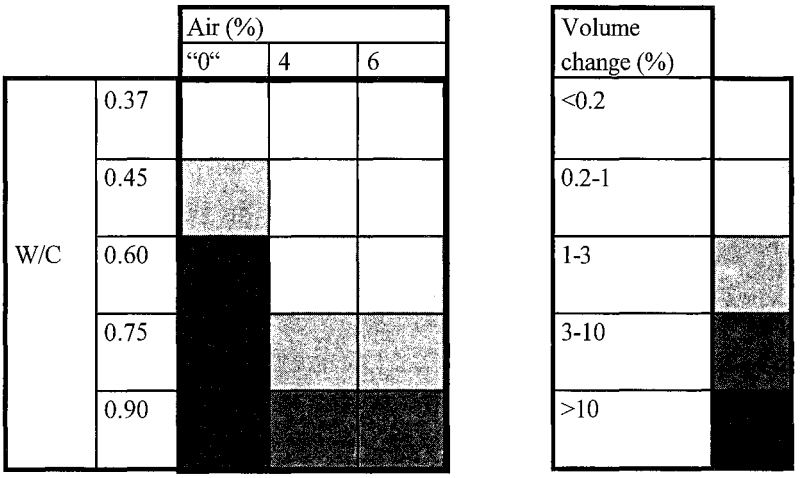

Figure 9. *Relation between air content, water/binder ratio and volume change for specimens exposed at the field exposure site at R40 for three winters.*

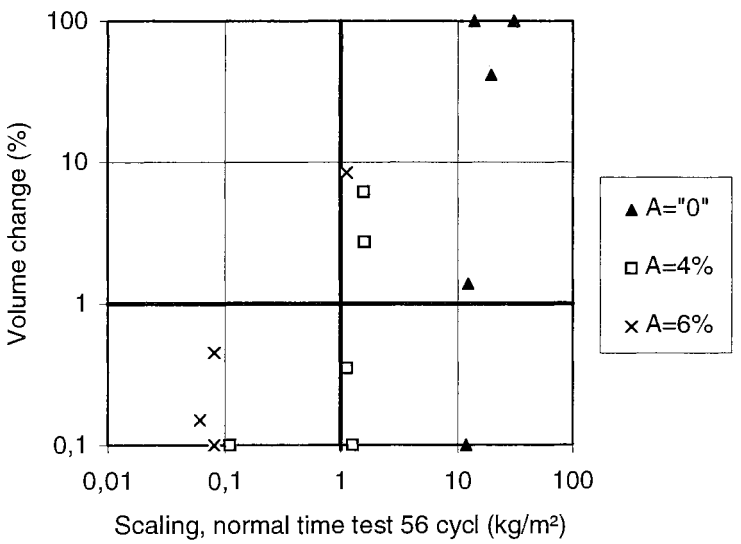

Fig. 10. *Volume change after three winters at the exposure site at R40 as function of results from normal time tests according to SS 13 72 44.*

change in the field exposure test. Moreover, there were two qualities, air content=4% with water/binder ratios of 0.37 and 0.6, that fulfilled the field exposure requirement and which were at the limit of the acceptable area for the normal time test. Of the other eight qualities that failed to fulfill the requirement for acceptable scaling resistance in the normal time test, seven also failed in the field exposure. The exception is the concrete without entrained air with a water/binder ratio of 0.37.

Test method SS 13 72 44 thus generally classified the qualities of concrete correctly in 13 of 14 cases. For concrete qualities that are normally used in environments aggressive towards concrete in Sweden, for which the method was primarily developed, i.e. concrete with entrained air and low water/binder ratio, the method classified all eight concrete qualities correctly. The results thus indicate that the method and the acceptance limits are suitable for testing concrete in an aggressive road environment, at least for high quality concrete with entrained air.

The results deviated for concrete without entrained air and with low water/binder ratio (0.37). The normal time test gave a great deal of scaling after 56 cycles, over 11 kg/m^2, while no damage at all occurred during the field exposure period! This observation agrees well with the results of the field exposure in the marine environment in Träslövsläge. Ageing had a positive effect, especially on concrete without entrained air, and when the water/binder ratio is less than 0.40 there were indications that concrete without entrained air also had considerable ability to tolerate freezing in environments aggressive towards concrete.

Concrete with low water/binder ratios (0.30-0.40) and no entrained air is not scaling-resistant in normal time tests, i.e. at an age of about one month. At that time, there is a high amount of freezable water in the capillary pores and without a functioning air pore system, the concrete disintegrates because of freezing. As the concrete ages, hydratation continues, and the volume of the capillary pores, and thus also the amount of freezable water, decreases. If the water/binder ratio is sufficiently low, the capillary pore volume becomes so small and the amount of water that can freeze so little that the concrete is protected from scaling even by a poor air-entrainment system, e.g. by the natural air that always exists in concrete. This is probably the explanation for the differences between the normal time tests and the field exposure tests for the quality of concrete without entrained air and with a water/binder ratio of 0.37. The effect may also be strengthened by other positive ageing effects.

There is also a significant difference between the normal time test and the results of the field exposure tests for the concrete with a water/binder ratio of 0.37 and

an air content of 4%. The result in the normal time test is also considerably poorer than the corresponding result for the concrete with the same air content but with a water/binder ratio of 0.45. This is probably explained by the fact that the concrete mixtures with a water/binder ratio of 0.37 always had an added water-reducing agent, which no other mixtures had. Investigations have shown that the combination of water reducing agents and air-entraining agents often leads to poor air-pore systems /5/. For the concrete with a water/binder ratio of 0.37 and 4% entrained air, there is obviously no protective air-pore system at the normal time test, although such a system is found in the concrete with a water/binder ratio of 0.45. This explains the differences in the normal time tests. With continued hydratation and ageing, the significance of a good air-pore system decreases at low water/binder ratios. For this reason, there are no demonstrable differences between water/binder ratio of 0.37 and water/binder ratio of 0.45 in the field exposure tests.

SS 13 72 44 thus normally underestimates the scaling resistance of concrete without entrained air and low water/binder ratios. In order to be able to fully exploit the potential of such qualities of concrete, the test methodology should be modified. It would probably be advantageous to carry out tests when the specimens are 56 days old or older, or perhaps more preferably, on test specimens that have been allowed to age outdoors for a number of months. The disadvantage is that the required testing time is extended, but it is difficult to see how this can be avoided. Concrete with low water/binder ratios is simply not "mature", from the viewpoint of scaling resistance, at an age of 28 days.

Large differences were seen in the normal time tests between concrete with 4% and 6% entrained air, except when the water/binder ratio was 0.37, and also when the water/binder ratio was 0.6 or higher. No corresponding difference was found in the field exposure tests. This supports the observations at Träslövsläge that indicate that the positive effects of ageing become clearer the poorer the quality of the air pore structure.

Conclusions

This paper gives the results of field experiments in which 34 qualities of concrete were exposed to a marine environment on the west coast of Sweden and in which 15 qualities of concrete were exposed to a de-iced road environment along Swedish national highway 40 between Borås and Göteborg. The conclusions from the investigation can be summarised in the following points:

- Normal time testing according to SS 13 72 44, procedure IA, classified the scaling resistance of the concrete correctly, i.e. in an expected way according to present experience.
- Concrete is often either good or very poor from the viewpoint of scaling resistance and is seldom classified in the classes between good or very poor. A functioning test method must thus primarily be able to distinguish between very good and very poor qualities. The experiments performed here show that SS 13 72 44 does so.
- No visible frost damage could be observed on any of the specimens after three years of exposure in a marine environment, except for specimens with a water/binder ratio of 0.75. These specimens showed surfaces that were weakly etched and edges with frost damage.
- For concrete qualities with entrained air, scaling is often up to ten times less in specimens aged in a marine environment than in specimens that were not aged at all. This difference decreases with increased scaling and, at values of about 1 kg/m^2 after 56 cycles, which is the limit for acceptable scaling resistance according to SS 13 72 44, there no longer seems to be any difference. The present acceptance limit thus seems adequate for concrete with entrained air in the marine environment in Sweden. For concrete with lower scaling, the method gives results that can be said to be on the safe side, i.e. the scaling in the normal time test is higher than the corresponding values for aged specimens.
- The results indicate that SS 13 72 44 underestimates the scaling resistance of concrete without entrained air that has been exposed to a marine environment. However, there is justification for a high safety margin for concrete without entrained air until the destruction mechanisms and ageing effects in the case of salt and frost damage are completely understood.
- For aged specimens without entrained air and with Portland cement as binder, scaling is very limited after 56 freeze/thaw cycles, when the water/binder ratio is 0.4 or lower. This indicates that it may be possible to produce concrete with good scaling resistance in the marine environment without the use of air-entrainment agents, providing that the water/binder ratio is sufficiently low.
- The results from the exposure of concrete to a highway environment indicate that SS 13 72 44 and its acceptance limits are adequate for classifying concrete for use in road environments aggressive towards concrete, at least for high quality concrete with entrained air.
- Ageing has a positive effect, especially on concrete without entrained air. When the water/binder ratio is less than 0.40, concrete without entrained air also seems to have a considerable ability to withstand freezing in an aggressive road environment.
- Many of the specimens exposed to the highway environment showed a great deal of damage after four seasons. This demonstrates that the environment of

a highway is significantly more aggressive than the marine environment of the west coast of Sweden, at least with respect to frost damage.

- Concrete manufactured according to present practices, i.e. with a water/binder ratio less than 0.45 and entrainement of 4-6% air, normally has good scaling resistance both in a marine environment and a road environment with de-icing agents.

References

1. *Petersson, P-E.* Scaling Resistance of Concrete - Field Exposure Tests. SP-Rapport 1995:73, Swedish National Testing and Research Institute, 1995.
2. *SS 13 72 44.* Concrete testing - Hardened concrete - Frost resistance. Swedish standard, second ed., 1988.
3. *Petersson, P-E.* The influence of silica fume on the salt frost resistance of concrete. SP-RAPP 1986:32, Swedish National Testing and Research Institute, 1986.
4. *Lagerblad, B and Utkin, P.* Silica granulates in concrete - dispersion and durability aspects. CBI-report 3:93, Swedish Cement and Concrete Research Institute, Stockholm, 1993.
5. *Petersson, P-E.* The use of air-entraining and plasticizing admixtures for producing concrete with good salt-frost resistance. SP-Report 1989:37. Swedish National Testing Institute, Borås, 1989.

Chloride Induced Corrosion in Marine Concrete Structures

Kyösti Tuutti, Skanska AB

Introduction

Corrosion of steel in concrete has been the main task in durability research activities world-wide the last decades. Thousands of reports have shown that chloride ions penetrate a normal uncracked concrete cover in a relative short period of time. However, high performance concrete could be an effective barrier for chloride ions, but such concrete has only been used the last decade for special applications. A normal situation is also that concrete structures are cracked. Such cracks will behave as channels for all type of chemicals in the surrounding environment. A question that must be answered is; could we expect a large number of collapse or maintenance activities for the major part of existing marine structures? The answer must be no; according to our experience that indicate a long service life for also relatively low quality concrete. In Scandinavian countries' concrete with a water cement ratio of about 0.50 has been in service for more than 50 years.

The main problem today is the lack of understanding, that even if laboratory results indicate a rapid penetration of chloride ions we must relate that type of negative results to the good practical experience. In other words it is only in special occasion a low chloride concentration will induce corrosion on steel in concrete. The tool we could use to understand things better is simple or advanced models that could give a general outlook of the effect of individual parameters. This report has the aim to point out the importance of all individual corrosion parameters in the evaluation procedure of the concrete service life.

Simplified model for the corrosion process

It is well known and accepted that the process of corrosion of steel in concrete must be divided into two phases:

- the ***initiation phase***, in which it is necessary to clarify the processes that take place during the time required to initiate the corrosion process, and
- the ***propagation phase***, in which it is necessary to clarify the processes that take place when corrosion has been initiated.

Initiation is achieved almost completely either by neutralisation of the concrete around the reinforcement, so-called carbonation, or by an excessive chloride concentration around the reinforcement. The rate of corrosion after initiation is determined by the electrochemical conditions in and around the corrosion area.

Initiation phase

Carbonation

Carbonation of concrete consists of a carbondioxide penetration into concrete and a chemical reaction with constituents in concrete. This process will reduce the pH-value to such a level that corrosion of steel will be possible. Mathematically it is possible to describe the carbonation process as a moving boundary. The mathematical equations are in more detail presented by Crank. The special case which applies to CO_2 diffusion in concrete have the solution

$$(C_X - C_1) / g\left(k / 2\sqrt{D}\right) + C_X - C_2 = 0$$

$$g\left(k / 2\sqrt{D}\right) = \sqrt{\pi}\left(k / 2\sqrt{D}\right) e^{\left(k^2/4D\right)} erf\left(k / 2\sqrt{D}\right)$$

$$X = k\sqrt{t}$$

where C_X = concentration at the carbonation front
C_1 = concentration in the environment
C_2 = concentration in the origin material
D = diffusion constant for CO_2
X = carbonation depth
t = time

In principle terms the rate of carbonation is thus dependent on

- the concentration of CO_2 in the surrounding environment
- the possible amount of CO_2 which will be absorbed by the concrete
- the permeability of the material

When these tree parameters are known it is possible to calculate the rate of the carbonation.

In practice we know that our structures are not homogenous especially not in the cover zone. The permeability will decrease as a function of depth and the moisture content in the material will increase as a function of depth, etc. Therefore the carbonation rate will slow down and in some cases almost reach infinite values. However, every thin section in the cover can be calculated with the equations showed above.

Carbonation is due to the low concentration of carbondioxide in air a very slow process in high quality concrete. Therefore, normal marine concrete will carbonate only a couple of millimetre's during a period of hundred years.

Chloride initiation

It is established that a certain chloride concentration in the pore water in concrete will cause corrosion. Chloride ions are able to penetrate concrete from the environment that is surround the structure. The competition between different binders as ordinary Portland cement (OPC), mixed products containing OPC, slag, pulverized fly-ash (PFA) etcs have increased research activity into the durability of concrete. The main field of this research has been the comparison of diffusion coefficients and the binding capacity of chlorides in the cement matrix. Unfortunately it is not sufficient to simply determine the chloride penetration because such values do not indicate the service life of the structure. It is also necessary to know the chloride content at the initiation moment.

The length of the initiation period is thus determined by how rapidly the concrete cover is depassivated as a result of the fact that chloride ions penetrate to the steel, and by the concentration which is required for the start of the corrosion process. The penetration sequence is normally described as a diffusion process. In practice, the transport is not always quite so clear-cut but is rather a combination of capillary suction and diffusion. One example of this is the fact that partly dried-out concrete absorbs a chloride solution through capillary action. On the other hand such a rapid chloride penetration can not be acceptable if we are expecting a service life longer than 30 years. Therefore a time dependent diffusion model can be used for high quality concrete, see chapter produced by Poulsen.

Mass transport as a result of diffusion gives the following parameters when studying the initiation period.

- concentration difference, the ambient concentration minus the initial concentration of chloride ions
- transport distance, the thickness of concrete cover
- the permeability of the concrete against chloride ions at different periods and sections of the concrete cover
- the capacity of the concrete for binding chloride ions
- the threshold value which is required for initiation of the process of corrosion

Theoretical calculations and modelling of the time of initiation in a chloride rich environment demonstrate the lack of knowledge for the important parameter,

the threshold value of chloride ion concentration, which changes the passive stage to an active corrosion stage. Normally the reader believes that the sample with the lowest chloride concentration is preferable. Figure 1 demonstrates that the situation can be the opposite.

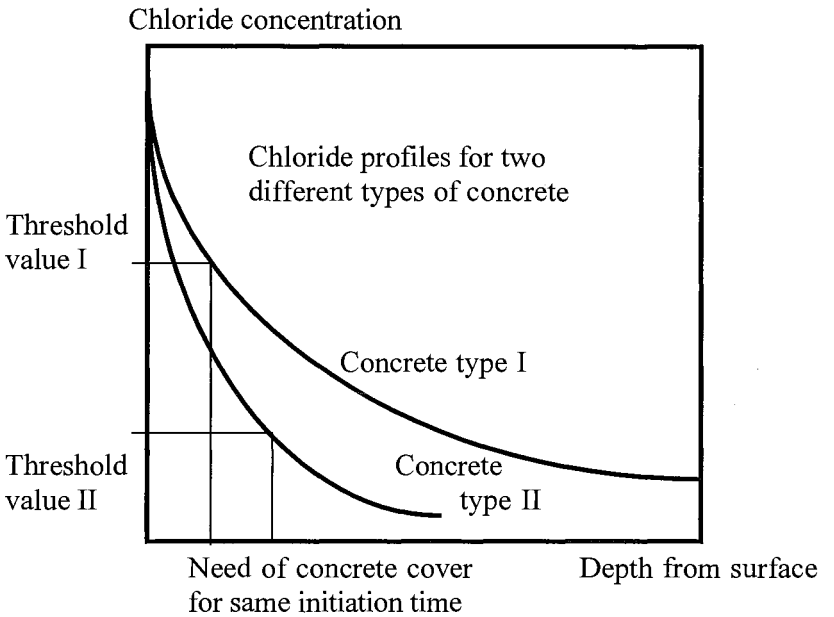

Figure 1. *Schematic sketch of initiation depth for two different concrete's.*

In research studies we like to analyse homogenous samples do to the difficulty to understand the complex corrosion process. However, it is easy to imagine that chloride ions will penetrate and reach the steel in cracked areas extremely fast. One year in this situation will be an overestimation in time. Is that short period the end of the service life? Certainly not with regard to practical experience.

In varying environmental conditions as the splash zone, concrete near de-iced roads etc the moisture conditions are varying by time. In drying periods water will evaporate from the concrete and the salts are remained in the pore water which is still in the pores. The concentrations of different salt solutions are then increasing in the pore-water as a function of evaporated water. In wet periods water is quickly absorbed through capillary suction which will increase the total amount of corrosive ions in the concrete if the water contains such substances. Structures that are not sheltered from rain will also be washed out of chloride ions when the rain water is flowing at the surface. The chloride concentration

will therefore be fluctuating in a surface zone, the convective zone, and reach a limit maximum value inside the concrete. A diffusion process will describe the chloride penetration behind this convective zone, see Figure 2.

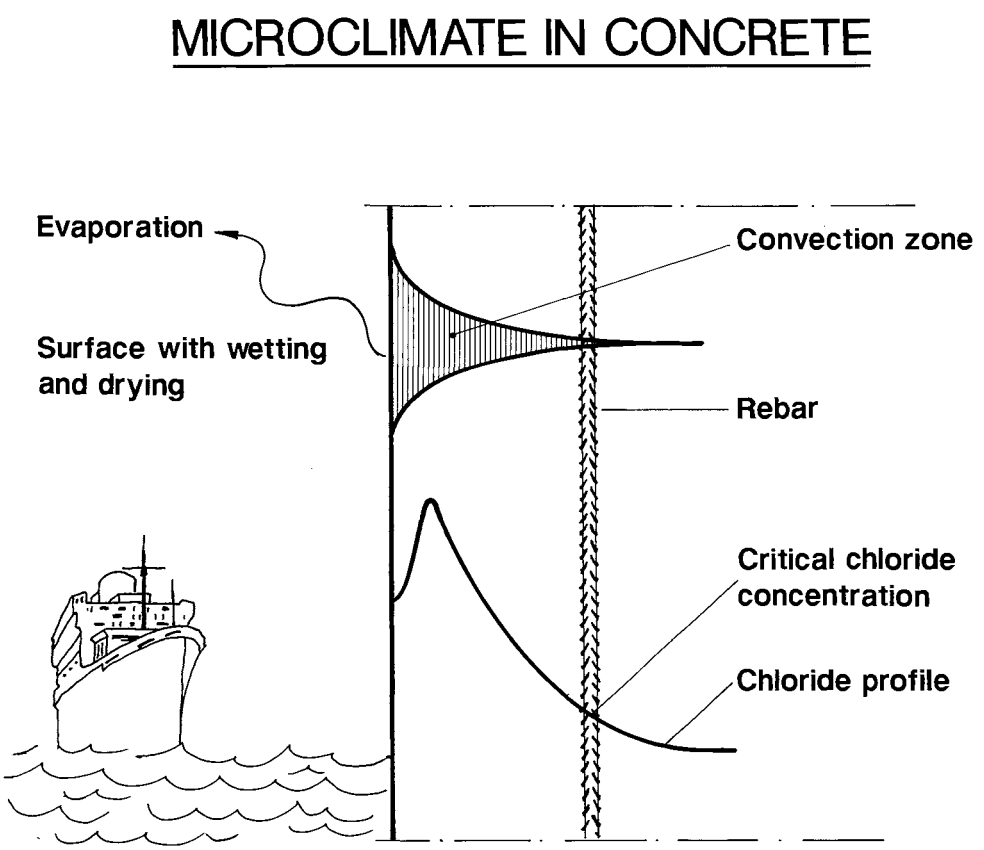

Figure 2. *Schematic sketch of the moisture and the chloride variation in concrete in the splash zone, Sandberg /1/.*

The depth of the convective zone depends on the

- wetting and drying time
- time of capillary suction during wetting
- permeability of the concrete against water
- difference in vapour pressure

A numerical calculation method of this convective zone, based on a material study, have been developed by Arfvidsson and Hedenblad /2/. The prediction method will also account the effect of a capillary suction in the wetting

procedure. Demonstration of the effect of the primary parameters will give one more piece in the corrosion puzzle, see Figure 3. Small concrete covers and/or high permeable concrete will decrease the internal environmental homogeneity as oxygen concentrations, ion concentrations and moisture conditions. These variations will primary influence on the chloride threshold value in the initiation procedure.

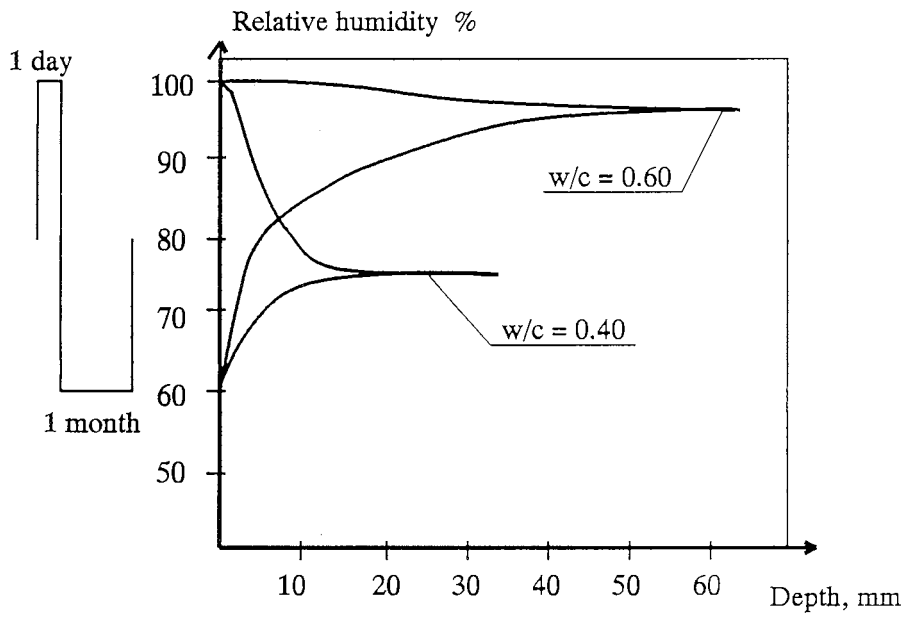

Figure 3. *Demonstration of the moisture variation in two different concrete's, W/C = 0.40 respective 0.60, with an environment cycling of 1 day capillary suction and 1 month drying in RH = 60 %, Arfvidsson and Hedenblad /2/.*

The chloride threshold level depends on so many parameters that we are today a little bit disorientated. Many investigations are reporting different critical chloride concentrations with a lowest value of around 0.2 - 0.4 % by weight of the cement content. Also several of national codes are using those low values as the allowable amount of chloride in concrete. On the other hand many investigations indicate higher threshold values around 1 - 2 % by weight of the cement content, Lambert, Page and Vassie /5/, Pettersson /6/, Pettersson and Woltze /7/.

Between 1950 and 1960 numerous results were obtained using calcium chloride admixtures as an accelerator. Laboratory and practical experiments showed that we could expect a threshold value of 2 - 3% by the weight of cement. These samples were both small and large, with a very homogeneous concrete

surrounding the reinforcement. The climate was with other words constant. Suppose such experiments were made under other climate conditions. Drying and wetting procedures would have increased the chloride concentration close to the steel surface, in an inhomogeneous way, which certainly would have changed the reported results. In the same manner thick concrete covers will increase the homogeneity around the embedded steel.

This difference indicates the problems we are dealing with. The most important parameter that will give such variable results, as mentioned above, is the transportation or the exchange of water, oxygen, corrosion inhibiting ions and corrosive ions. Therefore such variations must be taken into account in all comparison tests and life time predictions.

Chloride concentrations in the surrounding environment could be high or low. An increase of the chloride concentration in the environment will give the same effect as a reduction of the threshold value. All chloride concentration profiles are related to the concentration at the surface. The threshold value is on the other hand relatively constant, which will drop the relative position of the threshold line in the figures when the surface concentration is increased.

Recent results by Pettersson and Woltze /7/ indicate that all binder combinations will have different threshold values. The moisture situation will also complicate the exact prediction of the threshold value on structures in service. However, structures have to be designed in such a way that the concrete quality combined with the effect of the concrete cover will raise a minimum of moisture variations close to the steel surface. If these design roles is used, it is also possible to predict the service life of a concrete structure.

Threshold values could be measured with advanced electrochemical methods which will detect the start of the process of corrosion, see Andrade and Alonso /8/, Lambert, Page and Vassie /5/, Pettersson /9/. After initiation the pore water close to the steel surface must be analyzed which will give the threshold value. It should be pointed out that it is important to measure the free chloride concentration in the pore water in this stage. It is also important to do these measurements with an adequate concrete cover. Small concrete covers will give underestimated results because other elements transported in the system will give a strong influence on the threshold value.

Electrochemical measurements as potential mapping on concrete show that a high potential will occur in an oxygen rich environment, i.e. dry concrete and a low potential when oxygen is lacking, i.e. wet concrete. Sandberg /10/ has used Pourbaix diagram for illustration of threshold values as a function of the electrochemical potential. Use of this model it is possible to divide a bridge in a

marine environment in several climatic zones, see Figure 4. A small concrete cover will also give much shorter initiation time according to the fluctuation in potentials.

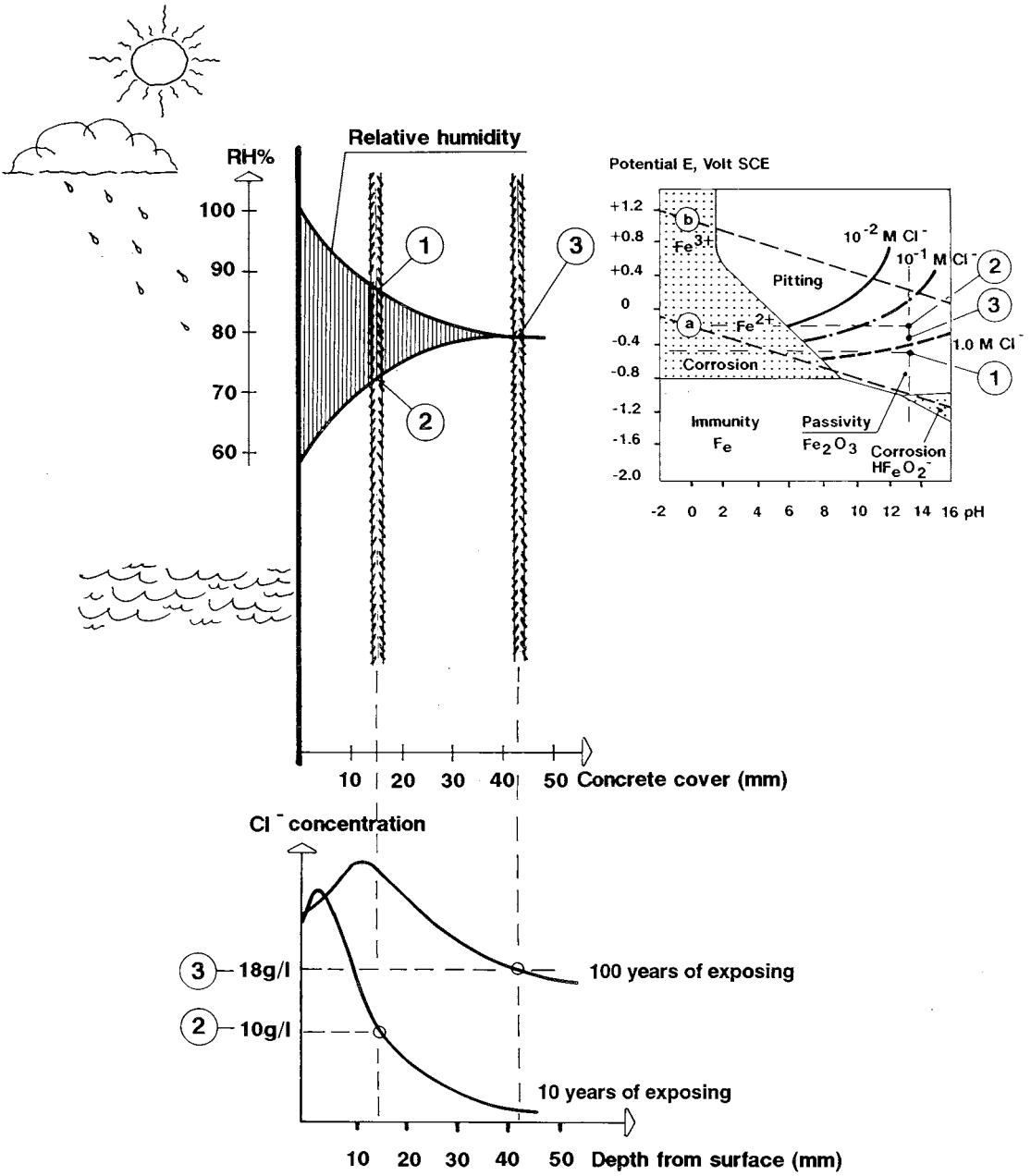

Figure 4. *Illustration of the effect on the chloride threshold value from concrete cover and the micro climatic variations around the steel surface.*

Norwegian studies of concrete bridges have also found that a bridge could contain many different environmental conditions as:

- completely water saturated concrete
- concrete in the splash zone in the main wind direction
- concrete in the splash zone sheltered from the rain and wind
- concrete above the splash zone sheltered or not sheltered from rain and wind etc.

An old Finnish colleague, Prof. Sneck, mentioned for 20 years ago some laboratory tests he was carried out. Rebars were first treated in a cementpaste with a watercement-ratio of about 0.40. Thereafter the rebars were cast into different concrete qualities with an initial chloride concentration. The problem was that Prof. Sneck could not create a corrosion process even when the chloride concentration was about 5% by weight of the cement content. This simple, not useful, test that time indicates that corrosion of steel in concrete could only be initiated in cavities or improper concrete around a steel surface.

On the other hand Fidjestöl and Nielsen /11/ made some tests with cracked concrete for 20 years ago. The samples were placed on the bottom of the harbour in Stavanger. He could almost immediately recognise that cracks in the concrete were sealed with magnesiumsalts and no corrosion were detected at all. The year, 1995, these old samples were once again examined without any sign of visual corrosion attack.

Propagation stage

Steel in concrete has both physical and electrochemical protection. The physical effect limits the mobility of various substances through the concrete, and the electrochemical protection is caused by the high hydroxide concentration in the pore water. As discussed in chapters above the electrochemical situation is changing with time and after a specific time the process of corrosion will start. The following factors affect the mean corrosion rate of steel after initiation:

- the chemical composition of the liquid that surrounds the steel.
- the conductivity of the electrolyte, which determines the contact between the anodic and cathodic areas.
- the oxygen supply to the cathodic areas.
- the temperature that affects the solubility of various substances and the mobility of those. Also chemical reactions are related to the temperature.

Variations of above mentioned factors in time could increase normally the corrosion rate by an increase of mobility of substances in the corrosion areas. Numerous other factors are often mentioned in the literature as controlling the

corrosion rate but these are in some way directly or indirectly controlled by the primary factors.

Moisture conditions inside the concrete was an important factor in the initiation stage. The electrolyte in concrete consists by the pore-water, which in electrolytic terms is relatively constant in conductivity for completely saturated material. Gjörv /11/ found that the resistivity of a concrete was changed by a factor of two when the W/C ratio is changed from 0.70 to 0.40. Also an increase of the chloride content to a level of 4% calcium chloride by weight of cement decreased the resistivity a factor 2. A dry concrete could on the other hand cause a situation where the contact between anodic and cathodic areas will be broken, which could be foreseen in high performance concrete with a water cement ratio below 0.40. This situation is important for many structures, where the initiation times are short but a low corrosion rate will give acceptable service lives.

A chemical composition could affect on the electrolytic situation by changing the hygroscopic properties of the material. Especially high chloride concentrations will increase the amount of water that will be bound to the pores in relatively dry air. The critical relative humidity where the corrosion rate will shortened the service life abruptly will decrease with increasing chloride content.

Oxygen will be retarded on the way to the cathodic areas if the pores are filled up with water. The cathode process, which consumes oxygen, is therefore a limiting factor in wet environments. Concrete below sea water level could be estimated to reach a dissolution of steel in the same order of magnitude as in a passive stage.

Often constant conditions are relatively non corrosive. Structures out of doors are not in a constant environmental condition even if they are sheltered from rain. Electrochemical measurements have indicated that changes in relative humidity, especially if free water is in contact with the concrete surface, will give strong electrochemical effects. Also the propagation stage is, thus strongly effected of the moisture variation and level of saturation of the concrete cover, which will be controlled by the climate around the structure.

The last environmental parameter of major significance is the temperature variation. Almost all chemical and electrochemical reactions are speeded up with increasing temperature. Situations when this is not the fact could be explained with a reduction of other main controlling parameters for example a drying out during the increasing temperature. An increase in temperature of 10 degrees will double the corrosion rate.

Reflections on reported studies

Reported results are very often specified with rough dimensions. The researcher is satisfied to test large pieces of concrete taken from one or a few deep locations in the structure. The chloride concentration is specified in per cent by weight of the total weight of concrete. Unfortunately, this type of rough measurement provides so little information that it cannot be used as reference material by other researchers. Modern methods are based on analysis of complete chloride profiles, millimetre by millimetre into the structure being studied. In such a complete analysis it is possible to see local variations at, for example, the steel surface or in parts of the covering layer, so that the transport mechanisms can be discussed in a completely different way. In addition to chloride profiles, these variations must be related to the material or amount of mortar, suitably via the measured calcium oxide content.

The electrochemical conditions in concrete structures are decided by the binder used as well as by the moisture conditions round the structure. The question to which an answer is still being sought is whether or not a concrete can be made so impermeable that even if the corrosion process is initiated, the rate of corrosion will be limited by the material's resistivity in a decisive way. Such resistivity measurements have been made for almost 20 years, but the results are only presented as a function of the concrete type. Why has nobody endeavoured to relate this type of measurement to an estimate of the duration of the corrosion period under different environmental conditions?

As regards moisture conditions, both the threshold levels and the rate of corrosion after initiation are probably affected in a decisive way by the climate closest to the steel surface. Moisture mechanics are a well-studied subject and there exist today instruments to calculate moisture conditions around reinforcement steel, even if the climate varies at the outside of the concrete surface. In simultaneous measurement of corrosion conditions and relative humidity interesting information has been obtained that increases understanding of the mechanisms acting in this type of decomposition. It is with pleasure that it is possible to note that contributions about moisture mechanics around reinforcement have become increasingly common in various corrosion seminars and congresses.

Finally, a trend is starting to emerge towards more detailed investigations of the corrosion complex. A structure as simple as a bridge pier in sea water can be divided into a number of micro environments according to their position relative to sea level. By mean of this type of accurate analysis of relevant conditions at different times, it will probably be possible to find new explanations for the way in which the surrounding environment affects the reinforcement. Statistical

methods can be used to advantage on as inhomogeneous a material as concrete. We have mostly assumed that there are no variations that exert a primary influence on the various component parameters that we present in reports and talks. As simple a circumstance as the fact that most structures contain cracks, from the invisible micro cracks to large ones that are accepted by concrete standards, are not dealt with as a result of the complexity. It is probable that an even more detailed division of the micro environment in concrete cover is required before it will be possible to make more correct predictions about the service life of a structure.

Concluding remarks

Summarizing this report the experience of the environmental effects are of great importance especially the micro environment close to steel surface. Simple chloride profiles will not give any information of the state of the corrosion process. With other words our simplifying procedures in codes or tests are not relevant to the corrosion processes that will occur in practice. We have to make better analysis that will take the micro climate into account inside the concrete. Therefore we could also expect that identical geometrical structures with different concrete qualities will behave completely different in

- moisture content
- results from electrochemical potential mapping
- threshold value
- corrosion rate
- critical crack width, etc

even when comparison is made in same sections.

References

1. *Sandberg, P.* Kloridinitierad armeringskorrosion i betong, University of Lund 1992, Building Materials, TVBM-7032.
2. *Arfvidsson and Hedenblad.* Calculation of moisture variation in concrete surfaces, University of Lund 1991, Building Materials & Building Physics.
3. *Kjaer, U.* Concrete for the fixed link across the Great Belt - Store Bält, Dansk Beton , No 4, 1990.
4. *Byfors, K.* Chloride initiated reinforcement corrosion. Swedish Cement and Concrete Research Institute, Report 1:90, Stockholm 1990.
5. *Lambert, Page and Vassie.* Investigations of reinforcement corrosion. 2. Electrochemical monitoring of steel in chloride-contaminated concrete. Materials and Structures, Vol. 24, No. 143, 1991.

6. *Pettersson, K.* Corrosion threshold value and corrosion rate in reinforced concrete, CBI Report 2:92, Swedish Cement and Concrete Research Institute, Stockholm 1992..
7. *Pettersson and Woltze.* Fältförsök beständiga marina betongkonstruk-tioner, Delrapport 1, Rapport nr 92057, Swedish Cement and Concrete Research Institute, Stockholm 1992.
8. *Andrade, Alonso.* The relationship of Icorr to Temperature and R.H. A contribution to the Brite/EuRam project BREU-CT92-0591.
9. Pettersson. Corrosion threshold value and corrosion rate in reinforced concrete. Cement- and Concrete Research Institute. Report 2:92. Stockholm 1992.
10. *Sandberg.* Critical evaluation of factors affecting chloride initiated reinforcement corrosion in concrete. Report TVBM-3068. Lund 1995.
11. *Fidjestöl, Nielsen.* Field test of reinforcement corrosion in concrete. ACI Publication SP-65, Performance of concrete in marine environment, pp 205 - 222, 1980.
12. *Gjörv.* Durability of Reinforced Concrete Wharves in Norwegian Harbours. Ingengörsförlaget A/S, 208 pp, 1968, Oslo.

Chloride Threshold Values in Reinforced Concrete

Karin Pettersson, Cement och Betong Institutet, 100 44 Stockholm

Abstract

Corrosion of steel in concrete occurs whenever the external influences change the composition of the pore solution to an aggressive condition. Chloride ions and carbonation of the concrete can destroy the passivity which results in corrosion of the steel.

The importance of chloride ions for reinforcement corrosion in concrete has lead to the concept of the chloride threshold level, which may be defined as the minimum chloride level at the depth of the reinforcement resulting in active pitting corrosion of the reinforcement.

Introduction

Chloride induced reinforcement corrosion is probably the most common durability problem associated with modern good quality reinforced concrete structures exposed for marine or deicing salts. Normally, steel in concrete is passivated in a moist, alkaline environment which is free of chlorides and other aggressive ions. The term passivity denotes that although ordinary steel reinforcement in concrete is thermodynamically not stable, the corrosion rate is depressed to an insignificant low level by the formation of a barrier of iron oxides on the steel surface. The state of passivation is maintained until the concrete in contact with the reinforcement becomes carbonated or until a sufficient concentration "the threshold level" of aggressive ions (normally chlorides) has reached the steel surface. The aggressive ions (e.g. chlorides) then trigger the dissolution of the iron oxide layer and later on the dissolution of steel.

Both the passivating formation of an oxide barrier on the steel surface and the chloride initiated reinforcement corrosion process in concrete can be divided into two sub-processes:
1) The anodic dissolution of steel (which is boosted by chloride ions).
$Fe \rightarrow Fe^{2+} + 2e^-$ (eq. 1)
2) The cathodic reduction of oxygen:
$1/2O_2 + H_2O + 2e^- \rightarrow 2OH^-$ (eq. 2)

The accumulated rate of the anodic and cathodic reactions must be the same in order to maintain the charge balance. In concrete, the chloride attack on the reinforcement is usually occurring as pitting corrosion, with an anodic attack concentrated into a small corrosion pit corresponding to a relatively large cathodic reaction area. The anodic and the cathodic area forms a corrosion cell, which size is limited by the resistivity of the electrolyte, which is the concrete surrounding the reinforcement.

The chloride threshold value in concrete can be defined as the highest chloride content that does not cause any risk of corrosion on the reinforcement. The chloride will get in contact with the concrete through sea water or deicing salt. The chloride content is most practically defined as the total chloride content compared to the cement content measured in the same sample, % Cl^- per cement. However, it is usually assumed that it is the free chloride content in the pore solution that is the most interesting for corrosion on the reinforcement. Different cement types have different content of alkali ions, and these ions are important for the chloride threshold value. When the critical chloride value for the onset of active corrosion has been reached, the corrosion will start and continue with a varying rate.

The threshold values usually presents as free chloride ions in the pore solution, mg Cl^-/l

and as the $\frac{[Cl^-]}{[OH^-]}$ ratio.

The chloride threshold value is not a fixed value. It should rather be grouped in intervals than be given in specific values. Figure 1, Brown /1980/ shows where the acceptable chloride content is presented for uncarbonated concrete in marine condition. The chloride threshold value is one of the most important factors for the lifetime of a concrete structure. Hausman /1967/ /1/ indicated critical chloride concentrations which initiate the corrosion process for steel in basic solutions. According to Hausmann, this threshold value is:

$\frac{[Cl^-]}{[OH^-]} \leq 0{,}61$, the Cl^- and OH^- are the concentration in mole per litre, M.

This relation should give values on the safe side for mortar and concrete since the embedded steel is surrounded by an alkaline cement paste which offers a physical protection of the steel surface.

Chloride concentration % Cl per cement weight	Possibility for corrosion
<0.4	negligible
0.4-1.0	possible
1.0-2.0	probable
>2.0	certain
Values usually agreed concerning the critical chloride content in not carbonated concrete around plain carbon steel. This table shows that the critical content in concrete has no constant v. It depend on other parameters than only the concrete mass.	

Fig. 1. *Accepted chloride concentration in uncarbonated concrete before corrosion starts.*

Factors affecting the chloride threshold values

Several parameters are likely to affect the chloride threshold level in concrete. Only very recently systematic approaches have been adopted in order to identify their relative importance. The following is a review of parameters which have some evidence of being important in controlling the threshold level, with the purpose of illustrating the variability associated with the chloride threshold level /2/.

Passive steel potential and concrete alkalinity

By analogy with stainless steel, a critical pitting potential is believed to exist for passivated ordinary steel in alkaline concrete. The critical pitting potential depends on the alkalinity of the pore solution in contact with the steel, as indicated in Figure 2. Below the critical pitting potential pitting corrosion cannot be established, since the steel potential would be too low for becoming anodic /3/. In the absence of pitting corrosion, low potential conditions in high quality concrete is usually harmless because of insignificant corrosion rates, provide that the reinforcement is properly embedded in concrete.

A potential - pH diagram for iron in aqueous solutions may serve as a schematic representation of the passivity regions for steel in concrete. Threshold levels for reinforcement steel exposed to solutions of various alkalinity and chloride concentrations are indicated in Figure 3. So far very few systematic investigations have been reported on threshold levels for reinforcement embedded in concrete as a function of passive steel potential and concrete alkalinity.

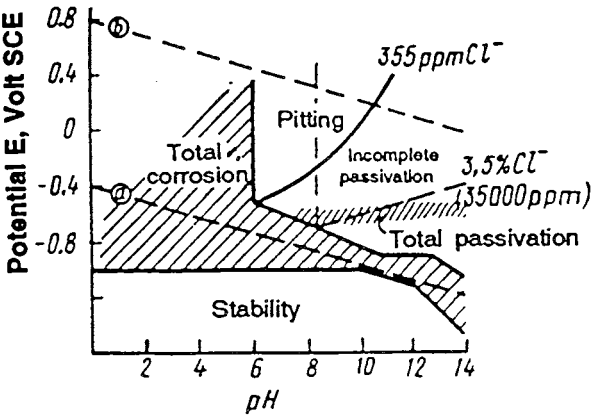

Fig. 2. Potential - pH diagram for the schematic stability of mild steel in concrete /4/. Pitting corrosion is impossible in and below the area marked "total passivation".

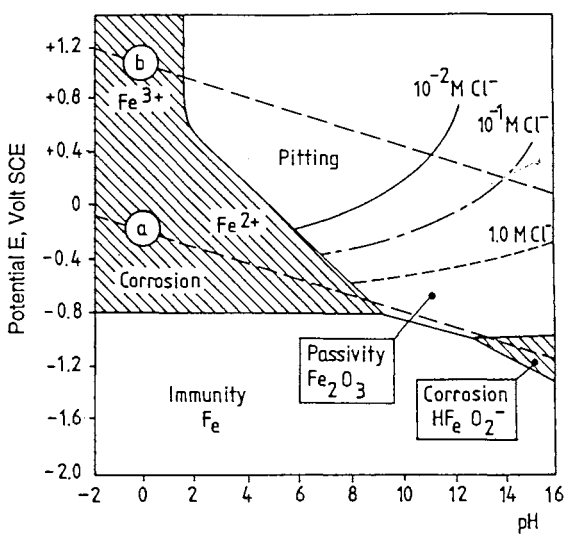

Fig. 3. Potential - pH diagram showing threshold levels for mild steel exposed in chloride solutions /2/.

Cast-in chlorides

Cast-in chlorides alter the hydration process for Portland cement as compared to when Portland cement is hydrated in chloride free water. Besides the increased chloride binding taking place when the aluminate phase is hydrated in presence of chlorides, the pore size distribution is altered which may lead to an altered permeability. On the other hand, cast-in sodium chloride causes an increased pH of the pore solution due to the formation of sodium hydroxide. Furthermore, the formation of passivating oxides on the steel surface is less efficient at higher chloride concentrations /5/. As a consequence different chloride threshold levels can be expected for concrete with cast-in chlorides when compared to originally chloride free concrete. In fact most chloride threshold levels reported are derived from short term experiments with cast-in chlorides. But apparently too little data exist to evaluate whether experiments with cast-in chlorides tend to underestimate or overestimate the chloride threshold level for originally chloride free concrete.

Cover thickness

Besides acting as a physical barrier preventing external chlorides from reaching the reinforcement, the cover also stabilises the micro environment at the depth of the reinforcement. In other fields it is well known that changes in moisture, temperature, oxygen, salinity, etc. often promotes corrosion as compared to a stable, not changing exposure condition /6/. By analogy, it is assumed that a thicker cover helps to increase the threshold level by reducing moisture- and oxygen variations as the depth of the reinforcement.

A thicker cover naturally also helps to prevent carbonation and leaching of alkali hydroxides at the depth of the reinforcement, thereby preserving the highly alkaline environment at the reinforcement.

Water to binder ratio

A lower water to binder ratio helps to stabilise the micro environment at the depth of the reinforcement in a similar way as a thicker cover, since the moisture permeability decreases, as illustrated by Tuutti /7/ in Figure 4. In addition, a lower water to binder ratio also may have the following positive effects on the threshold level:
-A higher concrete resistivity and denser steel-concrete interface, both factors resulting in less area available for corrosion cells to develop.

-Less chloride mobility, thereby preventing chloride accumulation in corrosion pits, with a potentially decreasing catalytic effect of chloride ions.

Typical results of the influence of the w/b on the chloride threshold values are shown in Figures 5 and 6.

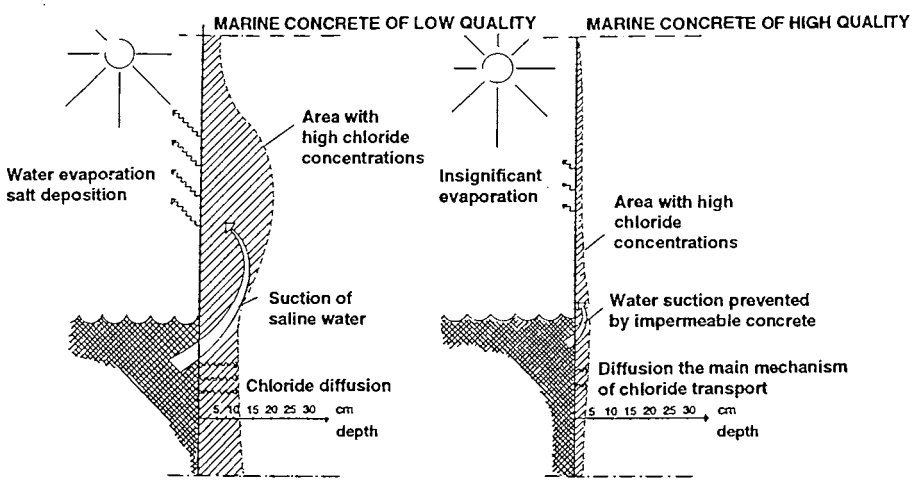

Fig. 4. *The effect of a low moisture permeability in concrete on the micro climate affecting the reinforcement /7/.*

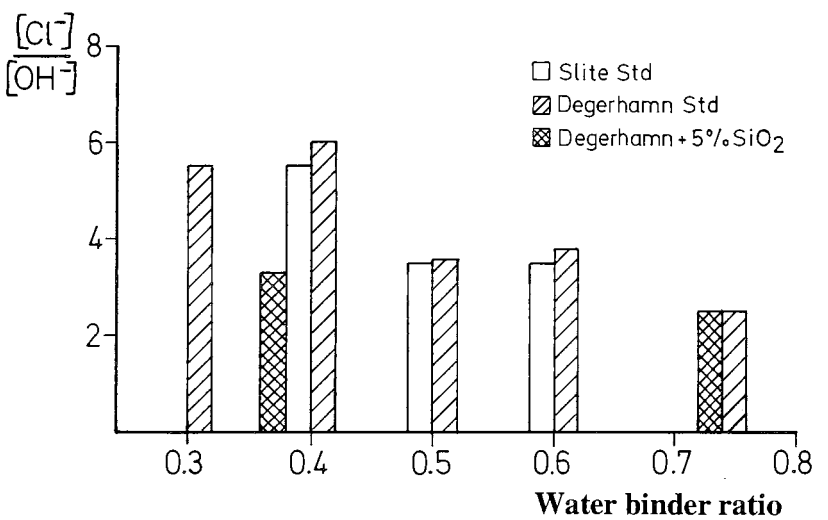

Fig. 5. *Chloride threshold value for mortar specimens versus the water-to-binder ratio.*

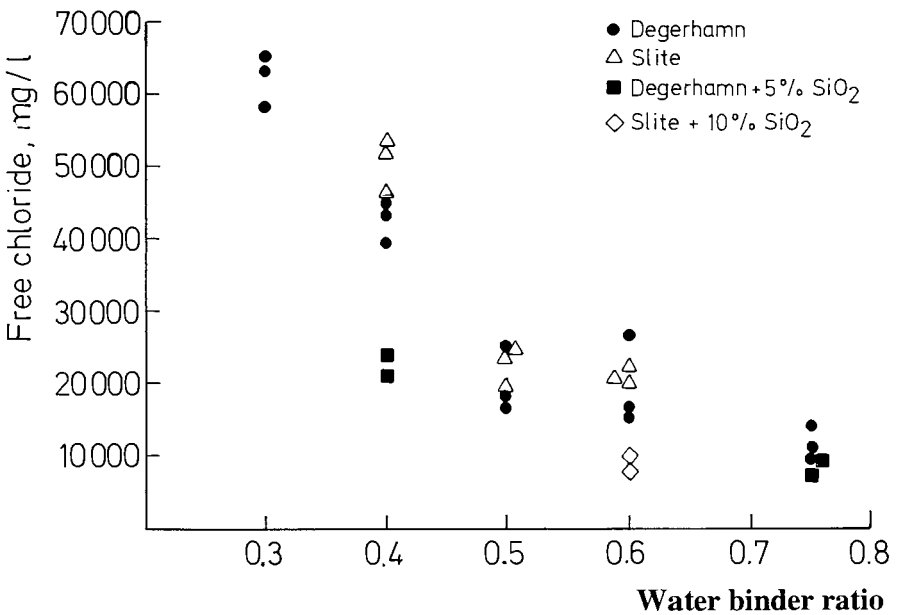

Fig. 6. *Chloride threshold value for mortar specimens versus the water binder ratio.*

Cracks

Macro cracks (0.1-0.8 mm wide at surface) in concrete generally accelerates the chloride transport rate and decrease the chloride threshold level. The effect of macro cracks on the chloride threshold value depends on the crack size, the exposure conditions and on the cover thickness /8,9/, as illustrated by experimental data from laboratory exposure in Figure 7. For submerged high performance concrete, 30 mm cover, water to binder ratio 0.30 and 0.4 mm crack width, the chloride threshold level was found to be marginally lower as compared to submerged uncracked concrete. On the other hand, for the same concrete exposed to air, the chloride threshold value was reduced to almost zero for 0.4 mm cracks as well as for 0.8 mm cracks.

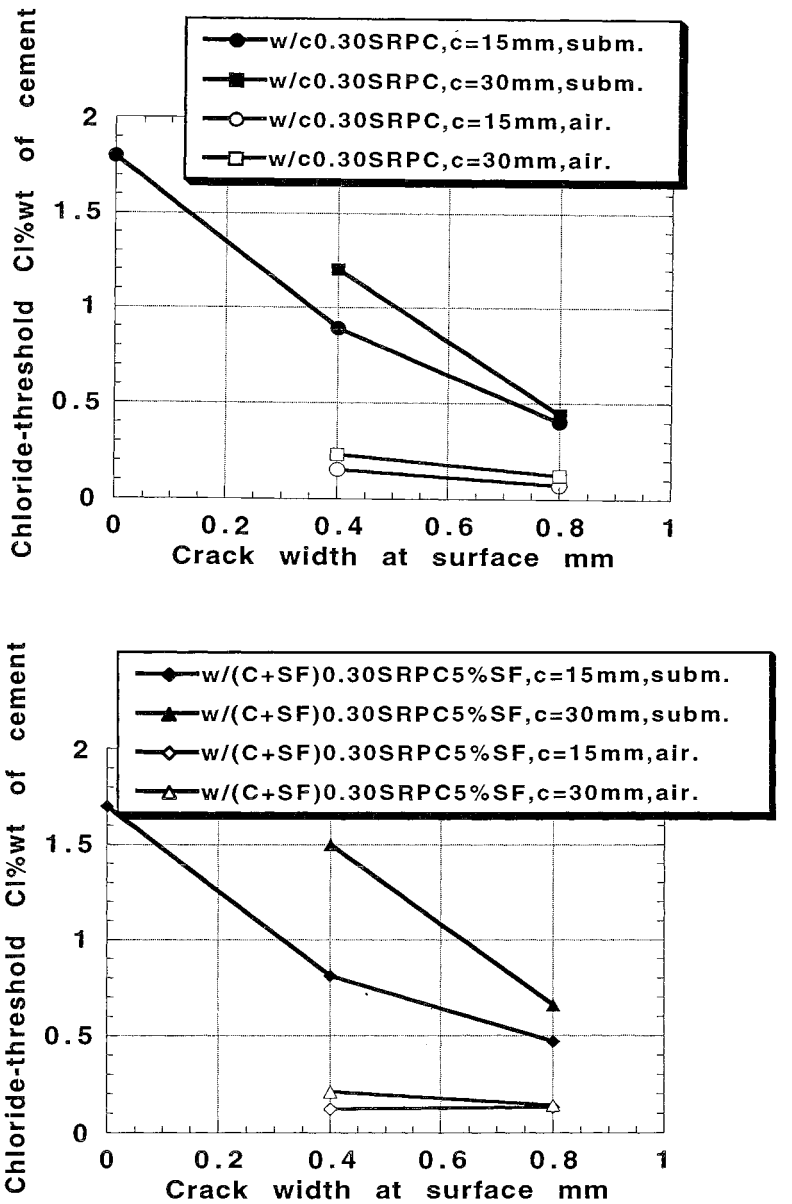

Fig. 7. Chloride threshold levels for laboratory submerged- or wet/dry exposed high performance concrete, w/(C+SF)=0.30; 15 and 30 mm cover /2/. A) Plain sulfate resisting Portland cement. B) With 5% silica fume as cement replacement.

Binder type

Reported results on the effect of cementitios or pozzolanic by-products (ground granulated blast furnace slag, fly ash or silica fume) on the chloride threshold level are somewhat conflicting. Bamforth & Chapman-Andrews /10/ and Thomas, Matthews & Haynes /11/ reported for ground granulated blast furnace slag (GGBS) respectively for fly ash (FA), that these cement replacement materials have no effect on chloride threshold level. On the other hand Thomas /12/ from an extensive field study later reported that a cement replacement for fly ash does affect the chloride threshold level negatively. MacPee & CaO /13/ found a negative effect of GGBS on the chloride threshold level. Hansson & Sørensen /14/ and Pettersson /15/ found a negative effect of silica fume (SF) on the chloride threshold level.

Conclusions

* The chloride threshold values appear to vary between 10 and 65 g chloride per litre pore solution compare to the water binder ratio.

* The chloride threshold value (Cl-)/(OH-) in mortar is between 3-6, which is 5-10 times higher than Hausmann /1967/.

* A thicker cover will stabilise the micro environment at the depth of the reinforcement which helps to increase the threshold value.

* Macro cracks generally decreases the chloride threshold values.

* Additives as micro silica and fly ash have small or no effect on the threshold value.

References

1. *Hausman, D.A.:* Steel Corrosion in Concrete. Materials Protection, Nov, pp 19-23. 1967.

2. *Pettersson, K., Sandberg, P.:* Chloride Threshold Levels and and Corrosion Rates in Cracked High Performance Concrete Exposed in a Marine Environment - Considerations for a definition of service life time for high performance concrete, to be presented at the 4th. CANMET/ACI Int. Conf. on Durability of Concrete, Sydney, August 17-22, 1997.

3. *Arup, H.:* The Mechanisms of the Protection of Steel by Concrete, Proc. Corrosion of Reinforcement in Concrete Construction, Ellis Horwood Ltd., Chichester, June 1983, pp 151-157.

4. *Alekseev, S. N., Ivanov, F. M., Modry, S., Schiessl, P.:* Durability of reinforced concrete in aggressive media, (ed. M. Majithia; S.K. Mallick), Russian Translation Series 96, A.A. Balkema /Rotterdam /Brookfield, 1993, pp. 164-247, 305-349.

5. *Yonezawa, T., Ashworth, V., Procter, R.P.M.:* Pore Solution Composition and Chloride Effects on the Corrosion of Steel in Concrete, Corrosion Engineering, Vol. 44, No. 7, July 1988, pp. 489-499.

6. *Mattsson, E.:* Electrochemistry and Corrosion Science, Swedish Corrosion Institute, Roos Produktion AB, Stockholm 1992 (in Swedish).

7. *Tuutti, K.:* Corrosion of Reinforcement in Concrete (in Swedish), Proc. Sem. Durability of Marine Concrete Structures, Danish Concrete Institute, Aalborg Portland, Cementa, Denmark - Sweden 1993, pp. 85-101.

8. *Pettersson, K., Jørgensen, O., Fidjestøl, P.:* The Effect of Cracks on Reinforcement Corrosion in High-Performance Concrete in a Marine Environment, Proc. 3rd CANMET/ACI Int. Conf. Performance of Concrete in Marine Environment, St. Andrews-by-the Sea, August 4-9, 1996.

9. *Pettersson, K.:* Criteria for Cracks in Connection with Corrosion in High Strength Concrete, Proc. 4th Int. Symp. on Utilization of High-Strength/High-Performance Concrete, Paris May 29-31, 1996.

10. *Bamforth, P.B., Chapman-Andrews, J.F.:* Long Term Performance of R.C. Elements under UK Coastal Exposure Conditions, Proc. Corrosion and Corrosion Protection of Steel in Concrete, ed R N Swamy, Sheffield Academic Press, 1994, Vol. 1, pp. 139-156.

11. *Thomas, M.D.A., Matthews, J.D., Haynes, C.A.:* Chloride Diffusion and Reinforcement Corrosion in Marine Exposed Concrete Containing Pulverised Fuel Ash, Proc. Corrosion of Reinforcement in Concrete, Ed C L Page, K W J Treadaway & P B Bamforth, Elsevier Applied Science, London, 1990, pp. 198-212.

12. *Thomas, M.D.A.:* Chloride Thresholds in Marine Concrete, Proc. Int. RILEM Workshop on Chloride Penetration into Concrete, Saint-Rémy-Les-Chevreuse, October 15-18, 1995.

13. *Macphee, D.E., CaO, H.T.:* Theoretical Description of Impact of Blast Furnace Slag (BFS) on Steel Passivation in Concrete, Magazine of Concrete Research, vol 45, no 162, 1993, pp. 63-69.

14. *Hansson, C.M., Sørensen, B.:* Threshold Concentration of Chloride in Concrete for the Initiation of Reinforcement Corrosion, Proc. Corrosion Rates of Steel in Concrete, ed N S Berke, V Chaker & D Whiting, ASTM STP 1065, 1990, pp. 3-16.

15. *Pettersson, K.:* Corrosion Threshold Value and Corrosion Rate in Reinforced Concrete. CBI Report 2:92 Swedish Cement and Concrete Research Institute, Stockholm, 1993.

A New Method for Determining Chloride Thresholds as a Function of Potential in Field Exposure Tests.

Hans Arup
Hans Arup Consult, Dyreborgskovvej 16
DK 5600 Faaborg

The Swedish project on concrete in the marine environment includes a determination of chloride threshold values as a function of applied potential. The principle of the test has been described in an earlier publication /1/ together with an analysis of the factors, which are important in this connection. Only a brief summary will be given here.

Experimental Technique.

It was decided from the beginning to have the specimens under potentiostatic control and to use the applied potential as an independent variable in the test. The onset of corrosion would then be detectable by a sudden increase of (anodic) current from the specimen. Instead of determining the chloride level at the surface of the specimen by post-event sampling (which was considered to be a difficult, even doubtful technique), chloride levels at a given time and depth is determined by numeric calculation from 2-3 chloride profiles produced at different times by step grinding using the testblock itself or an identical concrete sample exposed together with it. The pre-corrosion currents to and from the specimens are so small, that their effect on chloride migration is negligible. The small currents also permits to use one potentiostat to control several specimens at different potentials through the use of a voltage divider.

The test as described is essentially non-destructive, which makes it feasible to use a large number of specimens in each testblock. This permits testing of more variables or additional levels of each variable and can also be used to improve the statistical basis.

Design of Test Unit.

A further improvement of the experimental technique was sought by designing the test unit shown in Figure 1. Twenty specimens, an MnO_2-reference electrode (ERE 20) and two counter electrodes of activated Ti mesh are mounted in a precast slab of high resistivity mortar. Note that the electrodes are placed in precast blocks of low resistivity mortar. The 20 specimens are U-shaped - like stirrups - and the electrical connections and the epoxy coated ends are protected by being farther away from the chloride exposed face. The precast unit is made with great precision, so the variation in depth of cover is minimal. The test unit becomes the side or bottom of the form in which the test concrete is poured. If wanted, electrochemical control and monitoring can start immediately, because all electrodes and electrical connections are ready and in place.

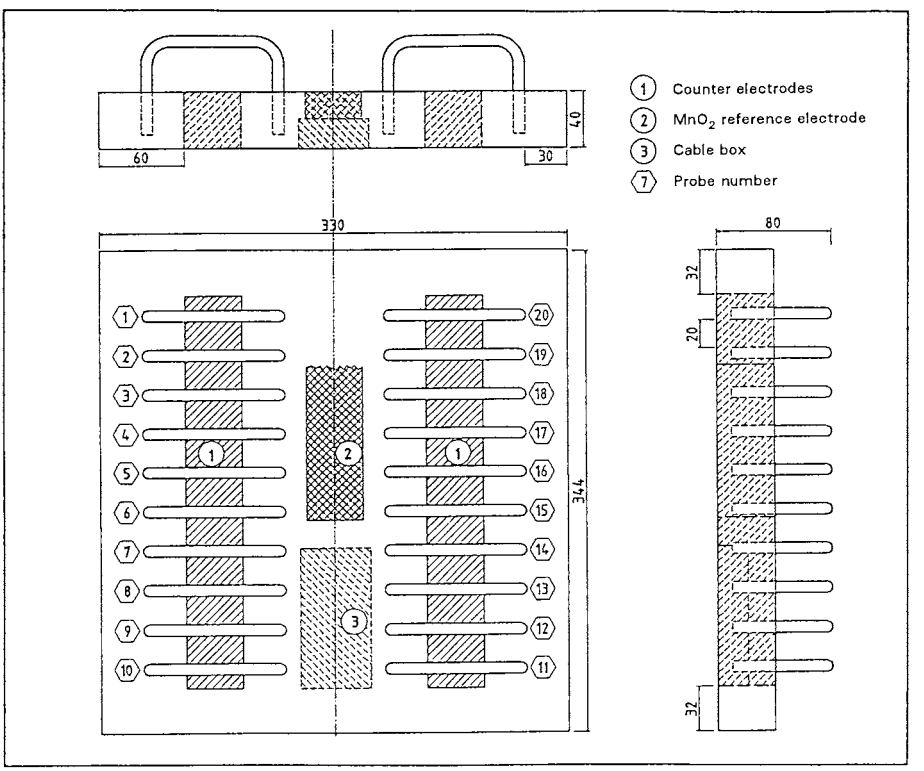

Figure 1. Drawing of precast unit with 20 specimens ready for being cast into test concrete. The unhatched part of the slab is filled with high resistivity mortar and contains the wired connections to the cable box.

In the Swedish test the concrete was cast with appr 10 cm "cover" above the specimens and allowed to cure 28 days. The desired cover of 10 mm was then produced by slitting the block with diamond grinding. Earlier tests had shown that a ground surface produces very consistent results in chloride penetration tests. The sawn-off slab was cut in smaller pieces, which were exposed with the testblock and used for profile grinding. The back and the sides of the testblock were coated with epoxi.

A detailed description of the test unit and the procedures in carrying out chloride threshold determination can be found in the document APM 303 by the AEC laboratory, who was responsible for the preparation of the testblocks, the profile grinding and some of the laboratory exposure tests /2/.

Electrochemical Control and Monitoring.

A special combined potentiostat/voltage divider was constructed for use

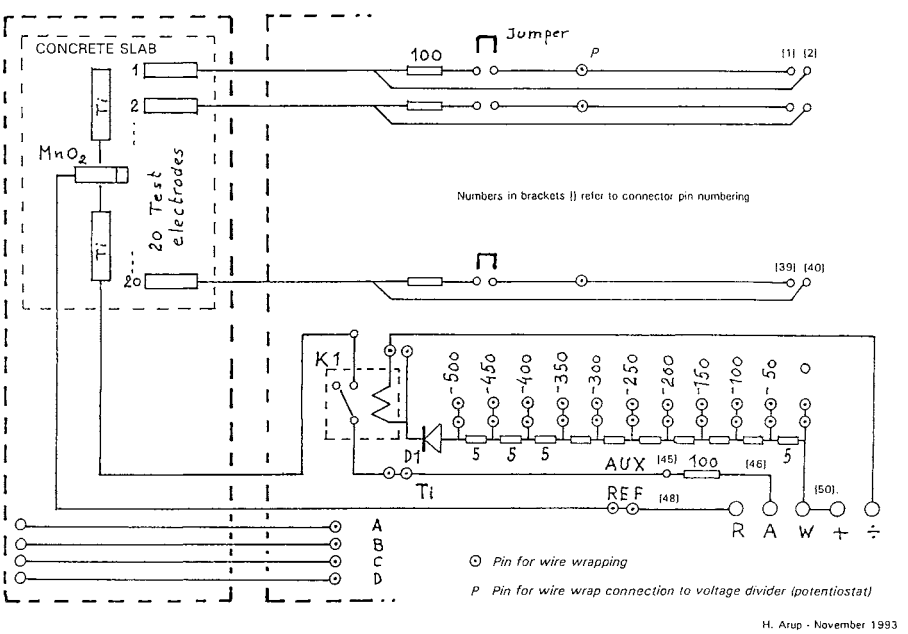

Figure 2. Simplified electrical diagram of the connector box. The points marked P are connected by wire wrapping to a point on the voltage divider. If the corresponding jumper is inserted, the specimen is potentiostatically controlled, and the current is monitored as the voltage drop over the 100 ohm resistor.

that a lot of effort and forethought has been applied in order to improve repeatability, this must have a repercussion not only on the ongoing work, but on any other work on steel in concrete.

Specimen Number	Potential vs MnO_2	Time to start of corrosion, days.	Repassivation	Threshold Cl in % of mass
2	free(ca −200)	221	556	1,7
8	−50	248	no	1,8
18	−50	262	no	1,8
9	−150	396	no	2,0
4	+50	513	no	2,4
6	0	531	no	2,4
15	−250	581	no	2,5
20	−100	609	no	2,5
7	−200	651	654	2,7

Table 1. Results from the first test in Lund. For explanation see text.

It must be noted, however, that all specimens at potentials below −250 mV, which is around −90 mV in the calomel scale, are still protected, so maybe the expected protective effect of a partial cathodic protection remains to become evident.

It is also interesting to see that the threshold values determined so far are in the high end of the range known from other published work. This may be due to the efforts made to make sound castings and the design of the specimens, which prevents e.g. crevice corrosion at the edge of the coating.

As said earlier, the specimens were disconnected from the potentiostat, as soon as corrosion has been detected, and the free potential of the specimen was monitored. In two cases, and after very different time intervals, these specimens repassivated as evident from a sharp potential increase of 100-200 mV. This can be explained by the fact that the potentiostatic control represents a coupling to an infinite area of cathodic passive surface. The small, freely corroding specimen has not enough cathode area to support a growing pit.

in these tests. It is connected with a 26-way flat cable to the test block and with a 50-way flat cable to a datalogger. Figure 2 shows a diagram for the internal connections in the instrument (leaving out the potentiostat, which is connected to "W", "R" and "A" in the diagram). The potential of one end ("W") of the voltage divider is set on the potentiostat. The steps on the voltage divider are 50 mV each, but can be set to 100 mV, giving a total range of 0-500 (1000) mV below the set potential. Each of the 20 specimens is connected by wire wrapping to a given step in the voltage divider, and the current to or from the specimen is read as the voltage drop across a current measuring resistor of 100 ohm. The datalogger has a resolution of 1 microvolt, corresponding to a current of only 0,01 microamp per specimen or 3 microamp per m^2. Freely corroding specimens are connected to "W" and the corresponding jumper removed. The datalogger will then monitor the potential relative to the potential set by the potentiostat (with a reversal of the sign).

The current flowing to or from the non-corroding samples is usually less than 1 microamp. The current rises steeply with the onset of corrosion. After corrosion has been recorded, the specimen is normally disconncted by removing the jumper, and the potential of the now freely corroding specimen is recorded (relative to the former fixed potential).

Early Results and Discussion.

In order to test the method described above, two identical test blocks were prepared, each with 20 specimens of 8mm smooth ground steel rod and made with a medium quality concrete with 330 kg/m^3 sulfate resistant Portland cement and a W/C ratio of 0,5. In each block, two specimens were corroding at free potential, the others were held two and two at 9 different potentials from +50 to −450 mV against MnO_2 (appr. +210 to −240 mV against Calomel). The cover was 10 mm. Exposure was in 10% NaCl at room temperature. One block was exposed at the AEC Laboratory, the other at Lund Technical University.

As an example of the results obtained so far, the following table 1 lists time to corrosion initiation and the corresponding calculated chloride threshold concentrations from the test in Lund:

The results are surprising in many ways and give rise to several questions. The scatter between duplicate specimens is very large - with the exception of the pair no 8/18, which agree well, all the other results are from one specimen in a pair, the other still not corroding. There is no clear influence of potential - certainly not in the expected way ! Considering

For this reason it can be argued, that the potentiostatic testing is a conservative test, which might be expected to give a safe value of the threshold. On the other hand, we probably have insufficient knowledge of the effect that time after casting in concrete and preexposure conditions has on the threshold. Could it be so that a specimen which has been potentiostatically held at a moderately high potential for some time will develop a more resistant oxide film ?

Regardless of the answers to these questions, it is clear that the tests have been made with "labcrete" with no attempts to reproduce defects as occurring in the field.

In the continuation of the program, therefore, a large number of specimens with artificial defects will be used. The new program, which has recently started, comprises a total of 15 testblocks, each with 20 specimens. Six blocks will be exposed in a natural marine environment, below and just above the waterline, the others will be tested in the laboratories.

The research programme referred to here is sponsored by CEMENTA, Sweden, and part of the work has been carried out at the AEC laboratories in Vedbæk, Denmark. The author acknowledges the inspiring collaboration with Palle Sandberg and Henrik Sørensen from the respective companies.

References.

/1/ Hans Arup: Bestemmelse af Chloridtærskelværdi, in Marina Betongkonstruktioners Livslängd, 1993.

/2 Test Method APM 303, AEC Laboratory, Vedbæk, Denmark, 1993.

Estimation of Chloride Ingress into Concrete and Prediction of Service Lifetime with Reference to Marine RC Structures

Ervin Poulsen, AEClaboratory. 20 Staktoften, DK-2950 Vedbæk

Abstract

This paper deals with three important topics related to chloride ingress into marine RC structures, namely determination of:

- The chloride profile $C = C(x, t)$.
- The ingress of a reference chloride concentration $C_r = C_r(t)$.
- The service lifetime defined as the period of initiation $t_{LT} = t_{cr}$.

It is assumed that the chloride ingress obeys Fick's 2nd law of diffusion, cf. Eq. 1, with time-dependent boundary condition $C(0, t) = C_{sa}(t)$, cf. Eq. 13, and time-dependent, achieved chloride diffusion coefficient $D_a = D_a(t)$, cf. Eq. 7. Furthermore, it is assumed that the chloride diffusion coefficient is independent of the location x in the concrete and the chloride concentration C of the concrete. The complete solution of Fick's 2nd law of diffusion found by Leif Mejlbro, cf. [1], is applied and numerical examples are given.

The influences of concrete properties and environment characteristics are taken into account and illustrated by numerical examples.

Keywords. Chloride ingress into marine concrete. Fick's 2nd law of diffusion. Time-dependent chloride diffusion coefficient and time-dependent surface chloride concentration.

Introduction

During the last decade marine RC structures have been carefully examined, and concrete specimens placed in seawater exposure stations have increased our knowledge significantly. There is still a need for more observations, but at present the mathematical models used to describe the chloride ingress into marine concrete do not take the results of the observations fully into account. However, the complete solution exists, and it is just as simple to apply as the well-known error-function solution.

Estimation of chloride ingress into concrete

In the early 1970s Collepardi et al, cf. [2] and [3], published a method for calculation of the chloride ingress into concrete structures by diffusion, Fick's 2nd law:

Eq. 1 $$\frac{\partial C}{\partial t} = \frac{\partial}{\partial x}\left(D\frac{\partial C}{\partial x} \right)$$

The error-function solution

By applying chloride diffusion parameters of constant values, i.e. independent of time t, chloride content C, and location x, the solution of Fick's 2nd law of diffusion yields the error-function solution:

Eq. 2 $$C(x,t) = C_i + (C_{sa} - C_i)\,\mathrm{erfc}\left(\frac{x}{\sqrt{4(t - t_{ex})D_0}} \right)$$

Here

$C(x,t)$ is the chloride concentration of the concrete at the distance x from the exposed surface at time t.
C_i is the initial chloride content of the concrete.
C_{sa} is the (constant) chloride concentration of the concrete at the surface.
x is the distance from the chloride exposed concrete surface.
t is the time (age) measured from the time of casting (origo).
t_{ex} is the time of the first chloride exposure.
D_0 is the (constant) chloride diffusion coefficient.
$\mathrm{erfc}(z)$ is the error-function complement, cf. Crank [4].

Mejlbro's Ψ-solution

The error-function solution Eq. 2 has the disadvantage of applying only to chloride ingress on condition that the diffusion constants C_{sa} and D_0 remain constant. In 1988 Takewaka et al, cf. [5], showed that the achieved diffusion coefficient is a function of time (exposure period), i.e. $D_a = D_a(t)$.

Furthermore, in 1990 Uji et al, cf. [6], showed that the surface chloride concentration is a function of time (exposure period), i.e. $C_{sa} = C_{sa}(t)$.

This means that the error-function solution is not valid if this information is taken into account.

The general solution. Leif Mejlbro, cf. [1], has solved Fick's 2nd law of diffusion, cf. Eq. 1, provided that $D = D(t)$ is time-dependent, and that $C_{sa} = C_{sa}(t)$ belongs to a family of functions as:

Eq. 3: $$C_{sa} = C_i + S\,[(t - t_{ex})\,D_a]^{\,p}$$

where S is a constant, depending on the environment and the type of binder, and the achieved chloride diffusion coefficient $D_a = D_a(t)$, cf. [7], obeys the following relation:

Eq. 4: $$D_a = \frac{1}{t - t_{ex}} \int_{t_{ex}}^{t} D(u)du$$

Mejlbro's Ψ-solution yields, cf. [1]:

Eq. 5: $$C(x,\,t) = C_i + S\,[(t - t_{ex})\,D_a]^{\,p}\,\Psi_p(z)$$

where z is given by:

Eq. 6: $$z = \frac{x}{\sqrt{4(t - t_{ex})D_a}}$$

The functions $\Psi_p(z)$ are tabulated by Mejlbro, cf. [1]. For $p = 0$ it is seen that C_{sa} remains constant, and in this case $\Psi_0(z) = \mathrm{erfc}(z)$, cf. [1].

$D_a(t)$ as a power function of time. It is a very special but important case of interest when the achieved chloride diffusion coefficient $D_a = D_a(t)$ yields a power function of time t, i.e.:

Eq. 7: $$D_a = D_{aex}\left(\frac{t}{t_{ex}}\right)^{\alpha}$$

Here α is an exponent which according to Maage et al, cf. [8], depends as well on the environment as on the w/c-ratio of the concrete. If the parameter α is not measured for the concrete and environment in question α could be estimated in the interval $0.25 \le w/c \le 0.45$ by Eq. 8 since the observations in the splash zone of α obey the relation:

Eq. 8; $$\alpha = 3 \times (0.55 - w/c)$$

However, there is a need for more observation of α.

In Eq. 7, the parameter D_{aex} denotes the value of the chloride diffusion coefficient at time $t = t_{ex}$, and if this parameter is not determined by the test method NT Build 443, cf. [9], (former APM 302) it could be estimated from the relation:

Eq. 9: $$D_{aex} = 50{,}000 \times \exp\left(-\sqrt{\frac{10}{w/c}}\right)$$

valid for concrete made from low-alkali sulphate resisting Portland cement in the interval $0.30 \leq w/c \leq 0.70$.

In the special case where the achieved diffusion coefficient $D_a = D_a(t)$ obeys Eq. 7, and the surface chloride concentration $C(0, t) = C_{sa}(t)$ obeys Eq. 3, the following non-dimensional variables are introduced:

Eq. 10: $$S_p = S \times (t_{ex}\, D_{aex})^p$$

Eq. 11: $$\tau = \left(\frac{t}{t_{ex}}\right)^{1-\alpha} - \left(\frac{t_{ex}}{t}\right)^{\alpha}$$

Eq. 12: $$z = \frac{0.5x}{\sqrt{t_{ex} D_{aex} \tau}}$$

Thus, the surface chloride concentration is written in the following way:

Eq. 13: $$C_{sa} = C_i + S_p \times \tau^p$$

and it is seen that Mejlbro's Ψ-solution yields the convenient form:

Eq. 14: $$C(x, t) = C_i + (C_{sa} - C_i) \times \Psi_p(z)$$

The application of Eq. 14 is shown in Example 1.

Calculation of chloride ingress into concrete

When the surface chloride concentration C_{sa} is time-dependent and could be estimated by a function as given by Eq. 13, the ingress x_r of a reference chloride concentration C_r can be determined by solving the following equation, cf. Eq. 14:

Eq. 15: $$C_r = C_i + (C_{sa} - C_i) \times \Psi_p(z_r)$$

where:

Eq. 16: $$z_r = \frac{0.5 x_r}{\sqrt{t_{ex} D_{aex} \tau}}$$

The parameter D_{aex} could be found by test method NT Build 443, cf. [9], (former APM 302) or estimated from Eq. 9. The variable τ is defined by Eq. 11, where α is given by Eq. 8. Thus, the solution of Eq. 16 yields

Eq. 17: $$x_r = 2 z_r \sqrt{t_{ex} D_{aex} \tau}$$

Here:

Eq. 18: $$z_r = \text{inv}\,\Psi_p\left(\frac{C_r - C_i}{C_{sa} - C_i}\right)$$

where inv Ψ_p is the inverse function of Ψ_p, cf. [1].

Prediction of service lifetime

The duration of the service lifetime of a marine RC structure is difficult to define and therefore also difficult to predict. Various opinions of the term »service lifetime« exist. Fidjestøl et al, cf. [10] declare that the consideration of lifetime versus rebar corrosion has a strong philosophical aspect. There are technical criteria (corrosion, cracking, spalling, loss of bearing capacity) as well as non-technical aspects (aesthetics, public opinion, loss of market value, public safety). When rebars of marine RC structures start to corrode due to ingress of chloride into the concrete, the mode of corrosion is pitting. When corroding rebars become pitted its properties change. Pitting is particularly vicious because it is a localized and intense form of corrosion, and failures often occur with extreme suddenness, cf. Fontana [11]. Marine RC structures like jetties are exposed to impact (ship) loads and need to be ductile. This indicates that the initiation stage is taken as the service lifetime of marine RC structures. Furthermore, the cost of rehabilitation of a marine RC structure during its initiation period is generally small compared with rehabilitiation during its propagation period, cf. de Sitter [12]. In this paper the service lifetime t_{LT} is defined as the initiation period t_{cr}. This paper considers two cases of lifetime prediction, namely:

- The service lifetime of a marine RC structure under design.
- The residual lifetime of a marine RC structure under service.

The main differences in these two cases are the information available, e.g. the properties of the concrete and the characteristics of the environment.

Mejlbro's Λ-solution

In case the achieved chloride diffusion coefficient $D_a(t)$ obeys Eq. 7 and the surface chloride concentration $C_{sa}(t)$ obeys Eq. 3, Mejlbro's Ψ-solution may be written as, cf. [1]:

Eq. 19: $$C(x, t) = C_i + S \times (0.5\, x)^{2p} \times \Lambda_p(z)$$

where z is defined by Eq. 12 and τ by Eq. 11. The functions $\Lambda_p(z)$, cf. [1], are defined as:

Eq. 20: $$\Lambda_p(z) = \frac{\Psi_p(z)}{z^{2p}}$$

and tabulated by Mejlbro, cf. [1]. Especially for $p = 0$, Eq. 20 yields:

Eq. 21: $$\Lambda_0(z) = \Psi_0(z) = \operatorname{erfc}(z)$$

Calculation of service lifetime

When as well the surface chloride concentration C_{sa} as the achieved chloride diffusion coefficient D_a are time-dependent and will obey Eq. 3 and Eq. 7 respectively the service lifetime defined as the initation period t_{cr} could be determined by solving the following equation:

Eq. 22: $$C_{\mathrm{cr}} = C_i + S \times (0.5c)^{2p} \times \Lambda_p(z_{\mathrm{cr}})$$

Here C_{cr} is the critical chloride concentration or the threshold value of the chloride concentration of the concrete with respect to the reinforcement, and c is the rebar concrete cover. The variable z_{cr} is defined by the relation:

Eq. 23: $$z_{\mathrm{cr}} = \frac{0.5c}{\sqrt{t_{ex} D_{aex} \tau_{\mathrm{cr}}}}$$

where τ_{cr} denotes:

Eq. 24: $$\tau_{\mathrm{cr}} = \left(\frac{t_{\mathrm{cr}}}{t_{ex}}\right)^{1-\alpha} - \left(\frac{t_{ex}}{t_{\mathrm{cr}}}\right)^{\alpha} \cong \left(\frac{t_{\mathrm{cr}}}{t_{ex}}\right)^{1-\alpha}$$

The approximation shown is valid since $t_{\mathrm{cr}} >> t_{ex}$ is the normal case. The solution of Eq. 22 with respect to z_{cr} yields:

Eq. 25: $$z_{\mathrm{cr}} = \mathrm{inv}\,\Lambda_p(y_{\mathrm{cr}})$$

where $\mathrm{inv}\,\Lambda_p$ is the inverse function of Λ_p, cf. [1], and

Eq. 26: $$y_{cr} = \frac{C_{cr} - C_i}{S \times (0.5c)^{2p}}$$

By introducing Eq. 23 and Eq. 24 into Eq. 25 and solving it with respect to t_{cr} the lifetime formula yields:

Eq. 27: $$t_{cr} = t_{ex} \times \left(\frac{0.5c}{\sqrt{t_{ex} D_{aex}} \times \text{inv}\Lambda_p(y_{cr})} \right)^{\frac{2}{1-\alpha}}$$

The application of Eq. 27 is shown in Example 3.

Calculation of residual lifetime

When calculating the service lifetime of a marine RC structure under design neither the aggressiveness of the marine environment nor the chloride diffusivity of the concrete is known. However, determination of the potential chloride diffusivity should be a part of the pretesting of concrete before the concrete structure is constructed.

When calculating the residual lifetime of a marine RC structure which has been in service for a (longer) period of time t_{in}, and the structure of which has been regularly under observation, the aggressiveness of the marine environment as well as the chloride diffusivity of the concrete can be estimated more accurately than is the case with a marine RC structure under design.

In principle the calculation of the residual lifetime of a marine structure in service does not deviate significantly from the calculation of the service lifetime of a marine RC structure under design, except that the observations obtained during the inspections are utilized in the latter. In the following a procedure for the calculation of the residual lifetime is recommended.

It is assumed that D_{aex} has been determined (test method NT Build 443) at the time when the concrete was exposed to chloride (seawater) for the first time. If this is not the case D_{aex} should be estimated by Eq. 9. However, it is also possible to determine the potential chloride diffusion coefficient at the time of inspection t_{in} by applying the test method NT Build 443, and value D_{aex}. In the splash zone the potential chloride diffusion coefficient usually decreases with time, cf. [13].

If a series of observations of D_a are avaiable from various inspections, it is possible to derive α from a linear regression analysis. If only one inspection has taken place and the achieved diffusion coefficient $D_a(t_{in})$ has been determined, α is found by the following formula:

Eq. 28: $$\alpha = \frac{\ln(D_{ain}/D_{aex})}{\ln(t_{ex}/t_{in})}$$

Hence, the residual lifetime yields:

Eq. 29: $$\mathrm{res}t_{cr} = t_{ex} \times \left[\left(\frac{0.5c}{\sqrt{t_{ex} D_{aex}} \times \mathrm{inv}\Lambda_p(y_{cr})} \right)^{\frac{2}{1-\alpha}} - \frac{t_{in}}{t_{ex}} \right]$$

Examples

In order to illustrate the application of the sets of formulae developed above the chloride profiles of a selected marine concrete are calculated by means of Eq. 14 and compared with observations made, cf. Example 1 and Figure 2. The case is selected among the concrete specimens tested at the Träslövsläge field exposure station, cf. [15] and [16].

The characteristics of the marine environment, p, S and S_p as defined by Eq. 3 and Eq. 10, and used in Example 2 are found by a regression analysis of the data presented by Swamy et al [14] from inspections of the surface chloride content up to the 30th year of exposure in the tidal zone and in the splash zone, cf. Figure 3.

Development of chloride profiles

Example 1. A series of concrete specimens (marked Ö) tested at the Träslövsläge field exposure station in Sweden, cf. [15] and [16], have the following properties and characteristics:

w/c	= 0.40	by mass
t_{ex}	= 0.04	year
C_i	= 0.03	% by mass cement
α	= 0.35	non-dimensional
S_p	= 2.20	% by mass cement
p	= 0.20	non-dimensional

The chloride profiles developed in the near-to-surface layer of concrete after 0.6 year, 1.0 year and 2.0 years of exposure have been measured and should be estimated by means of Eq. 14 of the paper.

The parameters S_p and p have been determined in order to fit the observed development of the surface chloride concentration C_{sa}, cf. Figure 1.

The chloride profiles after 0.6 year, 1,0 year and 2.0 years of exposure are determined by means of a spread sheet and shown in Figure 2.

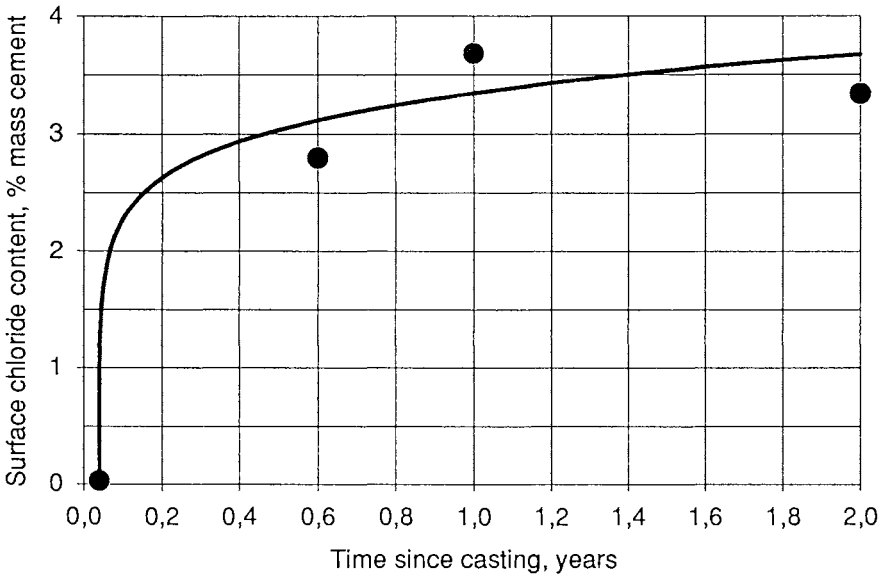

Fig. 1. *The development versus time of the surface chloride content C_{sa} and the achieved chloride diffusion coefficient D_a for the concrete specimens marked Ö in Trälövsläge field exposure station, cf. Example 1.*

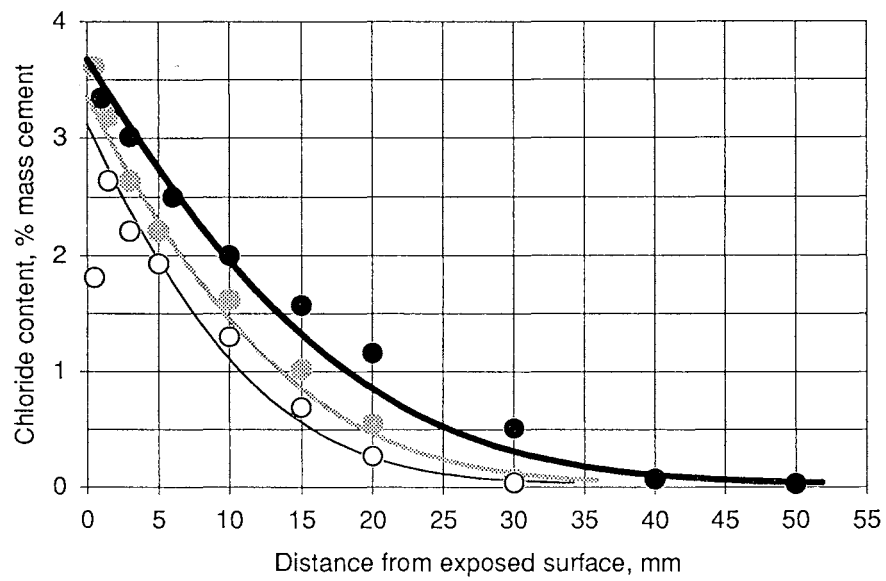

Fig. 2. *Calculated chloride profiles for exposure periods of 0.6, 1.0 and 2.0 years and the observations made, cf. Example 1. A fairly good agreement is observed.*

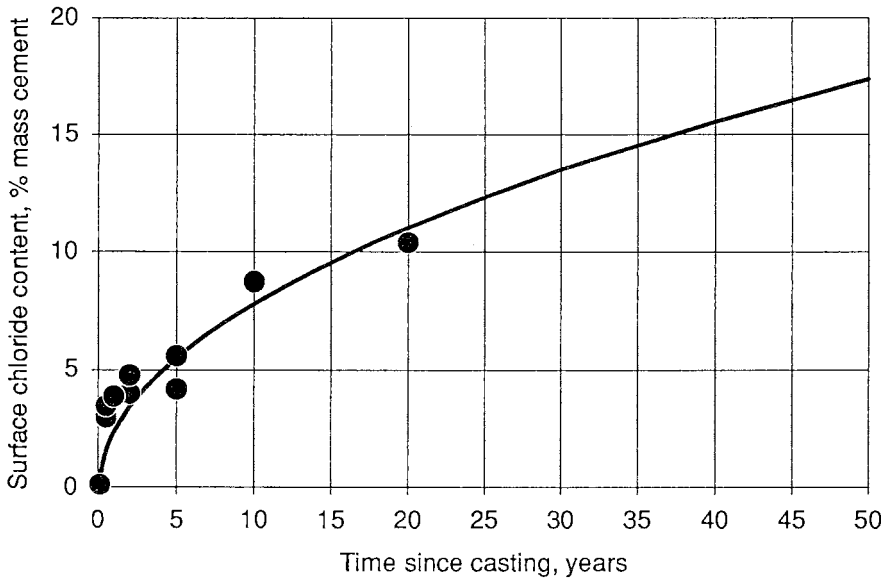

Fig. 3. *Development of the surface chloride content in the tidal zone and splash zone, cf [14]. The curve shown follows Eq. 13 of the paper with* S_P *=0.8 % by mass cement and with p=0.9.*

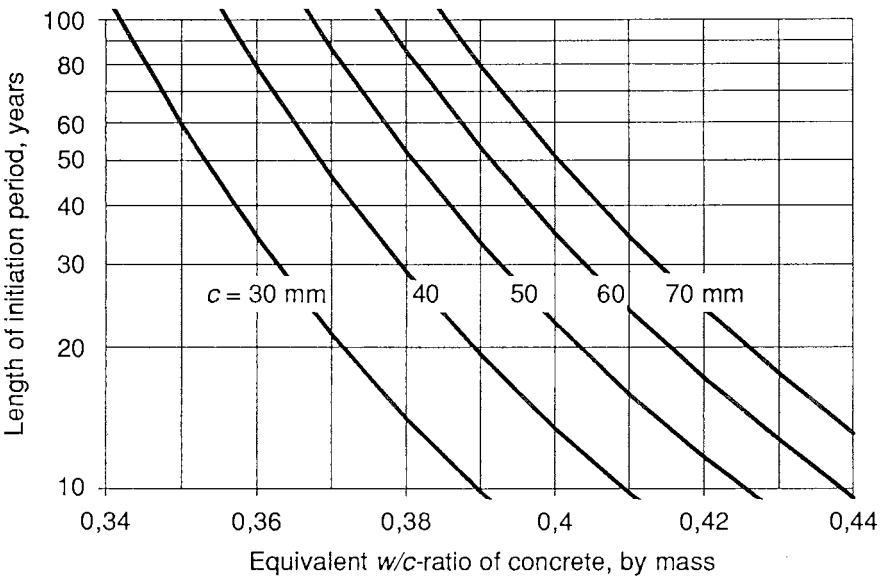

Fig. 4. *A »service for lifetime diagram« calculated by means of the step by step procedure shown in Example 2 and for the parameters* S_P*=0.8 and p=0.9 as demonstrated in Figure 3.*

Service lifetime

The expected service lifetime of a high performance concrete is calculated provided that the concrete properties and the environment characteristics are target values and that the chloride aggressiveness of the environment remains constant. The design service lifetime is determined in a similar way where the design values of the properties and the characteristics are used. There is no way of a checking the result today, therefore, the judgement of the result is placed in the reader's hands.

Example 2. A marine RC structure exposed to the splash zone of seawater has the following expected values of the decisive parameters:

c	= 40	mm
w/c	= 0.35	by mass
t_{ex}	= 0.1	year
C_i	= 0.0	% by mass cement
C_{cr}	= 0.8	% by mass cement
S_p	= 0.8	% by mass cement
p	= 0.9	non-dimensional

The calculation of the predicted length of the service lifetime (i.e. initiation period) is carried out in 6 steps. From Eq. 9 we get:

Step 1: $$D_{aex} = 50{,}000 \times \exp\left(-\sqrt{\frac{10}{0.35}}\right) = 239 \text{ mm}^2/\text{yr}$$

From Eq. 10 we get:

Step 2: $$S = \frac{0.8}{(0.1 \times 239)^{0.9}} = 0.0461 \text{ \% by mass cement per mm}^{1.8}$$

From Eq. 8 we get:

Step 3: $\alpha = 3 \times (0.55 - w/c) = 3 \times (0.55 - 0.35) = 0.60.$

From Eq. 26 we get:

Step 4: $$y_{cr} = \frac{C_{cr} - C_i}{S \times (0.5c)^{2p}} = \frac{0.80 - 0.0}{0.046 \times (0.5 \times 40)^{2 \times 0.9}} = 0.0791$$

From a table of $\Lambda_{0.9}(z)$, cf. [1], we get:

Step 5: $z_{cr} = \text{inv}\Lambda_{0.9}(0.0791) = 0.997$

Thus, the length of the predicted initiation period (expectation value) yields, cf. Eq. 27:

$$\text{Step 6:} \qquad t_{cr} = 0.1 \times \left(\frac{0.5 \times 40}{0.997 \times \sqrt{0.1 \times 337}} \right)^5 = 117 \text{ yr}$$

The above shown step by step procedure is used in order to draw the »service lifetime diagram« shown in Figure 4.

Concluding remarks

The chloride ingress into marine RC structures was introduced by means of a mathematical model about 25 years ago. During this period of time our knowledge about the basic behaviour of chloride ingress into concrete has increased significantly, particularly with respect to the influence of time on the decisive parameters of the problem.

State of the art

From an engineering point of view chloride ingress into concrete exposed to a marine environment can be estimated with an accuracy comparable to the best models available for predicting the bearing capacity of structural RC members on condition that the decisive parameters are known.

Need for further research

In order to bring the design of marine RC structures with respect to lifetime towards the standards of the design of RC structures with respect to bearing capacity, further research and examination are needed about:

- The critical chloride content (threshold value) in various types of concrete – the expectation values as well as the choice of their design values.
- Well-defined environmental zones of marine RC structures.
- The influence of time on the surface chloride content of various types of concrete for various surface treatments valid in the defined environmental zones – the expectation values as well as the choice of their design values.
- The influence of time on the achieved chloride diffusion coefficients of various types of concrete and the time of exposure valid for the defined environmental zones – the expectation values as well as the choice of their design values.

Acknowledgement

In connection with the application of mathematical modelling the author wishes to acknowledge the valuable advice and guidance provided by Leif Mejlbro, Department of Mathematics, the Technical University of Denmark. The author

also wishes to thank the Swedish BMB-group and the Norwegian LIGHTCON for the most inspiring co-operation in the field of marine RC structures.

References

[1] *Mejlbro, L.* »The complete solution of Fick's second law of diffusion with time-dependent diffusion coefficient and surface concentration«. Durability of marine concrete structures. CEMENTA, Danderyd. Sweden 1996.

[2] *Collepardi, M. et al.* »Kinetics of penetration of chloride ions into concrete«. Il Cemento No. 4. Italy 1970.

[3] *Collepardi, M. et al.* »Penetration of chloride ions into cement paste and concrete«. American Ceramic Society, Vol. 55. USA 1972.

[4] *Crank, J.* »The mathematics of diffusion«. Clarendon Press. UK 1986.

[5] *Takewaka, K., Mastumoto, S.* »Quality and cover thickness of concrete based on the estimation of chloride penetration in marine envi-ronments«. ACI SP 109-17, Detroit. USA 1988.

[6] *Uji, K., Matsuoka, Y., Maruya, T.* »Formulation of an equation for surface chloride content of concrete due to permeation of chloride«. Elsevier Applied Science, London. UK 1990.

[7] *Poulsen, E.* »On a model of chloride ingress into concrete having time-dependent diffusion coefficient«. Nordic miniseminar on chloride penetration into concrete structures, Gothenburg. Sweden 1993.

[8] *Maage, M., Helland, S., Carlsen, J. E.* »Practical non-steady chloride transport as a part of a model for predicting the initiation period«. RILEM workshop on chloride penetration into concrete. St-Rémy-Les-Chevreuse. France 1995.

[9] *NT Build 443.* »Concrete, hardened: Accelerated chloride penetration«. Approved 1995-11. NORDTEST register. Esbo. Finland 1996.

[10] *Fidjestøl, P., Tuutti, K.* »The importance of chloride diffusion«. RILEM workshop on chloride penetration into concrete. St-Rémy-Les-Chevreuse. France 1995.

[11] *Fontana, M. G.* »Corrosion engineering«. McGraw-Hill Book Company, London. UK 1986.

[12] *de Sitter, W. R.* »Cost for service life optimization – the law of fives«. CEB-RILEM workshop on durability of concrete structures. Copenhagen. Denmark 1984.

[13] *Tang, L., Nilsson, L. O.* »Chloride diffusivity in high strength concrete at different ages«. Nordic Concrete Research, publication No. 11, Oslo. Norway 1992.

[14] *Swamy, R. H., Hamada, H., Laiw, J. C.* »A critical evaluation of chloride penetration into concrete in marine environment«. Corrosion and Corrosion Protection of Steel in Concrete, University of Sheffield, Sheffield. UK 1995.

[15] *Sandberg, Palle.* »Betongsorter för Öresundbron testas i havsvatten i Träslövsläge«. Betong No. 3, Stockholm. Sweden 1993.
[16] *Malmström, K., Petersson, Per-Erik.* »Betong testas i havsklimat«. Betong No. 2, Stockholm. Sweden 1992.

The Complete Solution of Fick's Second Law of Diffusion with Time-dependent Diffusion Coefficient and Surface Concentration

Leif Mejlbro

Department of Mathematics, Technical University of Denmark, DK-2800 Lyngby, Denmark

ABSTRACT. Fick's Second Law of Diffusion with time-dependent diffusion coefficient and surface concentration is solved. Mimicking the classical solution, special time-dependent surface concentration functions are considered. These models are used in giving estimates of the lifetime of the structure, when the concrete cover is given, as well as estimates of the thickness of the concrete cover, when the expected lifetime is given.

KEYWORDS. Chloride ingress into concrete. Fick's Second Law of Diffusion. Time-dependent diffusion coefficient. Time-dependent surface concentration.

AMS CLASSIFICATION: 35K20

1 Introduction

It is generally accepted that chloride ingress into concrete in many cases follows Fick's Second Law of Diffusion, i.e. the chloride concentration $C(x,t)$ at the distance x from the surface and to time t satisfies the generalised *heat equation*

$$\frac{\partial C}{\partial t} = \frac{\partial}{\partial x}\left\{D(x,t)\frac{\partial C}{\partial x}\right\} \tag{1}$$

with some initial and boundary conditions. Here, $C = C(x,t)$ denotes the *chloride profile*, i.e. the chloride concentration of the concrete versus the distance x from the exposed surface at time t, and $D(x,t)$ is the *chloride diffusion coefficient.*

In the most general setup, the chloride diffusion coefficient D depends on many other parameters like e.g. the conditions when one particular pier is concreted, its maturity age, the constituents of the concrete, the size of its pores, the choride concentration itself, and the temperature. Hence, (1)

is only an approximation (a model) of the true situation. By solving (1) one obtains a mathematical description which can be tested. If the tests are in a reasonable concordance with the solutions of (1), then (1) is accepted as a model, which can be used in practice, until a better model has been established.

What transport of chloride is concerned, concrete is neither an isotropic medium nor a homogeneous material. These anomalies are conveniently described as functions in time t and location x. Here we shall not consider the more difficult nonlinear case, where D also depends on C. Thus, $D(x,t)$ depends only on how the pier is concreted and by which constituents (parameters given in advance), and of the time t and the location x (evolution parameters). For that reason we shall consider $D(x,t)$ as a chloride diffusion coefficient belonging to that particular pier, as well as to similar ones, depending only on x and t. This idealisation has the advantage that (1) can be understood by both civil engineers and mathematicians.

Hence, the diffusion coefficient $D(x,t) > 0$ depends in general on x and t. It was a big surprise to the author that no general solution formula for (1) can be found in the mathematical literature, where this formula should also be applicable in practice, in spite of the fact that (1) is only a slight generalisation of one of the classical partial differential equations. This observation has recently been confirmed from other sources, in the sense that the only possible authors who may have handled equations like (1) in special cases are Friedman, Ladyzhenskaja, Solonnikov and Uraltsev. All their work has not yet been checked, but the papers and books of them, which have been, cannot be used in this context.

The present contribution must therefore be considered as a step towards a solution of the general equation (1). The main objective here is that the solution should also be easy to apply in practice.

Although the value of $C(x,t)$ may be interesting in its own right, the author has in mind to give a simple method of estimating the time t_{cr}, when the chloride concentration $C(x,t)$ exceeds a critical value C_{cr}, at which the steel bars below the concrete cover (at distance x from the surface) start to corrode, causing physical damage to the structure, which will diminish the safety against failure according to the Code of Practice. The exact value of C_{cr} is not fixed. It was pointed out by E. Poulsen [12], that when noncarbonated concrete surrounding the reinforcement of black steel bars is considered, then corrosion can be neglected when $C(x,t)$ is below 0.4% by mass cement,

it may happen occasionally when $C(x,t)$ lies between 0.4% and 1.0%; it is quite probable when $C(x,t)$ lies between 1.0% and 2.0% by mass cement, and finally it is certain when $C(x,t)$ exceeds 2.0%. These figures are based on an English investigation, cf. R.D.Browne et al. [1]. In other situations we may get other limits.

The style of the paper will be that of a mathematician, where the results are formulated in propositions, theorems and corollaries. Realising that most of the readers probably do not know much about partial differential equations (and of course cannot be assumed to be experts within this particular field) the proofs have been kept as elementary as possible, leaving out the more delicate question of uniqueness, which requires harder mathematical methods. The prerequisites will therefore only be mathematics which is taught during the first couple of years at every technical university in the world.

Since only little is assumed from the theory of Partial Differential Equations, it has been chosen not to give any reference to this particular mathematical field. All that is needed is developed, and yet only the question of uniqueness is omitted, because it is surprisingly enough harder to handle.

In Section 2 a brief history of the problem is given. In Section 3 we consider the case where $D(t)$ only depends on the time t. By a change of variables the problem is reduced to a simpler one, which is solved completely in Section 4. In Section 5 we consider the special case, where $\tilde{\varphi}(T) = T^p$ for some $p \geq 0$, and the functions $\Psi_p(z)$ and $\Lambda_p(z)$ are introduced. It is here necessary to give a series expansion of $\Psi_p(z)$ from which the tables of these functions at the end of this paper have been derived. The results in Section 5 should be easy to implement. The connection with other approaches is discussed in Section 6. Finally, comments to the tables are given in Section 7.

ACKNOWLEDGEMENT. The author wants to express his gratitude towards Ervin Poulsen, who formulated this problem and stimulated this investigation, and for his help in finding the right formulations, such that this contribution should be possible to read for civil engineers and not just for mathematicians. Furthermore, my colleague Per W. Karlsson is thanked for his interest and support in this attempt to bridge the gap between pure mathematics and applied civil engineering, as well as for his help in finding the connection to the classical mathematical field of Special Functions.

2 Historical Background

In order to explain why the particular problem of only time-dependence of the diffusion coefficient is considered, it is worth while to present a brief historical record. The author is here in debt to Ervin Poulsen, who provided the relevant references and also wrote a list of the main events of the theory. Without his help this section could never have been written.

The roots of the mathematical theory go back to 1822, when J.B.J. Fourier formulated the socalled *heat equation*

$$\frac{\partial f}{\partial t} = \frac{\partial^2 f}{\partial x^2}$$

in order to describe heat conduction in materials. Fourier never thought of chloride penetration into concrete, so he is only mentioned here, because the heat equation from a mathematical point of view is identical with the simplest *equation of diffusion.*

In 1855, A. Fick created a mathematical model for diffusion in permeable materials with no mention, however, of chloride diffusion. That Fick's second law could be used for chloride diffusion into concrete was first realised by M. Collepardi et al. [3] in 1970. Since their paper was written in Italian, their work remained unnoticed outside Italy until 1972, when it was translated into English, cf. M. Collepardi et al. [4]. Having only results available from short time experiments, and probably also due to mathematical difficulties (the general equation is unsolved even today) they only considered the case of constant diffusion coefficient and constant surface chloride concentration, where an exact solution was known.

Based on inspection of Japanese marine constructions, K. Takewaka et al. [17] conjectured in 1988 that the chloride diffusion coefficient of concrete, besides depending on the water/cement proportion, also was time-dependent, and they suggested that $D(t)$ might have the structure $C_i + c \cdot t^p$. This was confirmed in 1993 by M. Maage et al. [8], who investigated Norwegian coastal bridges, and later on, in 1994, by P.S. Mangat et al. [9], who made a large full scale test.

In the meantime, in 1990, K. Uji [18] conjectured, also based on inspection of Japanese marine constructions, that the chloride concentration $C(0,t)$ at the surface (the *boundary condition* in mathematical terms) was also time-dependent. They suggested that it was proportional to the square root of

the time t. If so, Crank [5] could provide a solution. This hypothesis was confirmed in 1994 by R.N. Swamy et al. [16] for marine concrete in splash-zones, and in tidal zones, and in a marine atmosphere. However, for concrete under seawater the square root model does not describe the situation. The figures 7 and 18 of Swamy et al. [16] suggest that one might consider a logistic condition instead like e.g. $C(0,t) = S\{1 - B\exp(-At^{\alpha})\}$. In principle this can now be solved by applying Theorem 1 in Section 4, but the resulting integral is not easy to handle.

Without knowing this history, L. Mejlbro [10] solved in 1995 the special problem, when $D(x)$ only depends on the location x. The solution was used by A.S. Østerdal [11] in her thesis. It was later realised independently by Ervin Poulsen and the author that the combined results [10] and [11] actually implied that if $D(x,t)$ depends on both x and t, then the solution $C(x,t)$ is far less influenced by variations in x than by variations in t. After all, because a general solution does not exist in a closed form, it is therefore very natural first to study the case where the diffusion coefficient $D(t)$ and the surface chloride concentration both are time-dependent, and this is the object of this contribution.

3 Mathematical Formulation

We shall solve (1) completely under the assumptions that the diffusion coefficient $D(x,t) = D(t)$ and the boundary condition $C_i + \varphi(t)$ for $x = 0$ are only time-dependent, while the initial condition for $t = t_{ex}$, the *exposure time*, is a constant C_i. In mathematical terms this restricted problem can be formulated in the following way:

$$
\begin{aligned}
&\frac{\partial C}{\partial t} = D(t)\frac{\partial^2 C}{\partial x^2}, && x > 0,\ t > t_{ex},\\
&C(x,t_{ex}) = C_i, && x \geq 0,\\
&C(0,t) = C_i + \varphi(t) && t \geq t_{ex},\\
&\lim_{x\to+\infty} C(x,t) = C_i, && t \geq t_{ex},
\end{aligned}
\tag{2}
$$

where $\varphi(t)$ and $D(t)$ are continuous functions, and $\varphi(t_{ex}) = 0$, and $D(t) > 0$ "almost everywhere" for $t \geq t_{ex}$. In physical terms $C(x,t)$, and $\varphi(t)$, and

C_i are dimensionless, while the physical dimension of $D(t)$ is lenght^2/time; a suitable unit for $D(t)$ is mm^2/yr. It will be important in the following to keep account of the physical dimension in order to understand all the transformations.

In practice we always have $D(t) > 0$, but it might for theoretical reasons be convenient for the models also to allow $D(t) = 0$ as well as $D(t) = +\infty$ in "not too many points".

It is no restriction for the applications also to assume that $\varphi'(t)$ exists and is continuous for $t > t_{ex}$, though $\varphi'(t)$ may not exist for $t = t_{ex}$.

The last condition in (2) has been added to remind the reader that without a condition of this type one does not have uniqueness of the solution. From a technical point of view this is quite natural (the chloride concentration is constant at infinity), and as no uniqueness proof is presented here, it will be omitted in the rest of the paper and only tacitly assumed.

The trick of solving (2) is to perform the monotone change of variables

$$(3) \qquad \begin{aligned} T &= T(t) = \int_{t_{ex}}^{t} D(\tau)\,d\tau = (t - t_{ex})\left\{\frac{1}{t - t_{ex}}\int_{t_{ex}}^{t} D(\tau)\,d\tau\right\} \\ &= (t - t_{ex})D_a(t), \end{aligned}$$

where $D_a(t)$ denotes the mean value of the chloride diffusion coefficient over the interval from t_{ex} to $t > t_{ex}$. It is easily seen that the physical dimension of T is length^2, and we shall use the unit mm^2.

Introducing $\tilde{C}(x,t) = C(x,t) - C_i$ (dimensionless), and noting that

$$\frac{\partial \tilde{C}}{\partial t} = \frac{dT}{dt}\frac{\partial \tilde{C}}{\partial T} = D(t)\frac{\partial \tilde{C}}{\partial T},$$

it is easily seen that (2) is transformed into the equivalent problem

$$(4) \qquad \begin{aligned} &\frac{\partial \tilde{C}}{\partial T} = \frac{\partial^2 \tilde{C}}{\partial x^2}, && x, T > 0, \\ &\tilde{C}(x,0) = 0, && x \geq 0, \\ &\tilde{C}(0,T) = \varphi(t(T)) = \tilde{\varphi}(T), && T \geq 0, \end{aligned}$$

where $t(T)$ is the solution $t \geq t_{ex}$ of the equation

$$(t - t_{ex})D_a(t) = T.$$

If therefore $\tilde{C}$ is a solution of (4), then

$$C(x,t) = \tilde{C}(x,T(t)) + C_i = \tilde{C}(x,(t-t_{ex})D_a(t)) + C_i \tag{5}$$

is the solution of (2), where (3) has been used. We may thus in the following concentrate on solving (4).

4 Solution of Problem (4)

In order not to confuse the reader the notation of Section 2 is maintained, i.e., T is now the (transformed) time variable, and the functions involved are $\tilde{C}(x,T)$ and $\tilde{\varphi}(T)$.

Theorem 1 *Assuming that $\tilde{\varphi}(T)$ is continuous for $T \geq 0$, and differentiable for $T > 0$, and that $\tilde{\varphi}(0) = 0$, the solution of (4) is given by*

$$\begin{aligned} \tilde{C}(x,T) &= \int_0^T \tilde{\varphi}'(T-\tau)\mathrm{erfc}\left(\frac{x}{\sqrt{4\tau}}\right) d\tau \\ &= \int_0^T \tilde{\varphi}'(\tau)\mathrm{erfc}\left(\frac{x}{\sqrt{4(T-\tau)}}\right) d\tau. \end{aligned} \tag{6}$$

Here, $\mathrm{erfc}(u)$ denotes the complementary error function given by

$$\mathrm{erfc}(u) = \frac{2}{\sqrt{\pi}} \int_u^{+\infty} \exp(-s^2)\, ds.$$

PROOF. It suffices to check that (6) satisfies (4). First note that the two integrals in (6) are equal by the change of variables $\tau \to t - \tau$.

It is well known, or easy to check, that $\mathrm{erfc}(x/\sqrt{4T})$ is a solution of the differential equation in (4). Using this fact we get from the latter expression of (6) that

$$\begin{aligned} \frac{\partial \tilde{C}}{\partial T} &= \lim_{\tau \to T} \tilde{\varphi}'(\tau)\mathrm{erfc}\left(\frac{x}{\sqrt{4(T-\tau)}}\right) + \int_0^T \tilde{\varphi}'(\tau)\frac{\partial}{\partial T}\mathrm{erfc}\left(\frac{x}{\sqrt{4(T-\tau)}}\right) d\tau \\ &= 0 + \int_0^T \tilde{\varphi}'(\tau)\frac{\partial^2}{\partial x^2}\mathrm{erfc}\left(\frac{x}{\sqrt{t(T-\tau)}}\right) d\tau = \frac{\partial^2 \tilde{C}}{\partial x^2}, \end{aligned}$$

and $\tilde{C}(x,t)$ satisfies the differential equation of (4).

Since $\tilde{\varphi}(0) = 0$ by assumption, an integration by parts of the first integral in (6) gives for $x > 0$

$$\tilde{C}(x,T) = \frac{x}{\sqrt{4\pi}} \int_0^T \tilde{\varphi}(T-\tau) \frac{1}{\tau\sqrt{\tau}} \exp\left(-\frac{x^2}{4\tau}\right) d\tau. \tag{7}$$

Since the exponential function in the integrand tends faster to 0 than $\tau\sqrt{\tau}$ for $\tau \to 0+$, it follows that $\tilde{C}(x,0) = 0$, and the initial condition of (4) is satisfied. Arguing similarly we note that also $\lim_{x\to+\infty} \tilde{C}(x,T) = 0$, so the hidden condition assuring the uniqueness is satisfied as well.

Finally, when $x \to 0$ we get by $\tilde{\varphi}(0) = 0$,

$$\begin{aligned} \tilde{C}(x,T) &= \int_0^T \tilde{\varphi}'(\tau)\operatorname{erfc}\left(\frac{x}{\sqrt{4(T-\tau)}}\right) d\tau \to \int_0^T \tilde{\varphi}'(\tau)\operatorname{erfc}(0)\, d\tau \\ &= \int_0^T \tilde{\varphi}'(\tau)\, d\tau = \tilde{\varphi}(T), \end{aligned}$$

and the boundary condition is fulfilled, so Theorem 1 has been proved. □

Consulting books in mathematics on this subject one would find a formula similar to (7), but not to (6). For our purposes (6) is far more convenient than (7), where the only disadvantage is that we *must* assume that $\tilde{\varphi}(0) = 0$. There are, however, means to circumvene this obstacle, which will implicitly be used in the next section. Theorem 1 may be the starting point for future work, when specified functions $\tilde{\varphi}$ are considered. So far for most applications it is difficult to apply.

It is worth while here to note that if $\tilde{\varphi} = \tilde{\varphi}_1 + \tilde{\varphi}_2$, where $\tilde{\varphi}(0) = \tilde{\varphi}_1(0) = \tilde{\varphi}_2(0) = 0$, and $\tilde{\varphi}_1$ and $\tilde{\varphi}_2$ are differentiable for $T > 0$, then the solution of (4) is given by

$$\begin{aligned} \tilde{C}(x,T) &= \int_0^T \tilde{\varphi}'(\tau)\operatorname{erfc}\left(\frac{x}{\sqrt{4(T-\tau)}}\right) d\tau \\ &= \int_0^T \tilde{\varphi}_1'(\tau)\operatorname{erfc}\left(\frac{x}{\sqrt{4(T-\tau)}}\right) d\tau + \int_0^T \tilde{\varphi}_2'(\tau)\operatorname{erfc}\left(\frac{x}{\sqrt{4(T-\tau)}}\right) d\tau, \end{aligned}$$

cf. (6). This is actually the *principle of superposition* (mathematicians call this *linearity* of the problem). If therefore $\tilde{\varphi}$ is split into a (finite) sum of functions, which are easier to handle than $\tilde{\varphi}$ itself, e.g. if

$$\tilde{\varphi}(T) = \sum_{j=1}^{n} c_j T^{p_j} = \sum_{j=1}^{n} \tilde{\varphi}_j(T), \qquad \tilde{\varphi}_j(T) = c_j T^{p_j},$$

cf. Theorem 2 below, then one first solves the simpler problems, and then one adds all of them. Of course each c_j here is of dimension length$^{-2p_j}$, such that $\tilde{\varphi}(T)$ becomes dimensionless.

5 The case $\tilde{\varphi}(T) = T^p$ for some $p \geq 0$.

Let us consider the case, where $\tilde{\varphi}(T) = (T/T_0)^p$ for some $p \geq 0$, where we put $T_0 = 1$ mm^2 in order to make $\tilde{\varphi}(T)$ dimensionless. This particular case is chosen for three reasons:

- This special case is fairly simple to solve for general p.
- The structure is very similar, though more general, to the classical problem of constant D.
- It is possible by superposition to solve the general equation (2). (The procedure will only be sketched in Section 7.)

Consulting the literature one will find (cf. e.g. Carslaw and Jaeger [2] and Crank [5]) that the solution of (4) is known, when p equals $0, \frac{1}{2}, 1, \frac{3}{2}, 2, \ldots$. Here we shall solve the problem for general $p \geq 0$ by first proving that the structure of the solution is given by

$$\tilde{C}_p(x,T) = \left(\frac{T}{T_0}\right)^p \Psi_p\left(\frac{x}{\sqrt{4T}}\right), \quad p \geq 0, \tag{8}$$

where the functions $\Psi_p(z)$ satisfy an ordinary differential equation of second order which can be solved by means of a series expansion.

First note that if $p = 0$, then $(T/T_0)^p = 1$, and it is well known that the solution of (4) is given by

$$\tilde{C}_0(x,T) = \operatorname{erfc}\left(\frac{x}{\sqrt{4T}}\right) = \left(\frac{T}{T_0}\right)^0 \Psi_0\left(\frac{x}{\sqrt{4T}}\right),$$

where $\Psi_0(z) = \operatorname{erfc}(z)$. Note that $\tilde{\varphi}(0) = 1 \neq 0$ in this case, so Theorem 1 does not apply.

Proposition 1 *The solution of (4) with* $\tilde{\varphi}(T) = (T/T_0)^p$, $p \geq 0$, *is given by (8), i.e.*

$$\tilde{C}_p(x,T) = \left(\frac{T}{T_0}\right)^p \Psi_p\left(\frac{x}{\sqrt{4T}}\right), \quad T_0 = 1 \text{ mm}^2,$$

where $\Psi_p(z)$ *is the unique solution of the ordinary initial value problem*

$$\begin{cases} \Psi_p''(z) + 2z\Psi_p'(z) - 4p\Psi_p(z) = 0, \\ \\ \Psi_p(0) = 1, \quad \Psi_p'(0) = -2\Gamma(p+1)/\Gamma\left(p+\frac{1}{2}\right). \end{cases} \tag{9}$$

Even though this result fully describes the structure of the solutions, it is only called a proposition, because it is the stepping stone to the better result of Theorem 2.

PROOF. When $p = 0$, an easy check shows that $\Psi_0(z) = \operatorname{erfc}(z)$ is indeed the solution of

$$\begin{cases} \Psi_0''(z) + 2z\Psi_0'(z) = 0, \\ \\ \Psi_0(0) = 1, \quad \Psi_0'(0) = -2\Gamma(1)/\Gamma\left(\frac{1}{2}\right) = -2/\sqrt{\pi}. \end{cases}$$

Let $p > 0$. By Theorem 1, the solution of (4) is given by (6), where $\tilde{\varphi}(T) = (T/T_0)^p$, i.e. by the change of variables $\tau = T \cdot u$,

$$\begin{aligned} \tilde{C}_p(x,T) &= T_0^{-p} \int_0^T p(T-\tau)^{p-1} \operatorname{erfc}\left(\frac{x}{\sqrt{4\tau}}\right) d\tau \\ &= p\left(\frac{T}{T_0}\right)^p \int_0^1 (1-u)^{p-1} \operatorname{erfc}\left(\frac{x}{\sqrt{4T}} \cdot \frac{1}{\sqrt{u}}\right) du, \end{aligned}$$

which is precisely of the form (8), if we put

$$\Psi_p(z) = p \int_0^1 (1-u)^{p-1} \operatorname{erfc}\left(\frac{z}{\sqrt{u}}\right) du. \tag{10}$$

Here,

$$\Psi_p(0) = p\int_0^1 (1-u)^{p-1}\,du = 1,$$

so Ψ_p satisfies the first initial condition of (9).

Differentiating (10) we obtain

$$\Psi_p'(z) = -\frac{2p}{\sqrt{\pi}}\int_0^1 (1-u)^{p-1}u^{(1/2)-1}\exp\left(-\frac{z^2}{u}\right)\,du.$$

Hence, by using the definition of the B-function,

$$\begin{aligned}\Psi_p'(0) &= -\frac{2p}{\sqrt{\pi}}\int_0^1 (1-u)^{p-1}u^{(1/2)-1}\,du = -\frac{2p}{\sqrt{\pi}}\mathrm{B}\left(p,\frac{1}{2}\right)\\ &= -\frac{2p}{\Gamma(\frac{1}{2})}\cdot\frac{\Gamma(p)\Gamma(\frac{1}{2})}{\Gamma(p+\frac{1}{2})} = -2\frac{\Gamma(p+1)}{\Gamma(p+\frac{1}{2})},\end{aligned}$$

so Ψ_p also satisfies the second initial condition of (9).

In order to derive the differential equation of (9) we just insert (8) into Fick's Second Law of Diffusion (4). This gives after some tedious calculations

$$\Psi_p''\left(\frac{x}{\sqrt{4T}}\right) = 4p\Psi\left(\frac{x}{\sqrt{4T}}\right) - 2\cdot\frac{x}{\sqrt{4T}}\cdot\Psi_p'\left(\frac{x}{\sqrt{4T}}\right).$$

The substitution $z = x/\sqrt{4T}$ (note that z is dimensionless) and a rearrangement of the equation finally gives the differential equation of (9), and Proposition 1 is proved. □

Once Proposition 1 has been proved, it is easy to derive a far better result (Theorem 2 below). Since the differential equation in (9) has no singular points, and since its coefficients are entire functions, its unique solution is also an entire function, i.e. $\Psi_p(z)$ can be written as a series

$$\Psi_p(z) = \sum_{n=0}^{+\infty} a_{p,n}z^n, \quad a_{p,0} = \Psi_p(0) = 1, \quad a_{p,1} = \Psi_p'(0) = -2\frac{\Gamma(p+1)}{\Gamma\left(p+\frac{1}{2}\right)},$$

(11)

which is convergent for all $|z| < +\infty$, provided that $-2\Gamma(p+1)/\Gamma(p+\frac{1}{2})$ is finite, i.e. $p \neq -1,-2,-3,\cdots$. (Note that we put $a_{p,1} = 0$, when $p+\frac{1}{2} = 0,-1,-2,-3,\cdots$.) Incidentally we have therefore extended Proposition 1 to

every p which is not a negative integer. This is far more than we want. In a technical setup, only $p \geq 0$ makes sense, but the mathematical solution is still valid for negative p, as long as p is not an integer.

When (11) is inserted into (9) we get after some reduction the recursion formula

$$a_{p,n+2} = \frac{4(p - \frac{n}{2})}{(n+2)(n+1)} a_{p,n}, \quad n \geq 0.$$

Knowing $a_{p,0}$ and $a_{p,1}$ from (11), all coefficients can be calculated from this formula. Introducing the notation

$$q^{(0)} := 1; \quad q^{(n)} = q(q-1)\cdots(q-n+1) \quad (n \text{ factors}), \quad n \geq 1,$$

it is easily shown that

$$a_{p,2n} = \frac{4^n}{(2n)!} p^{(n)}, \quad a_{p,2n+1} = -2\frac{\Gamma(p+1)}{\Gamma(p+\frac{1}{2})} \cdot \frac{4^n}{(2n+1)!} \left(p - \frac{1}{2}\right)^{(n)}.$$

Hence, we have proved the following extension of Proposition 1:

Theorem 2 *The solution of (4) with* $\tilde{\varphi}(T) = (T/T_0)^p$, $p \geq 0$, (or just p not a negative integer) *is given by*

$$\tilde{C}_p(x,T) = \left(\frac{T}{T_0}\right)^p \Psi_p\left(\frac{x}{\sqrt{4T}}\right), \quad T_0 = 1 \text{ mm}^2,$$

where

$$\Psi_p(z) = \sum_{n=0}^{+\infty} \frac{1}{(2n)!} p^{(n)} (2z)^{2n} - \frac{\Gamma(p+1)}{\Gamma(p+\frac{1}{2})} \sum_{n=0}^{+\infty} \frac{1}{(2n+1)!} \left(p - \frac{1}{2}\right)^{(n)} (2z)^{2n+1}. \tag{12}$$

Due to the factorials in the denominators, the series in (12) converge very fast for $0 \leq z \leq 2$, which is the most interesting interval, when chloride ingress into concrete is considered. A programme for the pocket calculator HP-42S is given at the end of the paper.

One should note the following

Corollary 1 *The functions Ψ_p defined by (12) satisfy*

$$\Psi_p'(z) = -2\frac{\Gamma(p+1)}{\Gamma(p+\frac{1}{2})}\Psi_{p-(1/2)}(z),$$

$$\Psi_p''(z) = 4p\Psi_{p-1}(z),$$

$$4p\Psi_{p-1}(z) - 4z\frac{\Gamma(p+1)}{\Gamma(p+\frac{1}{2})}\Psi_{p-(1/2)}(z) - 4p\Psi_p(z) = 0,$$

whenever these expressions make sense, i.e. for $p \neq 0, -\frac{1}{2}, -1, -\frac{3}{2}, \cdots$. Note that the formula for $\Psi_p'(z)$ is also valid for $p = 0$.

PROOF. The expression for $\Psi_p'(z)$ follows by a differentiation of (12). Iterating this process we get

$$\begin{aligned}\Psi_p'' &= \left(-2\frac{\Gamma(p+1)}{\Gamma(p+\frac{1}{2})}\right)\cdot\left(-2\frac{\Gamma(p+\frac{1}{2})}{\Gamma(p)}\right)\Psi_{p-1}(z)\\ &= 4\frac{\Gamma(p+1)}{\Gamma(p)}\Psi_{p-1}(z) = 4p\Psi_{p-1}(z).\end{aligned}$$

Using these in (9) we finally get our last formula, which is a recursion formula, from which $\Psi_p(z)$ can be calculated, when $\Psi_{p-1}(z)$ and $\Psi_{p-(1/2)}(z)$ are known. □

Using the transformations (3) and (5) we easily get

Corollary 2 *The solution of the initial/boundary value problem*

$$\begin{aligned}&\frac{\partial C}{\partial t} = D(t)\frac{\partial^2 C}{\partial x^2}, && x > 0, t > t_{ex},\\ &C(x, t_{ex}) = C_i, && x \geq 0,\\ &C(0,t) = C_i + S\cdot\{(t-t_{ex})D_a(t)\}^p, && t > t_{ex}, p > 0 \text{ const.}\end{aligned}$$

is given by

$$\begin{aligned}(13)\ C_p(x,t) &= C_i + S\cdot\{(t-t_{ex})\cdot D_a(t)\}^p\cdot\Psi_p\left(\frac{x}{\sqrt{4(t-t_{ex})D_a(t)}}\right)\\ &= C_i + S\cdot\left(\frac{x}{2}\right)^{2p}\Lambda_p\left(\frac{x}{\sqrt{4(t-t_{ex})D_a(t)}}\right),\end{aligned}$$

where $\Psi_p(z)$ *is given by (12),and where* S *is of unit* mm^{-2p}, *and where* $\Lambda_p(z) := \Psi_p(z)/z^{2p}$ *for* $z > 0$.

Tables of $\Psi_p(z)$ and $\Lambda_p(z)$ can be found in Section 7. The functions $\Psi_p(z)$ would be preferred by mathematicians, but a closer examination shows that the functions $\Lambda_p(z)$ are also very useful in the applications, which will be demonstrated in an example below. More precisely, assuming that the model of Corollary 2 can be applied, the functions Ψ_p are used, when we want to estimate x for a given lifetime t, while the functions Λ_p are used, when we want to estimate the time t, when $C(x,t)$ exceeds a given critical level (threshold value) at location x. Thus Corollary 2 may e.g. be applied in the following way: Suppose that our model is described by Corollary 2 for some $D(t)$, or equivalently for some $D_a(t)$, together with some $p > 0$. Let C_{cr} denote the critical concentration of chloride in concrete. We want to estimate the time, when C_{cr} is reached at the distance $x = c$ from the surface, i.e. we want to solve the equation

$$C_p(c,t) = C_{cr}, \quad C_{cr} \gg C_i,$$

in t.

Putting $x = c$ and $T = (t - t_{ex})D_a(t)$, and finally $z = c/\sqrt{4T}$ into (13), this equation also reads

$$C_{cr} = C_i + S \cdot \left(\frac{c}{2}\right)^{2p} \Lambda_p(z),$$

from which by a rearrangement,

$$\Lambda_p(z) = \frac{C_{cr} - C_i}{S} \cdot \left(\frac{2}{c}\right)^{2p}. \tag{14}$$

The left hand side $\Lambda_p(z)$ of (14) is trivially decreasing continuously from $+\infty$ to 0, when z goes from 0 to $+\infty$. Hence, (14) has a unique solution z, which is easily found by tables of $\Lambda_p(z)$.

Once z has been found, we get T from

$$T = \left(\frac{c}{2z}\right)^2.$$

Finally, solving the equation

$$\int_{t_{ex}}^{t} D(\tau)\,d\tau = (t - t_{ex})D_a(t) = T = \left(\frac{c}{2z}\right)^2,$$

we obtain the critical time t, when corrosion starts at depth $x = c$.

EXAMPLE. The following is a modification of an example given by Ervin Poulsen in a letter to the author, who got the permission to include it here.

Suppose that we can use the model given by Corollary 2. Furthermore, assume that we have performed some measurements, which show that the *mean value chloride diffusion coefficient* $D_a(t)$ [not to be confused with $D(t)$ itself] is approximately given by

$$D_a(t) = D_0\left(\frac{t_{ex}}{t}\right)^{\alpha} \qquad \text{for } t \geq t_{ex} \tag{15}$$

for some $\alpha > 0$, where the dimension of D_0 is length^2/time. The point is that $D_a(t)$ is easier to measure than $D(t)$ itself. By differentiating (3) we get from (15) that we implicitly assume that

$$D(t) = D_0\left\{(1-\alpha)\left(\frac{t_{ex}}{t}\right)^{\alpha} + \alpha\left(\frac{t_{ex}}{t}\right)^{\alpha+1}\right\} \qquad \text{for } t \geq t_{ex},$$

from which we derive the important observation that

$$D_0 = D(t_{ex}) = D_a(t_{ex}).$$

Concerning the technical data we assume (% by mass concrete):

- Model parameter: $p = 0.2$
- Concrete cover: $c = 50$ mm
- Time of exposure: $t_{ex} = 0.1$ yr.
- Critical value: $C_{cr} = 0.1$ %
- Absorption of chloride during the first year: $S = 0.5$ %/yr^p
- Initial content of chloride: $C_i = 0.02$ %

- Water/cement proportion: $w/c = 0.37$.
- Exponent: $\alpha = 3 \cdot (0.55 - w/c) = 3 \cdot (0.55 - 0.37) = 0.54$
- Diffusion coefficient at time of exposure:

$$D_0 = 0.57 \cdot 10^6 \exp\left(-\sqrt{\frac{23}{w/c}}\right) \text{ mm}^2/\text{yr} = 215 \text{ mm}^2/\text{yr}.$$

Equation (14) now reads

$$\Lambda_{0.2}(z) = \frac{C_{cr} - C_i}{S} \cdot \frac{4^{0.2}}{c^{0.4}} = \frac{0.10 - 0.02}{0.5} \cdot \frac{4^{0.2}}{50^{0.4}} = 0.04415.$$

Using the tables of $\Lambda_p(z)$ it is seen that the solution of this equation is $z \approx 1.30$, from which

$$T = \left(\frac{c}{2z}\right)^2 = \left(\frac{50}{2 \cdot 1.30}\right)^2 = 369.82.$$

Finally, assuming that $t_{cr} \gg t_{ex}$,

$$(t_{cr} - t_{ex}) D_a(t_{cr}) \approx t_{cr} \cdot D_0 \cdot \left(\frac{t_{ex}}{t_{cr}}\right)^\alpha = D_0 {t_{ex}}^\alpha t_{cr}^{1-\alpha} \approx T,$$

i.e.

$$t_{cr} \approx \left\{\frac{T}{D_0 \cdot {t_{ex}}^\alpha}\right\}^{1/(1-\alpha)} = \left\{\frac{369.82}{215 \cdot 0.1^{0.54}}\right\}^{1/0.46} \approx 48.5 \text{ years},$$

which is the estimated lifetime. We see that an estimated critical time of $t_{cr} \approx 50$ years is quite reasonable. $\bigtriangledown$

EXAMPLE. Let us again assume that the mean value chloride diffusion coefficient $D_a(t)$ is modeled by (15), i.e.

$$D_a(t) = D_0 \left(\frac{t_{ex}}{t}\right)^\alpha \quad \text{for } t \geq t_{ex},$$

and let us assume that the boundary value is of the type

$$\begin{aligned} C_p(0,t) &\approx C_i + S\{(t - t_{ex}) D_a(t)\}^p \\ &\approx C_i + S \cdot D_0^p \cdot {t_{ex}}^{p\alpha} \cdot t^{(1-\alpha)p} \quad \text{for } t \gg t_{ex}, \end{aligned}$$

i.e.

$$C_p(0,t) \approx C_i + S_p t^{(1-\alpha)p}, \quad S_p = SD_0^p {t_{ex}}^{p\alpha}, \quad \text{for } t \gg t_{ex}.$$

Then (13) gives

$$C_p(x,t) \approx C_i + S\{(t-t_{ex})D_a(t)\}^p \Psi_p\left(\frac{x}{\sqrt{4(t-t_{ex})D_a(t)}}\right)$$

$$\approx C_i + S_p t^{(1-\alpha)p} \Psi_p(z), \tag{16}$$

where

$$x = \sqrt{4(t-t_{ex})D_a(t)} \cdot z \approx 2\sqrt{D_0 {t_{ex}}^{\alpha} t^{1-\alpha}} \cdot z. \tag{17}$$

Let C_{cr} be the critical level, and let $t \gg t_{ex}$ be given. We want to estimate the necessary concrete cover x for various values of p.

In the numerical example we keep the value of S_p fixed. Note, however, that we are forced to give S_p the strange physical dimension length$^{-(1-\alpha)p}$.

Ervin Poulsen has kindly provided the author with the following theoretical, though realistic technical data, where the values of C_{cr}, S_p and C_i are given as % of mass cement:

- Time of exposure: $t_{ex} = 0.1$ yr.
- Expected lifetime: $t = 100$ yr.
- Critical value: $C_{cr} = 0.8\%$
- Absorption of chloride during the first year: $S_p = 1.5\%/\text{yr}^{(1-\alpha)p}$.
- Initial content of chloride: $C_i = 0.15\%$
- Exponent: $\alpha = 0.45$
- Diffusion coefficient at time of exposure: $D_0 = 290$ mm^2/yr.

By (16) we get

$$\Psi_p(z) \approx \frac{C_{cr} - C_i}{S_p t^{(1-\alpha)p}} = \frac{0.80 - 0.15}{1.5 \cdot (100^{0.55})^p} = \frac{0.43333}{12.59^p}.$$

Solving this equation in z we finally get by (17),

$$x \approx 2\sqrt{290 \cdot 0.1^{0.45} \cdot 100^{0.55}} \cdot z \text{ mm } \approx 72 \cdot z \text{ mm}.$$

p	$(1-\alpha)p$	$\Psi_p(z)$	z	x/mm
0.0	0.000	0.43333	0.55	39.6
0.1	0.055	0.33637	0.64	46.0
0.2	0.110	0.26111	0.71	51.0
0.3	0.165	0.20268	0.78	56.2
0.4	0.220	0.15733	0.84	60.5
0.5	0.275	0.12213	0.90	64.8
0.6	0.330	0.09480	0.95	68.4
0.7	0.385	0.07359	1.00	72.0
0.8	0.440	0.05712	1.05	75.6
0.9	0.495	0.04434	1.09	78.5
1.0	0.550	0.03442	1.14	82.1

Table 1: Concrete cover for $t = 100$ years and $0.0 \leq p \leq 1.0$.

Note that the exponent $(1-\alpha)p$ of t in (16) resembles the exponent in the classical case for large t.

Using the tables of Ψ_p at the end of the paper we finally get Table 1, which describes how x depends on p in this model. We note that the expected concrete cover x for $0.0 \leq p \leq 1.0$ lies within the expected interval of the thickness of the concrete cover. Only measurements can give the right estimate of p. $\bigtriangledown$

6 Connections with other approaches

In [10] we have earlier considered the problem, when $D(x,t) = D(x)$ does not depend on time and the initial and boundary values are constant. When $D(x)$ is not constant, the solution is totally different in structure from what is presented here. This solution has been used in Østerdal [11].

Considering the present situation, Carslaw and Jaeger [2] solved the problem (4) for nonnegative integers p. Their solution was extended by Crank [5] to the case, where $2p$ is a nonnegative integer. According to Crank [5] we have

$$\begin{aligned} \Psi_0(z) &= \operatorname{erfc}(z) \\ \Psi_{0.5}(z) &= \exp(-z^2) - \sqrt{\pi}\, z \operatorname{erfc}(z), \end{aligned}$$

$$\Psi_1(z) \;=\; (1+2z^2)\mathrm{erfc}(z) - \{2/\sqrt{\pi}\}\, z\, \exp(-z^2),$$

where, by the extension of Proposition 1, we may add

$$\Psi_{-0.5}(z) = \exp(-z^2).$$

An easy, though tedious check shows that these functions are indeed given by the series (12) for $p = 0, \frac{1}{2}, 1$ (and for $p = -\frac{1}{2}$).

More generally, define an operator A by

$$Af(x) = \int_x^{+\infty} f(t)\, dt, \qquad x \in [0, +\infty[,$$

and by induction,

$$A^n f(x) = A(A^{n-1}f)(x) = \int_x^{+\infty} A^{n-1}f(t)\, dt, \quad n \in \mathbb{N},$$

whenever these expressions make sense. We supply these definitions with $A^0 f(x) = f(x)$. Choosing

$$f(x) = \mathrm{erfc}(x) = \frac{2}{\sqrt{\pi}} \int_x^{+\infty} e^{-t^2}\, dt = A\left(\frac{2}{\sqrt{\pi}}\, e^{-t^2}\right)(x),$$

it is easy to prove that the $A^n f(x)$ are all defined. The usual notation, cf. Carslaw and Jaeger [2] and Crank [5], is

$$\mathrm{i^n erfc}(x) = A^n(\mathrm{erfc})(x),$$

which obeys the recursion formula

$$2n\, \mathrm{i^n erfc}(x) = \mathrm{i^{n-2} erfc}(x) - 2x\, \mathrm{i^{n-1} erfc}(x), \qquad m \geq 2, \tag{18}$$

from which follows that there exist polynomials $p_n(x)$ and $q_n(x)$, such that

$$\mathrm{i^n erfc}(x) = p_n(x) \exp(-x^2) + q_n(x)\mathrm{erfc}(x).$$

It should be noted that the functions only enter the solution, when $D(x,t)$ is constant.

It follows from the results of Crank that if $2p$ is a nonnegative integer, then

$$\Psi_p(z) = \Gamma(p+1) \cdot 4^p \cdot \mathrm{i^{2p} erfc}(z).$$

The solution $\Psi_p(z)$ given by (12) has the following advantages compared with the classical solutions:

1. $\Psi_p(z)$ is defined for all $p \geq 0$ (in fact even for all $p \neq -1, -2, -3, \cdots$), while $\mathrm{i}^{2p}\mathrm{erfc}(z)$ is only defined, when $2p$ is a nonnegative integer.

2. $\Psi_p(0) = 1$, while $\mathrm{i}^{2p}\mathrm{erfc}(0) = 1/\{\Gamma(p+1) \cdot 4^p\}$.

3. The series (12) is converging rapidly for $0 \leq z \leq 2$ and converges for all $z \in [0, +\infty[$, while the recursion formula (18) is less easy to apply.

From a mathematical point of view it should be noted that $\Psi_p(z)$ can be expressed by the socalled *confluent hypergeometric functions*, or more specifically by Kummer's function (cf. Kummer [7]),

$$ {}_1F_1[a; b; x] = 1 + \frac{a}{b}\,x + \frac{a(a+1)}{b(b+1)}\,\frac{x^2}{2!} + \frac{a(a+1)(a+2)}{b(b+1)(b+2)}\,\frac{x^3}{3!} + \cdots . $$

It follows after some heavy calculations that

$$ \Psi_p(z) = {}_1F_1\left[-p; \frac{1}{2}; -z^2\right] - 2z\,\frac{\Gamma(p+1)}{\Gamma(p+\frac{1}{2})}\,{}_1F_1\left[-p+\frac{1}{2}; \frac{3}{2}; -z^2\right], $$

which can be "reduced" to

$$ \Psi_p(z) = \exp(-z^2)\,{}_1F_1\left[p+\frac{1}{2}; \frac{1}{2}; z^2\right] - 2z\,\exp(-z^2)\,\frac{\Gamma(p+1)}{\Gamma(p+\frac{1}{2})}\,{}_1F_1\left[p+1; \frac{3}{2}; z^2\right]. $$

The latest available tables of ${}_1F_1[a; b; x]$ for $a \in [-1, 1]$, for $b \in \left[\frac{1}{10}, 1\right]$, and for $x \in \left[\frac{1}{10}, 10\right]$, all with step $\frac{1}{10}$, can be found in Slater [14]. She also indicates some recursion formulæ, such that a general value of ${}_1F_1[a; b; x]$ can be calculated by means of these tables. These recursion formulæ are, however, worse in their appearence than e.g. (18) for $\mathrm{i}^n\mathrm{erfc}(x)$, so even if the Ψ_p are special cases of wellknown special functions, the direct approach (12) is still superior to this theory, when applications are considered.

7 Comments to the Tables

In this section are given tables of $\Psi_p(z)$ and $\Lambda_p(z)$, and a pocket calculator programme for $\Psi_p(z)$.

The tables of $\Psi_p(z)$ are given in the range $-0.50 \leq p \leq 1.00$ and in the range $0.05 \leq z \leq 2.00$, each with a step of 0.05. We note that $\Psi_p(0) = 1$

trivially, cf. (9) in Proposition 1. In practice one would only expect $0 \leq p \leq 1$. The tables for $-\frac{1}{2} \leq p \leq 0$ have been added in case that one also wants to calculate

$$\Psi_p'(z) = -2\frac{\Gamma(p+1)}{\Gamma(p+\frac{1}{2})}\Psi_{p-(1/2)}(z),$$

cf. Corollary 1, but are otherwise not necessary. We note in particular that $\Psi_{-0.50}(z) = \exp(-z^2)$, cf. Section 6.

Then follow the tables of

$$\Lambda_p(z) := \frac{\Psi_p(z)}{z^{2p}}$$

for $0.00 \leq p \leq 1.00$ and $0.05 \leq z \leq 2.00$. Note that $\Lambda_0(z) = \Psi_0(z)$ and that $\Lambda_p(0) = +\infty$ for $p > 0$. The usefulness of these tables was demonstrated in the comments and the example following after Corollary 2, when one wants to solve (14) with respect to z in order to obtain an estimate of the expected lifetime in one of these models. (The smaller z, the longer expected lifetime.)

For the time being the functions $\Psi_p(z)$ give the connection with the classical theory, but what lifetime is concerned one should rather concentrate on the functions $\Lambda_p(z)$ instead.

One extension should be mentioned here (cf. also the end of Section 4). If

$$\tilde{\varphi}(T) = c_0 + \sum_{j=1}^{n} c_j T^{p_j}, \tag{19}$$

where all $p_j > 0$, then the solution of (4) is given by

$$\begin{aligned} \tilde{C}(x,T) &= c_0\Psi_0\left(\frac{x}{\sqrt{4T}}\right) + \sum_{j=1}^{n} c_j T^{p_j}\Psi_{p_j}\left(\frac{x}{\sqrt{4T}}\right) \\ &= c_0\Lambda_0\left(\frac{x}{\sqrt{4T}}\right) + \sum_{j=1}^{n} c_j \left(\frac{x}{2}\right)^{2p_j}\Lambda_{p_j}\left(\frac{x}{\sqrt{4T}}\right), \end{aligned} \tag{20}$$

according to the principle of superposition. When the distance $x > 0$ is given, and $\tilde{C}_{cr}$ is the critical level for $\tilde{C}(x,T)$, then by (20) the expected transformed lifetime T can be found by solving the equations

$$c_0\Lambda_0(z) + \sum_{j=1}^{n} c_j \left(\frac{x}{2}\right)^{2p_j}\Lambda_{p_j}(z) = \tilde{C}_{cr} \quad \text{and} \quad T = \left(\frac{x}{2z}\right)^2.$$

The point is that if $0 \leq T \leq T_0$, then every continuous function $\tilde{\varphi}(T)$ can be approximated uniformly by a sum of the type (19) (Weierstraß' approximation theorem).

Finally, a simple pocket calculator programme for HP-42S is given for calculating $\Psi_p(z)$ for any allowed value p. The programme is run by first storing p in `STO 01`, then write z in the window followed by `XEQ ''PSI''`. After a couple of seconds the value of $\Psi_p(z)$ appears in the window, when z is not too large. The absolute error is here chosen $\leq 10^{-5}$. If another absolute error is preferred, one has to change the lines 52 and 88 accordingly. In some cases, when p or $p + \frac{1}{2}$ are integers, the programme may not run. Then one of the commands `GAMMA` should be replaced by the following three lines in the programme: `A: 1, B: -, C: N!`.

References

[1] **Browne, R.D. et al.**, Marine durability survey of the Tongue Sand Tower. Concrete-in-the-Oceans Technical Report. P4 Final Report. Cement & Concrete Association. 1980, London.

[2] **Carslaw, H.S. and Jaeger, J.C.**, Conduction of Heat in Solids, Clarendon Press, Oxford 1959.

[3] **Collepardi, M. et al.**, Kinetics of penetration of chloride ions in concrete (in Italian), Il Cemento no. 4, 1970.

[4] **Collepardi, M. et al.**, Penetration of chloride ions into cement paste and concrete. American Ceramic Society, vol. 55, USA 1972.

[5] **Crank, J.**, The Mathematics of Diffusion, Clarendon Press, Oxford 1975.

[6] **Gautefall, O.**, Methods for determination of chloride diffusivity in concrete, REPCON-report A 16, Statens vegvesen, Vegdirektoratet, Oslo 1994.

[7] **Kummer, E.E.**, Über die hypergeometrische Reihe $F(a; b; x)$, J. reine angew. Math. 14 (1836), 39–83.

[8] **Maage, M.**, Chloride Penetration in High Performance Concrete exposed to Marine Environment, Symp. Utilization of High Strength Concrete, Lillehammer 1993, 838–846, Norway.

[9] **Mangat, P.S. and Molloy, B.T.**, Prediction of long term chloride concentration in concrete, Materials and Structure, 1994, 338–346.

[10] **Mejlbro, L.**, Ficks anden lov for stedafhængig diffusionskoefficient, Mathematisk Institut, DTU, MAT-REPORT NR. 1995-11 (in Danish).

[11] **Østerdal, A.S.**, Analyse af chloridprofiler i beton, Thesis, IMM-EKS-1995-23, Lyngby 1995 (in Danish).

[12] **Poulsen, E.**, Bestemmelse af diffusivitet for forskellige betonkvaliteter (in Danish), in Marina betongkonstruktioners livslängd (1995), 103–124.

[13] **Purvis, R.L. et al.**, Life-Cycle Cost Analysis for Protection and Rehabilitation of Concrete Bridges Relative to Reinforcement Corrosion, Strategic Highway Research Program, National Research Council, Washington DC, 1994, 80–82.

[14] **Slater, L.J.**, Confluent Hypergeometric Functions, Cambridge at the University Press, 1960.

[15] **Spalding, D.B. and Gibson, M.M.**, The calculation of time-dependent diffusion processes with variable properties and chemical reaction, in *Diffusion processes*, Proc. Thomas Graham Memorial Symp. Univ. Strathclyde, vol. 2, 561–571, Gordon and Breach Science Publishers, London, New York, Paris.

[16] **Swamy, R.N. et al.**, A Critical Evaluation of Chloride Penetration into Concrete in Marine Environment, in *Corrosion and Corrosion Protection of Steel in Concrete*, Proc. Intern. Conf. Univ. Sheffield, 24–28 July 1994, ed. R.N. Swamy, 404–419. Sheffield Academic Press.

[17] **Takewaka, K. and Mastumoto, S.**, Quality and Cover Thickness of Concrete Based on the Estimation of Chloride Penetration in Marine Environments, Proc. Second Intern. Conf. St. Andrews by-the-Sea, Canada 1988, ed. V.M. Malhotra, 381–400, American Concrete Institute, Detroit.

[18] **Uji, K. et al.**, Formulation of an Equation for Surface Chloride Content of Concrete due to Permeation of Chloride, in *Corrosion of Reinforcement in Concrete*, ed. C.L. Page et al., (1990), 258–267, Society of Chemical Industry, Elsevier Applied Science, London and New York.

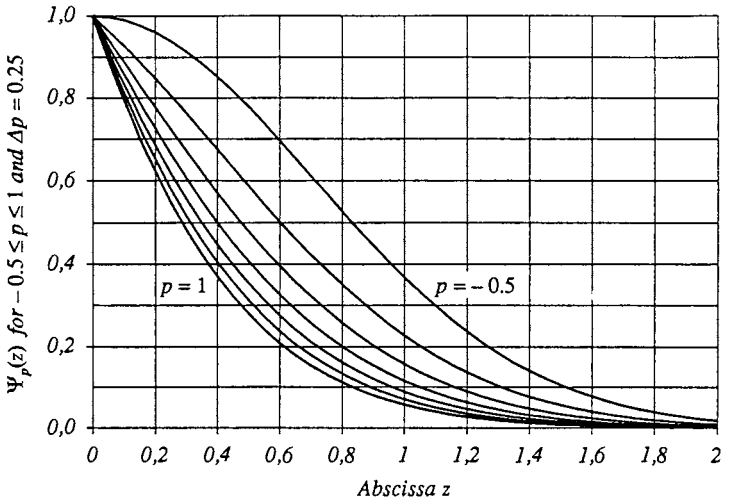

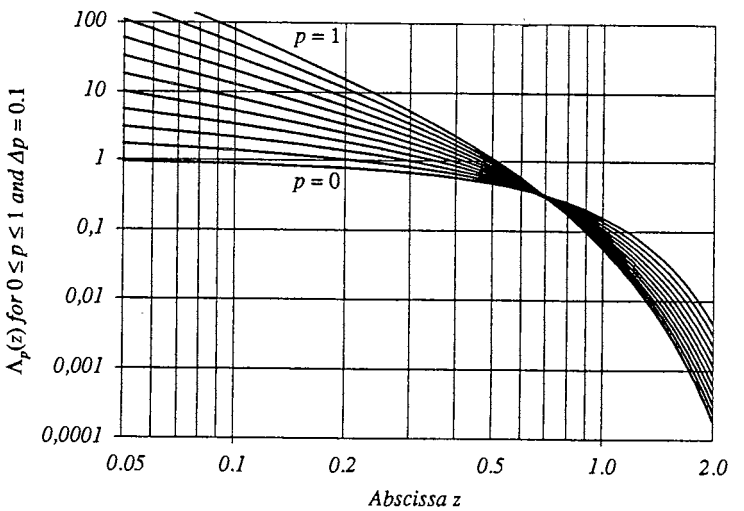

z	$\Psi_{-0.50}$	$\Psi_{-0.45}$	$\Psi_{-0.40}$	$\Psi_{-0.35}$	$\Psi_{-0.30}$	$\Psi_{-0.25}$	$\Psi_{-0.20}$	$\Psi_{-0.15}$
0.05	.99750	.98947	.98237	.97602	.97026	.96499	.96013	.95561
0.10	.99005	.97455	.96092	.94876	.93778	.92776	.91854	.91000
0.15	.97775	.95542	.93586	.91847	.90282	.88859	.87555	.86350
0.20	.96079	.93231	.90746	.88544	.86569	.84780	.83145	.81640
0.25	.93941	.90552	.87603	.85000	.82673	.80572	.78659	.76902
0.30	.91393	.87536	.84192	.81250	.78629	.76269	.74127	.72168
0.35	.88471	.84222	.80551	.77331	.74471	.71906	.69584	.67467
0.40	.85214	.80650	.76718	.73281	.70238	.67516	.65061	.62828
0.45	.81669	.76862	.72735	.69138	.65964	.63133	.60587	.58278
0.50	.77880	.72904	.68644	.64942	.61685	.58789	.56192	.53844
0.55	.73897	.68819	.64484	.60728	.57434	.54513	.51901	.49546
0.60	.69768	.64651	.60296	.56534	.53243	.50334	.47739	.45407
0.65	.65541	.60444	.56118	.52391	.49141	.46276	.43727	.41442
0.70	.61263	.56238	.51986	.48332	.45154	.42361	.39882	.37667
0.75	.56978	.52073	.47932	.44384	.41307	.38608	.36221	.34092
0.80	.52729	.47983	.43987	.40572	.37618	.35034	.32754	.30726
0.85	.48554	.44000	.40176	.36916	.34104	.31650	.29491	.27575
0.90	.44486	.40152	.36521	.33435	.30778	.28466	.26437	.24640
0.95	.40555	.36462	.33042	.30141	.27650	.25488	.23595	.21923
1.00	.36788	.32950	.29751	.27045	.24727	.22720	.20966	.19421
1.05	.33204	.29632	.26661	.24154	.22011	.20160	.18547	.17129
1.10	.29820	.26517	.23777	.21470	.19503	.17808	.16333	.15041
1.15	.26647	.23614	.21104	.18995	.17201	.15658	.14320	.13149
1.20	.23693	.20926	.18641	.16726	.15100	.13705	.12498	.11444
1.25	.20961	.18453	.16387	.14658	.13194	.11941	.10858	.09915
1.30	.18452	.16193	.14336	.12785	.11475	.10356	.09391	.08552
1.35	.16162	.14140	.12481	.11098	.09933	.08939	.08085	.07343
1.40	.14086	.12287	.10813	.09588	.08558	.07681	.06928	.06277
1.45	.12215	.10624	.09323	.08244	.07338	.06569	.05910	.05341
1.50	.10540	.09141	.07999	.07055	.06263	.05592	.05018	.04524
1.55	.09049	.07826	.06830	.06008	.05319	.04738	.04241	.03814
1.60	.07730	.06667	.05804	.05092	.04497	.03995	.03568	.03201
1.65	.06571	.05652	.04908	.04294	.03783	.03353	.02987	.02674
1.70	.05558	.04768	.04130	.03605	.03168	.02801	.02490	.02223
1.75	.04677	.04003	.03458	.03011	.02640	.02329	.02065	.01840
1.80	.03916	.03343	.02881	.02503	.02190	.01927	.01705	.01516
1.85	.03263	.02779	.02389	.02071	.01807	.01587	.01401	.01243
1.90	.02705	.02298	.01971	.01705	.01485	.01301	.01146	.01014
1.95	.02231	.01892	.01619	.01397	.01214	.01061	.00933	.00824
2.00	.01832	.01549	.01323	.01139	.00987	.00861	.00756	.00666

Table 2: $\Psi_p(z)$ for $-.50 \leq p \leq -0.15$.

z	$\Psi_{-0.10}$	$\Psi_{-0.05}$	$\Psi_{0.00}$	$\Psi_{0.05}$	$\Psi_{0.10}$	$\Psi_{0.15}$	$\Psi_{0.20}$	$\Psi_{0.25}$
0.05	.95137	.94739	.94364	.94006	.93666	.93341	.93030	.92731
0.10	.90204	.89457	.88754	.88088	.87457	.86855	.86280	.85730
0.15	.85230	.84183	.83200	.82273	.81396	.80563	.79769	.79011
0.20	.80245	.78946	.77730	.76586	.75507	.74484	.73513	.72589
0.25	.75280	.73774	.72364	.71049	.69808	.68637	.67527	.66473
0.30	.70363	.68692	.67137	.65684	.64320	.63035	.61821	.60672
0.35	.65523	.63728	.62062	.60509	.59056	.57692	.56406	.55191
0.40	.60784	.58902	.57161	.55542	.54032	.52617	.51288	.50035
0.45	.56171	.54237	.52452	.50797	.49257	.47819	.46471	.45203
0.50	.51707	.49750	.47950	.46286	.44741	.43302	.41956	.40695
0.55	.47409	.45458	.43668	.42017	.40488	.39068	.37743	.36505
0.60	.43296	.41374	.39614	.37997	.36503	.35118	.33830	.32628
0.65	.39380	.37507	.35797	.34229	.32784	.31449	.30209	.29056
0.70	.35672	.33865	.32220	.30715	.29332	.28056	.26875	.25779
0.75	.32180	.30453	.28884	.27453	.26141	.24933	.23818	.22785
0.80	.28910	.27273	.25790	.24440	.23205	.22072	.21028	.20063
0.85	.25863	.24324	.22933	.21670	.20518	.19462	.18492	.17598
0.90	.23039	.21604	.20309	.19136	.18069	.17093	.16199	.15376
0.95	.20437	.19107	.17911	.16830	.15848	.14953	.14134	.13382
1.00	.18051	.16828	.15730	.14740	.13843	.13027	.12282	.11600
1.05	.15874	.14757	.13756	.12856	.12042	.11303	.10630	.10015
1.10	.13900	.12885	.11980	.11166	.10432	.09768	.09163	.08612
1.15	.12117	.11203	.10388	.09657	.09000	.08406	.07867	.07376
1.20	.10517	.09698	.08969	.08317	.07731	.07203	.06725	.06291
1.25	.09088	.08358	.07710	.07132	.06614	.06147	.05726	.05344
1.30	.07818	.07172	.06599	.06089	.05633	.05224	.04854	.04520
1.35	.06696	.06127	.05624	.05177	.04778	.04420	.04098	.03808
1.40	.05709	.05211	.04772	.04382	.04035	.03724	.03445	.03194
1.45	.04846	.04412	.04031	.03693	.03392	.03124	.02884	.02668
1.50	.04094	.03719	.03390	.03098	.02840	.02610	.02404	.02219
1.55	.03444	.03121	.02838	.02588	.02367	.02171	.01995	.01838
1.60	.02883	.02607	.02365	.02152	.01964	.01797	.01648	.01515
1.65	.02403	.02168	.01962	.01782	.01623	.01482	.01356	.01244
1.70	.01994	.01795	.01621	.01469	.01335	.01216	.01111	.01017
1.75	.01646	.01479	.01333	.01205	.01093	.00994	.00906	.00828
1.80	.01353	.01213	.01091	.00984	.00891	.00808	.00736	.00671
1.85	.01107	.00990	.00889	.00800	.00723	.00655	.00595	.00541
1.90	.00902	.00805	.00721	.00648	.00584	.00528	.00478	.00435
1.95	.00731	.00651	.00582	.00522	.00470	.00424	.00383	.00348
2.00	.00590	.00524	.00468	.00419	.00376	.00339	.00306	.00277

Table 3: $\Psi_p(z)$ for $-0.10 \leq p \leq 0.25$.

z	$\Psi_{0.30}$	$\Psi_{0.35}$	$\Psi_{0.40}$	$\Psi_{0.45}$	$\Psi_{0.50}$	$\Psi_{0.55}$	$\Psi_{0.60}$	$\Psi_{0.65}$
0.05	.92444	.92166	.91898	.91639	.91388	.91144	.90906	.90675
0.10	.85202	.84694	.84204	.83731	.83274	.82831	.82402	.81985
0.15	.78286	.77590	.76921	.76276	.75655	.75054	.74474	.73911
0.20	.71706	.70861	.70051	.69273	.68524	.67803	.67107	.66434
0.25	.65469	.64511	.63595	.62717	.61874	.61064	.60284	.59532
0.30	.59580	.58541	.57549	.56601	.55694	.54823	.53987	.53183
0.35	.54041	.52948	.51908	.50917	.49970	.49064	.48195	.47362
0.40	.48851	.47730	.46666	.45653	.44688	.43767	.42887	.42043
0.45	.44009	.42880	.41811	.40797	.39833	.38914	.38038	.37201
0.50	.39508	.38390	.37334	.36334	.35385	.34484	.33626	.32808
0.55	.35343	.34250	.33221	.32248	.31327	.30455	.29626	.28837
0.60	.31503	.30448	.29456	.28522	.27639	.26804	.26012	.25261
0.65	.27979	.26971	.26026	.25137	.24299	.23846	.22761	.22053
0.70	.24757	.23804	.22911	.22074	.21287	.20545	.19846	.19184
0.75	.21825	.20931	.20096	.19314	.18581	.17892	.17243	.16631
0.80	.19168	.18336	.17561	.16838	.16160	.15525	.14927	.14365
0.85	.16770	.16003	.15289	.14624	.14003	.13421	.12876	.12364
0.90	.14616	.13913	.13261	.12654	.12088	.11560	.11066	.10603
0.95	.12689	.12049	.11457	.10908	.10397	.09920	.09475	.09059
1.00	.10973	.10395	.09861	.09366	.08907	.08480	.08082	.07711
1.05	.09451	.08932	.08454	.08012	.07602	.07222	.06868	.06539
1.10	.08108	.07645	.07219	.06827	.06463	.06127	.05814	.05524
1.15	.06928	.06517	.06141	.05794	.05474	.05178	.04904	.04648
1.20	.05895	.05534	.05202	.04898	.04617	.04358	.04119	.03897
1.25	.04996	.04679	.04389	.04124	.03879	.03654	.03446	.03254
1.30	.04217	.03941	.03689	.03458	.03246	.03052	.02872	.02706
1.35	.03544	.03305	.03087	.02888	.02706	.02538	.02384	.02242
1.40	.02967	.02760	.02573	.02402	.02246	.02103	.01971	.01850
1.45	.02473	.02296	.02136	.01990	.01856	.01735	.01623	.01521
1.50	.02052	.01902	.01765	.01641	.01528	.01425	.01331	.01245
1.55	.01696	.01568	.01453	.01348	.01253	.01166	.01087	.01015
1.60	.01396	.01288	.01191	.01103	.01023	.00950	.00884	.00824
1.65	.01144	.01053	.00972	.00898	.00832	.00771	.00716	.00666
1.70	.00933	.00858	.00790	.00729	.00673	.00623	.00578	.00536
1.75	.00758	.00695	.00639	.00589	.00543	.00502	.00464	.00430
1.80	.00613	.00561	.00515	.00473	.00436	.00402	.00371	.00343
1.85	.00494	.00451	.00413	.00379	.00348	.00321	.00296	.00273
1.90	.00396	.00361	.00330	.00302	.00227	.00254	.00234	.00216
1.95	.00316	.00288	.00262	.00240	.00220	.00202	.00185	.00170
2.00	.00251	.00228	.00208	.00190	.00173	.00159	.00146	.00134

Table 4: $\Psi_p(z)$ for $0.30 \leq p \leq 0.65$.

z	$\Psi_{0.70}$	$\Psi_{0.75}$	$\Psi_{0.80}$	$\Psi_{0.85}$	$\Psi_{0.90}$	$\Psi_{0.95}$	$\Psi_{1.00}$
0.05	.90450	.90231	.90017	.89808	.89603	.89403	.89207
0.10	.81580	.81186	.80802	.80427	.80062	.79706	.79357
0.15	.73366	.72836	.72321	.71821	.71333	.70858	.70395
0.20	.65783	.65153	.64541	.63948	.63371	.62811	.62265
0.25	.58807	.58105	.57426	.56769	.56132	.55513	.54913
0.30	.52409	.51662	.50941	.50244	.49570	.48917	.48284
0.35	.46561	.45790	.45048	.44332	.43641	.42973	.42327
0.40	.41235	.40458	.39712	.38994	.38302	.37635	.36991
0.45	.36400	.35633	.34897	.34190	.33510	.32856	.32226
0.50	.32027	.31281	.30566	.29881	.29224	.28593	.27986
0.55	.28086	.27369	.26685	.26030	.25403	.24802	.24226
0.60	.24547	.23867	.23219	.22600	.22009	.21444	.20902
0.65	.21381	.20742	.20135	.19557	.19005	.18478	.17975
0.70	.18558	.17965	.17401	.16865	.16356	.15870	.15406
0.75	.1 052	.15505	.14986	.14495	.14027	.13583	.13160
0.80	.13835	.13335	.12862	.12414	.11989	.11585	.11202
0.85	.11882	.11428	.10999	.10594	.10211	.09847	.09503
0.90	.10167	.09758	.09373	.09009	.08665	.08340	.08033
0.95	.08668	.08302	.07958	.07633	.07328	.07039	.06766
1.00	.07363	.07037	.06732	.06444	.06174	.05919	.05679
1.05	.06231	.05943	.05673	.05421	.05183	.04960	.04749
1.10	.05253	.05000	.04764	.04542	.04335	.04140	.03957
1.15	.04412	.04191	.03985	.03792	.03612	.03443	.03285
1.20	.03691	.03499	.03321	.03154	.02999	.02853	.02717
1.25	.03076	.02910	.02757	.02613	.02480	.02355	.02239
1.30	.02553	.02411	.02280	.02157	.02043	.01937	.01838
1.35	.02111	.01990	.01878	.01774	.01677	.01587	.01503
1.40	.01739	.01636	.01541	.01452	.01371	.01295	.01224
1.45	.01426	.01339	.01259	.01185	.01116	.01052	.00993
1.50	.01165	.01092	.01025	.00963	.00905	.00852	.00803
1.55	.00948	.00887	.00831	.00779	.00731	.00687	.00646
1.60	.00768	.00718	.00671	.00628	.00588	.00552	.00518
1.65	.00620	.00578	.00540	.00504	.00472	.00442	.00414
1.70	.00498	.00464	.00432	.00403	.00376	.00352	.00329
1.75	.00399	.00371	.00345	.00321	.00299	.00279	.00261
1.80	.00318	.00295	.00274	.00255	.00237	.00221	.00206
1.85	.00252	.00234	.00217	.00201	.00187	.00174	.00162
1.90	.00199	.00184	.00171	.00158	.00147	.00136	.00127
1.95	.00157	.00145	.00134	.00124	.00115	.00106	.00099
2.00	.00123	.00113	.00105	.00097	.00089	.00083	.00077

Table 5: $\Psi_p(z)$ for $0.75 \leq p \leq 1.00$.

z	$\Lambda_{0.00}$	$\Lambda_{0.05}$	$\Lambda_{0.10}$	$\Lambda_{0.15}$	$\Lambda_{0.20}$	$\Lambda_{0.25}$	$\Lambda_{0.30}$
0.05	.94364	1.2684	1.7053	2.2929	3.0834	4.1471	5.5782
0.10	.88754	1.1090	1.3861	1.7330	2.1673	2.7110	3.3919
0.15	.83200	.99461	1.1896	1.4233	1.7037	2.0401	2.4436
0.20	.77730	.89959	1.0418	1.2071	1.3994	1.6231	1.8834
0.25	.72364	.81614	.92113	1.0403	1.1757	1.3295	1.5041
0.30	.67137	.74088	.81831	.90457	1.0007	1.1077	1.2270
0.35	.62062	.67207	.72854	.79048	.85842	.93291	1.0146
0.40	.57161	.60872	.64899	.69264	.73993	.79112	.84653
0.45	.52452	.55020	.57787	.60762	.63958	.67385	.71058
0.50	.47950	.49608	.51394	.53311	.55361	.57551	.59883
0.55	.43668	.44605	.45631	.46742	.47940	.49223	.50592
0.60	.39614	.39988	.40429	.40934	.41499	.42122	.42802
0.65	.35797	.35736	.35734	.35787	.35890	.36039	.36231
0.70	.32220	.31830	.31500	.31224	.30996	.30811	.30665
0.75	.28884	.28254	.27689	.27180	.26723	.26310	.25937
0.80	.25790	.24991	.24264	.23600	.22991	.22431	.21914
0.85	.22933	.22025	.21195	.20435	.19734	.19087	.18488
0.90	.20309	.19339	.18453	.17642	.16896	.16207	.15570
0.95	.17911	.16916	.16011	.15184	.14426	.13729	.13085
1.00	.15730	.14740	.13843	.13027	.12282	.11600	.10973
1.05	.13756	.12793	.11925	.11139	.10425	.09774	.09178
1.10	.11980	.11060	.10235	.09492	.08821	.08212	.07657
1.15	.10388	.09523	.08752	.08060	.07439	.06878	.06371
1.20	.08969	.08166	.07454	.06820	.06251	.05743	.05284
1.25	.07710	.06974	.06325	.05749	.05237	.04780	.04370
1.30	.06599	.05932	.05345	.04828	.04371	.03964	.03603
1.35	.05624	.05024	.04499	.04040	.03635	.03277	.02960
1.40	.04772	.04237	.03772	.03367	.03011	.02699	.02424
1.45	.04031	.03558	.03149	.02795	.02486	.02215	.01978
1.50	.03390	.02975	.02619	.02311	.02044	.01812	.01609
1.55	.02838	.02477	.02168	.01903	.01674	.01476	.01304
1.60	.02365	.02054	.01788	.01561	.01366	.01198	.01053
1.65	.01962	.01695	.01468	.01275	.01119	.00968	.00847
1.70	.01621	.01393	.01200	.01037	.00898	.00780	.00679
1.75	.01333	.01140	.00977	.00840	.00724	.00626	.00542
1.80	.01091	.00928	.00792	.00678	.00581	.00500	.00431
1.85	.00889	.00753	.00639	.00544	.00465	.00398	.00341
1.90	.00721	.00608	.00514	.00435	.00370	.00315	.00269
1.95	.00582	.00488	.00411	.00347	.00293	.00249	.00212
2.00	.00468	.00391	.00327	.00275	.00232	.00196	.00166

Table 6: $\Lambda_p(z)$ for $0.00 \leq p \leq 0.30$.

z	$\Lambda_{0.35}$	$\Lambda_{0.40}$	$\Lambda_{0.45}$	$\Lambda_{0.50}$	$\Lambda_{0.55}$	$\Lambda_{0.60}$	$\Lambda_{0.65}$
0.05	7.5040	10.096	13.583	18.278	24.596	33.100	44.548
0.10	4.2447	5.3129	6.6510	8.3274	10.428	13.060	16.358
0.15	2.9278	3.5089	4.2064	5.0437	6.0489	7.2559	8.7054
0.20	2.1862	2.5386	2.9488	3.4262	3.9821	4.6295	5.3833
0.25	1.7025	1.9278	2.1839	2.4750	2.8058	3.1818	3.6094
0.30	1.3598	1.5078	1.6727	1.8565	2.0613	2.2895	2.5440
0.35	1.1041	1.2022	1.3098	1.4277	1.5570	1.6987	1.8541
0.40	.90646	.97129	1.0414	1.1172	1.1992	1.2878	1.3836
0.45	.74991	.79200	.83703	.88517	.93665	.99167	1.0505
0.50	.62365	.65002	.67802	.70771	.73918	.77252	.80783
0.55	.52049	.53594	.55230	.56959	.58783	.60706	.62731
0.60	.43537	.44326	.45169	.46065	.47014	.48017	.49074
0.65	.36463	.36734	.37041	.37383	.37759	.38167	.38607
0.70	.30555	.30477	.30429	.30410	.30416	.30447	.30502
0.75	.25601	.25297	.25022	.24775	.24552	.24352	.24173
0.80	.21436	.20994	.20583	.20200	.19844	.19511	.19200
0.85	.17931	.17412	.16927	.16474	.16049	.15649	.15273
0.90	.14978	.14427	.13913	.13432	.12981	.12557	.12159
0.95	.12490	.11937	.11423	.10944	.10496	.10076	.09683
1.00	.10395	.09861	.09366	.08907	.08480	.08082	.07711
1.05	.08632	.08130	.07668	.07240	.06845	.06478	.06137
1.10	.07152	.06689	.06265	.05876	.05517	.05186	.04880
1.15	.05910	.05491	.05109	.04760	.04440	.04146	.03876
1.20	.04871	.04496	.04156	.03848	.03566	.03309	.03074
1.25	.04003	.03672	.03373	.03103	.02859	.02637	.02435
1.30	.03280	.02990	.02731	.02497	.02286	.02096	.01924
1.35	.02679	.02428	.02204	.02004	.01824	.01663	.01518
1.40	.02181	.01966	.01774	.01604	.01452	.01316	.01195
1.45	.01770	.01586	.01424	.01280	.01153	.01039	.00938
1.50	.01432	.01276	.01139	.01019	.00912	.00818	.00735
1.55	.01154	.01023	.00909	.00808	.00720	.00643	.00574
1.60	.00927	.00818	.00722	.00639	.00567	.00503	.00447
1.65	.00742	.00651	.00572	.00504	.00445	.00393	.00347
1.70	.00592	.00517	.00452	.00396	.00348	.00306	.00269
1.75	.00470	.00408	.00356	.00310	.00271	.00237	.00208
1.80	.00372	.00322	.00279	.00242	.00211	.00183	.00160
1.85	.00293	.00253	.00218	.00188	.00163	.00141	.00123
1.90	.00230	.00197	.00170	.00146	.00126	.00109	.00094
1.95	.00180	.00154	.00132	.00113	.00097	.00083	.00072
2.00	.00140	.00119	.00102	.00087	.00074	.00063	.00054

Table 7: $\Lambda_p(z)$ for $0.35 \leq p \leq 0.65$.

z	$\Lambda_{0.70}$	$\Lambda_{0.75}$	$\Lambda_{0.80}$	$\Lambda_{0.85}$	$\Lambda_{0.90}$	$\Lambda_{0.95}$	$\Lambda_{1.00}$
0.05	59.959	80.705	108.64	146.24	196.87	265.04	356.83
0.10	20.492	25.673	32.168	40.309	50.516	63.313	79.357
0.15	10.446	12.537	15.049	18.067	21.693	26.061	31.287
0.20	6.2614	7.2843	8.4760	9.8645	11.483	13.368	15.566
0.25	4.0955	4.6484	5.2773	5.9926	6.8064	7.7324	8.7861
0.30	2.8277	3.1440	3.4968	3.8902	4.3291	4.8187	5.3649
0.35	2.0246	2.2114	2.4164	2.6412	2.8878	3.1584	3.4553
0.40	1.4872	1.5993	1.7204	1.8514	1.9930	2.1462	2.3119
0.45	1.1133	1.1804	1.2521	1.3287	1.4106	1.4980	1.5914
0.50	.84520	.88475	.92658	.97083	1.0176	1.0671	1.1194
0.55	.64861	.67100	.69452	.71921	.74513	.77233	.80085
0.60	.50186	.51354	.52577	.53859	.55199	.56599	.58062
0.65	.39079	.39581	.40114	.40676	.41269	.41892	.42544
0.70	.30578	.30674	.30791	.30927	.31081	.31252	.31441
0.75	.24013	.23872	.23747	.23637	.23543	.23462	.23395
0.80	.18909	.18636	.18380	.18140	.17915	.17703	.17503
0.85	.14918	.14583	.14265	.13965	.13680	.13410	.13153
0.90	.11783	.11429	.11093	.10776	.10475	.10189	.09917
0.95	.09314	.08966	.08638	.08329	.08036	.07760	.07497
1.00	.07363	.07037	.06732	.06444	.06174	.05919	.05679
1.05	.05819	.05524	.05247	.04989	.04747	.04520	.04308
1.10	.04597	.04334	.04090	.03863	.03652	.03454	.03270
1.15	.03628	.03398	.03186	.02990	.02809	.02640	.02484
1.20	.02859	.02662	.02480	.02314	.02160	.02018	.01887
1.25	.02250	.02082	.01929	.01788	.01660	.01541	.01433
1.30	.01768	.01627	.01498	.01381	.01274	.01176	.01087
1.35	.01387	.01269	.01162	.01065	.00977	.00897	.00824
1.40	.01086	.00987	.00899	.00820	.00748	.00683	.00624
1.45	.00848	.00767	.00695	.00630	.00572	.00519	.00472
1.50	.00661	.00595	.00536	.00483	.00436	.00394	.00357
1.55	.00513	.00460	.00412	.00370	.00332	.00299	.00269
1.60	.00398	.00355	.00316	.00282	.00252	.00226	.00202
1.65	.00308	.00273	.00242	.00215	.00191	.00171	.00152
1.70	.00237	.00209	.00185	.00164	.00145	.00128	.00114
1.75	.00182	.00160	.00141	.00124	.00109	.00096	.00085
1.80	.00140	.00122	.00107	.00094	.00082	.00072	.00064
1.85	.00107	.00093	.00081	.00071	.00062	.00054	.00047
1.90	.00081	.00070	.00061	.00053	.00046	.00040	.00035
1.95	.00062	.00053	.00046	.00040	.00034	.00030	.00026
2.00	.00047	.00040	.00034	.00030	.00026	.00022	.00019

Table 8: $\Lambda_p(z)$ for $0.70 \leq p \leq 1.00$.

01:	LBL ''PSI''	25:	XEQ A	49:	STO+ 00	73:	×
02:	2	26:	XEQ B	50:	STO 04	74:	RCL 05
03:	×	27:	XEQ C	51:	ABS	75:	×
04:	X↑2	28:	XEQ D	52:	1E-5	76:	RCL 03
05:	STO 02	29:	LBL D	53:	X > Y?	77:	2
06:	1	30:	RCL 00	54:	RTN	78:	×
07:	STO 00	31:	RTN	55:	1	79:	STO 07
08:	STC 03	32:	LBL A	56:	STO+ 03	80:	÷
09:	STO 04	33:	RCL 06	57:	GTO A	81:	RCL 07
10:	1	34:	RCL 03	58:	LBL B	82:	1
11:	RCL 01	35:	-	59:	1	83:	+
12:	+	36:	RCL 02	60:	STO 03	84:	÷
13:	STO 06	37:	×	61:	RCL 05	85:	STO+ 00
14:	GAMMA	38:	RCL 04	62:	STO+ 00	86:	STO 05
15:	RCL 01	39:	×	63:	RCL 06	87:	ABS
16:	0.5	40:	RCL 03	64:	0.5	88:	1E-5
17:	+	41:	2	65:	-	89:	X > Y ?
18:	GAMMA	42:	×	66:	STO 06	90:	RTN
19:	÷	43:	STO 07	67:	RTN	91:	1
20:	+/-	44:	÷	68:	LBL C	92:	STO+ 03
21:	RCL 02	45:	RCL 07	69:	RCL 06	93:	GTO C
22:	SQRT	46:	1	70:	RCL 03	94:	END
23:	×	47:	-	71:	-		
24:	STO 05	48:	÷	72:	RCL 02		

Table 9: Programme for HP-42S, calculating $\Psi_p(z)$.

Temperature Cracking

Mats Emborg & Jan-Erik Jonasson
Betongindustri AB, Box 473, 100 74 Stockholm
Division of Structural Engineering
Luleå University of Technology, 971 87 Luleå

Summary

Research and practical experiences show that the quality and life time of concrete structures largely depends on the curing conditions in the early life time of concrete. Inadequate curing leads to malfunction and cracking, and thus considerable decrease of durability and service life time. A major source of this cracking is the restrained volume changes related to hydration temperatures and shrinkage phenomena. The tendency of concrete cracking due to temperature movements during hydration is a problem that is known since the "childhood" of concrete technology.

The risk of cracking has almost solely been estimated from temperature criteria, which is a most uncertain method. Modern research show that a lot of additional factors play a dominant role for the risk of cracking, and nowadays most of these factors can be taken into account when estimating the risk of cracking in most casting situations.

In this chapter the modern way of making analyses of cracking risks is presented, and examples of two typical cases will be shown. The chosen material parameters and the used models will be given. The difference between temperature and stress criteria for the reduction of cracks will be discussed. Results from laboratory tests with the Thermal Stress Testing Machine, developed at the Luleå University of Technology, will also be shown.

The presented way of making crack risk analyses has for instance been used by Betongindustri AB, see the reference list.

Introduction

Within the European Community many billions of ECU are invested in infrastructural concrete projects such as reactor enclosures, roads, tunnels and important marine structures e g dams, locks, bridges and marine tunnels.

Many of these are located in harsh environments. Increasing service life time, reducing initial malfunction (e g lacking tightness) and reduction of maintenance and repair costs would result in enormous cost savings.

Research and practical experiences show that the quality and life time of concrete structures largely depends on the curing conditions in the early life time of concrete, as inadequate curing leads to malfunction and cracking. A major source of this cracking, that occur at casting of both massive and thin structures, is the restrained volume changes related to hydration temperatures and shrinkage phenomena.

Judgements of crack risks must be based on knowledge of the temperature field in the young concrete, on the maturity development, and on the stresses that occur. The interactions of different factors are very complex, and realistic judgements must be based on computer analyses.

It is very important that the models for cracking risk estimations are based on carefully documented material tests on concrete at early ages. In this chapter two examples of marine structures are studied theoretically. Finally, results from laboratory tests are shown where thermal stresses are recorded in concrete specimens.

It must be mentioned, that, by establishing new techniques for estimations of cracking risks in the building industry, the following main benefits can be obtained

- optimisation of technical effects and costs of alternative construction procedures, all fulfilling quality requirements set up by codes
- reduced construction costs by optimised processes
- improved knowledge when specifying requirements
- reduced maintenance costs and increase service life time. Potential saving are in the order of 200 - 300 MECY/year

This article gives a survey of basic feature of this new technique for cracking risk computations.

Choice of cases to analyse

Traditionally two types of temperature cracks may be defined as:

I = through cracks
II = surface cracks

In the first case it is a restraining effect between different parts of the structure, for example between old and new concrete, or between the structure and the surroundings. One example is casting directly on rock, where through cracks may occur. The second type of cracks is caused by temperature differences inside the newly cast concrete.

Here two structures have been chosen to study these two types of cracks as:

I = vertical section through a long column cast on a earlier cast basement, Figure 1a.
IIa = horizontal section through a homogeneous column without cooling, see Figure 1b.
IIb = horizontal section through the same column as in the case IIa but with embedded pipes for air cooling, see Figure 1c.

The calculation of temperatures are done with the finite element method, and due to symmetrical reasons only the parts marked with solid lines in Figure 1 are studied, see the chosen element meshes in Figure 2.

The study is here done for a mixture called concrete A, and the chosen variation for parameters describing air and casting temperatures are presented in Table 1.

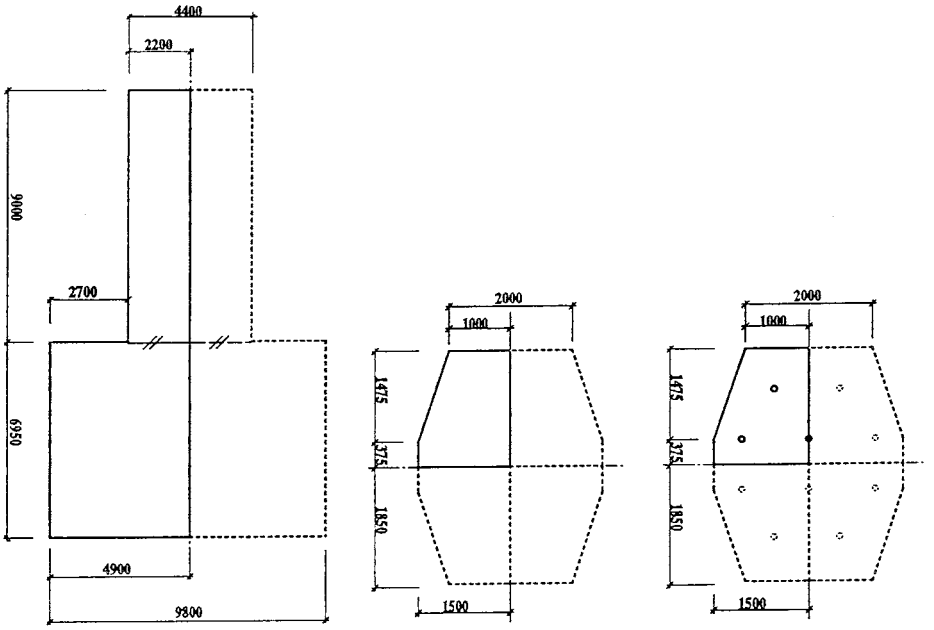

a)I = long column *b)IIa = homogeneous column, no cooling* *c)IIb = homogeneous column, air cooling*

Fig. 1. *Sections of studied structures.*

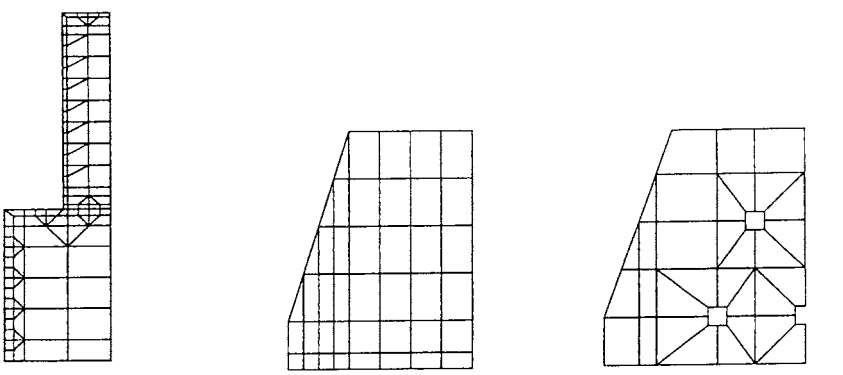

a)I = long column *b)IIa = homogeneous column, no cooling* *c)IIb = homogeneous column, air cooling*

Fig. 2. *Chosen element meshes for the studied sections shown in Figure 1.*

Table 1. *Parameter variations at the study of risk of thermal cracking.*

Structure	Concrete	Air temperature [°C]	Casting temperature [°C]
I = Figure 2a	A	20	10
			15
			20
			25
		0	10
			15
			20
IIa = Figure 2b	A	20	10
			15
			20
		0	10
			15
			20
IIb = Figure 2c	A	20	10
			15
			20
		0	10
			15
			20

The parameters shown in Table 1 are examples of variations in:

- *working method* (casting temperature and cooling)

and

- *environmental conditions* (air temperature)

The casting temperature may also be considered as a material parameter from the view of the working site, as it is common that the "material" concrete including a chosen starting temperature can be ordered from the ready mixed factory.

Concrete parameters for the temperature calculation

General

Here the concrete called A has been chosen as a "typical" concrete for the use in a bridge structure. This concrete is of class K45 (classification of cube strength) with a cement content = 430 kg/m^3 and a water/cement ratio of 0.42.

Data for temperature calculation

At the calculation of temperature in this study the heat conduction equation is applied to two-dimensional heat flow due to:

$$k_x \frac{\partial^2 T}{\partial x^2} + k_y \frac{\partial^2 T}{\partial y^2} + P_c = \rho_c c_c \frac{\partial T}{\partial t} \qquad (1)$$

where T[°C] = temperature, t[s] = time, k_x[W/(m°C)] and k_y [W/(m°C)] are heat conductivity in x[m] and y[m] direction, respectively, P_c[W/m^3] is hydration heat of the concrete, ρ_c[kg/m^3] = density of the concrete, and c_c[J/(kg°C)] = specific heat of the concrete. Here only constant conductivity are used, and the numerical values have been chosen to $k_x = k_y = 1.9$ [W/(m°C)], which is believed to be within the expected area for young concrete.

One of the most important concrete parameters is the heat of hydration , which for the actual concrete is described in Figure 3, where the vertical axis shows the hydration heat per weight of cement, and the horizontal axis shows the equivalent time of maturity (t_{equ}) described by

$$t_{equ} = \int_0^t \beta_T dt + \Delta t_{equ}^o \qquad (2)$$

where β_T is the temperature factor ("maturity function") shown in Figure 4, the term Δt_{equ}^o is formally the equivalent time of maturity at time t=0. The parameter Δt_{equ}^o can be used to describe the equivalent tine of maturity at start of calculation or to simulate a casting sequence or the filling rate at casting.

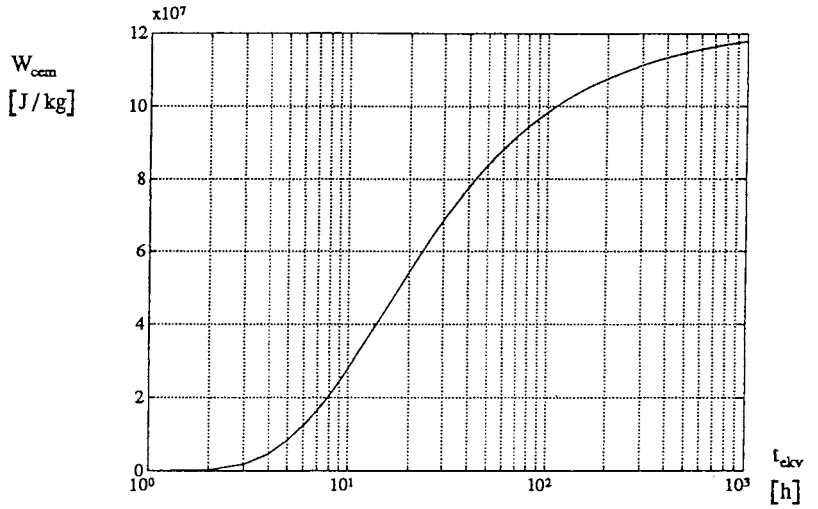

Fig. 3. *Hydration heat for the studied concrete expressed as developed heat per cement weight as a function of equivalent time of maturity.*

For the use of heat of hydration presented in Figure 3 the values of concrete density and specific heat are restricted to the following values:

$$\text{Use of Figure 3} \Rightarrow \begin{cases} \rho_c = 2350 \text{ kg/m}^3 \\ c_c = 1000 \text{ J/(kg°C)} \end{cases} \tag{3}$$

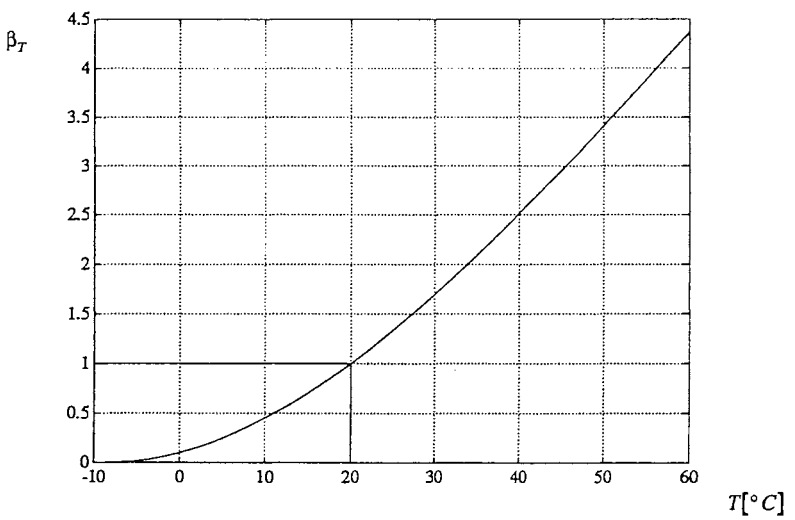

Fig. 4. *Temperature factor, β_T, as a function of temperature for actual concrete. (The factor β_T is also known as "maturity function".)*

Compressive strength

In addition to the information on the temperature field from a calculation with Eq. (1), the use of Eq. (2) gives a description of the maturity development within the structure. This can be used to calculate the strength growth in order to determine form stripping times or to estimate necessary protection against damage at early freezing at winter concreting. The compressive strength, measured on 150 mm cubes for the studied concrete, is shown in Figure 5.

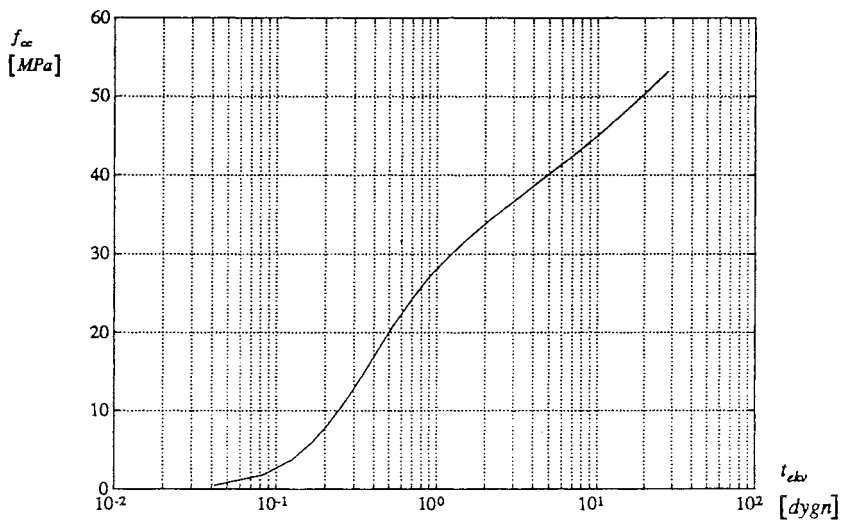

Fig. 5. Compressive strength as a function of equivalent time of maturity for 150 mm cubes for the studied concrete.

Calculated temperature development

General

The illustrations shown here are aimed to give a typical picture of the temperature development, and for this purpose a *summer case* ($T_{air} = T_{cast} = 20$ °C) and a *winter case* ($T_{air} = 0$ °C and $T_{cast} = 10$ °C) have been chosen. For each case the temperature field is presented along a chosen section during the heating phase, which means during the time up to the maximal temperature has been reached in the newly cast structure. At last some temperature differences as a function of time are presented for the whole studied period, which is chosen to be 10 days (240 h) for case I = long column on a basement and to be 6 days (144 h) for the case II = homogeneous column.

Long column on basement

For the vertical mid-section of the long column at level = 0 m the temperature distribution during the heating phase (time = 6 h) is presented in Figure 6. The column is placed from level = 0 m to level = 9 m. The bottom of the basement is placed on level = - 7 m. The start temperatures in the basement is the temperature that has occurred after the casting approximately 5 weeks before the start of the column casting. As can be seen from the figure, the summer case reaches a maximal temperature of about 68 °C, and the winter case about 57 °C. In comparison with the casting temperature, this means about the same temperature increase, i. e. in these cases the dimensions of the columns are so big, that the environmental conditions do not play a dominant role during the heating phase, see Figure 1. From 6 days to 10 days the temperatures decrease only about 1 á 2 °C, which reflects a slow cooling rate. Furthermore, it is seen from Figure 6 that during the heating phase the upper part of the column increases its temperature while lower parts of the column have a slow cooling phase.

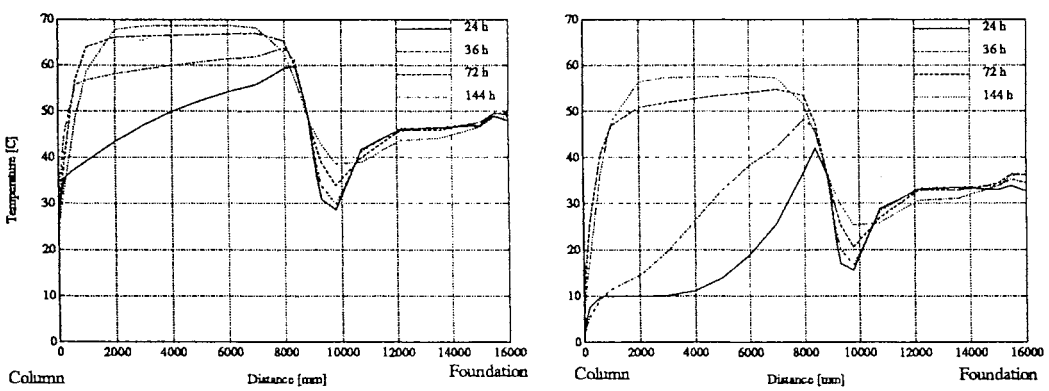

a) Summer case *b) Winter case*

Fig. 6. *Calculated temperature distribution along the vertical mid-section for case I = long column during heating phase until reaching the maximal temperature in the column.*

For the long column the temperature differences between the maximal temperature and a point in the basement situated about 20 centimetres from the top of the basement is shown in Figure 7 as a function of time. From the figure it can be seen that the summer case gives a maximal temperature difference of about 22° C, and for the winter case about 24° C. The fact that these differences decrease very slowly from time = 6 days to time = 10 days reflects that the cooling rate is very slow.

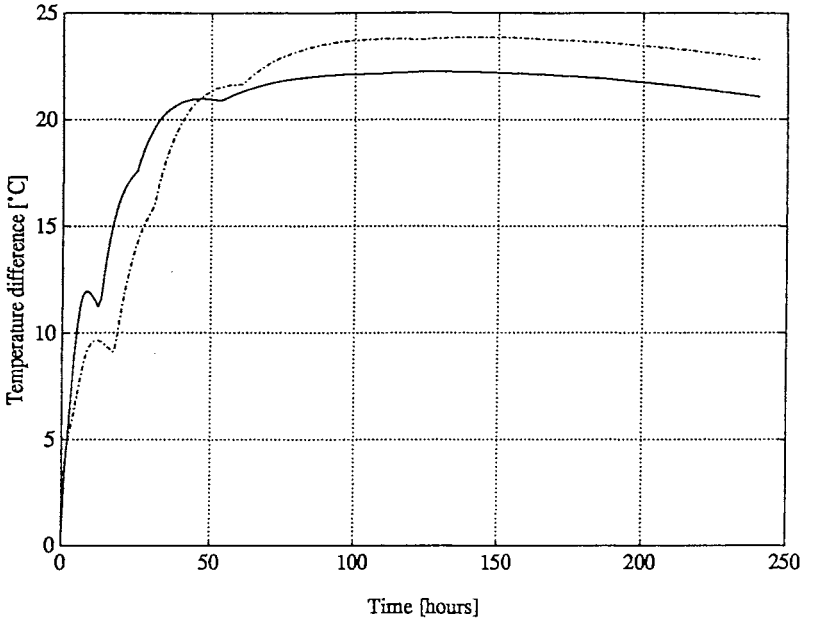

***Fig.** 7. Temperature difference (case I) between maximal temperature in the column and the temperature about 20 centimetres from the top of the basement as a function of time. The solid line is for the summer case, and the dashed-dotted line denotes the winter case.*

Homogeneous column

For the homogeneous column it has been chosen to present the temperature distribution along a section in the shortest direction of the column placed 375 mm from the mid-section of the column. This section is cutting the embedded cooling pipes, see Figures 1 and 2. Figure 8 shows the temperature distribution for the non-cooled section of the case IIa, and Figure 9 shows the corresponding distribution for the section through the cooling pipers of the case IIb.

In Figures 8 and 9 the distance = 0 m means the surface of the column, and distance = 1.5 m means the centroid of the column. The maximum temperature in the column is reached about 36 h after casting for the non-cooled case, and for the case with air cooling the maximum temperature is reached about 24 h after casting. Without cooling the maximum temperature rise is about 45°C for the summer case and about 40 °C for the winter case, which means that for the mid-section of the column the environmental conditions have only a influence of about 10 per cent on the temperature rise. With the use of cooling pipes the summer case has a calculated temperature rise of about 38°C, while the winter

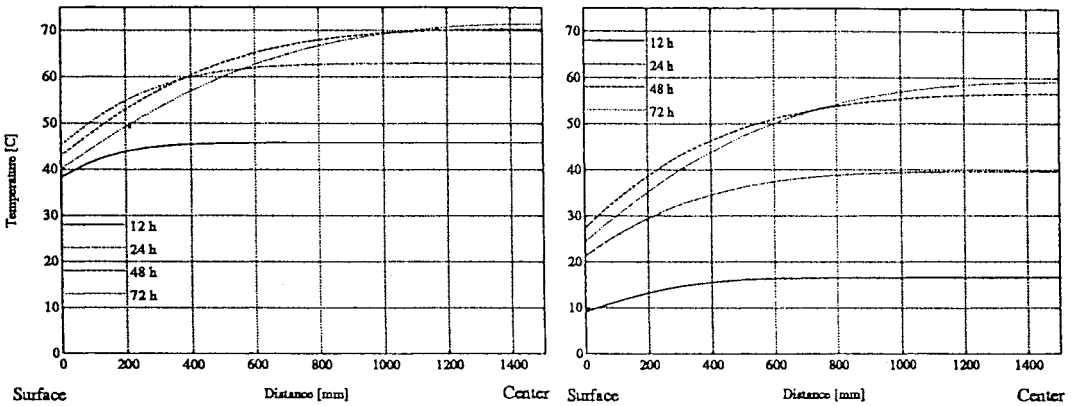

a) Summer case *b) Winter case*

Fig. 8. *Calculated temperature distribution along a section in the shortest direction of the column situated 375 mm from the vertical mid-section for case II a = non-cooled homogeneous column during heating phase until reaching the maximum temperature in the column.*

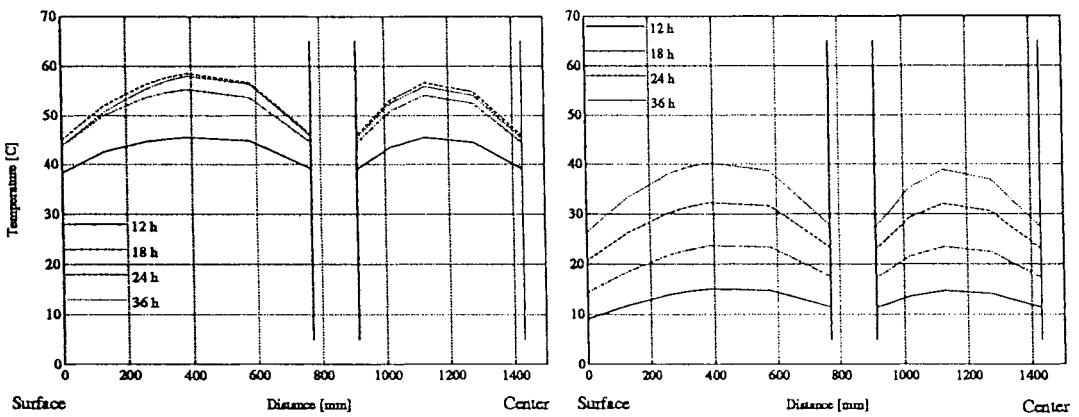

a) Summer case *b) Winter case*

Fig. 9. *Calculated temperature distribution along a section in the shortest direction situated 375 mm from the vertical mid-section for case IIb = air cooling of a homogeneous column during the heating phase until maximal temperature is reached in the column. The chosen section is cutting the cooling pipes in the middle of the structure in the shortest direction.*

case has increased the maximum temperature with only about 22 °. Although, the largest effect of the cooling pipes is that the temperature gradients within the structure decrease strongly, which can be seen in figure 10, where the cooling pipes give a decrease of the temperature differences from about 32 á 37 °C in the non-cooled case to about 14 á 15 °C when using cooling pipes. The result that the temperature differences maintain in time for the non-cooled cases means that the cooling takes place in such a way that the temperature differences is kept inside the column. On the contrary, for the cases with air cooling there is a decrease of the temperature gradients during the cooling phase.

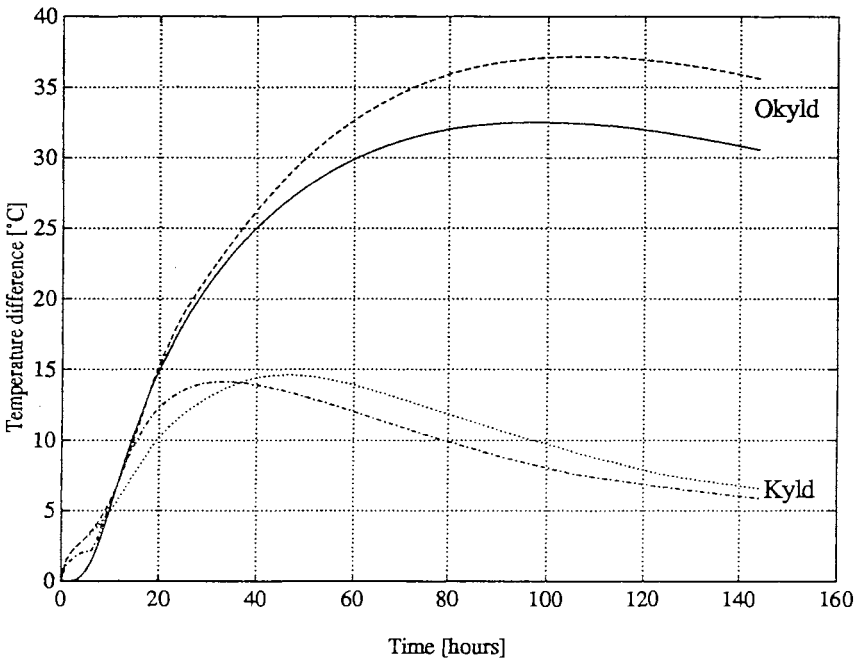

***Fig. 10**. The temperature differences between the maximum temperature in the column and the surface temperature for the homogeneous column as a function of time. The solid line represents non-cooled structure for the summer case, dashed line represents non-cooled structure for the winter case, dashed-dotted line represents air cooling for the summer case, and the dotted line represents air cooling for the winter case.*

Mechanical properties of concrete

At calculation of temperature stresses and crack risks caused by hydration heat it is important that the mechanical properties of young concrete is taking into account in a correct way. The necessary properties are:

* strength development
* elastic and creep behaviour (viscoelastic behaviour)
* temperature expansion and contraction
* fracture mechanics properties

Strength development

The compressive strength can be calculated by analytical expressions or determined by tests, see Figure 5. The tensile strength, f_{ct}, is usually calculated from the compressive strength, for instance in the following way

$$
\begin{aligned}
&f_{cc}^{*}(t) = 0.8 \cdot f_{cc}(t) \\
&f_{ct}(t) = 0.115 \cdot f_{cc}^{*}(t) - 0.022 \qquad \text{for } f_{cc}^{*}(t) \le 20 \text{ MPa} \\
&f_{ct}(t) = 0.105 \cdot (f_{cc}^{*}(t) - 20)^{0.839} + 2.28 \qquad \text{for } f_{cc}^{*}(t) > 20 \text{ MPa}
\end{aligned}
\tag{4}
$$

Direct testing of tensile strength is rather difficult to do, and it is usually carried through only in connection with larger building projects. Figure 11 shows tensile strength development for young concrete due to Eq. 4. When analysing crack risks the slow temperature loading rate should be considered as the tensile strength of concrete hereby will be reduced. For the time periods that usually exist, the reduced tensile strength can be in the order of 65 to 80 per cent of the short time strength.

Viscoelastic behaviour

The elastic and creep deformations can be expressed by

$$\varepsilon_{tot}(t,t') = \varepsilon_{el}(t') + \varepsilon_{c}(t,t') = \frac{\sigma(t')}{E(t')\left[1 + \varphi(t,t')\right]} \tag{5}$$

where $\varepsilon_{tot}(t,t')$ is the total deformation at time t caused by a loading at time t'; $\varepsilon_{el}(t')$ and $\varepsilon_{c}(t,t')$ are elastic and time dependent deformation at time t caused by a loading at time t'; $\sigma(t')$ is the applied stress at time t'; $E(t')$ is the Young's modulus at time t', and $\varphi(t,t')$ is the creep function at time t for loading at t'.

A simpler model is to avoid splitting into elastic and creep parts, and only to consider the total deformation by

$$\varepsilon_{tot}(t,t') = J(t,t')\sigma(t') \tag{6}$$

where $J(t,t')$ is the compliance function [1/Pa] at time t for loading at time t', which can be expressed with the so called modified Triple-Power law.

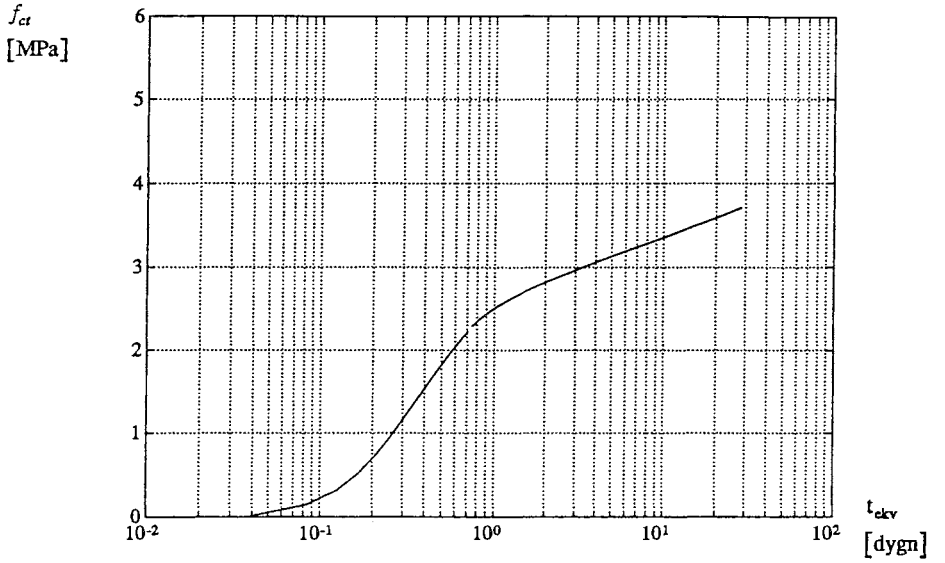

Fig. 11. Tensile strength for young concrete calculated from compressive strength development due to Figure 5 and Eq. 4.

Characteristic for time dependent deformations of young concrete is the strong dependency of the loading time, see for instance the creep curves tested for the actual concrete in Figure 12.

Temperature movements

Measurements of free movements of young concrete in accordance with a pre-chosen time dependent temperature curve gives different temperature movement coefficients at heating and at cooling. Therefore it is suitable to define a temperature heating coefficient, α_h, and a temperature cooling coefficient, α_c. The following values have been used in the present study

$$\alpha_h = 9.4 \cdot 10^{-6} / ^\circ C \text{ and } \alpha_c = 8.6 \cdot 10^{-6} / ^\circ C$$

Constitutive equation

Temperature stresses are calculated by taking into account the temperature development, the associated temperature movements, the mechanical properties, and the restraint conditions for the newly cast concrete. A constitutive model illustrated in Figure 13 has been used, which gives the following expression for the calculated strains

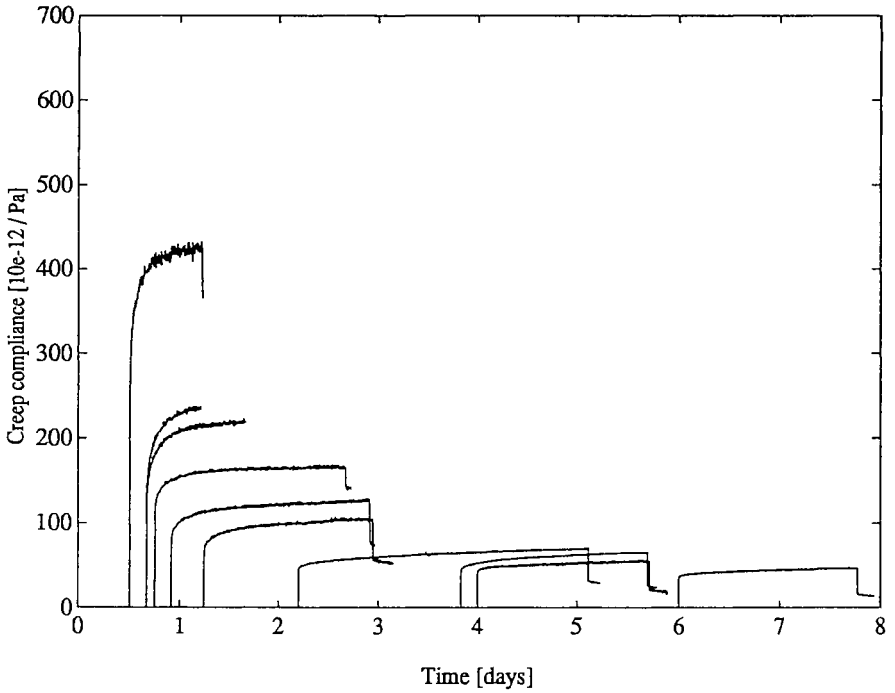

Fig. 12. Results from creep tests expressed as compliance function at early ages for the studied concrete. Every curve shows the sum of elastic and delayed deformations.

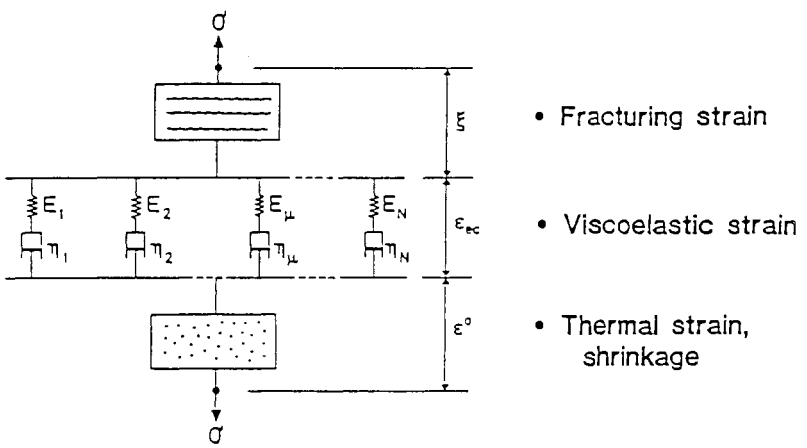

Fig. 13. Illustration of the constitutive model at calculation of temperature stresses and crack risks.

$$\varepsilon = \varepsilon_{ec} + \xi + \varepsilon^{o} \qquad (7)$$

where ε is the external total strain, that is zero for a completely restraint situation ($\varepsilon = 0$ at 100 % restraint conditions); ε_{ec} is the viscoelastic strain; ξ is the strain at softening behaviour (fracture mechanics behaviour); and ε^{o} is the temperature related non-elastic strain.

Temperature cracks

At a complete estimation of risks of temperature cracks the following parameters must be taken into account

- temperature development
- mechanical properties
- degree of restraint
- temperature of connected structures and in the environment

How these parameters are influenced by concrete grade, casting conditions, geometry etc. is very complex, see Figure 14.

The effect of restraining on temperature stresses is often decisive compared with other parameters, which is illustrated for the case of a wall on a completely stiff basement in Figure 15, where totally different temperature stresses are reached at different levels in spite of identical temperature development. For the point marked (1) in the wall high tensile stresses are reached which gives high risks of cracking for through cracks during the cooling phase - i. e. similar as in case I above. The point marked (2) shows early tensile stresses at the surface and risk of surface cracks - i. e. similar as in case II above.

Cracking risks of studied cases

With the constitutive model of Eq (7), with equations of material properties and with material data of actual concrete, partly shown above, thermal cracking analyses have been performed for varied situations of casting according to Table 1.

For Case I, the results from temperature computations showed maximum temperatures of the columns between 58° C and 74° C, temperature differences $\Delta T_1 = T^{max}_{column} - T_{air}$ between 38 °C and 68 °C and $\Delta T_2 = T^{max}_{column} - T_{found.}$ between 15° C and 31° C. Further, about the same temperature increase (maximum temperature - casting temperature) are obtained for all cases, i. e. the effect of temperature of environment can, as mentioned earlier, be neglected for actual massive sections.

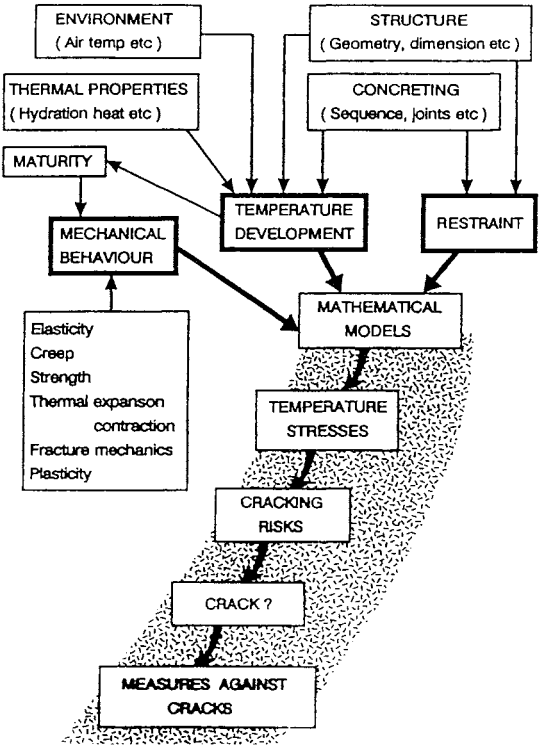

Fig. 14. Block diagram showing the complex relationships between different parameters influencing temperature stresses and crack risks in a

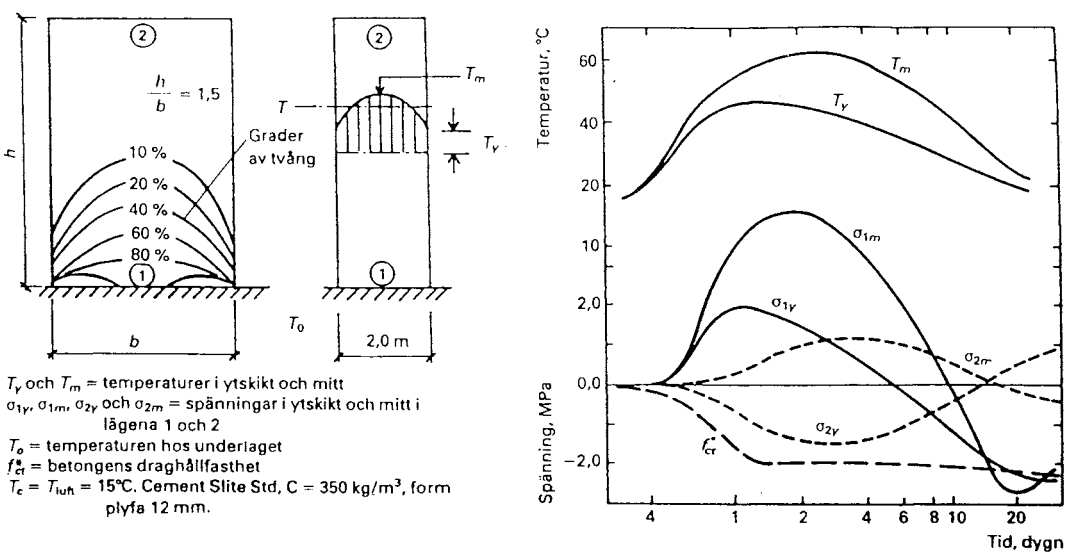

Fig. 15. A wall cast on completely stiff basement. Influence of restraint on the size and sign of the temperature stresses at two different levels from the basement with the same temperature development.

The risks of through cracking in the bottom part the column, η_1^{max}, at the cooling are very high for all cases, see Table 2. According to general estimations and general opinion in Sweden, a cracking risk over 0.7 should be avoided.

Table 2. *Results from temperature- and thermal stress computations of Case I - casting of bridge column on foundation. ΔT_1 and ΔT_2, see text. η_1^{max} and η_2^{max} denote the maximum cracking risk in lowest part of column and in foundation respectively*

T_{cast} [°C]	T_{air} [°C]	T_{max} [°C]	ΔT_1 [°C]	ΔT_2 [°C]	η_1^{max}	η_2^{max}
25	20	73.8	53.8	25.8	0.57	>1
20	20	68.7	48.7	22.3	0.57	>1
15	20	63.6	43.6	18.7	0.62	>1
10	20	58.5	38.5	15.4	0.76	>1
20	0	68.3	68.3	31.2	0.75	>1
15	0	63.0	63.0	27.5	0.73	>1
10	0	57.7	57.7	23.7	0.82	>1

Cracking can appear also in the upper part of the column due to a fast cooling of the upper surface. Also, a considerable risk of cracking η_2^{max} is present in the foundation as it is affected by the newly cast column that tends to expand, see Figure 16. However, possible cracks in the foundation are closed during cooling.

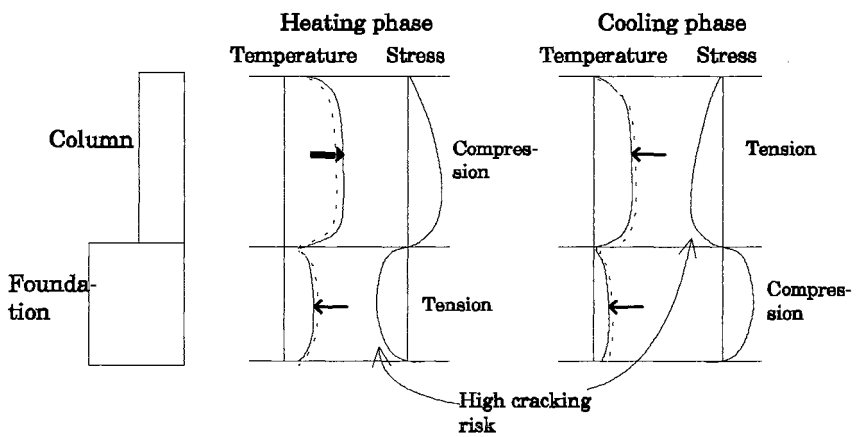

Fig. 16. *Temperature and thermal stress distributions (risks of through cracking), shown schematically when casting a bridge column on a foundation.*

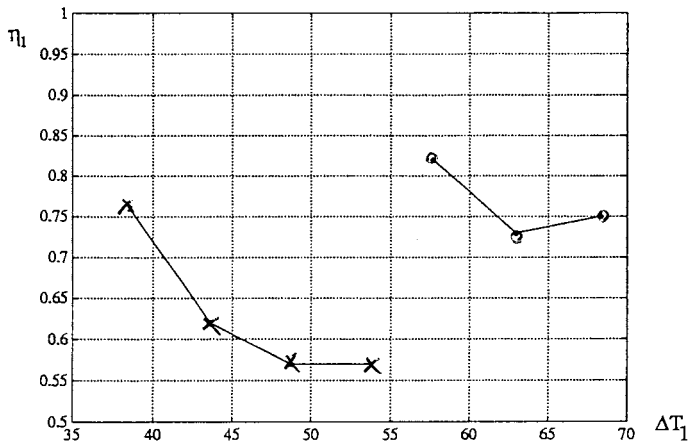

Fig. 17. *Risk of through cracking in the lowest part of the column as a function of the temperature difference* $\Delta T_1 = T^{max}_{column} - T_{air}$. *The curve marked with* **x** *denote summer cases and the curve with legend* **o** *is for winter situations.*

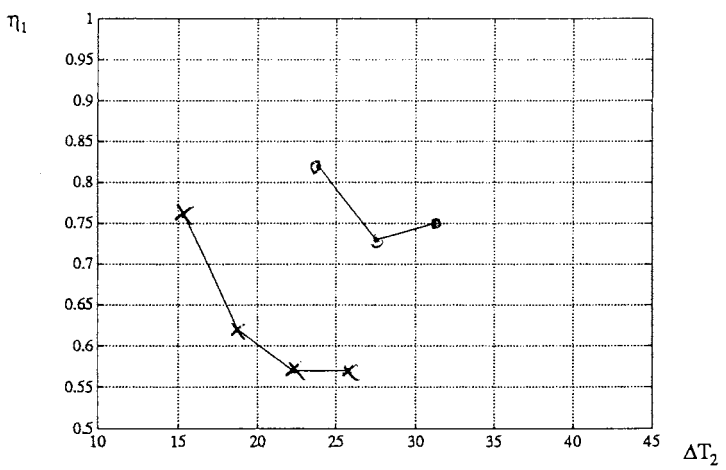

Fig. 18. *Risk of through cracking in the lowest part of the column as a function of the temperature difference* $\Delta T_2 = T^{max}_{column} - T_{found}$. *Notation see Figure 17.*

Plot of cracking risks in the columns as a function of temperature differences ΔT_1 and ΔT_2 give *lower* cracking risk for *higher* temperature differences, see Figures 17 and 18.

Computations for Case IIa, risk of surface cracking of a non-cooled column, show very high cracking risks for all cases according to Table I. The winter cases ($T_{air} = 0$ °C), imply lower cracking risks than the summer cases ($T_{air} = 20$ °C), see Table 3.

Plots of the cracking risks as a function of the temperature differences $\Delta T_3 = T_{max} - T_{air}$ and $\Delta T_4 = T_{max} - T_{surface}$ (Figures 19 and 20) show both decreasing and increasing cracking tendency when the temperature differences are increased. (T_{max} is the maximum temperature in the centre of the column).

An use of embedded cooling pipes, Case IIb, implies strong reductions of cracking risks, see Table 3, Figures 19 and 20. The cracking risks of cooled sections seems to be rather insensitive to the temperature differences ΔT_3 and ΔT_4.

Further, Figures 21 and 22 show the positive effect of the cooling on the distributions of temperatures and thermal stresses for two studied cases .

Table 3. *Results from temperature- and thermal stress computations of Case II - risk of surface cracking. ΔT_3 and ΔT_4, see the text. $\eta_{surface}$ denotes the maximum cracking risk of the surface.*

Case	T_{cast} [°C]	T_{air} [°C]	T_{max} [°C]	ΔT_3 [°C]	ΔT_4 [°C]	$\eta_{surf.}$
IIa	20	20	71.5	51.5	32.5	0.97
non-cooled	15	20	66.3	46.3	29.3	0.98
	10	20	61.4	41.4	26.3	>1
	20	0	70.0	70.6	44.3	0.90
	15	0	65.0	65.0	40.8	0.822
	10	0	59.2	59.2	37.2	0.73
IIb	20	20	59.0	39.0	14.1	0.24
cooled	15	20	54.6	34.6	12.7	0.25
	10	20	50.9	30.9	11.4	0.27
	20	0	50.5	52.5	18.7	0.12
	15	0	46.6	46.6	16.7	0.10
	10	0	40.8	40.8	14.6	0.08

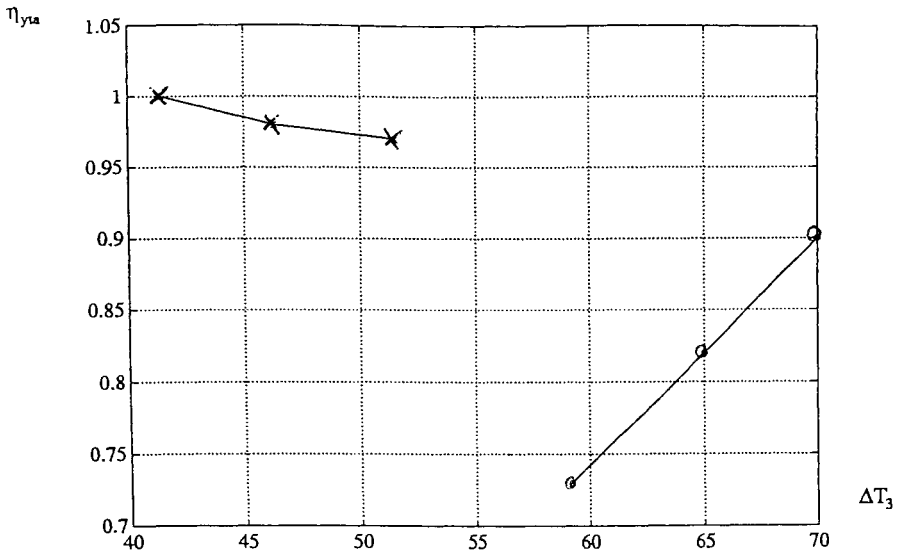

a) Case IIa without cooling pipes

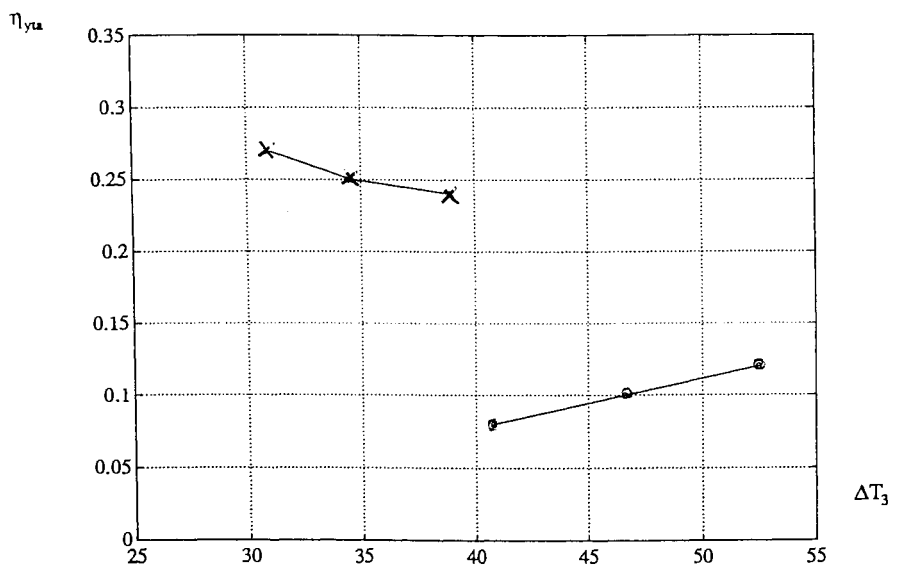

b) Case IIb with embedded cooling pipes

Fig. 19. *Cracking risks as a function of* $\Delta T_3 = T_{max} - T_{air}$. *Lines with* **x** *is the summer case* (T_{air} = 20° C) *and lines marked with* **o** *is the winter case* (T_{air} = 0° C).

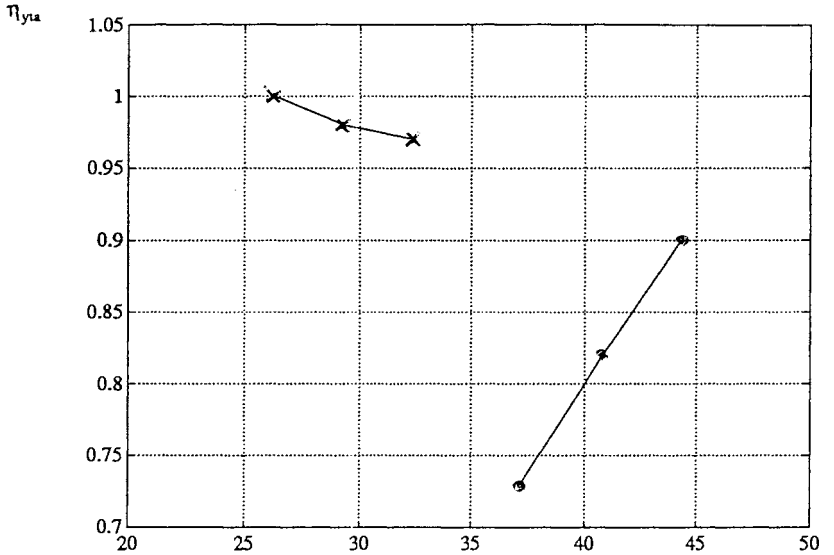

a) Case IIa without cooling pipes

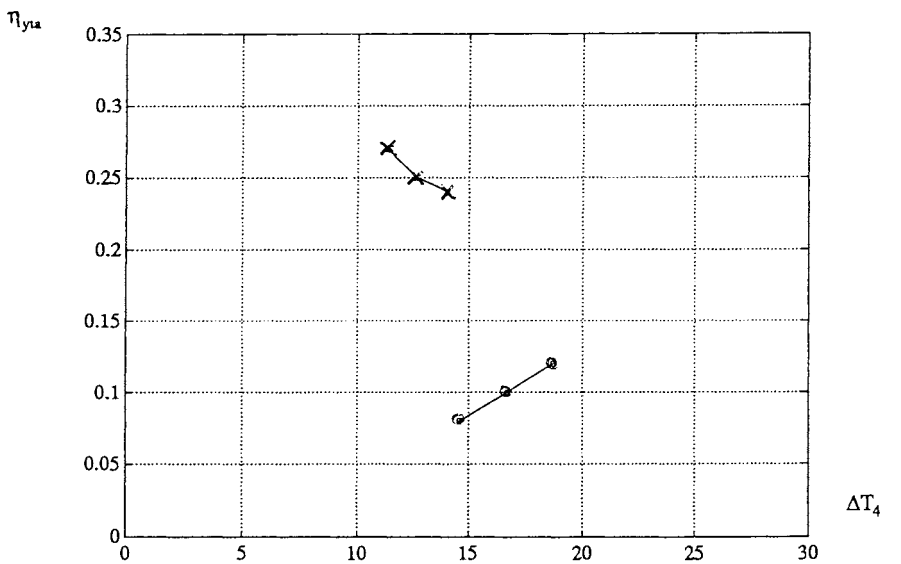

b) Case IIb with embedded cooling pipes

Fig. 20. *Cracking risks as a function of* $\Delta T_4 = T_{max} - T_{surface}$. *Lines with* ***x*** *is the summer case* (T_{air} = 20° C) *and lines marked with* ***o*** *is the winter case* (T_{air} = 0 ° C).

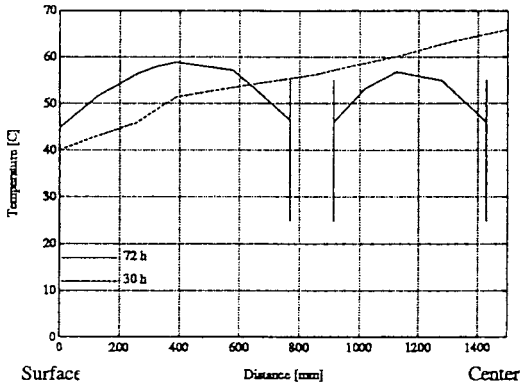

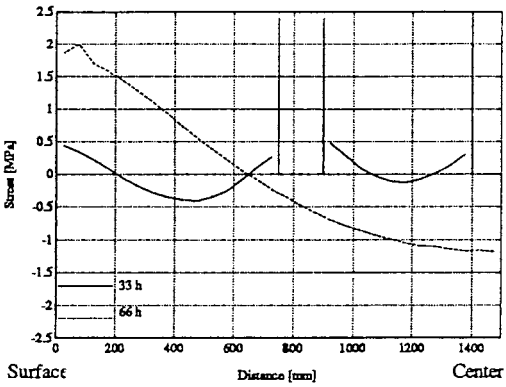

a) Maximum temperature *b) Maximum tensile stresses levels*

Fig. 21. *Maximum temperatures and tensile stress levels in a cooled section (dashed lines) and non-cooled section (solid lines), summer case (T_{air} = T_{cast} = 20° C).*

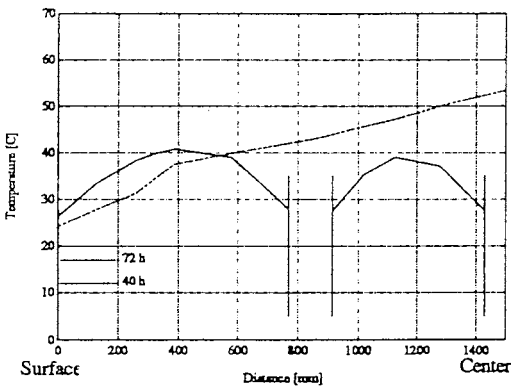

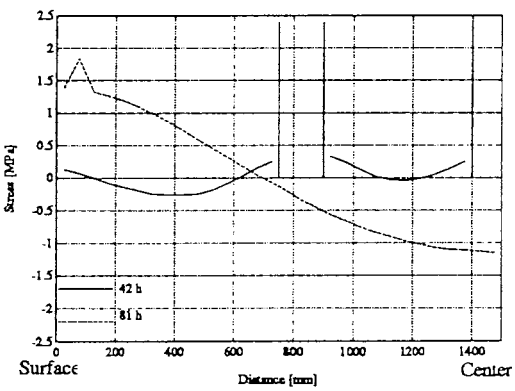

Fig. 22. *Maximum temperatures and tensile stress levels in a cooled section (dashed lines) and non-cooled section (solid lines), winter case (T_{air} = 0° C, T_{cast} = 10° C).*

Tests in the thermal cracking frame

Laboratory work where thermal stresses are studied has been done in several Universities and Institutes of Europe, see e g /6/. Since 1980 such a tests have carried out at the Luleå University of Technology where small concrete cylinders immediately after casting where placed in a servo-hydraulic testing machine and were heated by surrounding water. Thermal stresses were recorded

when the ends of the specimen were fixed, i. e. 100 % end restraint. Test methodology and tests results are shown in /7/.

Since a couple of years the test method has been refined by making the tests horizontally with a larger specimen, see Figure 23 and /8/. The heating is performed by blowing temperated air into a climate box surrounding the specimen. The temperature stresses are recorded by a load cell of the servohydraulic cylinder. With the test method, the total thermal stress and cracking behaviour can be studied for varying temperature curves - simu-lating a wide range of constructive situations - for different concrete mixes, cements types etc. This serve as an important source for calibration of models of computer programs and for optimisation of concrete for applications of interest.

Figure 24 shows examples of results from such a tests. Three different concrete mixes are studied with different properties regarding heat of hydration and mechanical behaviour. The temperature curves of Figure 24 a are obtained by theoretical computations based on adiabatic calorimetry tests and simulate the temperature development of a 0.7 m thick wall. The thermal stresses of Figure 24 b, obtained directly from the tests at 100 % restraint (inflexible supports), show large differences between the concrete mixes. It is clear that mix C is the most suitable for this case.

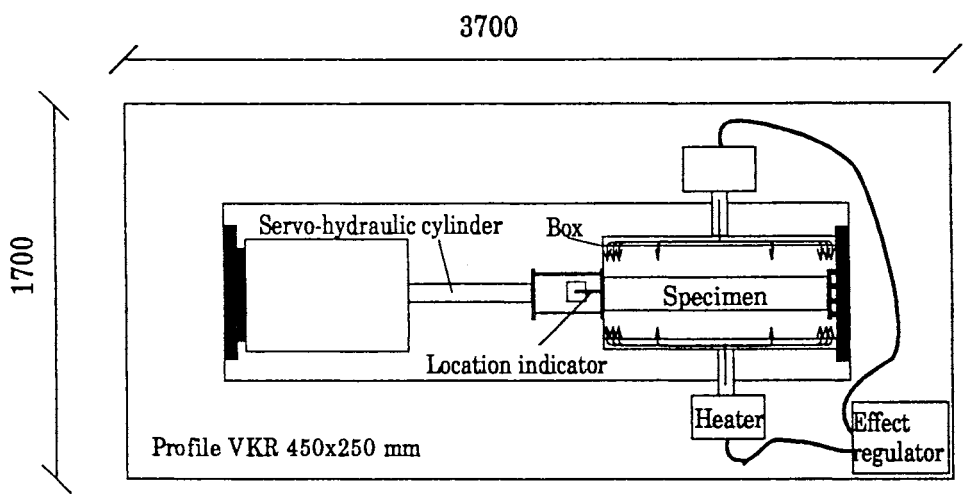

Fig. 23. *Thermal cracking frame, schematically shown, for studying thermal stresses at different simulated constructive situations (from /8/).*

Conclusions

It is demonstrated in this paper and in other research of Luleå University of Technology that thermal crack estimations should be based on *all* influencing factors of Figure 14. Thus, many factors other than temperature should be considered, such as

- varying degrees of restraint in different elements of studied structures
- influence of transient mechanical properties of the young concrete

Crack criteria that are purely based on temperature differentials, which often are used by engineers, offer a poor basis for crack predictions in hardened concrete. This is shown by three examples of Table 3 where criteria based on stress computations are compared with pure temperature related criteria, see Table 4. In the table, the discrepancies between cracking risks obtained from temperature computations and stress computations are clearly demonstrated. Compare for instance the correlation factors of cooled and non-cooled summer case.

By the method of cracking analysis described in the article, it is possible to compare effects of different methods for reduction of cracking risks. For the studied cases a cooling with embedded cooling pipes has a significant positive effect on tensile stresses and cracking risks. On the other hand, a lowering of the placing temperature has a very small effect on risk of cracking. In fact, in some cases, a *higher* risk is obtained with a *lower* placing temperature.

The results of the laboratory tests with the cracking frame support the general conclusion that all influencing factors, not only temperature, must be included in an analysis and in a choice of crack arresting methods.

Table 4. *Comparisons between temperature related and stress related criteria avoidance of thermal cracks.*

Case	II (winter)	IIa (summer)	IIb (summer, cooling)
T_{cast}	10	20	20
T_{air}	0	20	20
Max temp difference within structure ΔT_4 [°C]	37.2	32.5	14.1
Stress related criteria η_{surf}	0.73	0.97	0.24
Temperature related criteria $\Delta T_4/\Delta T_{crack}$ *	1.86	1.62	0.70
Correlation factor $(\Delta T_4/\Delta T_{crack})/\eta_{surf}$	2.54	1.67	2.93

**) Here, the often used temperature related criteria $\Delta T_{crack} = 20°C$ is chosen which means that the temperature difference within cast section can not be higher than 20 ° C*

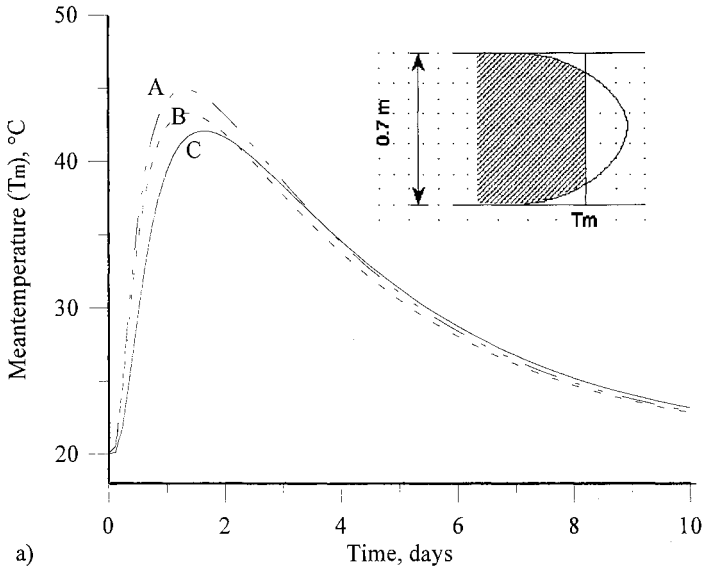

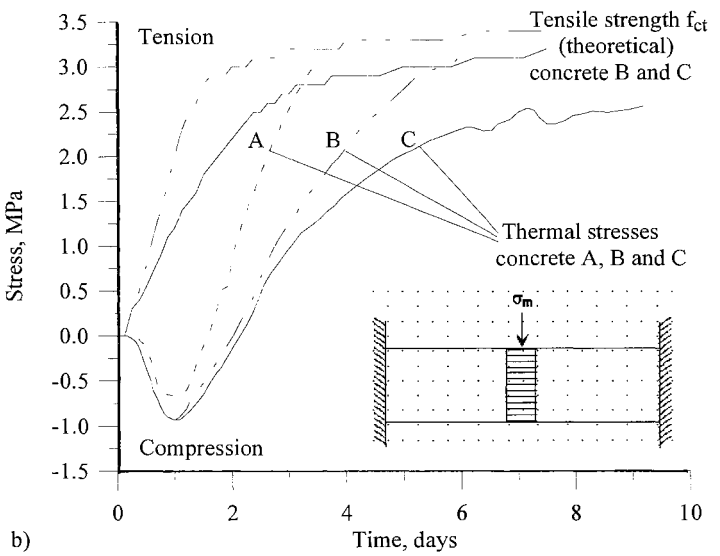

Fig. 24 a) *Mean temperature development of a 0,7 m thick wall Computations with HETT program.*
b) *Recorded thermal stresses at 100 % end restraint the with frame of Figure 23.*

References

1. *Bernander S, Emborg M.* Cracking in massive concrete structures, Chapter 27 in the Handbook for Concrete Design - Workmanship, Svensk Byggtjänst, Stockholm 1992, Sweden, 639 - 666 (in Swedish).

2. *Jonasson, J-E, Emborg M, Bernander S.* Temperature, maturity development and thermal stresses in young concrete. Chapter 16 in the Handbook for Concrete Design - Material, Svensk Byggtjänst, Stockholm 1994, Sweden, 547 - 607 (in Swedish).

3 *Emborg M, Bernander S.* Assessment of the risk of thermal cracking in hardening concrete. Journal of Structural Engineering (ASCE), New York, Vol 120, No 10, October 1994, pp 2893 - 2912.

4. *Jonasson J-E.* Modelling of temperature, moisture and stresses in young concrete, Division of Structural Engineering, Luleå University of Technology, Doctoral Thesis, 1994:153D, Luleå 1994, 225 pp.

5. The Crack Free Program - A program for avoiding thermal cracking, Betongindustri AB, Stockholm 1993, 10 pp.

6. *Rilem.* Proceedings from International Rilem Symposium on Thermal Cracking in Concrete at Early Ages (edited by R Springensmid), 10 - 12 October, Munich, 1994.

7. *Emborg M.* Thermal stresses in concrete structures at early ages. Division of Structural Engineering, Luleå University of Technology, Doctoral Thesis, 1989:73D, Luleå 1989, 285 pp.

8. *Westman G.* Thermal cracking in high performance concrete. Viscoelastic models and laboratory tests. Division of Structural Engineering, Luleå University of Technology, Licentiate Thesis, 1995:27L, Luleå 1995, 123 pp.

9. *Ekerfors K.* Maturity development in young concrete. Temperature sensistivity, strength and heat of hydration, Division of Structural Engineering, Luleå University of Technology, Licentiate Thesis, 1995:34L, Luleå 1995, 136 pp (in Swedish).

Concrete Specifications for the Öresund Link

Göran Fagerlund,
Lunds Tekniska Högskola, avd. byggnadsmaterial

The Öresund Link – a short presentation

A combined bridge and tunnel link between the Swedish city Malmö and the Danish capital Copenhagen is now under construction. The construction works started in the autumn of 1995, and according to the plans, the link will be opened in the year 2000. The total length of the link is about 15.5 km consisting of a submerged tunnel (3.8 km), two approach bridges (6.4 km), a high bridge (1.1 km), and an artificial island (4.2 km). The link is designed for combined train and car traffic.

The submerged tunnel consists of prefabricated concrete elements which are exposed to sea water without being protected by a membrane of any kind; steel, bitumen or polymer.

The bridge sub-structure (bottom slabs and pier shafts) is made of concrete. The concrete is cast in special element factories on shore. The elements are floated to the building site where they are placed. The pylons for the cable stayed high bridge are cast in situ, in "open sea".

The bridge super-structure is made of framework steel girders with an upper bridge deck made of concrete. The car traffic runs on the upper bridge deck and the train traffic runs inside the steel girder in a concrete tray. The high bridge is cable stayed with a free span of 492 m and a clearance to the water table of 57 m.

Table 1. *Concrete volumes.*

Part of the link	m^3
High bridge	55 000
Approach bridges	260 000
Tunnel	650 000
Ballast concrete [1)]	40 000
Total amount	1 005 000

1) used for increasing the weight of the tunnel

The service life requirement

The Owner clearly states, that he wants a service life of the Öresund Link that is at least 100 years. The following is cited from the "Explanatory Document of the Construction Requirements for the Concrete Works":

"100 years of service life shall be ensured for all concrete structures. Easy replaceble concrete components (e.g. crash barriers) can have a service life of 50 years. The service life is defined as the period within which full function is maintained. Reinforcement corrosion is not allowed to start within the 100 years of service life. Maintenance shall be performed, but major repair-work or replacement shall be avoided.....".

It must be observed that "service life" is not a deterministic property signifying that the whole structure will lose its function after exactly 100 years. Instead, it is an extremely complex property composed of many "sub-properties". Therefore, service life is subject to a certain variation; also different parts of the same structural part will have a considerable spread in service life. The spread is even bigger for the entire structure. Service life can, therefore, be defined as a certain point on the service life probability density function; e.g. it might be defined by the lower 5% fractile, meaning that only 5% of the structure will have a service life below 100 years. This probabalistic approach is visualized in Figure 1.

The Owner is aware of the fact that a quantified service life requirement, expressed in years, cannot be used as a functional requirement in a building

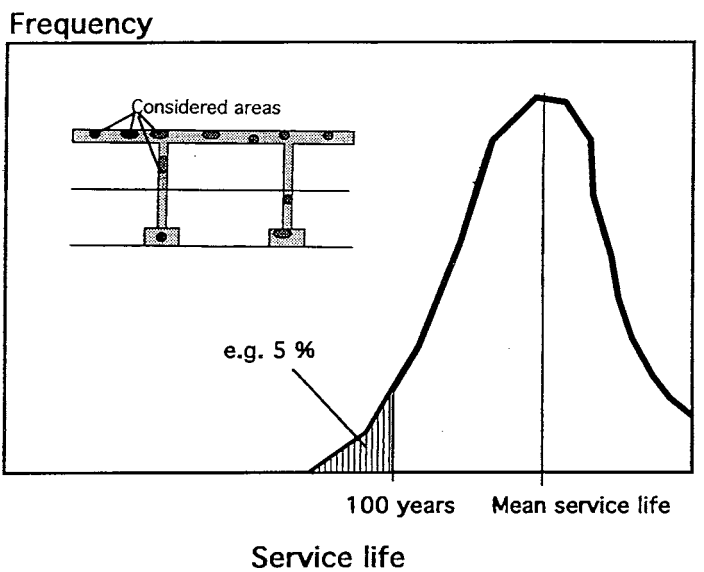

Fig. 1. *A definition of service life.*

contract. It is not possible in the negotiation phase to judge different tenders in a fair way when it comes to compare the different technical solutions, and their ability to give the desired service life. Besides, it would be almost impossible to prove, during the building phase, by taking samples of the fresh or hardened concrete, that the structure will obtain the service life aimed at. Therefore, the service life requirement is translated into substituting properties that are coupled to service life. Important properies are:

1: Maximum water/cement ratio
2: Minimum air content
3: Minimum concrete cover
4: Maximum crack width
5: Required composition of the cement and other binders

These requirements are supplemented with strict requirements concerning the pre-testing of the concrete mixes to be used in the structures, and strict requirements concerning the control of the mix, and the production. Important properties to be pre-tested are:

1: Frost resistance, and salt scaling resistance
2: Thermal and mechanical properties of the young concrete during hardening. These measurements are to be supplemented by a theoretical analysis of the thermal crack risk during the construction phase

The requirements are to a great extent based on knowledge obtained from research performed during the last years, and on modern field studies of concrete exposed for shorter or longer times to the real environment. Much of the back-ground information comes from research presented in the previous papers in this report. A short description and discussion of the requirements is made below.

The requirements are almost the same for the bridges as for the tunnel. There are some differences, due to the different environments to which the two types of structures are exposed. Only major differences are treated below.

Overview of concrete types

The tunnel, and the bridge, are divided in different climate zones. A certain concrete quality is required for each zone. Principally, there are two types of concrete prescribed:
Type A, with a maximum water/binder ratio of 0.40
Type B, with a maximum water/binder ratio of 0.45

Table 2. Principles for selecting concrete types.

Tunnel		
Zone 1	Severe marine anvironment *Outer walls, roof, floor*	A
Zone 2	Non-marine environment *Inner walls. Part of portal buildings*	B
Zone 3	Frost environment *Ramps. Parts of portal buildings*	A with air
Zone 4	Marine environment No static function *Ballast concrete*	B
Bridges		
Zone 1	Marine environment *Constantly below water (<-3m)*	B
Zone 2	Severe marine environment *The splash zone (-3m to +6m)*	A with air
Zone 3	Marine environment with de-icing salt *(+6m to 6m above bridge deck)*	A with air
Zone 4	Marine environment with frost *(>6m above bridge deck)*	B with air

Each concrete type shall be airentrained or non-airentrained depending on whether it is exposed to frost or not.

The concrete cover is different in different zones. The following values are valid:

* Outer surfaces of tunnel walls and portal buildings: 75 mm
* All outer surfaces of the bridge: 75 mm
* Internal surfaces in the tunnel: 50 mm
* Internal surfaces in bridge piers, etc: 50 mm
* Top surface of bridge deck covered with membrane: 50 mm

There are also restrictions concerning the types of binders allowed. The differences depend on the different types of environment for the tunnel and the bridges:

The tunnel:

* Ordinary portland cement of type low alkali/sulfate resisting.
* Fly ash, maximum 15% of the binder. Efficiency factor 0,3.
* Silica fume, maximum 5% of the binder. Efficiency factor 2.
* Sulfate resisting slag cement with at least 66 % of ground granulated blastfurnace slag.

* Fly ash and silica fume are allowed to be used in combination, but only together with portland cement. No additions are allowed to slag cement.

The bridges:

* Ordinary portland cement of type low alkali/sulfate resisting.
* Silica fume, maximum 5% of the binder. Efficiency factor 2.

The basis for these limitations to cement is further discussed below.

Frost resistance

All concrete parts exposed to frost shall be frost resistant. There are two types of frost damage to cope with; (i) internal damage causing loss of cohesion of the concrete, and loss of bond to the reinforcement; see Figure 2, /1/; (ii) surface scaling, gradually reducing the concrete cover protecting the reinforcement, /2/, and causing æsthetic damage.

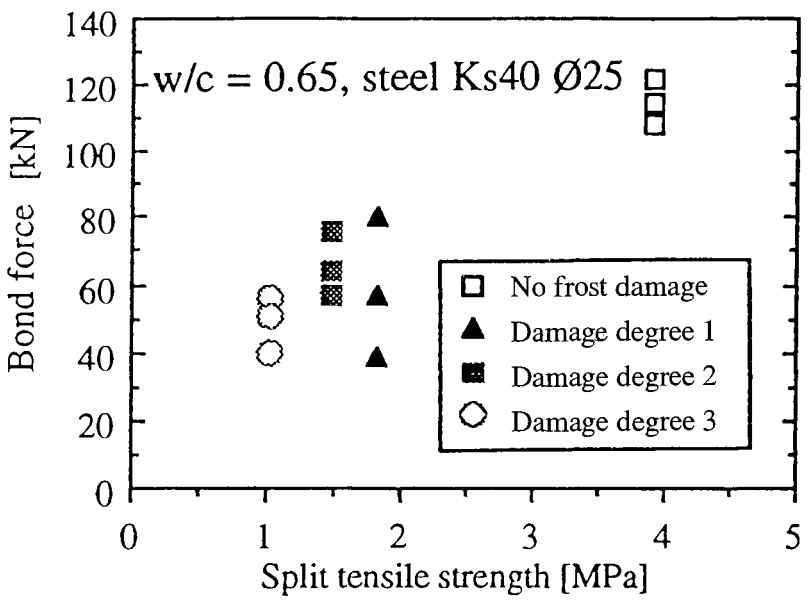

Fig. 2. *Effect of frost damage on the bond between concrete and reinforcement. The extent of frost damage is expressed in terms of the residual split tensile strength; /1/.*

Internal frost damage-theoretically

Internal damage occurs when the concrete is more than critically saturated. The best manner to avoid this situation is to introduce an entrained air-pore system

of a sufficiently high quality. Then, the cement paste will be protected, and, therefore, the concrete will be frost resistant, provided the aggregate is non-porous, and provided there are no other defects in the concrete structure.

Many parts of the concrete structure, such as the pier shafts in the splash zone, will be constantly exposed to water. Therefore, one must assume that the water content in the concrete will gradually increase due to a dissolution-of-air/replacement-by-water process in the air-pores. This process is described in /3/. Sooner or later, the critical saturation is reached, and the concrete fails when it freezes. The water absorption can be described by:

$$S = a + b \cdot t^c$$

Where S is the degree of saturation of the concrete (S=0 when the concrete is completely dry, and S=1 when it is completely saturated), a, b, and c are constants, that are determined by the permeability of the concrete, and by the shape of the air-pore system; /3/. t is the exposure time.

The service life is ended when S equals the critical degree of saturation, S_{cr}, which is, as a first approximation, supposed to be time-independent. The service life of the constanly water exposed concrete, therefore, is:

$$t_{life} = \{(S_{cr} - a)/b\}^{1/c}$$

S_{cr} is a material constant, that can be determined experimentally, /4/, or be calculated theoretically /5/. The constants a, b, and c can also be determined experimentally by a capillary absorption experiment, /4/. The coefficient a corresponds closely to the water content when all pores exept the air-pores are water-filled /3/. Thus, the higher the air content, the lower the value of a, and the longer the service life. The exponent c is of the order 0.25, /3/. The coefficient b depends on the diffusivity of dissolved air. Its value is almost totally unknown. Some tests indicate that it is of the order 10^{-4} for a dense concrete when t is expressed in seconds, /3/. Theoretically, these values of the constants a, b and c give a service life of 100 years for a concrete with a water/cement ratio 0,40 and an air content of 3%, provided the critical degree of saturation exceeds about 0,80. This is a rather low value. Normal values of S_{cr} for concrete is 0.80 to 0.90. Therefore, the service life of such a concrete might even be higher than 100 years. Practical experience show, that a concrete, containing at least 3 to 3.5% of entrained air in its hardened structure, is normally frost resistant, also when it is exposed to a very moist environment during a very long time.

Even if the air content seems to be in order, as shown by the salt scaling test, there might be structural defects, that do not influence the salt scaling resistance, but which might change the situation as regards internal frost attack; viz. it can be shown theoretically that a very small amount of freez-able water, 5 to 10 liters per m^3 of concrete, might be high enough to cause severe internal frost damage /6/. Freezable water, that might cause trouble, can be located in the following places; (i) in some air-pores. The risk is particularly big when the air-pore system is collapsed forming more or less continuous channels. This might happen when an unsuitable combination of water reducing or plasticizing admixture, air-entraining admixture and cement is selected; (ii) in aggregate pores and cracks; (iii) in interfaces between aggregate and cement paste; (iv) in cracks inside the concrete. Such defects can only be revealed by a freeze/thaw test, such as the dilation test described below.

Internal frost damage-requirements and pre-tests

Due to the uncertainties in the equation above for service life, this is not utilized for ensuring the internal frost resistance. Instead it is assumed that an air-pore system with an inferior shape will be rejected by the comprehensive salt scaling tests performed; see below. Besides, it is prescribed, that the air content of the hardened concrete shall not be below a certain value, that shall be determined by the salt scaling test described below.

The eventual negative effects of defects in the internal structure, mentioned above, will be investigated during the pre-testing of the mixes to be used. The test is a so-called dilation test of cylinders cast in a representative manner. The cylinders are stored in water during prescribed times, up to half a year. After the prescribed water storage, the cylinder is directly exposed to a single slow freeze cycle to -20°C. The length change is monitored. Any deviation from the extrapolated pre-freezing contraction curve is a sign of a frost effect. The deviation, or dilation, might be positive (expansion), or negative (contraction). Principally, no positive dilation should be accepted. In practice it is reasonable, however, to accept an expansion that might be a certain fraction of the tensile fracture strain; e.g 50% of this, or about 0.05‰. The test is inspired by the American test ASTM C671, "Critical Dilation of Concrete Specimens Exposed to Freezing".

It can be shown theoretically, that also a small amount of freezable water in the coarse aggregate, or in interfaces, might be high enough to cause severe trouble; /6/. Examples of test results of a dilation test similar to that prescribed are seen in Figure 3; /7/. By this method, unsuitable aggregate, containing too many cracks or pores, and unsuitable admixture types, causing unstable air-pore systems, will be rejected.

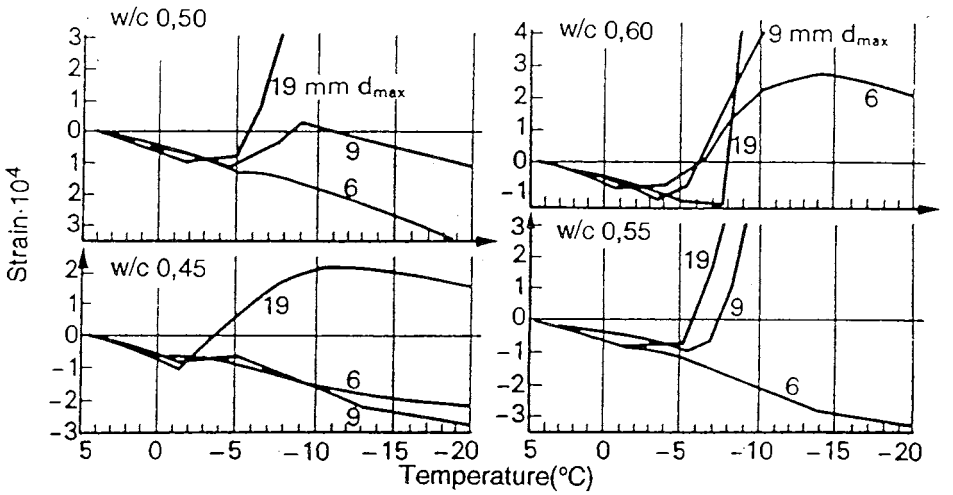

Fig. 3. Example of the result of dilation tests. Concretes with different aggregates are tested. The dilation is a function of the size of the aggregate and of the water/cement ratio; /7/

A new dilation test must be performed if major changes are made in the concrete mix; such as a change in the type of coarse aggregate.

Salt scaling-theoretically

Salt scaling of the concrete surface might occur when this is exposed to weak salt solutions in connection with freeze/thaw. Each new freezing cause additional scaling. This seems to be a function of the minimum freezing temperature. Thus, it seems as if the most severe freezings, down to rather low temperatures, are of the main interest for salt scaling.

The mechanism behind salt scaling has never been clarified. For ordinary concrete it seems as if an outer salt concentration of the order 3% is most severe; e.g. /8, 9/. For very dense concretes, it seems as if the absolute level of the salt concentration is of less importance; /10/. Even for such concrete it is quite clear, however, that pure water in contact with the concrete surface is much less harmful than is also a very weak salt solution. According to a theory just put forward, salt scaling might be a phenomenon of a similar type as frost heave in the ground; /11/. Ice, that has been formed close to the surface, will

suck water from the salt solution outside the concrete. Therefore, the ice bodies will grow and expose the concrete to pressure as long as there is thermal equilibrium at the ice front; i.e. as long as equal amounts of heat are leaving the ice and transferred to the ice. The water transfer is propelled by differentials in free energy between the ice and the unfrozen water. The mechanism is a variant of the microscopic ice lens segregation theory; /12/.

The salt scaling can be retarded, linear, or accelerated. Accelerated scaling cannot be allowed, because it normally leads to rapid destruction. The total amount of scaling after 100 years must be below 10 to 20 mm if the protective action of the concrete cover shall be maintained; /2/. This means that a scaling of less than 0.005 mm to 0.01 mm can be accepted at each freezing, if the number of severe freezings is supposed to be 20 each year. This corresponds to a weight loss of about 0.01 to 0.02 kg/m^2 for each cycle.

It has turned out, that some very dense concretes, containing mineral by-products, such as silica fume, might have a very low scaling during the first cycles. Then, rather suddenly, after a number of cycles, they get an accelerated scaling, that might lead to total destruction under test conditions; /13/. The reason for this behaviour is not clarified. One imaginable explanation is that the air-pore system becomes inactivated by water absorption; /3/. It might be that this inactivation occurs more rapidly in concretes containing mineral by-products.

Salt scaling-requirements and pre-tests

The concrete mix to be used shall be pre-tested with regard to its salt scaling resistance. The test method is the Swedish method SS 13 72 44 also called "The Borås Method". The test is prolonged to 112 cycles considering the dense concretes to be used, and considering the allowed use of silica fume. The test specimens are drilled out of big blocks, that are manufactured in a manner, as regards mixing, transport, placing and compaction, that as closely as possible resembles the real production technique.

The requirement for an accepted mix is that the average scaling of all specimens shall be below 0.3 kg/m^2 after 56 cycles and below 1.0 kg/m^2 after 112 cycles. There are also requirements for the maximum scaling of single specimens. The 112 cycle scalings correspond to about 10 mm of scaling after 100 years provided there are 20 severe freezings each year, and provided every new cycle gives the same amount of scaling.

Many concrete recipes must be tested, and the most favourable selected. The aim of the test is to find the minimum air contents of the fresh and hardened concrete, that are needed for a high enough salt scaling resistance. The fresh air

content is determined after different stages in the production process: (i) after mixing; (ii) after transport, but before pumping; (iii) after pumping. The last air content is used as the target air content during the production phase. It might, however, be replaced by the air content after mixing, once the relation between the two air contents has been established.

A new pre-testing must be performed every time a major change is made in the concrete mix; such as a change of cement or admixture, or a change in the consistency. Then, the whole programme has to be repeated, and new target air contents has to be established. This is necessary, since rather small changes might drastically change the salt scaling resistance.

Frost resistance-production tests

The comprehensive pre-testing programme, during which robust mixes are developed, makes it less meaningful to make production testing of frost resistance. This is instead secured by frequent measurements of the air content of the fresh mix. Batches with too low air contents will be rejected.

Another problem of using freeze/thaw tests as production tests is that they are very time consuming. Therefore, they cannot be used for rapid control and necessary changes of the mix and of the production technique.

As a means of controlling the general quality level of the finished structure, specimens are drilled out at certain intervals. So for example, specimens can be taken shortly after the start of production of new types of elements. The drilled out specimens are controlled with regard to the air content and the salt scaling resistance. Then, the acceptance criterion for scaling is increased to 0.5 kg/m^2 at 56 cycles. Principally, these tests can be used for rather rapid changes in the concrete mix, and/or in the production technique. They can also be used as a criterion for stopping production, in cases where the salt scaling results are repeatedly unacceptable.

Reinforcement corrosion

Marine exposure of the bridges

A very conservative calculation of the service life of the concrete in the splash zone is made using the following assumptions:

1: The chloride concentration is 0.46 mole/litre. (This is the same as in the North Sea, but somewhat higher than what is normal in Öresund.)
2: There is an accumulation of free chloride in the surface by a factor of 2, to 0.92 mole/litre.

3: A low alkali cement is used, giving a free OH-concentration in the pores at the bars of 1.04 mole/litre
4: The threshold concentration of free chloride for onset of corrosion is given by the Hausmann criterion; /15/:

$$[Cl^-]/[OH^-] > 0{,}60$$

Thus, the threshold concentration is; $0.60 \cdot 1.04 = 0.62$ mole/litre
5: The concrete cover is 75 mm.
6: A service life of at least 100 years ($3.154 \cdot 10^9$ seconds) before start of corrosion is required
7: The concrete has a water/binder ratio of 0.40, or lower

Then, assuming the chloride diffusion coefficient being constant over time, the maximum tolerable value of this can be obtained by Fick's law. Inserting the values above gives:

$$0.62/0.92 = erfc\{0.075/(4 \cdot 3.154 \cdot 10^9 \cdot d_{eff})^{1/2}\}$$

This gives a diffusion coefficient of maximum $5 \cdot 10^{-12}$ m^2/s.

There are also other possibilities, or cases, to consider, such as:
Case 1: The accumulation occurs at the surface by a factor 3. Then, the maximum allowable diffusivity becomes $1.5 \cdot 10^{-12}$ m^2/s
Case 2: The threshold concentration is increased by 25%. Then, the maximum allowable diffusivity becomes $24 \cdot 10^{-12}$ m^2/s
Case 3: The threshold concentration is increased by 25% and the accumulation occurs by a factor 3. Then, the maximum allowable diffusivity becomes $2.6 \cdot 10^{-12}$ m^2/s
Case 4: The threshold concentration is doubled. *Then, corrosion is impossible*
Case 5: The same assumptions as in the first calculation, but all alkalies (Na^+ and K^+) are assumed to be leached out. Then, the threshold concentration is reduced to about 0.02 mole/litre. The maximum diffusivity becomes $1.4 \cdot 10^{-13}$ m^2/s
Case 6: The same as case 5:, but the threshold concentration is increased by a factor 5. Then, the maximum diffusivity is $3.3 \cdot 10^{-13}$ m^2/s
Case 7: The concrete is made with a sulfate resisting slag cement with the same water cement ratio as in the other cases. Observations indicate that the OH-concentration might be lowered to 50% of that of the portland cement concrete; /15/. Thus, assuming the same criterions as in the

first calculation, the maximum diffusivity of the slag cement concrete becomes about 20 % of that of portland cement or $1 \cdot 10^{-12}$ m^2/s.

The following conclusions can be drawn:

1: The values of the maximum allowable diffusion coefficient for unleached concrete, with the low threshold concentrations assumed are of the order obtained in field tests; the first calculation, and cases 1: and 3:.
2: The value for a doubled threshold concentration compared with the Hausmann criterion, makes corrosion impossible; case 4:.
3: The cases where total leaching is considered give maximum chloride diffusivities that are low also compared with diffusivities obtained in field studies; cases 5: and 6:. Total leaching on a depth of 75 mm is, however, very unlikely, considering the very dense concrete.
4: The maximum allowable diffusivity of the slag cement concrete is low, but it is well-known that slag cement concrete has a low effective chloride diffusivity in reality. A big field test perfomed in the North Sea shows that the long-term diffusivity of slag cement is only 33% of that of pure portland cement; /16/. Thus, the OPC concrete and the slag cement concrete with the same water/cement ratio obtain almost the same service life before start of corrosion: case 7:.

All these calculations indicate that it is reasonable to assume, that a concrete with a water/binder ratio below 0.40 and a cover not smaller than 75 mm, ought to obtain a service life of at least 100 years in the marine environment, provided the cover is uncracked. The assumptions behind these calculations are conservative, especially the threshold criterion for onset of corrosion. It might very well be that initiation of corrosion is not possible at all in uncracked concrete in the actual environment, and with the actual water/cement ratio.

Marine exposure of the tunnel

The enclosure walls of the submerged tunnel are unprotected. Thus, there will be a constant water flow across the walls bringing with it chloride, that might accumulate at the inner surface of the tunnel walls. It is, therefore, very important that the permeability of the concrete is very low. An estimation has been made of the total flow in uncracked concrete during a period of 100 years. The basis of the calculation is long-term measurements of the equilibrium moisture flow across concrete specimens stored with one end in water and the other in 33% RH; /17/. This measured flow has been transformed into a calculated flow across the one meter thick walls of the tunnel. The walls are also exposed to an outer sea water pressure corresponding to a water depth of about 35 meters. This has been considered in the calculations.

The calculations indicate that the maximum flow is of the order 10 kg/m^2 during 100 years. This will bring with it a maximum amont of chloride of 0.16 kg/m^2. Then, it is assumed that the chloride flow is 100% convective, which is an assumption very much on the safe side. Assuming a cement content of 400 kg/m^3, and a concrete cover of 50 mm, the chloride content in the cover will as an average be maximum 0.7% of the cement weight. This is a level which will hardly cause corrosion. Besides, in reality, most of the cloride transport occurs by slow diffusion. Therefore, after 100 years the chloride front will most probably not even reach the bars at the inside face.

The bars at the upstream face cannot corrode due to lack of oxygen in the saturated very dense concrete.

If the concrete walls obtain through cracks, very large amounts of salt water will penetrate. This will certainly cause both reinforcement corrosion and other inconveniences. Therefore cracking - e.g. thermal cracking during the production phase- must be avoided.

Deicer salt exposure of the bridges

The bridge deck, the upper parts of the pier shafts, and the lower parts of the pylons will be exposed to deicing salts. Today, we have no possibility to calculate the service life with regard to reinforcement corrosion for this exposure type. We lack information concerning; (i) how to consider the moisture variations in the concrete cover. Some simplified calculations have been made, /17/, but they have not been calibrated against real structures in the field; (ii) how to estimate the effective chloride diffusion coefficient in concrete with constantly varying moisture conditions; (iii) how to estimate the threshold concentration. Probably, it is lower than the treshold concentration in marine environment due to the more varying moisture conditions.

As a consequence of these difficulties, no service life calculation, of the type described above for the marine environment, has been made for the deicing environment. It seems reasonable to assume, however, that a concrete with a water/binder ratio below 0.40 and a concrete cover of 75 mm will have a very long initiation time before onset of corrosion. The moisture content at the level of the bars will certainly be very stable, yielding a high value of the threshold concentration, and the transport of chloride will be slow considering that the cover is not always saturated. Besides, experience of the behaviour of edge beams of real bridge structures exposed to de-icing salts for a long time, indicates that reinforcement corrosion is rare also in structures with moderately thick concrete cover, provided the water/cemen ratio is low (<0,45).

Thermal cracking

As said above, the risk of reinforcement corrosion is low in crack-free concrete. In cracked zones corrosion starts early. Possibly, it soon stops due to counter-diffusion of alkalies into the crack zone, or due to self-healing of the cracks. One shall, however, not rely upon these healing mechanisms. So for example, there ought to be a maximum crack width for self-healing to take place. Above this size, corrosion at the crack tip will continue. The size of this maximum crack width for different types of concrete, and for different types of environment (sea or deicing), has not been clarified. Therefore, it is extremely important that the concrete in the bridge is crack-free in such parts, that are exposed to the most severe climate; the splash zone and the bridge deck zone. The tunnel walls must be completely crack-free in order to hinder constant flow of salt water.

The contractor must select a concrete mix and a production technique so that no cracks appear during the construction phase. Therefore, it is also required that he shall perform numerical calculations of the risk of thermal cracking before he starts his construction work. These calculations shall be made with an advanced computer programme, that makes possible an analysis for all parts of the structure, of the stress-strain fields appearing during and after the casting operation. The material properties to be used in the calculation shall be determined experimentally for the actual mix. The data required are:

1: The heat development
2: The strength development (compressive and tensile)
3: The development of deformation properties (elastic, viscous, plastic)

All these data shall be expressed in terms of the maturity of the concrete. Thus, also the calculated crack risk will be expressed as a function of maturity. The most difficult data to obtain are the deformation properties. These shall be determined by loading and unloading specimens of the actual mix and monitoring the deformations. Loading is made at different age of the young concrete, and to different levels relative to the actual strength at loading. The concrete can be looked upon as a so-called Burgers Body, the deformability of which is described by two "dash-pots" and two springs. The viscosities and the spring constants are functions of the maturity, and are determined by the experiment described above. There are of course also other possibilities of expressing the constitutive laws of hardening concrete.
The crack risk must not exceed a certain value, which is different for different parts of the structure:

* Outer tunnel walls and in the splash zone: Crack risk < 0.7
* Other exposed parts of the bridge and tunnel: Crack risk < 1.0

By changing the mix, by adjusting the pouring process, and by introducing cooling, a production technique can be selected that will satisfy these requirements.

Comments to the cement requirements

Slag cement

Some field tests show that concrete with high amounts of slag as a binder is less durable to frost than comparative concretes made with pure portland cement, or with portland cement containing small additions of silica fume; /18/. Similar results have been obtained in the laboratory; /19/. Therefore, considering the very long required service life, and the severe "frost environment", slag is not allowed in the bridges, not even in the submerged parts.

The tunnel is not exposed to frost, except for the ramps leading down to the tunnel, and the portal buildings. Therefore, slag cement is allowed.

Field and laboratory tests have indicated that concrete with slag cement might be more prone to thermal cracking than portland cement; /20, 21/. The lower heat development occurring in slag cement is certainly a positive factor, but it often seems to be more than counteracted by a more brittle behaviour. Despite this, slag cement is allowed in the tunnel, partly due to the long experience with this type of cement used in submerged tunnels in The Netherlands. It is assumed that possible negative behaviour with regard to thermal cracking will be revealed in the calculation of thermal cracking, and in the full scale trial castings described below.

Portland cement

The cement shall be of type low alkali/high sulfate resistance; LA/SR. There is an upper C_3A-limit of 5% prescribed. Often, there is also a lower C_3A-limit specified, due to the common belief that C_3A binds chlorides, and that a cement with low C_3A content, therefore, gives a lower risk of reinforcement corrosion. In many modern field and laboratory tests it has not been possible to verify this effect. There seems to be other factors, that are just as important for chloride diffusion, as the C_3A content. Therefore, no lower C_3A-limit is used.

Portland cements of type LA/SR often give concrete with better air-pore systems and, therefore, better frost resistance than normal portland cements. Besides, the risk of secondary cement reactions, such as delayed ettringite formation, ought to be reduced in comparison with an ordinary high alkali/high C_3A portland cement.

Fly ash

Fly ash is allowed in the tunnel, but not in the bridge. The reason is that the bridge is exposed to severe frost, which is not the case with the tunnel. Concrete containing fly ash normally has a much higher variation in the air content than concrete without fly ash. Thus, considering that the only rational way of securing a high frost resistance of the bridge is to control, that the air content is not below a certain target value, the use of fly ash is for-bidden in the entire bridge structure.

In the tunnel, a maximum of 15% of fly ash is allowed. Fly ash can give some advantages. It often increases the workability of the mix, and it might reduce the diffusivity of chlorides. On the other hand, it probably reduces the OH^- concentration of the pore water, which ought to lower the threshold concentration for onset of chloride induced corrosion. The combined effects are, however, hardly negative with regard to service life.

The efficiency factor of the fly ash is settled at 0.3. This is the figure used in the Swedish Standards, but it is lower than the value 0.5 used in the Danish Standard. The value 0.3 is a bit conservative for high quality fly ash, but it is reasonable considering the extremely high requirements for service life.

Silica fume

5 % of silica fume is allowed in the mix, both for the bridges, and for the tunnel This is reasonable, since small amounts of silica fume has been found to increase the workability of concrete. It also decreases the permeability to water and chloride. The lowering effect, that silica fume probably has on the threshold chloride concentration for start of corrosion, is probably more or less totally compensated for by the lower chloride permeability.

The eventual negative effects of silica fume on the long-term salt scaling resistance, that are described above, are coped with by increasing the salt scaling pre-test to 112 cycles, which is supposed to be enough to reveal eventual negative effects.

The efficiency factor is settled at 2. This is the same as in the Danish Standards, but higher than in the Swedish where it is settled at 1. The Swedish figure is low, and is based on eventual negative effects of silica fume on the carbonation of concrete. This is not a problem in the actual type of concrete. Besides, the value of the efficiency factor is of small importance, considering the low amount of silica fume that is allowed.

Comments to the water/binder ratio

Generally, the permeability is reduced when the water/binder ratio is reduced. Therefore, it might be tempting to reduce the maximum water/binder ratio to a very low value, in order to make possible a significant reduction of the concrete cover, without reducing the service life. This possibility has not been utilized in the specifications. The maximum water/binder ratio is specified to 0.40, with a target value of 0.38, taking natural variations into consideration. The reason behind this decision is that low water/binder ratios are connected with some problems:

1: The risk of internal micro-cracking, due to self desiccation, is imminent at low water/binder ratios. It also seems as if the risk increases with increased use of mineral by-products, especially silica fume. The eventual negative effects of micro-cracks have never been clarified, but they are hardly positive.
2: The concretes become more difficult to cast and to compact. The vibration time increases, and form vibration might become impossible. Besides, the finishing of concrete surfaces can be very difficult. In order to compensate for these negative factors, it is often necessary to use high dosages of superplastizisers. This might cause significant retardation of the stiffening of the concrete and disturbances in the production cycle, with loss in concrete quality as a consequence. It has also turned out that the air-pore system might be impaired when the stiffening time is prolonged. This will have a very negative effect on the frost resistance.

Thus, it is quite possible that an "optimum" quality is achieved with a water/binder ratio around 0.40. This is a value that has been used for bridge building in the Nordic countries during the last decade. Experiences from the use of this type of concrete is also very good. Besides, measurements of the chloride diffusivity of concretes, exposed for a long time in the field, indicate that a long service life can be obtained also with a concrete having a water/binder ratio of 0.40, provided that the cover is thick enough.

For concrete that is exposed to low chloride contents, but to frost, a water/binder ratio of maximum 0.45 is allowed, provided the concrete is protected with a proper air entrainment. This value is also based on long term experience.

Comments to the aggregate

The aggregate shall be of very high quality. Thus, the water absorption shall be

lower than 1%. Both the fine and the coarse aggregate shall be tested with regard to the potential risk of different types of harmful aggregate reaction.
The potential risk, that the coarse aggregate shall cause destruction to the concrete during freezing, is revealed in the dilation test, that is performed on concrete that has been stored in water during half a year; see above.

Full scale trial castings

An important link between pre-testing and production is the full scale trial castings that shall be made. They are used as a proof, that the concrete mix and the production method are suitable for full scale production. All requirements on the fresh concrete, and the hardened concrete, shall be fulfilled at the full scale trial casting. Therefore, numerous tests are made during, and after the casting. They include freeze-thaw tests, tests of the internal structure by thin section analyses, tests of the heat generation and cracking.

A full scale casting shall be made for each new type of structural element. The construction work is not allowed to start until an approved full scale trial test has been executed.

References

1. *Fagerlund, G, Janz, M., Johannesson, B.:* On the effect of frost damage on the bond between the reinforcement and the concrete. Div. of Building Materials, Lund Institute of Technology, Report TVBM-9016, Lund 1994.
2. *Fagerlund, G., Somerville, G., Tuutti, K.:* The residual service life of concrete exposed to the combined effect of frost attack and reinforcement corrosion. Int. Conf. "Concrete Across Borders", Odense, June 22-25, 1994.
3. *Fagerlund, G.:* Predicting the service life of concrete exposed to frost action through a modelling of the water absorption process in the air-pore system. In Jennings et al (eds.) "The Modelling of Microstructure and its Potential for Studying Transport Properties and Durability". Kluwer Academic Publishers, 1996.
4. The critical degree of saturation method of assessing the freeze/thaw resistance of concrete. Materials and Structures, Vol 10, Nr 58, 1977.
5. *Fagerlund, G.:* Prediction of the service life of concrete exposed to frost action. in "Studies on concrete technology". Swedish Cement and Concrete Research Institute, Stockholm, 1979.
6. *Fagerlund, G.:* Frost resistance of high performance concrete - some

theoretical considerations. In Sommer (ed.) "Durability of High Performance Concrete". RILEM Workshop, Vienna, Febr. 14-15, 1994. RILEM, Cachan, 1995.

7. *MacInnis, C., Lau, E.C.:* Maximum aggregate size effect on frost resistance of concrete. ACI Journal, Proceedings 1971(68):2.

8. *Verbeck, G.J., Klieger, P.:* Studies of salt scaling of concrete. Highway Research Board, Bulletin 150, 1957.

9. *Sellevold, E., Farstad, T.:* Frost/salt testing of concrete. Effect of test parameters and concrete moisture history. In Fagerlund, Setzer (eds.) "Freeze-Thaw and Deicing Resistance of Concrete". Div. of Building Materials, Lund Institute of Technology, Report TVBM-3048, Lund 1992.

10. *Lindmark, S.:* Influence of testing conditions on salt frost resistance of concrete. Division. of Building Materials, Lund Institute of Technology, Internal report M2:05, Lund 1995.

11. *Lindmark, S.:* Private communication. To be published in a report from a Nordic Research Seminar held at the Div. of Building Materials, Lund Institute of Technology in April, 1996.

12. *Powers, T.C., Helmuth, R.A.:* Theory of volume changes in hardened portland cement paste during freezing. Highway Research Board, Proceedings No 32, 1953.

13. *Petersson, P-E.:* The influence of silica fume on the salt frost resistance of concrete. Swedish National Testing and Research Institute, Technical Report 1986:32, Borås, 1986.

14. *Hausmann, D.A.:* Steel corrosion in concrete. Materials Protection, Nov. 1967.

15. *Bijen, J.:* Can we construct durable marine structures with neat concrete, and can we repair durably? Delft University and INTRON, Jan. 1989.

16. *Polder, R.B., Larbi, J.A.:* Investigations of concrete exposed to North Sea water submersion for 16 years. TNO Report 93-BT-R0619-02, 1993.

17. *Hedenblad, G.:* Moisture permeability of mature concrete, cement mortar and cement paste. Div. of Building Materials, Lund Inst. of Technol., Report TVBM-1014, 1993.

18. *Bremner, T.W., Carette, G.G., Malhotra, V.M.:* Role of supplementary cementing materials in concrete for the marine environment. In Chandra (ed.) "Durability of concrete. Aspects of admixtures and Industrial By-products". Swedish Council for Building Research, Document D9:1989.

19. *Stark, J., Ludwig, H-M.:* The influence of the type of cement on the freeze-

thaw/freeze-deicing salt resistance of concrete. In Sakai et al (eds.) "Concrete Under Severe Conditions". E&F Spon, London, 1995.

20. *Bamforth, P.B.:* In situ measurements of the effect of partial portland cement replacement using either fly ash or ground granulated blastfurnace slag on the performance of mass concrete. Proc. Inst. Civil Eng. Part 2, Sept, 1980.

21. *Emborg, M.:* Thermal stresses in concrete structures at early ages. Luleå University of Technology, 1989:73D, Luleå, 1989.

CEMENTA

Cementa AB Box 144 182 12 Danderyd